CHARACTERIZATION OF THE ACID-PRODUCING POTENTIAL AND INVESTIGATION OF ITS EFFECT ON WEATHERING OF THE GOATHILL NORTH ROCK PILE AT THE QUESTA MOLYBDENUM MINE, NEW MEXICO

by

Samuel Tachie-Menson

Submitted in Partial Fulfillment
of the Requirements for the

Master of Science in Mineral Engineering

New Mexico Institute of Mining and Technology
Department of Mineral Engineering

Socorro, New Mexico
May, 2006

To Danielle and Kate

ABSTRACT

As part of investigations into the effect of weathering on the physical stability of rock piles at the Questa molybdenum mine, samples from the Goathill North (GHN) rock pile were subjected to static, mineralogic and chemical tests to characterize the current levels of acidity and future acid producing potential within the rock pile, and investigate the implications for weathering of the rock pile material. There were differences between the paste pH results from the stable and unstable portions of the pile. In the stable portion, paste pH was lowest near the surface and the base of the pile. The concentration of high pH samples reduced from higher to lower elevations in the stable portion. In the unstable portion, the samples had generally lower pH values than those in the stable portion, and they did not show any recognizable trend with distance from the face of the pile. There was a higher concentration of high pH samples at lower elevations than higher elevations in the unstable portion of the pile. The differences between pH distribution in the stable and unstable portions of the pile is the result of prior sliding movement of the unstable portion, which resulted in greater accessibility of air and moisture to increase oxidation at the interior of the pile. Samples with lower paste pH had the greater potential to generate acid in future. Samples rich in Amalia Tuff had lower neutralization potential than samples rich in andesite because the Amalia Tuff has higher pyrite content from QSP alteration.

ACKNOWLEDGMENTS

I would like to acknowledge the support and direction received from the following individuals and organizations:

- Molycorp Inc. funded the thesis project and most of my Master's program through the New Mexico Bureau of Geology and Mineral Resources.
- The New Mexico Bureau of Geology and Mineral Resources (NMBGMR) provided office and laboratory space and equipment for my thesis work.
- Dr. Virginia McLemore, my thesis and research supervisor, offered most of the guidance and technical advice, without which this thesis would have been impossible to complete.
- Dr. Navid Mojtabai, my academic advisor, and my other thesis committee members, Dr. William Chávez Jr. and Lynn Brandvold also offered technical advice and a lot of encouragement.
- The Questa Rock Pile Weathering Stability Project team played a major role in this work from sampling through laboratory tests to data analysis. I am particularly grateful to Alex Tamm, Donald Wenner, Nathan Wenner, Sean Wentworth, Luiza Gutierrez, Heather Shannon, Vanessa Viterbo, Christian Kruger (NMT students), Richard Lynn, Kelly Donahue, Erin Philips, Patrick Walsh, (Geologists at NMBGMR), Jack Adams (WSU, Ogden, UT) and G. Ward Wilson (UBC, Vancouver, Canada), for their help with field sampling and sample preparation.

Kelly Donahue was in charge of the XRF analysis and Erin Philips did the modal mineralogy analysis. Shannon Archer, Stefani Bennett, Soloman Wenzel, Todd White, Kayode Olanrewajo, Anthony Odura-Darkwa, Kwaku Boakye, Armando Fernandes de Vegga Rodrigues, Claudia Duarte da Conceicao, and Jario Pires Jr. (NMT students) did most of the paste pH, paste conductivity, ABA and NAG tests. A lot of technical guidance was received from Dr. Andrew Campbell (E&ES department, NMT), Dr. Virgil Lueth and Dr. Nelia Dunbar (NMBGMR), and Mark Logsdon (Geochimica Inc., Aptos, CA).

- The Socorro section of WAAIME supported my Masters program with much needed scholarship-loans.
- My wife, Kate, and my daughter, Danielle, did not complain much but did their best to make life normal for us all when I had to stay in the office most of the days and nights writing my thesis.
- My family in Ghana, Christina (my mother), Joseph Ernest (my father who passed away in May 2005), Rebecca (my sister) and Joseph and Josiah (my brothers) contributed towards my education in many different ways and I wish them every blessing from heaven.
- The vicar, Rev. Fr. Woody Peabody, and members of Epiphany Episcopal Church in Socorro provided a lot of needed moral, spiritual and financial support during my Master's program to make life a lot easier for me and my family.

There are many other people who contributed toward this thesis report and my Master's program but are not mentioned here. Their contributions were, all the same, appreciated.

TABLE OF CONTENTS

Page

LIST OF TABLES

Table Page

LIST OF FIGURES

Figure Page

This thesis is accepted on behalf of the
Faculty of the Institute by the following committee:

Advisor

Date

I release this document to the New Mexico Institute of Mining and Technology.

Student's Signature Date

1 INTRODUCTION

1.1 Introduction

This thesis investigates the present level and distribution of acidity and the potential for future acid generation in the Goathill North rock pile at the Questa molybdenum mine in New Mexico and the implications for weathering of the rock pile material. Acidity of mine soils is mostly due to the oxidation of sulfide minerals such as pyrite and pyrrhotite (Stumm and Morgan, 1981) and results in acidic, iron- and sulfate-rich waters which accelerate the oxidation of rock-forming minerals (White et al., 1999). The potential for acidic waters to increase the rate of mineral dissolution or weathering and increase the release of heavy metals into waters is well known and documented in numerous publications based on studies done in many different locations worldwide (see section 2.2.4). The release of acidic waters with high metal concentrations is called Acid Rock Drainage (ARD). Most of the studies done in the past have dwelt on the release of toxic metals into water bodies through acid drainage (e.g. Higgs et al., 1997; King, 1995; Thomson et al., 1997). The focus of the current study is the effect of soil acidity on the weathering of rock pile materials in Goathill North. This work is part of a multi- and inter-disciplinary research effort being undertaken by a team of scientists and engineers to investigate how weathering affects the physical stability of mine rock piles at the Questa mine.

1.2 Thesis Overview

The thesis is organized into six chapters as follows:

Chapter 1: Introduction to the entire research project in general and the thesis work in particular, and an in-depth description of the project site.

Chapter 2: Review of literature relevant to the thesis.

Chapter 3: Methods used in sampling and laboratory tests.

Chapter 4: Presentation of laboratory tests results.

Chapter 5: Discussions of test results.

Chapter 6: Conclusions and recommendations.

1.3 Project Background

The Questa Rock Pile Weathering Stability Project was initiated by Molycorp Inc., the owners and operators of the Questa molybdenum mine, in 2002. Molycorp decided to carry out investigations into the geochemical and physical weathering effects over time on the mine rock pile fabric, water movement through the piles, and mechanical properties of the piles. In 2002, Molycorp solicited for letters of intent from qualified university researchers and research groups for the purpose of investigating the potential effect of chemical and physical weathering on the stability of rock piles at the mine (Molycorp Inc., 2002).

The University of Utah put together, a team of university researchers and consultants from the United States and Canada to undertake the rock pile weathering study which is now known as the Questa Rock Pile Weathering Stability Project. The team consists of geologists, geophysicists, geochemists, hydrologists, biologists, geotechnical engineers,

students and other supporting staff from the following academic and consulting organizations:

- Geochimica Inc., Aptos, CA, USA
- Minnesota Department of Natural Resources, St. Paul, MN, USA
- New Mexico Bureau of Geology and Mineral Resources, Socorro, NM, USA
- New Mexico Institute of Mining and Technology, Socorro, NM, USA
- R^2 Incorporated, Denver, CO, USA
- SoilVision Systems Ltd., Saskatoon, SK, Canada
- Spectral International Inc., Arvada, CO, USA
- The University of Utah, Salt Lake City, UT, USA
- University of British Columbia, Vancouver, B.C., Canada
- University of California, Berkley, CA, USA
- University of Nevada, Reno, NV, USA
- Weber State University, Ogden, UT, USA

The project is divided into three phases. The first phase is focused on the characterization of the rock piles, which was started in August 2003 to be completed in May 2006. This thesis project is part of the Phase I characterization program.

1.4 Project Scope and Objectives

The scope of the Phase I program as stated in the Phase I work plan (Molycorp Project Team, 2004) is to address the key question, "*Will the rock piles become gravitationally unstable over time*?" by focusing on the following critical issues:

1. Understanding weathering processes, both at the surface and within the mine rock piles,
2. Measuring the rate at which such weathering processes occur over time, and
3. Determining the effect of these processes on the long-term physical stability of the piles.

Molycorp decided to regrade the Goathill North (GHN) rock pile in 2004 because of concerns about its stability. The deconstruction exercise brought a unique opportunity to examine the interior of the pile without incurring the cost of drilling. Therefore Phase I investigations were focused on the Goathill North rock pile.

The specific objectives of the Phase I program were to:

1. Document the deconstruction of Goathill North rock pile, using trenches to map and obtain samples that will characterize the structure, mineralogy, geochemistry, hydrology and geotechnical properties of the materials that were excavated.
2. Define the mineralogy, chemistry, isotopic composition, hydrological, geotechnical, and biogeochemical characteristics of spatially distributed samples of rocks and mine soils within the GHN rock pile.
3. Define the mineralogy, chemistry, isotopic composition, geotechnical, and biogeochemical characteristics of spatially distributed samples and determine the age and geologic history of selected alteration scars.
4. Determine a weathering index and the change in mineralogy, chemistry, isotopic, geotechnical and biogeochemical characteristics with time.

5. Use the geologic and geochemical data to determine rates of weathering, including rates of acid production within the rock pile and in the scars as a basis for final design of the weathering cells in Phase 2.
6. Develop the data that would be used in subsequent phases to predict the geochemical and mineralogical weathering of the rock pile.
7. Begin preliminary development and short term testing of the geochemical model.

The objectives of the current thesis work are to:

1. Characterize the present level and spatial distribution of acidity and soluble solids in the Goathill North rock pile by laboratory measurement of paste pH and paste conductivity of rock pile samples taken from trenches and drill holes.
2. Determine the potential for future generation or consumption of acidity in the rock pile by performing static Net Acid Generation (NAG) and Acid-Base Accounting (ABA) tests on the rock pile samples.
3. Investigate the effects of lithology on acidity and potential acid generation by comparing results of paste pH, NAG and ABA with chemical and mineralogical compositions of the samples.

1.5 Site Description

1.5.1 Location

The Questa molybdenum mine is located 5.6 km (3.5 miles) east of the village of Questa in Taos County, north central New Mexico, in a region with a long history of mining (Figure 1.1). The mine is on the south facing slopes of the north side of the Red

River Valley between an east-west trending ridgeline of the Sangre de Cristo Mountains at approximately elevation 3,200 m (10,500 ft) and State Highway 38 adjacent to the Red River at approximately elevation 2,438 m (8,000 ft). State Highway 38 connects the village of Questa on the west to the town of Red River on the east of the mine.

1.5.2 Mine History

In about 1914, two local prospectors staked multiple claims in an area of the Sangre de Cristo mountain range called Sulphur Gulch. During their exploration they discovered an unknown dark, metallic material. The common belief at the time was that it was graphite and it was rumored to have been used for a myriad of functions from lubricating wagon axles to shoe polish. In 1917 a sample of the ore was sent out to be

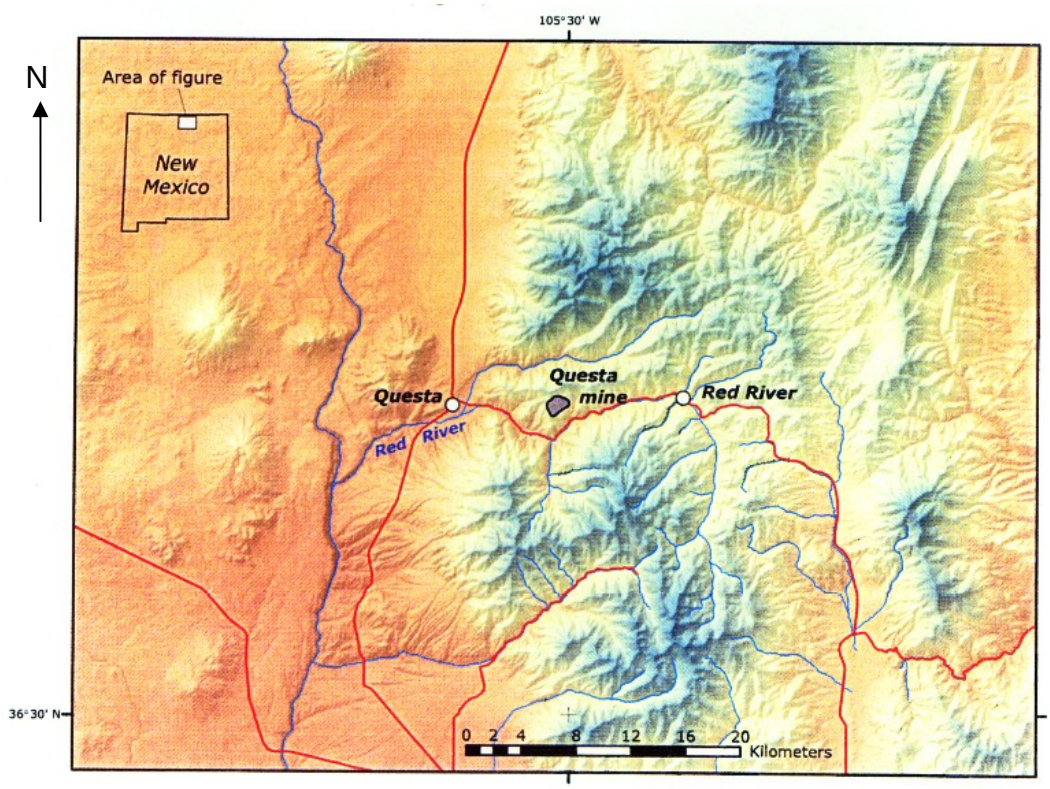

Figure 1.1: Location Map of Questa Mine (Ludington et al., 2004).

assayed for gold and silver. The report included a mention of molybdenum and its rising value resulting from an increase in usage during WWI.

Early in the summer of 1918, the R & S Molybdenum Mining Company began underground mining in Sulphur Gulch of the high grade molybdenum veins. On June 1, 1920, the Molybdenum Corporation of America was formed and acquired the R&S Molybdenum Mining Company (which later became Molycorp). By August of 1923 Molycorp had acquired the Junebug mill, which could produce one ton of molybdenum concentrate daily from every 25 tons of ore. All molybdenum production during this period was from high grade, vein molybdenite (MoS_2) with grades running as high as 35% molybdenum. This mill was one of the first floatation mills in North America.The mill was rebuilt several times and operated on a continuous basis until 1956 when the underground mining operations ceased. In 1963 the mill was dismantled to make way for the current mill.

From 1957 to 1960, exploration was conducted under contract with the Defense Minerals Exploration Act. After completion of the contract, Molycorp continued exploration and in early 1963 core drilling from the surface and underground was accelerated to determine whether or not an open pit mine was economically feasible. By 1964, sufficient reserves had been blocked out to justify the development of an open pit mine and the construction of a mill which could handle 10,000 tons per day. Pre-production stripping was started in September, 1964, and the first ore from the pit was delivered to the mill in January 1966.

Molycorp was acquired by Union Oil Company of California in August of 1977. In November 1978, development of the existing underground mine was begun with two vertical shafts bottoming out at approximately 396 m (1,300 ft) deep, and a mile-long decline was driven from the existing mill area to the haulage level. The mill floatation area was modernized to accommodate the higher grade of underground ore.

In January 1982, mining from the open pit ceased and in August of 1983, the new underground mine began operating. Employment at this time reached approximately 900 workers. In 1986, an extremely "soft" market caused the first shutdown of the mine in recent history. The mine was restarted in 1989 and continued to operate until January 1992 when the mine was shut down again due to low prices. The mine restarted in 1995 and most of that year was devoted to mine dewatering and repair. Production began in late 1996 and over the next several years approximately 13.6 million kg (30 million pounds) of molybdenum concentrate were produced. Development of the current ore body began in 1998, and its production in October 2000. This ore body and 3 adjacent ones have sufficient ore reserves for production to continue for several decades. (Wagner, 2005)

1.5.3 Mine Features

Figure 1.2 shows the location of surface features at the Questa mine site. The most conspicuous features at the mine site are nine mine rock piles that were constructed from 317.5 million metric tons of overburden and mine rock during the surface mining period (URS Corporation, 2000). The piles are located on the mountain slopes adjacent

to the open pit and include Sugar Shack South, Middle and Old Sulphur (or Sulphur Gulch South) rock piles whose toes are along State Highway 38 and can be seen by drivers on the road. These piles are referred to as the "Front Rock Piles" and are, together with Sugar Shack West, on the south-facing slopes of the mountain. On the east side of the pit are Spring Gulch and Blind Gulch/Sulphur Gulch North rock piles. Capulin, Goathill North and Goathill South rock piles are on west-facing mountain slopes on the west side of the open pit. The mine rock piles cover a surface area of about 2.75 million m^2 (275 ha) and extend vertically from just above the elevation of the Red River (2,470 m (~8,100 ft)) to approximately 2,990 m (9,810 ft), resulting in some of the highest mine rock piles in North America (Wels et al., 2002). They are typically at angle of repose and have long slope lengths (up to 610 m (2000 ft)), and comparatively shallow depths (30.5 – 61 m) (Lefebvre et al., 2002).

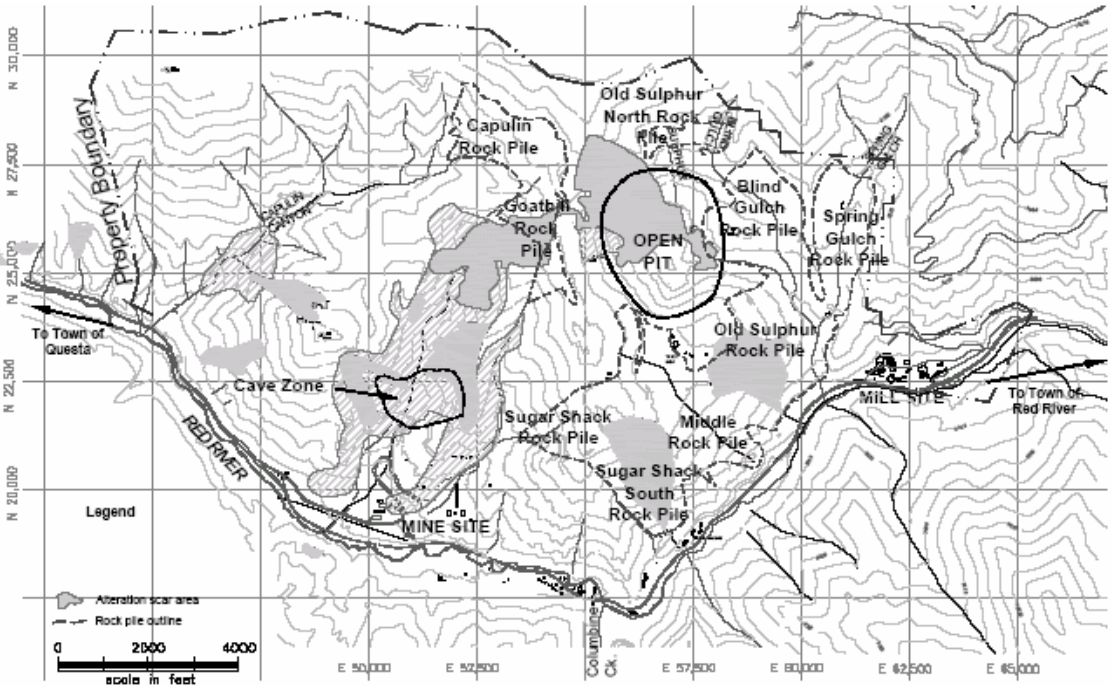

Figure 1.2: Map of Questa Mine Site Showing Surface Facilities (Shaw et al., 2002).

The mine offices are situated on the south-western corner of the mine property and the Mill Site is on the south-eastern corner towards the town of Red River.

1.5.4 Geology

The geology and mineralogy of the Red River Valley have been described by Schilling (1956), Rehrig (1969), Lipman (1981), Carpenter (1968), and Meyer and Leonardson (1990; 1997), and are summarized in this section. Figure 1.3 is a simplified geologic map of the Questa-Red River area. The Red River Valley is located along the southern edge of the Questa caldera and contains complex structural features (Caine, 2003) and extensive hydrothermal alteration. Volcanic and intrusive rocks of Tertiary age are underlain by metamorphic rocks of Precambrian age that were intruded by granitic stocks. The volcanic rocks are primarily intermediate to felsic composition (andesite to rhyolite); granites and porphyries have intruded the volcanics and are the apparent source of hydrothermal fluids and molybdenite mineralization.

The mineral deposits in the Red River Valley are considered Climax-type deposits (Figure 1.4) that are associated with silica- and fluorine-rich rhyolite porphyry and granitic intrusions. Climax-type hydrothermal alteration produces zones of alteration assemblages with a central zone of fluorine-rich potassic alteration, a quartz-sericite pyrite (QSP) zone (often with a carbonate-fluorite veinlet overprint), and a propylitic zone. In the potassic zone, rocks are altered to a mixture of biotite, potassium feldspar, quartz, fluorite, and molybdenite; these rocks usually contain less than 3 percent sulfide

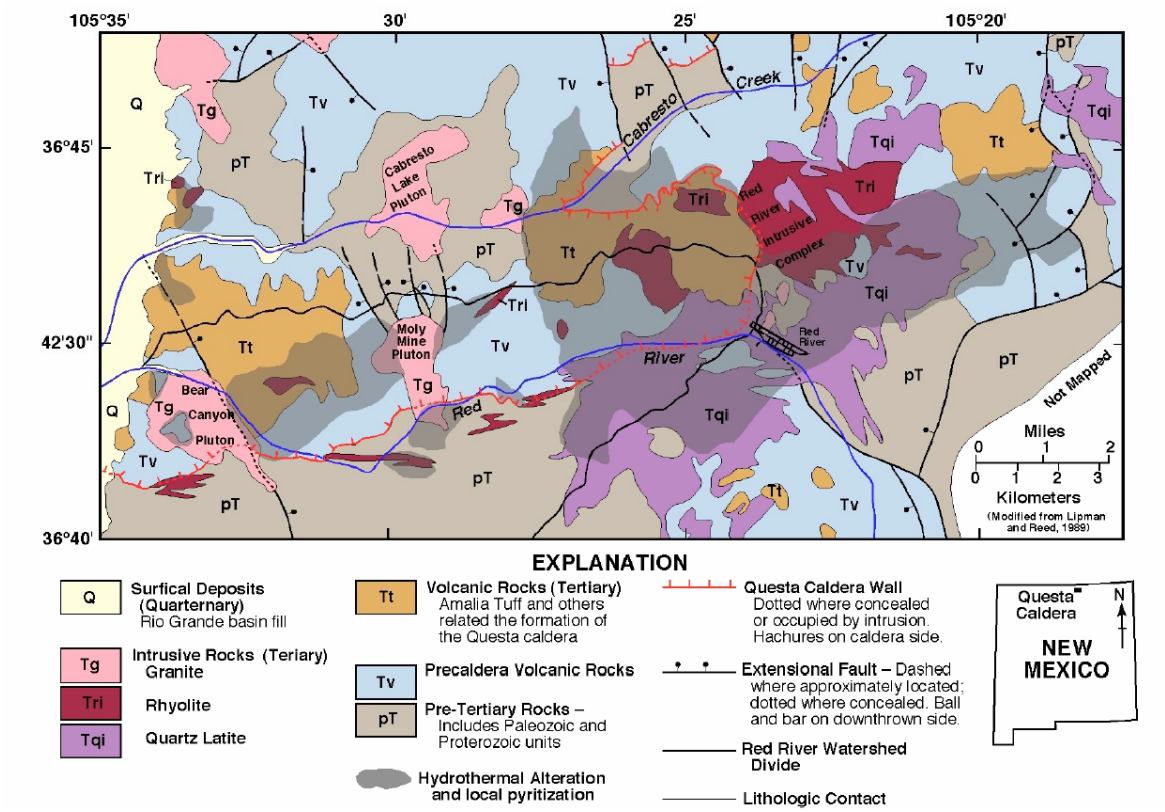

Figure 1.3: Simplified geologic map of the southern portion of the Questa Caldera in the vicinity of Red River, New Mexico from Caine (2003) modified from Lipman and Reed (1989).

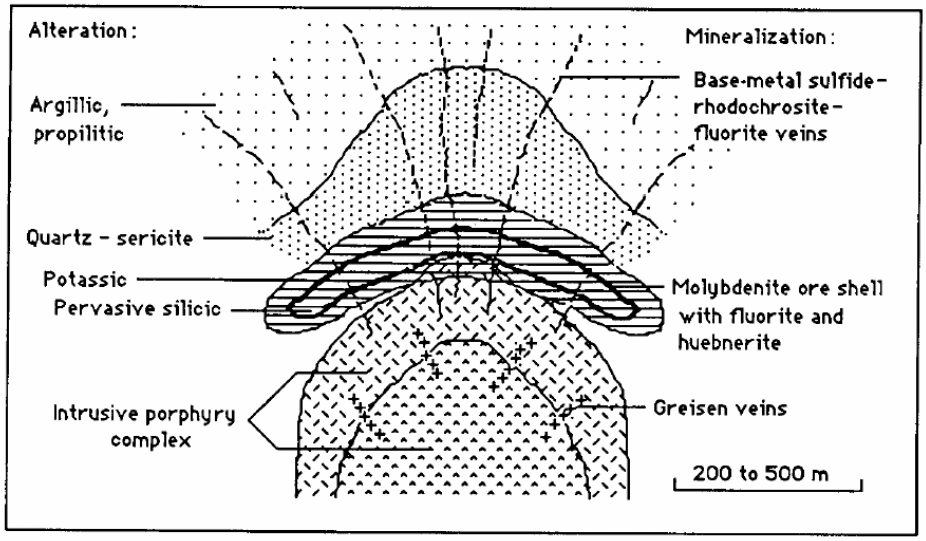

Figure 1.4: Schematic cross section of a Climax-type molybdenum deposit showing relationship of ore and alteration zoning to porphyry intrusions (Mutschler et al., 1981)

(including molybdenite). Quartz-sericite-pyrite (QSP) alteration, as the name implies, produces a mixture of quartz, pyrite (as much as 10 percent), and fine-grained mica (sericite) or illite. Chlorite, epidote, albite, and calcite typically are found in the propylitic zones.

Ore deposits in the Red River Valley contain quartz, molybdenite, pyrite, fluorite, calcite, manganiferous calcite, dolomite, ankerite, and rhodochrosite. Lesser amounts of galena, sphalerite, chalcopyrite, magnetite, and hematite also are present. The hydrothermal alteration related to mineralization overprints an older, regional propylitic alteration. In these areas, rocks can contain a mixture of quartz, pyrite, and illite clays replacing feldspars, chlorite, carbonates, and epidote. Abundant minerals in overburden rock produced by mining activities include chlorite, gypsum, illite, illite-smectite, jarosite, kaolinite, and muscovite (Gale and Thompson, 2001).

Andesite volcanic and volcaniclastic rocks are present in most scar-area bedrock outcrops and are the predominant bedrock units in the Straight Creek, South and Southeast Straight Creek, South Goat Hill, Sulphur Gulch, and Southwest Hansen scars. Amalia Tuff, a mildly alkaline, rhyolitic ash-flow tuff (ignimbrite), is the predominant rock type in the Goat Hill and Hansen scars, and quartz latite porphyry is the main rock type in the June Bug and Southeast Hottentot scars. Rhyolite porphyry is the main rock type in the Hottentot scar, and quartz latite and rhyolite porphyries form the hill slopes of many scars. Advanced argillic alteration was identified in the Hansen and Hottentot scars and in areas southwest of the Molycorp open pit. Propylitized andesite bedrock is

present in the La Bobita drainage, an area that does not contain alteration scars (Nordstrom et al., 2005).

1.5.5 Climate, Vegetation and Drainage

The Red River Valley is located within an alpine, semi-arid desert that receives precipitation throughout the year and sustains moderate biodiversity. The annual average temperature is 4°C and the annual average precipitation and snowfall are approximately 50 and 371 centimeters, respectively. Daily temperatures generally fluctuate by 18°C throughout the year (Western Regional Climate Center, 2003).

Climate and vegetation vary greatly within short distances, primarily because of differences in topography. Orographic effects of mountainous topography lead to precipitation on the windward slopes and localized storms within tributary valleys. Prevalent vegetation in the Red River Valley is representative of the following altitude zones: piñon-juniper woodland (1,800-2,300 m in altitude), mixed conifer woodland (2,300-2,700 m in altitude), and spruce-fir woodland (2,700-3,700 m in altitude) (Knight, 1990). Willows, cottonwoods, shrubs, perennial grasses, and flowering vegetation are common near the banks of the Red River. Widely spaced piñon pines and junipers extend from the river. Gains in altitude give rise to an abundance of ponderosa and limber pines, while Douglas- and white-fir are found at higher altitudes (Nordstrom et al., 2005).

The Sangre de Cristo Mountains are drained by intermittent tributaries of the Red River, including Bitter, Hottentot, Straight, Hansen, and Cabresto Creeks (Figure 1.5).

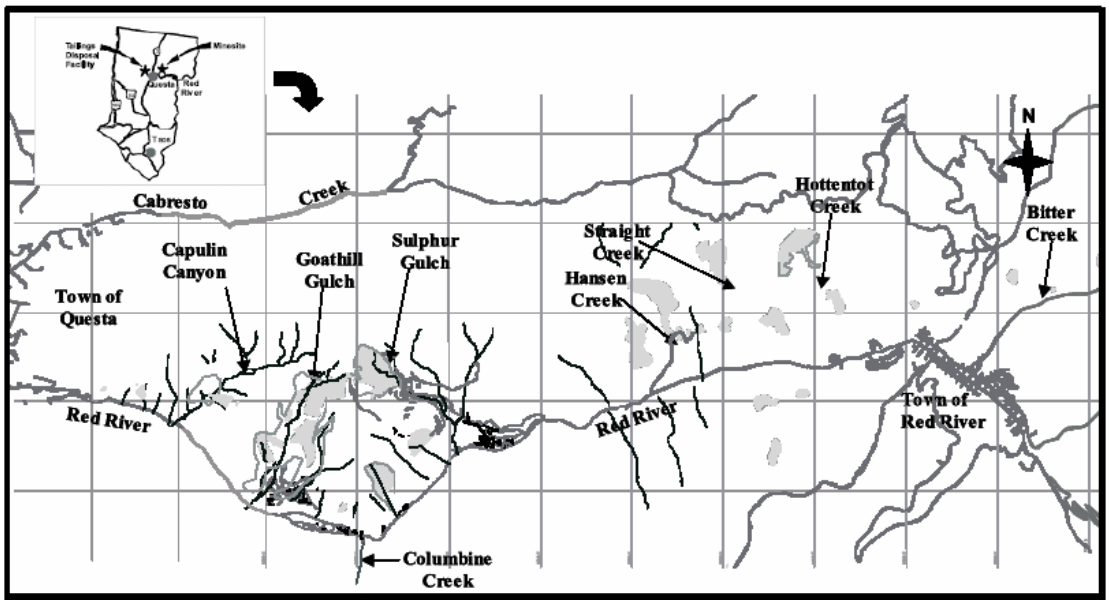

Figure 1.5: Drainage of the Questa-Red River Area (Shaw et al., 2003)

1.6 Goathill North Rock Pile

The Goathill North (GHN) rock pile was constructed between 1964 and 1974 with approximately 4.2 million cubic meters (5.5 million yrd^3) of material and has a maximum height of about 183 m (600 ft) (Norwest Corporation, 2004). It is the first among the nine rock piles constructed with material from the open-pit. Due to sliding of a portion of the pile, the GHN rock pile has been characterized as having a stable portion and an unstable portion. Figure 1.6 is a view of the GHN rock pile from West.

1.6.1 Stability Problems

Indications of movement in the northern portion of the GHN rock pile had been a concern to the mine for years until mitigation efforts were initiated. Studies conducted by Norwest Corporation in 2003 revealed that the rock pile was constructed in an area

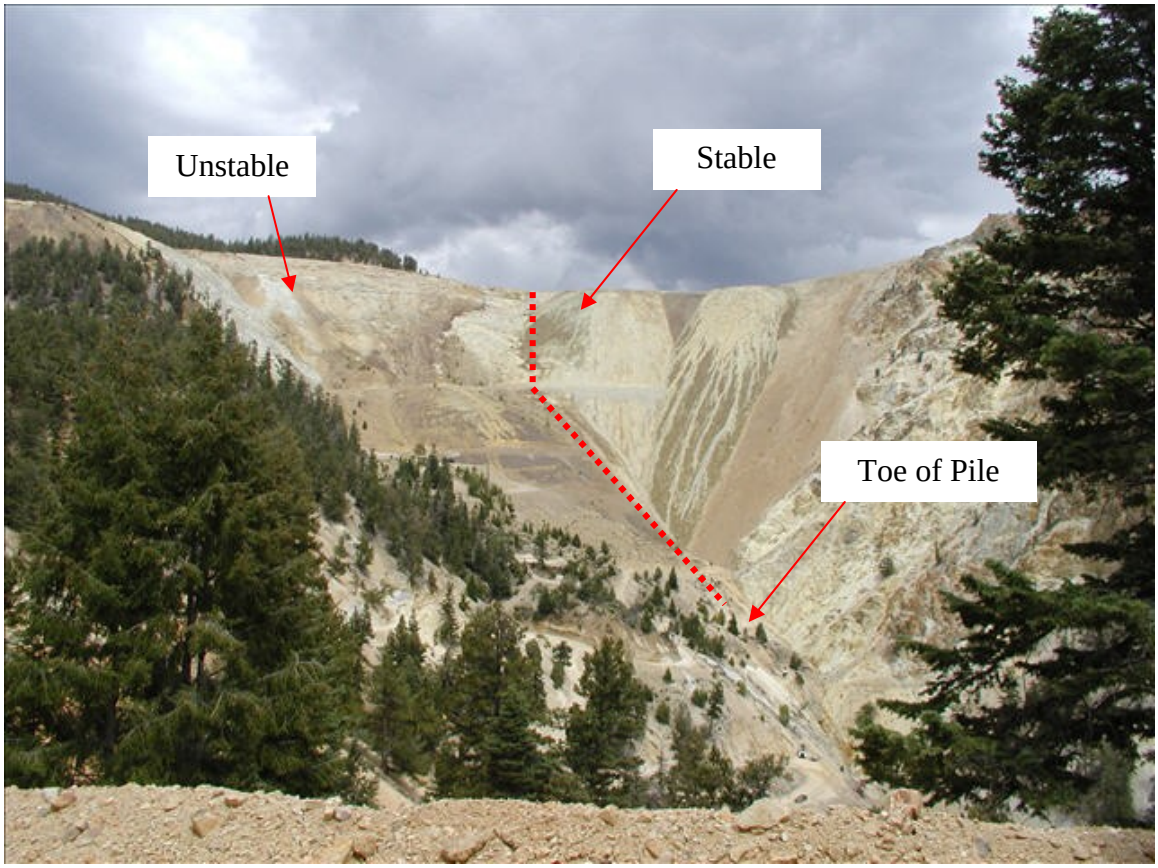

Figure 1.6: Goathill North Rock Pile viewed from the west before deconstruction

characterized by alteration scars. These scars have high bedrock pyrite contents which produce acid drainage and are more susceptible to weathering. In addition, there is a shallow perched water table in the weathered zone at Goathill North which contributes pore pressures to trigger slide movements in the bedrock. The seepage also acts as the solution for chemical weathering and the medium for transporting away any dissolved components of the weathered bedrock material. All these factors contributed to a weak foundation for the rock pile and triggered sliding soon after the rock pile placement started. Foundation movements associated with the initial development of the slide occurred between 1969 and 1973, and continued to occur after more than 30 years since their initiation. The total slide volume at Goathill North, based on the slip surface and

topographic contours, was estimated as 1.91 million m^3, comprising 1.34 million m^3 of mine rock and 0.57 million m^3 of valley colluvium. The slide zone was approximately 15.2 to 22.9 m thick and sliding was occurring along a surface that was dipping at approximately 20 degrees beneath the colluvium bench and approximately 30 degrees beneath the rock pile. (Norwest Corporation, 2004)

1.6.2 Deconstruction

Based on their findings about the stability status of the GHN rock pile (Norwest Corporation, 2003), Norwest recommended a four-phase mitigation plan to arrest the movement of the rock pile. The plan was to regrade the entire rock pile to reduce its slope angle and move material from the upper portion of the pile to the bottom to serve as a buttress against further movement. The four phases of the proposed project are summarized in Table 1.1.

The GHN deconstruction project began in the Spring of 2004 with the construction of the rock pile under-drain, Phase 1. Aplite rock from the northeastern corner of the mine property was crushed into coarse gravel size, transported and dumped at the toe of the rock pile to form a drainage layer on which the buttress would be placed. Starting from the Fall of 2004, the actual down slope pushing of the stable part of the rock pile began. Bulldozers were used to push the material at the upper part of the pile onto the drain rock at the toe. This was the second phase of the project and it was completed by the end of 2004. In the early spring of 2005, the third phase began. The upper portion of the unstable, slide area was pushed by bulldozers to the toe of the pile to serve as additional

Table 1.1: Summary of Proposed Mitigation Measures for GHN Rock Pile (Norwest Corporation, 2004)

Phase	Operation	Location	Cut/Fill	Finished Slope	Volume m^3 (yd^3)
1	Rock pile under drain construction	Main valley drainage at toe of rock pile	Imported fill	Follows topography	15,290 (20,000)
2	Stable pile cut and initial toe buttress fill	Stable south rock pile slope	Cut 'A'	2H:1V	152,910 (200,000)
		Initial toe buttress fill	Fill 'B'	1.5H to 2.5:1V	152,910 (200,000)
3	Slide unloading and regrading and final buttress fill and toe berm	Upper slide unloading	Cut 'C'	Follows shear plane	344,050 (450,000)
		Upper slide regrading	Cut 'D'	2H and 2.5H:1V	57,342 (75,000)
		Upper slide regrading	Fill 'E'	2H and 2.5H:1V	49,696 (65,000)
		Final buttress toe berm fill	Fill 'F'	1.5H to 2.5:1V	332,581 (435,000)
4	Surface water controls	Rock pile, colluvium and buttress fill slopes	Cut and fill	1.5H to 2.5:1V	19,114* (25,000)

*assuming rough grading included in Phase 3 and not including rip rap.

buttress. Following this phase was the final phase, the construction of surface drains to control flow of runoff water on the pile. Figure 1.7 shows how the rock pile looked like after about half of the deconstruction had been completed.

Figure 1.7: A view of GHN Rock Pile from north about midway in the deconstruction exercise

2 LITERATURE REVIEW

2.1 Mine Rock Piles

Mine rock piles, also called waste rock piles, waste piles or waste dumps, are some of the largest man-made structures by volume, weight or height at a mine (Robertson, 1982). In 1996 the International Commission on Large Dams (ICOLD) estimated that the weight of mine rock and tailings disposed of globally almost certainly exceeds 5,000,000,000 tonnes per annum. Considering that some highly priced commodities occur in their ores in concentrations of grams or carats per tonne, and that many individual mines extract in excess of 50,000,000 tonnes of ore per annum, even ICOLD's estimate is probably much too low (Blight and Fourie, 2005). Rock piles and tailings dams are the two major types of facilities containing geologic materials which are considered "waste" in mining and milling operations (Robertson, 1985; Sracek et al., 2004). But there are other types of "mine waste". Table 2.1 is a list of definitions of some of the different types of "mine waste".

2.1.1 Characteristics and Types of Mine Rock Piles

Mine rock piles contain overburden material and can take one or a combination of many different configurations such as valleyfill, crossvalley, sidehill, ridge, and heaped depending on the topography of the area (Figure 2.1) (Zahl et al., 1992). As the name

Table 2.1: Terms and Definitions for Mine Waste (Van Zyl et al., 2002).

Term	Definition
Overburden	The rock above the mineral resource that must be removed in order to mine the mineral resource.
Waste rock	Barren or uneconomic mineralized rock that has been mined, but is not of sufficient value to warrant treatment and is therefore removed ahead of processing. It may include overburden.
Low grade ore stockpiles	Rock that has been mined and stockpiled with sufficient value to warrant processing, either when blended with higher-grade rock or after higher-grade ore is exhausted, but often left as 'waste'.
Tailings	The solid product of the treatment and mineral concentration process that are considered too low grade to be treated further. Tailings are the finely ground host rock materials from which the desired mineral values have been largely extracted.
Heap leach spent ore	Rock remaining after recovery of metals and some soluble constituents through heap leaching and heap rinsing of ores.

indicates, a valley-fill rock pile fills a valley. The top surface is usually sloped to eliminate water ponding. Construction begins at the upstream end of the valley and dumping proceeds along the downstream face. This type of embankment can also be started as a cross-valley structure where the area is subsequently filled upstream. A cross-valley structure crosses the valley bottom, but the valley is not completely filled upstream. A side-hill structure lies along the side of a hill or valley but does not cross the valley bottom. A ridge embankment straddles the crest of a ridge, and overburden material is placed along both sides of the area. A diked embankment is constructed on nearly level terrain and can either impound fine-grained or coarse-grained material. If fines are impounded by coarser rock, the structure is considered a dike. If the embankment is homogeneous and coarse, it is termed a heap. In-pit dumps are another common type of rock pile configuration. They are just like valley-fill rock piles except that the rock is dumped in a mined-out open pit instead of a natural valley.

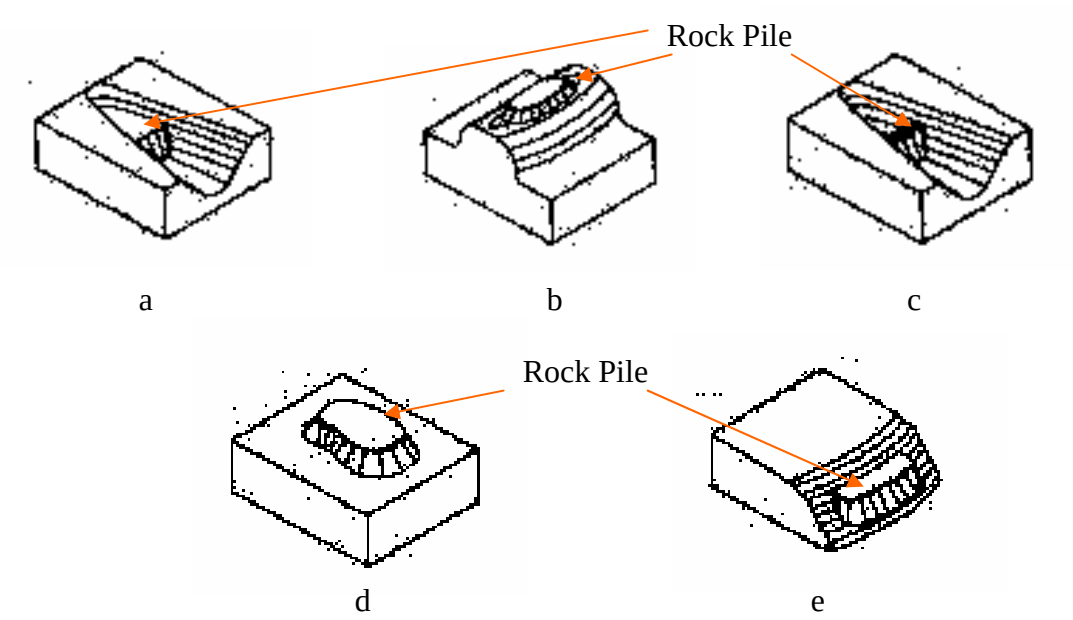

Figure 2.1: Configuration of Rock Piles Depending on Topography. (a) Valley-fill (b) Ridge, (c) Cross-valley, (d) Heaped, (e) Side-hill (Zahl et al., 1992).

The method of dumping of rock piles can also be used to classify rock piles into two main groups: end-dumped and layer-placed embankments (Robertson, 1982). End-dumped rock piles are advanced by tipping the rock from the crest of a hill and allowing it to roll down the slope and settle, with the surface and resulting layers at angle of repose and sub-parallel to the original slope. Side-hill piles are a common type of end-dumped rock piles. There is continuous raveling and sheet failure along the rock pile slope during the dumping process (McLemore et al., 2005; Robertson, 1982, 1985). End-dumping generally results in the segregation of materials with the finer-grained material at the top and coarser-grained material at the base. McLemore et al. (2005) described five zones of segregation in the Goathill North rock pile at the Questa molybdenum mine (Figure 2.2) and Nichols (1987) also recognized segregation in rock piles. Figure 2.2 illustrates the following zones in the rock pile:

1. Upper traffic surface

2. Top of the rock pile, where fines were more concentrated than coarser material

3. Intermediate zone, where material is well graded and evenly distributed

4. Toe of the rock pile, where mostly coarse material is concentrated

5. Basal rubble zone of cobbles and boulders along the contact between the rock pile and the original bedrock or colluvium.

Unlike end-dumped rock piles, layer-placed piles are constructed by dumping the rock in heaps on a level ground. The rock may be dumped by side-casting with a dragline as in coal operations. This is called dragline spoiling. New heaps are placed on old heaps

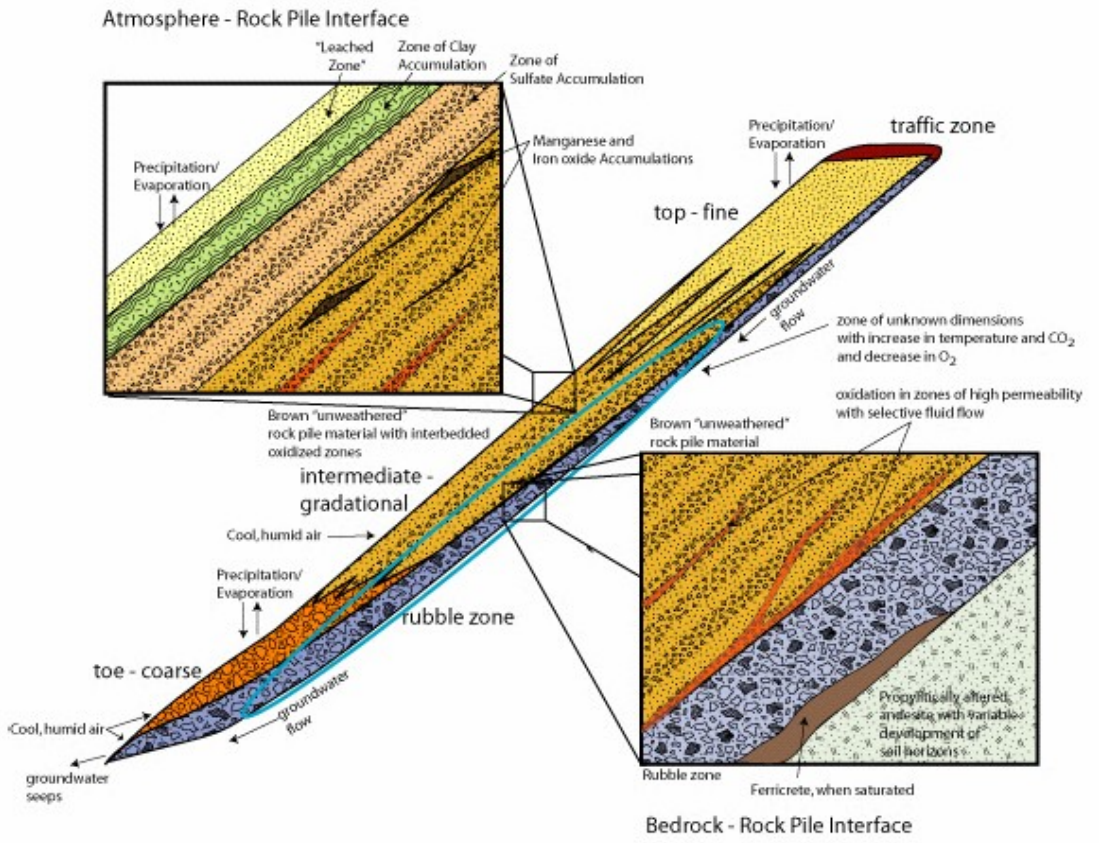

Figure 2.2: Conceptual model of an end-dumped rock pile (McLemore et al., 2005).

to make a big dump without any compaction. The more common practice in metal mines is to dump the rock with off-highway trucks, level the heaps out with bulldozers and dump more rock on the leveled heap. This method is called push-dumping and results in some level of compaction and little segregation at the traffic surfaces with coarse particles at the toe. The free-dumping method is similar to push-dumping. However, in free-dumping, the heaps are leveled, graded and compacted in smaller lifts to achieve a more compact embankment with no segregation. This method is used in the construction of tailings dam walls with mine rock. In some layer-placed piles, mine rock and tailings materials are mixed together (Quine, 1993; Shum, 1999).

2.1.2 Environmental Issues Related to Mine Rock Piles

The major environmental issues that arise from mine rock piles can be grouped into three categories namely, visual impacts and land use constraints, stability and erosion, and leaching (acid drainage). Generally, mining changes the topography and land use capabilities of the land. It is desirable that following reclamation the facility blends into or is compatible with the surrounding terrain, and that the surface of the facility be capable of a land use equivalent to or better than the original surface. This usually requires the facility surface to be stable, of gentle slope with positive drainage and with a topsoil cover layer (Robertson, 1985).

Erosion is a major mechanism for long-term dispersion of mine waste contaminants and has become an important consideration in the design of long-term reclamation for waste dumps and tailings impoundments alike (Robertson, 1985). Rock piles are eroded by

both wind (Schwendiman et al., 1980) and water (Walters, 1983). Design measures to limit erosion have been reviewed in the literature (Beedlow, 1984; Beedlow and Parker, 1985; Li et al., 1983; Nelson et al., 1983). Stability and leaching problems associated with mine rock piles are discussed separately in the following sections.

2.1.3 Mine Rock Pile Stability

The long-term stability of rock pile slopes (especially piles that are constructed by crest tipping) can decrease as a result of increase in the groundwater table due to groundwater accumulation and due to changes in the permeability of the rock pile materials resulting from weathering and the washing in of fines; and possible decrease in the pile material strength due to weathering. Changes such as these are responsible for many tragic rock pile failures, some of which are discussed in the next section. Long term stability analyses must, therefore, take into account the potential long-term strength and phreatic surface changes. (Robertson, 1985)

A rock pile failure is the uncontrolled or unscheduled release of the pile material beyond the confines of the pile (Robertson and Skermer, 1988). Pile failures are caused by disruptive actions that can be examined in two ways:

- Sudden, intense or extreme events such as floods that cause liquefaction (Hutchinson, 1988), earthquakes, volcanic action, and glaciation, which apply forces exceeding the values for which the impoundments were originally designed, and

- Slow, but perpetual actions of wind and water erosion, frost action, other forms of weathering and decomposition, chemical reaction and biological actions such as intrusion by roots, animals and man.

The various failure modes that occur in mine waste embankments have been summarized by Caldwell and Moss (1981) and others who review the methods of analysis. These failure modes are illustrated in Figure 2.3. Surface or edge slides may occur as material moves down the slope. This mode of failure is most likely to occur in crest tipped embankments. If sufficient water enters the slope and flows parallel to the face, a shallow flow slide may occur. Rock piles placed on flat ground of competent soil are least likely to fail. However, if the flat ground is covered by a thin layer of weak material, base failure may occur. If the ground is inclined, base failure is more likely to occur. This mode of failure has been experienced in both end-dumped and layer placed embankments. Block translation can occur where a dump is formed on inclined ground and the soil cover is relatively thin and weak. Unusually high water tables in the embankment, earthquakes or the decay of organic material beneath the dump may start such a failure. Circular arc failure through the dump material is most common where the dump material contains a significant percentage of fine grain soil. Similarly, a circular arc failure surface may develop through a deep foundation soil deposit of fine grained soils (Caldwell and Moss, 1981). Over the past century, there have been some rock pile failures worldwide. Table 2.2 is a summary of some of these failures.

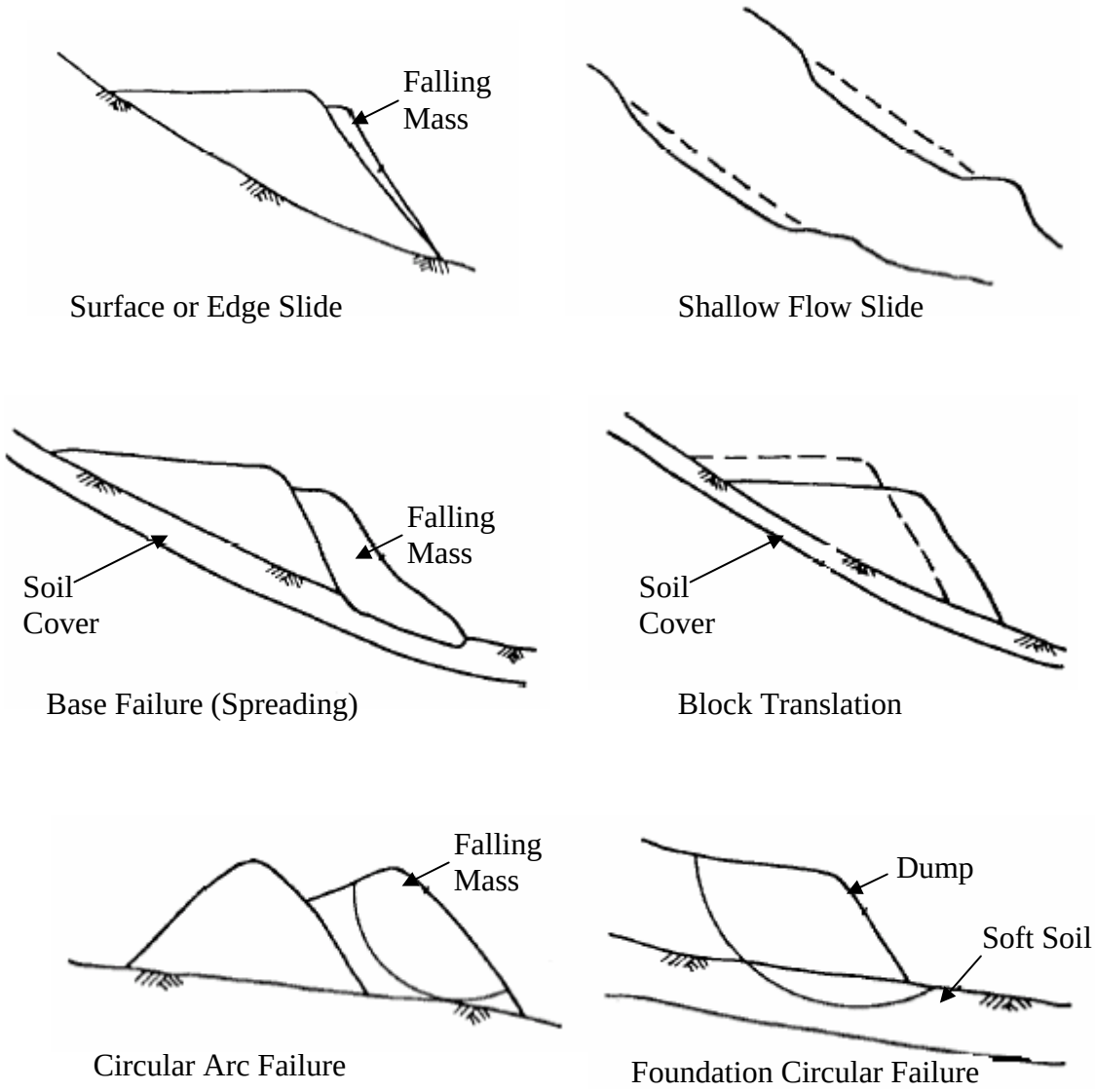

Figure 2.3: Possible Failure Modes in Mine Rock Piles (Caldwell and Moss, 1981)

Table 2.2: Some Historical Mine Rock Pile Failures

Date	Location	Description	Consequence	Reference
-	Derbyshire, UK	Flow slide of limestone dump	No fatalities	Robertson and Skermer (1988)
1961	Jupille, Belgium	Fly ash dump failure	11 fatalities and houses destroyed	Blight and Fourie (2005)
1965	Vlakfontein, South Africa	Basal slip beneath quartzite dump	No fatalities	Blight (1969)
October 21, 1966	Aberfan, South Wales	Coal mine dump failure	144 fatalities on surface, 89 miners killed underground	Blight and Fourie (2005); Johnes and McLean (1999)
1967	English China Clays, Cornwall, UK	Rapid flow	No fatalities	Robertson and Skerme (1988)
1972	Buffalo Creek, USA	Overtopping of coal dump	118 fatalities, 4000 rendered homeless and $50 million damage	Blight and Fourie (2005)
1974	Clinton Creek Asbestos, Yukon, Canada	Slope failure of rock pile due to weak foundation, thawing of foundation resulting in excess pore pressures		Robinson et al. (2005)
1982	Nye Nye, Liberia	Iron ore dump failure	200 fatalities	NCE (1982)
September 9, 1985	Quintette Marmot, BC, Canada	2.5 million m^3 coal dump failure caused by pore pressure resulting from collapse settlement	Environmental damage – river valley filled with failed material for 2.5 km	Blight and Fourie (2005); Dawson et. al. (1998)
October 26, 1989	Fording River, BC. Canada	3 million m^3 pile at 400 m height failed	Pile flowed a distance of 800 m	Dawson et al. (1998)

Table 2.2 Continued

Date	Location	Description	Consequence	Reference
May 11, 1992	Greenhills Couger No. 7, BC, Canada	Failure of 200,000 m^3 pile	Material flowed a distance of 700m	Dawson et al. (1998)
2001	Bonner, Silverton, Colorado, USA	Failure of a 19-m tall rock pile during remediation of adits	Runnout was less than 100 m	Stormont and Farfan (2005)
February 5, 2005	Newmont Gold Quarry Mine, Nevada, USA	10 million-t pile failure.	About 400 m of Nevada Route 766 was covered by pile material	Sonner (2005)

2.2 Acid Rock Drainage (ARD)

There are a number of published definitions for Acid Rock Drainage (ARD). Some of them are presented below.

> "Contaminated drainage that occurs as a result of natural oxidation of sulfide minerals contained in rock which is exposed to air and water." (Barton-Bridges and Robertson, 1989a)
>
> "The formation and movement of highly acidic water rich in heavy metals." (King, 1995)
>
> "Drainage that occurs as a result of natural oxidation of sulfide minerals contained in rock that is exposed to air and water." (American Geological Institute, 1997)
>
> "Contaminated effluent from mines and mining wastes that results from the oxidation of iron-sulfide minerals exposed to air and water." (White et al., 1999)

The formation of acid drainage and the contaminants associated with it has been described by some as the largest environmental problem facing the U.S. mining industry (Ferguson and Erickson, 1988; Lapakko, 1993; USDA Forest Service, 1993). In the

eastern U.S., more than 7,000 km of streams are affected by acid drainage from coal mines (Kim et al., 1982). In the western U.S., the Forest Service estimates that between 20,000 and 50,000 mines are currently generating acid on Forest Service lands, and that drainage from these mines is impacting between 8,000 and 16,000 km of streams (USDA Forest Service, 1993). It is also estimated that approximately 19,300 km of rivers and streams and more than 728 m^2 (180,000 acres) of lakes and reservoirs in the continental U.S. have been seriously damaged by acid drainage (Kleinmann, 1989). In addition to the acid contribution to surface waters, ARD may cause metals such as arsenic, cadmium, copper, silver, and zinc to leach from geologic materials (U.S. EPA, 1994).

As an example of the extremes to which waters can develop acidity and high metal concentrations, the analyses of four of the most acidic mine waters ever reported are shown in Table 2.3 together with the US Environmental Protection Agency's drinking water standards and measurements from other known acid drainage waters. These waters were found in the Richmond mine workings at Iron Mountain, California (Nordstrom, 1991). Note that all samples have negative pH values and metal concentrations in grams per liter. A survey of the literature indicates that only one known determination for copper, one for zinc, and one for arsenic have been found to be higher than those from the Richmond mine waters. Although these extreme values are rare, they do indicate the dramatic changes in water quality caused by natural processes and enhanced by mining activities.

Table 2.3: Comparison of four of the most acidic mine waters at Iron Mountain, California with the most acidic and metal rich mine waters reported in the world and the US EPA maximum contaminant levels (* secondary standards) for drinking water. (pH values in standard units, concentrations in g/L, except EPA standards in mg/L; n.d. = not determined, n.a. = not available) Adopted from Nordstrom and Alpers (1999) and US EPA website.

Parameter	Iron Mountain				Other Sites	EPA Standard
pH	-0.7	-2.5	-2.6	-3.6	0.67	6.5-8.5*
Cu	2.3	4.8	3.2	n.d.	48	1.3
Zn	7.7	23.5	20	n.d.	50	5.0*
Cd	0.048	0.21	0.17	n.d.	0.041	0.005
As	0.15	0.34	0.22	n.d.	0.40	0.01
Fe (total)	86.2	111	101	16.3	48	0.3*
Fe (II)	79.7	34.5	34.9	9.8	48	n.a.
SO_4	360	760	650	n.d.	209	250*

2.2.1 Cause of ARD

The oxidation of iron sulfide minerals such as pyrite and pyrrhotite is responsible for the majority of acid production by mine soils (Stumm and Morgan, 1981). Many metallic mineral deposits that form beneath the Earth's surface contain sulfide minerals. Sulfide minerals that are exposed to atmospheric oxygen or oxygenated ground waters are subjected to weathering to produce sulfuric acid (Plumlee, 1999). Bacterially catalyzed oxidation of sulfides is well known as the predominant cause of acid-rock drainage (Nordstrom and Alpers, 1999). Mining can accelerate natural processes: the development of underground workings, open pits, ore piles, mill tailings, and spoil heaps and the extractive processing of ores can enhance the likelihood of releasing chemical elements to the surrounding area in large amounts and at increased rates relative to unmined areas (King, 1995). It is important to note, however, that pyrite (or sulfide) oxidation also occurs in the absence of mining and there are numerous localities

world-wide where naturally acidic waters containing high concentrations of metals are known (Runnells et al., 1992).

2.2.2 Pyrite Oxidation

Acid rock drainage occurs where sulfides in rock oxidize resulting in reduction in pH of infiltrating water and possible leaching of metals (Broughton and Robertson, 1991). Table 2.4 is a list of summarized versions of some common chemical reactions that generate acidity in natural environments. The majority of acid drainage problems have been attributed to pyrite oxidation because pyrite is the dominant gangue sulfide mineral in many rock piles worldwide (Blowes and Jambor, 1990) and the least resistant to oxidation. There is a great deal of literature on the subject of ARD (e.g. Evangelou, 1995; Goldhaber, 1983; Lowson, 1982; McKibben and Barnes, 1986; Moses and Herman, 1991; Moses et al., 1987; Nordstrom, 1982).

Table 2.4: Examples of sulfide oxidation reactions and other mineral dissolution reactions that may generate acid. (n.a. = not available) (Nordstrom and Alpers, 1999; Plumlee, 1999) The reactions depicted are idealized, and likely do not represent the appropriate reaction products for the entire range of ambient chemical conditions.

Mineral	Formula	Acid generation/consuming reaction	Moles acid
Pyrite	FeS_2	$FeS_2 + 3.5O_2 + H_2O = Fe^{2+} + 2SO_4^{2-} + 2H^+$	2
		$FeS_2 + 3.75O_2 + 0.5H_2O = Fe^{3+} + H^+ + 2SO_4^{2-}$	1
		$FeS_2 + 3.75O_2 + 3.5H_2O = 2SO_4^{2-} + 4H^+ + Fe(OH)_{3(s)}$	4
		$FeS_2 + 14Fe^{3+} + 8H_2O = 15Fe^{2+} + 2SO_4^{2} + 16H^+$	16
Pyrrhotite	$Fe_{1-x}S$	$x = 0.1$: $Fe_{0.9}S + 1.95O_2 + 0.1H_2O = 0.9Fe^{2+} + SO_4^{2-} + 0.2H^+$	0.2
		$x = 0.1$: $Fe_{0.9}S + 2.175O_2 + 0.7H^+ = 0.9Fe^{3+} + SO_4^{2-} + 0.35H_2O$	-0.7
		$x = 0.1$: $Fe_{0.9}S + 2.175O_2 + 2.35H_2O = SO_4^{2-} + 2H^+ + 0.9Fe(OH)_{3(s)}$	2
		$x = 0.1$: $Fe_{0.9}S + 7.8Fe^{3+} + 4H_2O = 8.7\ Fe^{2+} + SO_4^{2-} + 8H^+$	8

Table 2.4 continued.

Mineral	Formula	Acid generation/consuming reaction	Moles acid
Sphalerite Covellite Galena	ZnS CuS PbS	$MS + 2O_2 = M^{2+} + SO_4^{2-}$ (M = Zn, Cu, Pb)	0
		$MS + 8Fe^{3+} + 4H_2O = M^{2+} + 8Fe^{2+} SO_4^{2-} + 8H^+$	8
Galena	PbS	$PbS + 2O_2 = PbSO_4$ (anglesite)	0
		$PbS + 0.5O_2 + 2H^+ = Pb^{2+} + H_2O + S^0$ (native sulfur)	-2
Chalcopyrite	$CuFeS_2$	$CuFeS_2 + 4O_2 = Cu^{2+} + Fe^{2+} + 2 SO_4^{2-}$	0
		$CuFeS_2 + 16Fe^3 + 8H_2O = Cu^{2+} + 17Fe^{2+} + 2SO_4^{2-} + 16H^+$	16
Enargite	Cu_3AsS_4	$Cu_3AsS_4 + 8.75O_2 + 2.5H_2O = 3Cu^{2+} + HAsO_4^{2-} + 4SO_4^{2-} + 4H^+$	4
		$Cu_3AsS_4 + 35Fe^3 + 20H_2O = 3Cu^{2+} + 35Fe^{2+} + HAsO_4^{2-} + 4SO_4^{2-} + 4SO_4^{2-} + 39H^+$	39
Arsenopyrte	FeAsS	$FeAsS + 3.25O_2 + 1.5H_2O = Fe^{2+} + HAsO_4^{2-} + SO_4^{2-} + 2H^+$	2
		$FeAsS + 3.5O_2 + H_2O = Fe^{3+} + HAsO_4^{2-} + SO_4^{2-} + H^+$	1
		$FeAsS + 13Fe^3 + 8H_2O = 14Fe^{2+} + HAsO_4^{2-} + SO_4^{2-} + 15H^+$	15
		$FeAsS + 3.5O_2 + 3H_2O = SO_4^{2-} + 2H^+ + FeAsO_4.2H_2O$ (scorodite)	2
Native Sulfur	S^o	$S^o + H_2O + 1.5\ O_2 = 2H^+ + SO_4^{2-}$	2
Realgar	AsS	$AsS + 2.75O_2 + 2.5H_2O = HAsO_4^{2-} + SO_4^{2-} + 4H^+$	4
		$AsS + 11Fe^{3+} + 8H_2O = 11Fe^{2+} + HAsO_4^{2} + SO_4^{2-} + 15H^+$	15
Siderite	$FeCO_3$	$FeCO_3 + H^+ = Fe^{2+} + HCO_3^-$	-1
		$FeCO_3 + 2H^+ + 0.25O_2 = Fe^{3+} + 0.5H_2O + HCO_3^-$	-2
		$FeCO_3 + 0.25O_2 + 2.5H_2O = Fe(OH)_3 + H^+ + HCO_3^-$	1
Alunite	$KAl_3(SO_4)_2(OH)_6$	$KAl_3(SO_4)_2(OH)_6 + 6H^+ = K^+ + 3Al^{3+} + 2SO_4^{2-} + 6H_2O$	-6
		$KAl_3(SO_4)_2(OH)_6 + 3H_2O = K^+ + 3Al(OH)_3 + 2SO_4^{2-} + 3H^+$	3

The chemical reaction responsible for the formation of acid waters requires three basic ingredients: pyrite, oxygen and water (Nordstrom and Alpers, 1999), and bacteria catalyze the process. The overall reaction is often written as:

$$FeS_{2(s)} + 3.75\ O_{2(g)} + 3.5\ H_2O_{(l)} = Fe(OH)_{3(s)} + 2\ H_2SO_{4(aq)} \quad (2.1)$$

where one mole of ferric hydroxide and 2 moles of sulfuric acid are produced for every mole of pyrite oxidized.

When pyrite oxidizes there are two species that can oxidize: the ferrous iron and the sulfidic sulfur. In studies on acid waters and pyrite oxidation, it has long been recognized that iron easily leaches out of pyrite but tends to stay in the ferrous state in acid solutions. Historical information indicates the production of ferrous sulfate and sulfuric acid from washing of pyritiferous ores and shales (Nordstrom and Alpers, 1999). Hence, another common representation of the pyrite oxidation reaction is:

$$FeS_{2(s)} + 3.5\ O_{2(g)} + H_2O_{(l)} = Fe^{2+}_{(aq)} + 2\ SO_4^{2-}{}_{(aq)} + 2\ H^{+}_{(aq)} \quad (2.2)$$

The sulfur moiety in pyrite oxidizes more quickly than the iron, but it must transfer a large number of electrons (14 times as many as iron per mole of pyrite) (Nordstrom and Alpers, 1999). Consequently, there are several possible side reactions and sulfur intermediates that may occur during oxidation. Two such side reactions that are documented are the formation of elemental sulfur (Bergholm, 1955; Clarke, 1966; Stokes, 1901); and the formation of intermediate sulfoxyanions of lower oxidation state than that found in sulfate: i.e. thiosulfate ($S_2O_3^{2-}$), polythionates ($S_nO_6^{2-}$), and sulfite (SO_3^{2-}) (Goldhaber, 1983; Granger and Warren, 1969; Moses et al., 1987; Steger and Desjardins, 1978; Williamson and Rimstidt, 1993).

Aside oxidation of pyrite by oxygen, it is also known that ferric iron rapidly oxidizes pyrite (Stokes, 1901). Experiments carried out by Garrels and Thompson (1960) and McKibben and Barnes (1986) have confirmed the balanced reaction stoichiometry:

$$FeS_{2(s)} + 14\ Fe^{3+}_{(aq)} + 8\ H_2O_{(l)} = 15\ Fe^{2+}_{(aq)} + 2\ SO_4^{2}{}_{(aq)} + 16\ H^{+}_{(aq)} \quad (2.3)$$

for the oxidation of pyrite by aqueous ferric ions. This reaction is considerably faster than the reaction with oxygen as the oxidant (Equation 2.2), but significant concentrations of oxidized iron only occur at low pH values because of the low solubility of hydrolyzed ferric iron at near-neutral pH values. Hence, it is thought that pyrite oxidation is initiated by oxygen at near-neutral pH (Equation 2.2), but as pH values reduce to about 4, the rate of oxidation becomes governed by Equation 2.3. Oxygen is still required to replenish the supply of ferric iron according to

$$Fe^{2+}_{(aq)} + 0.25\ O_{2(g)} + H^{+}_{(aq)} = Fe^{3+}_{(aq)} + 0.5\ H_2O_{(l)} \quad (2.4)$$

but the oxygen does not have to diffuse all the way to the pyrite surfaces. It is quite possible for pyrite to oxidize in the absence of dissolved oxygen. Nevertheless, the overall rate of pyrite oxidation in a rock pile will largely be determined by the overall rate of oxygen transport (advection and diffusion) (Nordstrom and Alpers, 1999).

2.2.3 Factors Influencing ARD

The acidity and dissolved constituents of acid drainage depends on the nature and reactivity of the sulfides involved, the chemical constituents of the host rock and the physical and chemical controls limiting the rates of oxidation and leaching (Broughton

and Robertson, 1991); the availability of oxygen and water, bacterial activity, temperature and pH (Barton-Bridges and Robertson, 1989b). This subsection discusses some of these factors that control the generation of acid drainage in the field.

Acid-Generating Minerals

The amount of acid generated by sulfide oxidation is a complex function of the sulfide minerals present in the rock, their resistance to weathering, whether the sulfides contain iron, whether oxidized or reduced metal species are produced by the oxidation, whether other elements such as arsenic are major constituents of the sulfides, whether oxygen or aqueous ferric iron is the oxidant, and whether hydrous metal oxides or other minerals precipitate as a result of the oxidation process (Plumlee, 1999). Table 2.5 is a list of some sulfide minerals in order of their relative resistance to oxidation. Grain size, texture and trace element content can substantially shift the relative resistance of the different sulfide minerals; for example, trace element-rich botryoidal pyrite and marcasite generally oxidize much more rapidly than coarse, euhedral sphalerite (Plumlee, 1999).

Iron sulfides (pyrite, FeS_2; marcasite, FeS_2; pyrrhotite, $Fe_{1-x}S$), sulfides with metal/sulfur ratios less than 1, and sulfosalts such as enargite (Cu_3AsS_4), generate acid when they react with oxygen and water. Other sulfides with metal/sulfur ratios equal to 1, such as sphalerite (ZnS), galena (PbS), and chalcopyrite ($CuFeS_2$) tend not to produce acid when oxygen is the oxidant. However, as mentioned in the previous section with respect to pyrite, aqueous ferric iron is a very aggressive oxidant that, when it reacts with sulfides, generates significantly greater quantities of acid, and more rapidly, than

Table 2.5: Factors affecting resistance of sulfide minerals to oxidation, listed in order of increasing resistance from top to bottom of table (Plumlee, 1999)

Mineralogy	Grain Size	Texture	Trace Element Content	Resistance to Oxidation
Pyrrhotite	Fine	Framboidal	High	Low
Chalcocite		Colloform		
Galena				
Sphalerite		Botryoidal		
Arsenopyrite				
Pyrite	Medium			Medium
Enargite		Massive		
Marcasite				
Bornite				
Chalcopyrite				
Argentite				
Cinnabar				
Molybdenite	Coarse	Euhedral	Low	High

are generated by oxygen-driven oxidation alone (Nordstrom and Alpers, 1999). Thus, because of their role in producing aqueous ferric iron, the amounts of iron sulfides present in a mineral assemblage play a crucial role in determining whether acid will be generated during weathering. In general, sulfide-rich mineral assemblages with high percentages of iron sulfides or sulfides having iron as a constituent (such as chalcopyrite or iron-rich sphalerite) will generate significantly more acidic waters than sphalerite- and galena-rich assemblages without iron sulfides (Plumlee, 1999).

Precipitation of hydrous oxides during the sulfide oxidation process can also lead to the formation of acid. In fact, some non-sulfide minerals such as siderite ($FeCO_3$) and alunite ($KAl_3(SO_4)_2(OH)_6$) can locally generate acid during weathering if hydrous iron or aluminum oxides precipitate (Table 2.4) (Plumlee, 1999).

Acid-Consuming Minerals

In most mineral deposits, acid-generating sulfide minerals are either intergrown with or occur in close proximity to a variety of carbonate and aluminosilicate minerals that can react with and consume acid generated during sulfide oxidation. However, like the sulfides, the ease and rapidity with which these minerals can react with acid varies substantially (Plumlee, 1999). The balance between the rates of acid production by iron-sulfide mineral oxidation and host rock buffering will determine the acidity of the mine drainage (White et al., 1999).

The most effective minerals for neutralizing acid are those containing calcium carbonate and magnesium carbonate such as calcite ($CaCO_3$), magnesite ($MgCO_3$), dolomite ($CaMg(CO_3)_2$) and ankerite ($CaFe(CO_3)_2$) (White et al., 1999). Equations 2.5 and 2.6 represent the dominant dissolution reaction of calcite with acid above pH 6.4 and below pH 6.4 respectively (Drever, 1997). The dissolution rates for the calcite reactions shown are relatively rapid (White et al., 1999).

$$CaCO_{3(s)} + H^{+}_{(aq)} = HCO_3^{-}{}_{(aq)} + Ca^{2+}_{(aq)} \quad (2.5)$$

$$CaCO_{3(s)} + 2H^{+}_{(aq)} = H_2CO_{3(aq)} + Ca^{2+}_{(aq)} \quad (2.6)$$

Dissolution of silicates such as plagioclase-feldspar minerals like anorthite (Equation 2.7) (Busenberg and Clemency, 1976) and olivine minerals like forsterite (Equation 2.8) (Hem, 1970) can also neutralize acid under acidic conditions, but their dissolution rates (and subsequent acid neutralization) are slow relative to the carbonate minerals.

$$CaAl_2Si_2O_{8(s)} + 2H^+_{(aq)} + H_2O = Ca^{2+}_{(aq)} + Al_2Si_2O_5(OH)_{4(s)} \quad (2.7)$$

$$Mg_2SiO_{4(s)} + 4H^+_{(aq)} = 2Mg^{2+}_{(aq)} + H_4SiO_{4(aq)} \quad (2.8)$$

The effectiveness of silicate-mineral neutralization is thought to be optimized when the acid production rate is relatively slow; feldspar minerals comprise a significant percentage of the overall mineralogy; and the available silicate-mineral surface area is large (Morin and Hutt, 1994).

Microbially-Catalyzed Sulfide Oxidation

It was first suggested in the early 1900's that pyrite oxidation and the consequent acid drainage from coal deposits may be catalyzed by bacteria (Carpentor and Herndon, 1933; Powell and Parr, 1919). In the mid 1900's scientists showed that microbial degradation of pyrite was an important factor in the production of acid waters (Colmer and Hinkle, 1947; Colmer et al., 1950; Temple and Colmer, 1951; Temple and Delchamps, 1953). Bacteria have been shown to increase the ferrous iron oxidation rate by 10^5 over the abiotic rate, from about 3×10^{-12} mol L^{-1} s^{-1} to about 3×10^{-7} mol L^{-1} s^{-1} (Singer and Stumm, 1968, 1970a, b). Some of the bacteria that are known to catalyze pyrite oxidation are *Thiobacillus thiooxidans* and *Thiobacillus ferrooxidans* (Mills, 1999). A study of the types of bacteria populations in the Goathill North rock pile is being undertaken as part of the rock pile weathering project.

Physical Factors

Since pyrite oxidation depends on the availability of oxygen and water, physical factors that control the accessibility of these weathering agents to the pyrite grains will also influence the rate of pyrite oxidation and acid-generation. Some of the physical factors that influence acid drainage generation are geology (geomorphology, structure, petrology, geophysical features), hydrology (water budget, porosity, permeability, flow direction, flow rate, dispersion, mixing, surface transport characteristics), and the effects of mining and mineral processing (Nordstrom and Alpers, 1999).

2.2.4 Effects of ARD on Weathering

There is considerable evidence in the literature to prove that acidic waters increase the rate of chemical weathering of rock-forming minerals. The presence of readily weathered sulfides in a mineral assemblage can increase the reactivity of other, less readily weathered sulfides due to the formation of corrosive acids (Plumlee, 1999). Plumlee (1999) observed monominerallic bornite that had remained unoxidized after 20 years of mining on one side of a mine drift. On the other side of the mine drift, bornite intergrown with reactive marcasite had undergone extensive oxidation to secondary copper sulfate salts. The acid generated by marcasite oxidation had triggered the breakdown of the more resistive bornite (Plumlee, 1999). Similar observations have been made in a weathering massive sulfide deposit, where the abundance of readily weatherable pyrrhotite in the deposit could be directly correlated with the rate at which the intergrown sphalerite and pyrite oxidized (Boyle, 1994).

The high concentrations of metals in acidic waters have been used as an indication of weathering of rock-forming minerals and a number of researchers have used this concept with mass-balance calculations to determine the minerals and weathering processes controlling drainage chemistry in water basins. Examples of such studies are those conducted on the Sierra Nevada Springs in California and Nevada (Garrels and Mackenzie, 1967); the Mackenzie River system in Canada (Reeder et al., 1972); and the Amazon River in Brazil (Gibbs, 1967, 1970, 1972; Stallard, 1985; Stallard and Edmond, 1981, 1983, 1987). Laboratory testing of pore waters extracted from soil samples collected in the Montagne des Aiguilettes in the Beaujolais (Rhoˆne, France) showed a convincing negative correlation between log [Si] and pH, indicating that active, in situ chemical weathering of silicates may be proton promoted (Gerard et al., 2003). In general, the evidence in the literature suggests that higher levels of ARD are indicative of both more advanced stages of weathering and greater rates of future weathering.

2.3 Prediction of Acid Rock Drainage

Numerous laboratory procedures have been developed over the last 30 years for predicting acid rock drainage and potential weathering rates of geologic materials. These predictive tools have been grouped into static and kinetic tests (e.g. Bethune et al., 1997; U.S. EPA, 1994; White et al., 1999). Some of the different predictive tests are discussed in this section.

2.3.1 Static Test Methods

Static tests are short term (usually measured in hours or days) and relatively low cost. Their objective is to provide an estimate of a sample's capacity to produce acid and its capacity to neutralize acid. One shortcoming of static tests is that they measure only the capacities for acid production and consumption and do not consider the differences between the respective dissolution rates of acid-producing and acid-consuming minerals. Another potential source of error inherent to static-test-data interpretation is the assumption that all acid-producing and acid-consuming minerals present will react completely, an assumption which ignores the influence of acid-producing and acid-consuming mineral particle-size and morphology (White et al., 1999). The most commonly used static test is known as acid-base accounting (ABA) (Ferguson and Erickson, 1988). Other static tests are the paste pH test (Sobek et al., 1978) and the Net Acid Generation (NAG) test (White et al., 1999).

Acid-Base Accounting

Several variations of the ABA test are in use in the United States and Canada (Lapakko, 1992) and five of them are compared in Table 2.6. The standard ABA method for determining NP, and the hydrogen peroxide method for AP were used in this study and the procedures are presented in detail in Chapter 3.

ABA measures the balance between the acid-producing potential (AP) and acid-neutralizing potential (NP) of each sample. Generally, AP is determined by sulfur assay using either total sulfur or sulfide sulfur content to estimate the quantity of acid-producing minerals present (Lapakko, 2002). The total sulfur content will overestimate the actual AP of samples containing substantial non acid-producing sulfate minerals

Table 2.6: Summary of acid-base accounting test methods and their advantages and disadvantages. Modified from US EPA (1994)

Acid Base Accounting (Smith et al., 1974; Sobek et al., 1978)	Modified Acid Base Accounting (Coastech Research Inc., 1989; Lawrence, 1990)	BC Research Initial (Bruynesteyn and Duncan, 1979; Duncan and Walden, 1975)	Alkaline Production Potential: Sulfur (Caruccio et al., 1981; Coastech Research Inc., 1989)	Acid Potential with H_2O_2 (Cruywagen et al., 2003; Smith et al., 1974; Sobek et al., 1978)
Acid Production Determination				
Acid potential = 31.25 * Total S	Acid Potential = 31.25 * Sulfide S	Total Acid = 31.25 * Total S	Total S used as indicator but AP is not calculated	Sample is leached with HCl, oxidized with 30% H_2O_2 and titrated to pH 7.0.
Neutralization Potential Determination				
-60 mesh (0.24 mm) sample Add HCl as indicated by fizz test, boil one minute than cool Titration endpoint pH 7.0	-60 mesh (0.24 mm) sample Add HCl as indicated by fizz test, agitate for 24 hours at room temperature pH 1.4 - 2.0 required after six hours agitation Titration endpoint pH 8.3	-400 mesh (0.038 mm) sample Titrate sample to pH 3.5 with 1.0 N H_2SO_4	-0.023 mm sample 20 mL 0.1 N HCl to 0.4g solid for 2 hours at room temperature Titration endpoint pH 5.0	Does not determine NP
Advantages And Disadvantages				
May overestimate AP and/or NP	May underestimate AP and /or NP. Takes more steps to determine AP.	Requires automatic titrator. More time-consuming.	May underestimate NP.	Determines actual reactive S. Does not require furnace. More time-consuming.

(e.g. barite and gypsum). On the other hand, the sulfide-sulfur measurement will underestimate the actual AP of samples containing substantial acid-producing sulfate minerals (e.g. melanterite and jarosite). Knowledge of the material's sulfate mineralogy will indicate if the sulfate minerals present, if any, are acid producing and allow selection of the more appropriate AP quantification (Lapakko, 2002). The AP value is calculated based on the assumption that two moles of acid will be produced for each mole of sulfur present (equation 2.1).

Because one mole of calcium carbonate will neutralize the two moles of acid (equation 2.6), the percent sulfur obtained from the sulfur assay is multiplied by 31.25 to yield AP in units of tonnes calcium carbonate equivalent per thousand tonnes of material or kg calcium carbonate equivalent per tonne of material (White et al., 1999). NP is generally determined by subjecting the sample to some form of acid digestion and represents the amount of acid-neutralizing carbonate minerals present in the sample (Kleinmann, 2001; White et al., 1999). The NP value is reported in the same units as the AP value.

Net-neutralizing potential (NNP), which is the difference between AP and NP (NP – AP = NNP), is one of the measurements used to classify a sample as potentially acid or non-acid producing (White et al., 1999) and is also called the "acid-base account" of the sample. The value for NNP may be either positive or negative (U.S. EPA, 1994). Recent ABA classifications have also used the ratio of NP to AP (NP/AP) to classify samples (i.e. if NP > AP, then NP/AP > 1; conversely, if NP < AP, then NP/AP < 1) (White et al., 1999).

Paste pH

Perhaps the most commonly measured soil characteristic is pH (Sobek et al., 1978). Although pH was originally defined by the Danish biochemist, S.P.L. Sorensen, as the negative logarithm of the concentration of hydrogen ions in 1909, the hydrogen-ion activity is measured instead of hydrogen-ion concentration (Sobek et al., 1978). Paste pH is the pH measured on a mixture of soil and deionized water which forms a slurry or paste. A known volume of deionized water is added to a known mass, or volume, of soil of a given particle size and stirred to form the paste. A calibrated pH meter with an electrode is used to measure the paste pH. The ratio of sample to deionized water is commonly 1:1 (mass of soil in grams to volume of deionized water in mL).

Six common factors that affect the measurement of paste pH are the dryness of the sample before testing; the soil:water ratio used; soluble salts content; seasonally influenced carbon-dioxide content; the size of the soil particles; and electrode junction potential (Jackson, 1958; Peech, 1965). Paste conductivity, redox potential and total dissolved solids (TDS) are other measurements that are usually done alongside paste pH in mine site characterization programs (e.g. McLemore et al., 2005; Shaw, 2000; Shaw et al., 2002; Wagner and Harrington, 1995). A detailed description of the paste pH and conductivity test procedure used in this work may be found in Chapter 3.

Net Acid Generation (NAG) Test

The static NAG test is based on hydrogen peroxide oxidation procedure developed for determining the pyrite content of coal overburden (Finkleman and Giffin, 1986). It

measures the net acid remaining, if any, after complete oxidation of the material with hydrogen peroxide and allowing complete reaction of the acid formed with the neutralizing components of the materials (Lewis et al., 1997). After neutralization is complete, the remaining H_2SO_4, if any, is titrated with NaOH. The amount of NaOH needed is expressed as kg of $CaCO_3$ equivalents per ton of material and is equal to the NAG of the material. Non-acid forming materials have a NAG = 0 whereas potentially acid forming materials have a NAG > 0 (Lewis et al., 1997). The NAG and ABA tests are often used together in predicting acid drainage (e.g. Andrina et al., 2003; Fines et al., 2003; Miller et al., 2003; Tran et al., 2003b; Williams et al., 2003). Details of the NAG test procedure are presented in Chapter 3.

2.3.2 Interpretation of Static Test Results

The interpretation of ABA results as presented in the literature is very variable. Different researchers have classified mine materials (as acid generating, non-acid-generating or uncertain) differently using static test results (Brodie et al., 1991; Day, 1989; Ferguson and Morin, 1991; Morin and Hutt, 1994). As an example of the diversity of static test results interpretation, Table 2.7 is a summary of different criteria for interpreting static test results for different applications. Considering the level of inconsistency presented by the interpretation of ABA and other static test results, Perry (1998) concludes that a universal ABA criterion for separating acid and alkaline producing rocks does not exist. The lack of universal criteria is not surprising since mine drainage quality is a product of the interaction of many geologic, hydrologic, climatic, and mining factors (Perry, 1998). For metal mines, it has been suggested that

ABA criteria are site specific and mineral dependent (Miller and Murray, 1988; Morin and Hutt, 1994).

Table 2.7: Summary of some suggested criteria for interpreting static test results developed for classification of individual rock samples. (Perry, 1998)

Criteria	Application	Reference
Rocks with NNP less than -5 kg $CaCO_3$/ton are considered potentially toxic.	Coal overburden rocks in northern Appalachian basin for root zone media in reclamation; mine drainage quality.	(Skousen et al., 1987; Smith et al., 1976; Smith et al., 1974; Surface Mine Drainage Task Force, 1979)
Rocks with paste pH less than 4.0 are considered acid toxic.	Coal overburden rocks in northern Appalachian basin for root zone media, mine drainage quality. Base and precious metal mine waste rock in Australia and southeast Asia.	(Smith et al., 1976; Smith et al., 1974; Surface Mine Drainage Task Force, 1979) (Miller and Murray, 1988)
Rocks with greater than 0.5% sulfur may generate significant acidity.	Coal overburden rocks in northern Appalachian basin, mine drainage quality. Base and precious metal mine waste rock in Australia and southeast Asia.	(Brady and Hornberger, 1990) (Miller and Murray, 1988)
Rocks with NP greater than 30 kg $CaCO_3$/ton and "fizz" are significant sources of alkalinity.	Coal overburden rocks in northern Appalachian basin, mine drainage quality.	(Brady and Hornberger, 1990)
Rocks with NNP greater than 20 kg $CaCO_3$/ton produce alkaline drainage.	Coal overburden rocks in northern Appalachian basin. Base and precious metal mine waste rock and tailings in Canada.	(Skousen et al., 1987) (British Columbia AMD Task Force, 1989; Ferguson and Morin, 1991)
Rocks with NNP less than -20 kg $CaCO_3$/ton produce acid drainage.	Base and precious metal mine waste rock and tailings in Canada.	(British Columbia AMD Task Force, 1989; Ferguson and Morin, 1991)
NP/AP ratio less than 1 likely results in acid drainage.	Base and precious metal mine waste rock and tailings in Canada.	(Ferguson and Morin, 1991; Patterson and Ferguson, 1994)

Table 2.7 continued.

Criteria	Application	Reference
Rocks with NNP greater than 0 kg $CaCO_3$/ton do not produce acid. Tailings with NNP less than 0 kg $CaCO_3$/ton produce acid drainage.	Base and precious metal mine waste rock and tailings in Canada.	(Ferguson and Morin, 1991; Patterson and Ferguson, 1994)
NP/AP ratio is classified as less than 1, between 1 and 2, and greater than 2.	Base and precious metal mine waste rock and tailings in Canada.	(Ferguson and Robertson, 1994)
Theoretical NP/AP ratio of 2 is needed for complete acid neutralization.	Coal overburden rocks in northern Appalachian basin, mine drainage quality.	(Cravotta et al., 1990)
Use actual NP and AP values as well as ratios to account for buffering capacity of the system	Base metal mine overburden rock, United States.	(Filipek et al., 1991)

Environmental Geochemistry International of Australia uses NAG results to group samples into three categories as in Table 2.8. This criterion is also used by Miller (1999). The value of 5 can range up to 10 depending on site-specific factors (Miller, 1999). To better characterize samples based on static tests, NAG and ABA results can be compared to assess the level of agreement between the two tests (e.g. Miller, 1999). It is expected that samples with lower NNP results will have lower NAG pH and higher NAG values.

Table 2.8: Interpretation of NAG results (Environmental Geochemistry International, 2004)

NAGpH	NAG (kg $CaCO_3$/t)	Acid Potential of Sample
≥ 4.5	0	Non-acid forming (NAF)
< 4.5	≤ 5	Potentially acid forming – lower capacity (PAF-LC)
< 4.5	> 5	Potentially acid forming (PAF)

Kinetic Tests

Kinetic tests are long-term (usually measured in months and sometimes years) and expensive. Their objectives are to confirm or reduce uncertainty in static-test classifications (i.e. whether a sample is acid or non-acid producing), identify dominant chemical weathering reactions, and determine acid-generation rates and temporal variations in leachate water quality. This is accomplished by accelerating the natural weathering rate of a sample under closely controlled laboratory conditions (Lapakko, 1988; Lawrence, 1990; White and Jeffers, 1994). One shortcoming of kinetic tests is the extended amount of time required to perform the tests, as it is not uncommon for these tests to continue for at least 29 weeks (e.g. Lapakko and Wessels, 1995). Kinetic test methods are widely discussed in the literature (e.g. EPA and Hardrock Mining, 2003; Lapakko, 2002; U.S. EPA, 1994) and six common types are compared in Table 2.9.

Table 2.9: Summary of kinetic test methods and their advantages and disadvantages. Adopted from US EPA (1994)

Humidity Cells (Sobek et al., 1978)	Soxhelet Extraction (Singleton and Lavkulich, 1978; Sullivan and Sobek, 1982)	Column Tests (Bruynesteyn and Hackl, 1982; Hood and Oertel, 1984)
Summary of Test Method		
-2.38 mm particle size 200g of rock exposed to three days dry air, three days humidified air, and rinsed with 200 mL on day seven	Particle size not presented T=70 C T=25 C Water passed through sample is distilled and recycled through sample	Variable particle size Columns containing mine waste are leached with discrete volumes of recirculating solutions

Table 2.9 continued

Humidity Cells	Soxhelet Extraction	Column Tests
Advantages and Disadvantages		
Models AP and NP well and models wet/dry conditions. Approximates field conditions and rate of acidity per unit of sample.	Simple, results in short time, and assessment of interaction between AP and NP.	Models AP and NP, models effect of different rock types, models wet/dry, and models different grain sizes.
Moderate to use, results take long time. Need special equipment. Moderate ease of interpretation. Large data set generated.	Moderate to use and need special equipment. Moderate interpretation in developmental stage. Relationship to natural processes not clear.	Difficult interpretation, not practical for large number of samples. Large volume of sample used, lots of data generated, long time, and potential problems: uneven leachate application, channelization.

BC Research Confirmation (Duncan and Walden, 1975)	Batch Reactor (Halbert et al., 1983)	Field Tests (Edgar and Lapakko, 1985)
Summary of Test Method		
-400 mesh particle size. 15-30g added to bacterially active solution at pH 2.2 to 2.5, T=35^{o}C. If pH increases, sample is non acid producer, if pH decreases, 1/2 original sample mass is added in each of two increments.	-200 mesh particle size. Sample/water slurry is agitated 200g/500 mL.	Field scale particles. 800 to 1300 metric ton test piles constructed on liners, flow and water quality data collected, tests began in 1977 and are ongoing
Advantages and Disadvantages		
Simple to use, low cost, assesses potential for biological leaching. Moderate to use, longer time needed, and some special equipment needed. Difficult interpretation if pH change is small, does not model initial AP step, and long time for pH to stabilize.	Able to examine many samples simultaneously and relatively simple equipment. Subject to large sampling errors and lack of precision.	Uses actual mine material under environmental conditions. Can be used to determine drainage volume. Mitigation methods can be tested. Expensive initial construction. Long time.

2.3.3 Mine Rock Pile Characterization

The environmental problems posed by mine rock piles have made it necessary for rock piles to be characterized. A typical rock pile characterization program involves field and laboratory measurements to determine the physical, hydrological, geological geochemical and geotechnical properties of the pile as a whole and/or the materials within it. Rock pile characterization programs have been carried out in a number of mines worldwide for reasons such as preparing Environmental Impact Statements (EIS), predicting acid drainage potential, predicting pile failure, and identifying suitable remediation methods and mine closure plans. Also, some characterization programs have been done during deconstruction of rock piles because of the opportunity to examine the interior of the rock piles without expensive drilling programs. Table 2.10 is a summary of some rock pile characterization programs that have been conducted using acid drainage prediction tools: some of these characterization programs also included physical, geotechnical and hydrological investigations which are not mentioned in Table 2.10. A summary of static test results reported for some mine rock piles is presented in Table 2.11.

Questa Rock Piles Characterization

The rock piles at the Questa molybdenum mine in New Mexico have been characterized by several research and consulting organizations with several different tools and objectives. Robertson GeoConsultants Inc. (RGC) carried out a drilling, instrumentation and monitoring project to determine the static geochemical characteristics of the material in four of the rock piles; the current location of the oxidation, acid and

Table 2.10: Summary of some rock pile characterization programs using static and kinetic test methods. ABA = acid base accounting, ABCC = acid-buffering characteristic curve; AP = acid potential; ARD = acid rock drainage; INAP = International Network for Acid Prevention, NAG = net acid generation; NAPP = net acid producing potential, NNP = net neutralization potential; NP = neutralization potential; TDS = total dissolved solids.

Site or Project	Location	Objective	Tools	Summary Results/Conclusion
Zortman and Landusky Mines (Miller and Hertel, 1997; Shaw, 2000; Shaw et al., 2000)	Phillips County, Montana	To identify contaminant loads and prioritize reclamation schemes	Paste pH, modified ABA, forward acid titration, multi-element ICP	Paste pH and NNP ranges: 4.9 to 6.3, and 0.9 to 1.3 for Zortman; 5.9 to 8.7, and -8.9 to 215.4 for Landusky
INAP Rock Pile Characterization Project (Fines et al., 2003; Tran et al., 2003a; Tran et al., 2003b)	Site 1 in South Carolina, USA and Site 2 in Sudbury Ontario, Canada	Opportunity to characterize rock piles during relocation of the piles to pit	Paste pH, ABA, NAG, kinetic and sequential NAG, ABCC, multi-element scan and mineralogical analysis	Site 1 samples are more weathered and contain less acid-buffering material and total sulfur than site 2 material
Restigouche Mine (Mattson and Carreau, 2003)	New Brunswick, Canada	To identify criteria for distinguishing between potentially acid-forming and non-acid forming material	ABA, humidity cells, EDS, EPMA.	Material with < 0.1% S designated non-acid, and > 4% S designated potentially acid forming
Grasberg Mine (Andrina et al., 2003; Miller et al., 2003)	Papua Province, Indonesia	To quantify acid/metal leaching rates and evaluate pile geochemistry control options	ABA, NAG, kinetic and sequential NAG, column leach, trial dump and test pads	Time frame to maximum acid generation is within two to three years of exposure
Ok Tedi Mine (Rumble et al., 2003)	Papua New Guinea	Assess overall NAPP of rock pile and optimize limestone addition	ABA and NAG	Bulk NNP of pile was 165; design NNP of 153 required to minimize acid generation.

Table 2.10 continued

Site or Project	Location	Objective	Tools	Summary Results/Conclusion
Ekati Diamond Mine (Day et al., 2003)	Northwest Territories, Canada	Investigate the mechanism(s) by which elevated TDS and acidity in the seepage from coarse kimberlite rejects were being generated	Rinse pH and conductivity, ABA, humidity cells, XRF, XRD.	High TDS attributed to low precipitation and fine grained reactive pyrite.
Standardization of static test methods for South African collieries (Cruywagen et al., 2003; Usher et al., 2003)	South Africa	To compare different static and kinetic test methods and define standard methods for ARD prediction	Paste pH, different ABA methods, standard and modified versions of humidity cell tests	AP method with hydrogen peroxide gives better indication of reactive sulfides than the Leco furnace method
Cadia Hill Gold Mine (Williams et al., 2003)	New South Wales, Australia	To evaluate ARD potential designation scheme of mine rock piles	ABA and NAG	The ARD potential designation scheme was confirmed to be appropriate
Samatosum Silver Mine (Ghomshei et al., 1997)	B. C., Canada	To determine acid drainage potential from a rock pile	ABA and column leach test	Channeling and flushing enhance ARD potential although there is excess NP in the dump

contaminant fronts within the piles, and the temporal variation of temperature, oxygen and carbon dioxide in the piles. The characterization results were to be used to plan and implement an investigative program to allow the remaining piles to be characterized, modeled and closure measures to be designed and verified.

Table 2.11: Summary of some reported static test results from different mine rock piles.

Site	Paste pH	Paste TDS	NNP	NP/AP	$NAG_{4.5}$	NAGpH
	s.u.	mg/L	kg $CaCO_3$/t		kg $CaCO_3$/t	s.u.
Zortman (Shaw, 2000)	-	316	-	-	-	-
Landusky (Shaw, 2000)	6.2	364	-	-	-	-
INAP Site 1 (Tran, 2003)	4.6	-	-7	1	7	4.2
INAP Site 2 (Tran, 2003)	6.53	-	-36	1	12	3.64
Restigouche Mine (Mattson and Carreau, 2003)	-	-	-19.45	3.15	-	-
Ok Tedi Mine (Rumble et al., 2003)	-	-	165	1.5 - 266	-	> 7.0
Ekati Diamond Mine (Day et al., 2003)	8.2	-	204	17.02	-	-
Samatosum Silver Mine (Ghomshei et al., 1997)	-	-	-43	0.57	-	-

Nine boreholes were drilled in four of the rock piles and sampled at 1.52-m (5-ft) intervals for tests including paste pH and acid base accounting. The test results and the acid generation potentials assigned to the boreholes are summarized in Table 2.12. (Robertson GeoConsultants Inc., 1999a, b, 2000)

Table 2.12: Summary of ABA and paste pH results on Questa rock pile samples. (Robertson GeoConsultants Inc., 2000)

Rock Pile	Drill Hole Number	Paste pH range s.u.	Avg. NNP kg $CaCO_3$/t	NP/AP	Acid Generation Potential
Spring Gulch	WRD-1	7.8-8.2	0.6	1.2	Uncertain
	WRD-2	4.0-6.4	-73.7	<0.1	Acid- generating
Sugar Shack South	WRD-3	5.8-7.7	-25.7	0.5	Potentially acid-generating
	WRD-4	6.5-7.9	-27.4	0.3	Potentially acid-generating
	WRD-5	4.7-8.0	-31.0	0.3	Potentially acid-generating
Sugar Shack West	WRD-6	4.1-7.8	-42.3	0.2	Potentially acid-generating
	WRD-7	4.5-7.6	-50.9	0.2	Potentially acid-generating
Capulin	WRD-8	3.7-4.5	-29.4	<0.1	Acid- generating
	WRD-9	3.9-5.6	-23.9	<0.1	Acid- generating

3 METHODOLOGY

Both field and laboratory methods were used in this research work. Field work included sampling of rock pile materials at various locations for testing. Laboratory procedures included paste pH and paste conductivity measurements, ABA and static NAG tests, X-ray fluorescence and modal mineralogy determination. The procedures used for the field and laboratory methods are presented in this chapter and Appendix B.

3.1 Sampling

Samples were collected from the surface of the GHN rock pile, and from trenches and boreholes in the interior of the rock pile. The samples are more like mine soil material rather than rock material, therefore tests used to characterize soils were used. The samples ranged in particle size from clay-size to cobbles as defined by ASTM D 422 and D 653 (American Society for Testing and Materials, 1980). A list of all the samples used for this thesis work and their respective locations is presented in Appendix A. Some of the samples were taken in duplicates and triplicates for quality assurance purposes, so there are some samples with different IDs but the same location information.

During sampling some of the sample locations were measured in feet with respect to some stations of known coordinates and elevation. However, for consistency and simplicity of presentation and analysis, all the sample locations are reported in North American Datum of 1927, Universal Transverse Mercator (NAD27 UTM) Zone 13N projection in meters. Elevations are also stated in meters above mean sea level with feet listed in parenthesis.

3.1.1 Surface Samples

Samples were collected from the surface of the GHN rock pile during sampling campaigns from May to September 2004. The samples were for surface mapping of the rock pile and during field tension infiltrometer measurements. They were mostly composite samples taken from 15-cm to approximately 1-m channels either along the face of the pile or just below the surface of the pile. Picks, shovels and hand trowels were used for sampling and the samples were stored in either clean one-gallon Ziploc bags or five-gallon plastic buckets. The bags were labeled in the inside and on the outside with water proof markers. Bagged samples were put into buckets before transportation. All buckets were tightly sealed and labeled on the lid and the side before transportation.

After sampling, the sample field description (including color, grain size, plasticity, alteration and moisture content) and location were recorded in a sample note book with a water-proof pen. The location of the sample was determined with either a hand-held or a differential Geographic Positioning System (GPS), or measured with a tape and

compass with respect to some known location. The data from the field sample note book was later transferred into the project database (McLemore et al., 2004). Figure 3.1 shows some students examining a site after collecting a sample. More details on the sampling procedures are presented in McLemore et al. (2005).

3.1.2 Trench Samples

Samples were collected from trenches that were dug into the GHN rock pile just before and during remediation construction of the pile. During the Summer and Fall of 2004, eight trenches were dug in the stable portion of the pile, and eleven trenches were dug in the unstable portion of the pile during late Winter to Spring of 2005 (Figure 1.6

Figure 3.1: Samuel Tachie-Menson and Luiza Gutierrez examining the material for soil properties after collecting a sample. In front of Samuel are a soil temperature probe and a hand-held GPS.

shows the different portions of the GHN rock pile). Each trench was sampled and mapped and various instruments were used to measure in-situ properties such as permeability, matric suction and bulk density.

The trenches were dug in benches (usually four benches per trench) with each bench measuring approximately 1.2 m (4 ft) tall and 1.7 m (5.6 ft) wide. Figure 3.2 is a section through the width of a typical trench. The trenches were aligned approximately east-west with their lengths perpendicular to the face of the pile (see Figures 3.3 and 3.4). Figure 3.5 is a map of the GHN rock pile showing the location of the trenches. The red lines in the upper half of the map are the trenches in the unstable portion and those in the lower half of the map are the trenches in the stable portion of the pile. The trenches were named with a three-letter plus three-digit naming system (e.g. LFG-005) and all the benches in all the trenches (except the first two, LFG-003 and LFG-004) were identified with consecutive numbers from 1 to 54. With this system, a sample could be identified with both the trench and bench from which it was taken, aside its own sample ID. Benches in the first two trenches were numbered separately so the bench numbering for LFG-004 did not follow from those for LFG-003. Numbering of benches in the unstable portion of the pile was not always consistent with the aforementioned numbering system because of some differences in the order in which the trenches were dug.

The procedure for collecting trench samples was the same as used for the surface samples discussed above, except that the bench faces had to be cleaned with picks,

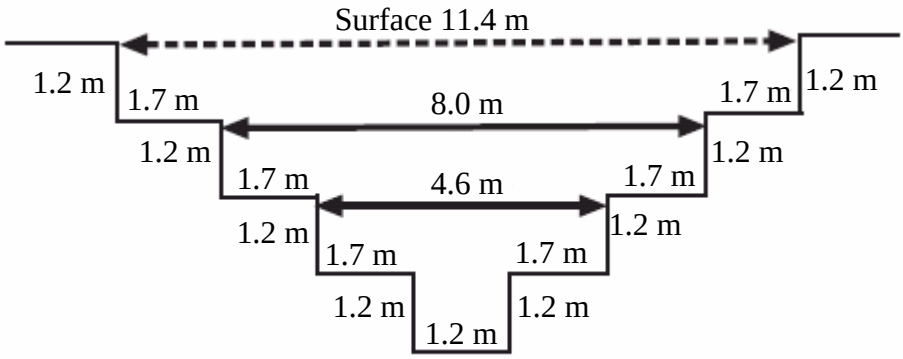

Figure 3.2: Schematic drawing showing a transverse cross section through a typical trench in the GHN rock pile. Horizontal dimensions are inside the section and vertical dimensions are outside.

shovels and brooms before sampling. This was necessary because, as bulldozers and excavators dug the trenches, loose materials from upper benches fell on the walls of lower benches. Another unique procedure that was used in the trenches was the identification and mapping of different layers of materials along the bench walls. These layers were identified by their field properties such as color and particle size and were mapped as units. McLemore et al. (2006; 2005) presents detailed information on the rock pile units in GHN. Most of the samples were collected from the vertical faces of the bench walls. On some of the benches, the samples were taken systematically at intervals of 1.52 m (5 ft) along the benches. Other samples were collected at specifically chosen locations and a few were collected from the floor of the benches. Tables 3.1 and 3.2 are list of trenches and benches and their respective numbers of samples in the stable and unstable portions of the pile respectively. In all, 712 samples from trenches were tested for this study.

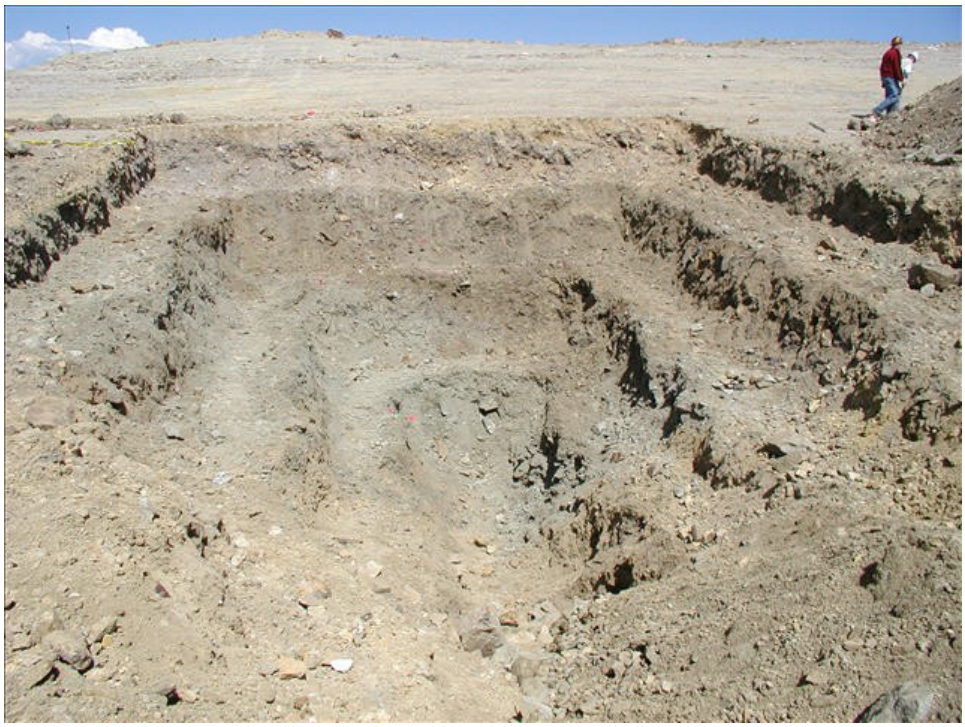

Figure 3.3: A view of trench LFG-004, from east looking west towards the front of the rock pile, after the trench was completed dug.

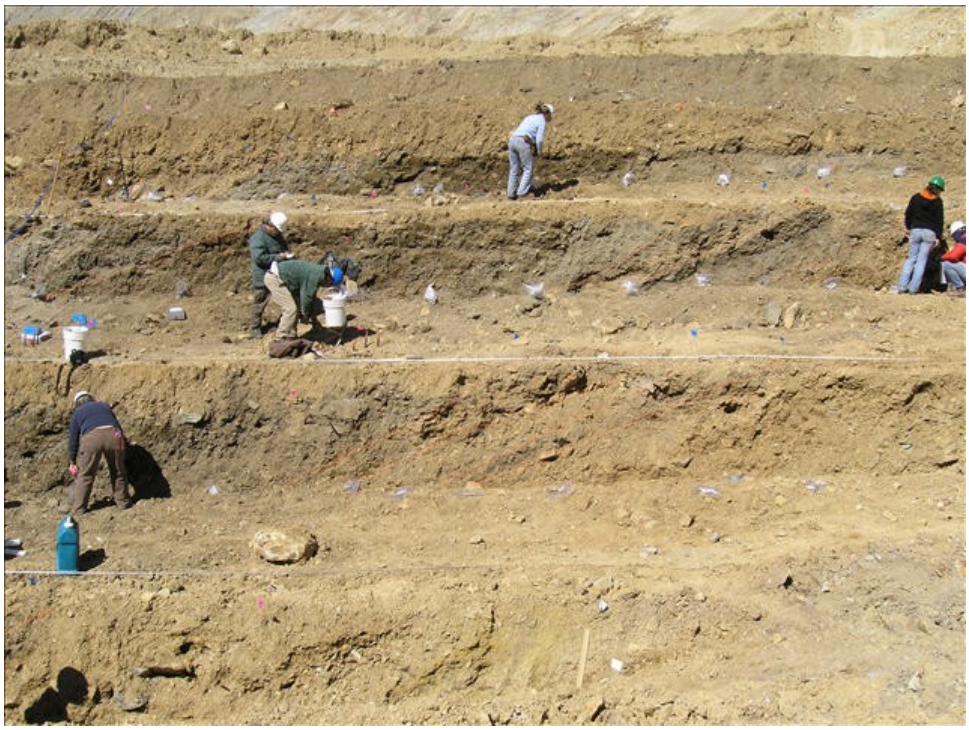

Figure 3.4: A view at the north wall benches of trench LFG-008 as workers take samples. The face of the rock pile is to the left. The little bright objects that are about equally spaced on the ground are Ziploc bags containing samples.

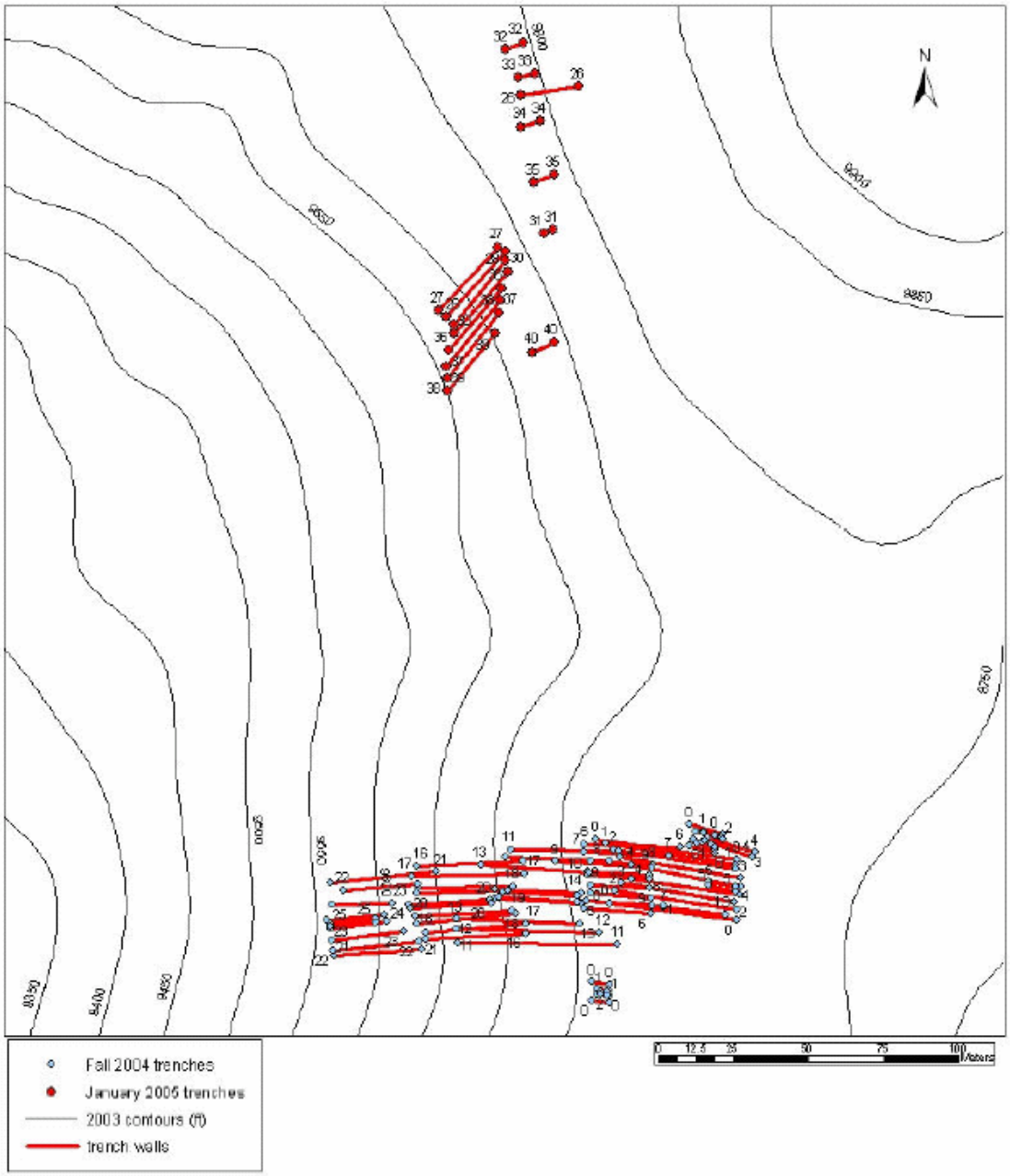

Figure 3.5: Map showing location of GHN trenches. The red lines represent trench walls; blue dots represent the corners of trenches in the stable portion of the pile; red dots represent the corners of trenches in the unstable portion of the pile. The black lines are 2003 elevation contours.

Table 3.1: List of trenches, benches and their respective numbers of samples in stable portion of GHN rock pile

Trench ID	No. of Benches	Bench nos.	No of samples on bench	Total no. of samples in trench
LFG-003	4	1	3	20
		2	5	
		3	8	
		4	4	
LFG-004	2	1	4	7
		2	3	
LFG-005	5	1	42	156
		2	36	
		3	33	
		4	37	
		5	8	
LFG-006	4	7	27	111
		8	24	
		9	39	
		10	21	
LFG-007	4	12	37	118
		13	32	
		14	34	
		15	15	
LFG-008	4	17	12	82
		18	24	
		19	29	
		20	17	
LFG-009	4	22	25	72
		23	33	
		24	8	
		25	6	
Total number of samples from stable portion trenches				566

Table 3.2: List of trenches, benches and their respective numbers of samples from the unstable portion of the GHN rock pile

Trench ID	No. of Benches	Bench nos.	No of samples on bench	Total no. of samples in trench
LFG-011	10	28	2	104
		29	27	
		30	24	
		32	1	
		37	5	
		43	1	
		44	20	
		45	1	
		46	22	
		47	1	
LFG-012	2	28	2	10
		31	8	
LFG-013	1	41	3	3
LFG-015	1	34	3	3
LFG-016	1	35	2	2
LFG-017	1	40	2	2
LFG-018	1	41	3	3
LFG-019	1	49	3	3
LFG-020	1	50	1	1
LFG-021	2	51	5	10
		52	5	
LFG-022	2	53	3	5
		54	2	
Total number of samples from unstable portion trenches				146

3.1.3 Drill Cuttings

Many boreholes have been drilled in the rock piles at Questa. The boreholes were drilled for investigative purposes such as slope inclinometer and piezometer installation, and temperature and pore gas monitoring. During drilling, some of the rock pile material extracted from the boreholes was sampled and stored in five-gallon buckets for future testing. Each bucket of sample represents a hole-thickness of approximately 1.52 m (5 ft). For the purpose of this project, splits of the drill cuttings were sampled from

the buckets for laboratory tests. Figure 3.6 shows the drill holes that were sampled for acid characterization tests.

A mechanical soil splitter (Figure 3.7) was used for sampling the drill cuttings. The sample in each bucket was poured into three separate clean buckets and the split in each of the three buckets was further split through the soil splitter to homogenize the whole sample. About 1 gallon of the sample was then placed in a labeled Ziploc bag. Between six and twelve bags of sample were stored in a 5-gallon bucket and the bucket was labeled and sealed before transportation to the lab. The drill cutting samples were described by their texture, color, the hole they came from and the depth at which they were sampled among other properties. This information was recorded in a note book and later transferred onto the project database. Sometimes, the information was typed straight into the database. Table 3.3 lists the boreholes that were sampled for this study and the number of samples collected from each of them. A list of the individual samples and their locations is presented in Appendix A.

Table 3.3: List of boreholes that were sampled from the stable and unstable portions of the GHN rock pile and number of samples from each borehole.

Portion of Pile	Borehole ID	No. of samples	Total no. of samples
Stable	SI-30	16	101
	TH-GN-01	32	
	TH-GN-06	53	
Unstable	SI-3	16	94
	TH-GN-02S	34	
	TH-GN-04S	20	
	TH-GN-07S	24	
Total number of samples from boreholes			195

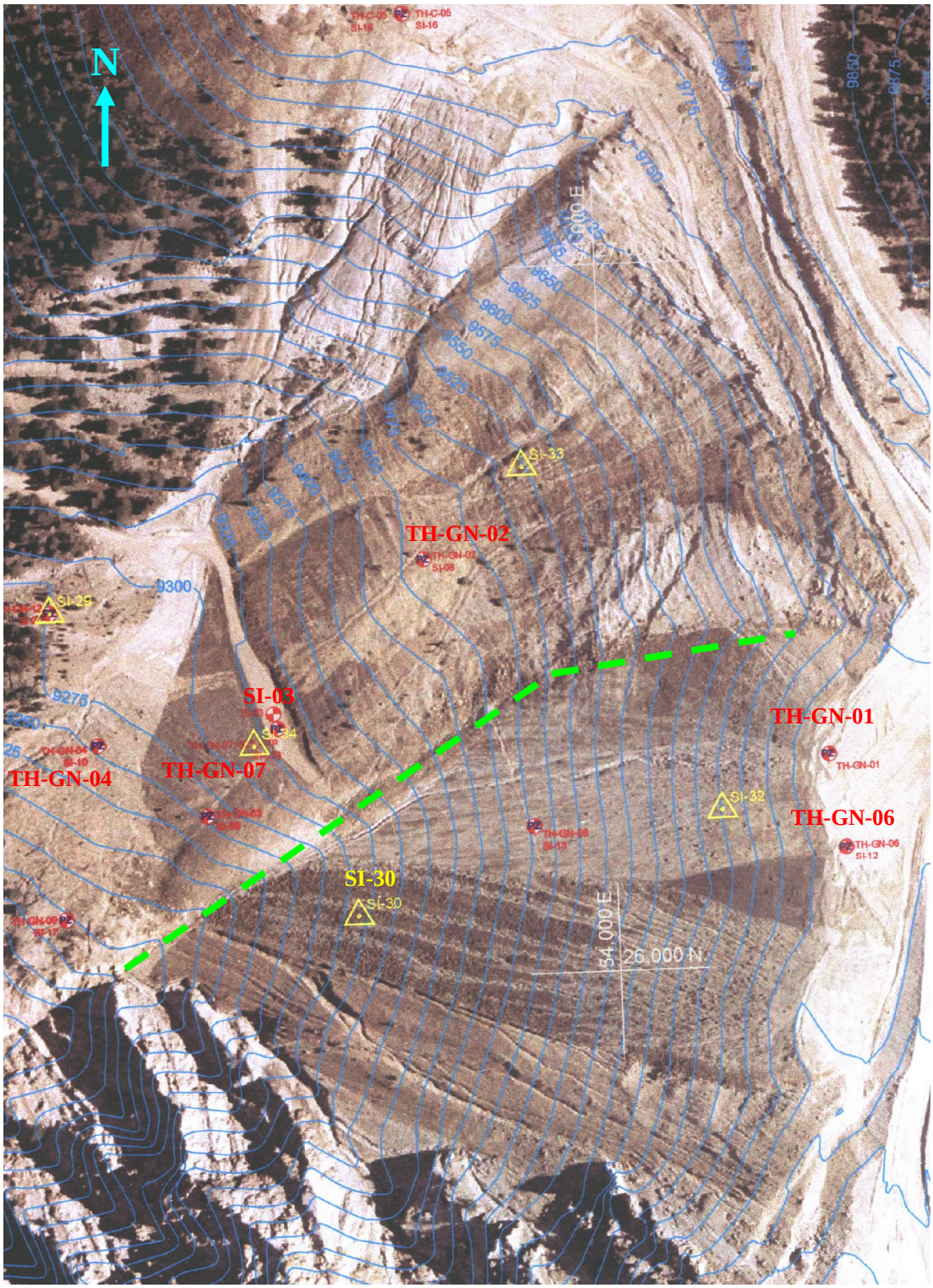

Figure 3.6: Arial photograph of the GHN rock pile showing locations of boreholes. The yellow triangles are slope inclinometer holes; the red and blue circles are piezometer holes; the blue lines are elevation contours. The bright green dashed line separates the stable portion (south) from the unstable portion (north).

Figure 3.7: Splitting of drill cuttings with a soil splitter.

3.2 Sample Preparation

Sample preparation procedures included drying, crushing and pulverizing. Figure 3.8 depicts the unit processes involved in sample preparation. Typically, the sample is taken out of the bag and air-dried indoors. The dried sample is run through a laboratory-size jaw crusher (The Mine & Smelter Supply Co., Denver, CO.) to break the bigger particles into pea-size fragments, which are then put into a tungsten carbide grinding set and shaken in a pulverizing machine (BICO Inc., Burbank, CA.) for one minute to grind the sample into powder (less then no. 60 mesh, 0.25 mm).

Figure 3.8: Sample preparation processes applied to GHN rock pile samples. The sample is air dried, crushed in a jaw crusher to pea-size, put into a tungsten carbide grinding set and pulverized in a pulverizing machine to get a powdered sample.

Not all the tests required the samples to be powdered. Paste pH and conductivity, clay mineralogy and petrographic analysis were performed on dried samples before or after crushing, but not pulverized. The paste pH test that forms part of ABA analysis was, however, done on powdered samples and the results are differentiated from those of the unpowdered samples. ABA, NAG and XRF analysis were performed on powdered samples. Some of the samples were oven dried at 105^{o}C for paste pH and conductivity tests.

3.3 Static Tests

Static tests included in this work are paste pH and paste conductivity, acid-base accounting (ABA), and static net acid generation (NAG) tests. The procedures used for these tests are described below. More detailed step by step procedures may be found in Appendix B.

3.3.1 Paste pH and Paste Conductivity

These two tests are considered together because they were always done together. A Corning 308 pH/Temperature meter and a HACH conductivity/TDS meter were used to measure pH and conductivity, respectively. The pH meter was calibrated with pH 4.0 and 7.0 buffer solutions before testing each batch of samples. The conductivity meter was calibrated with a 992 μS/cm calibration solution. The tests were performed on dried samples before or after crushing. Paste pH was measured in standard pH units and paste conductivity in mS/cm.

Twenty-five grams of particles less than 2 mm in size were extracted from the sample with a clean spatula or by sieving with a 2 mm sieve and put into a 50-mL glass beaker. A measuring cylinder was used to measure 25 mL of deionized (DI) water and added to the sample. In some cases, less than 25 g of the right particle size of sample could be obtained so a corresponding volume of DI water was added to make 1:1 soil-mass: water-volume mixture. The mixture of sample and water was stirred with a stirring rod and left to stand for at least 10 minutes.

After ten minutes, the suspension separated into three layers: water at the top, slurry of fines in the middle, and sandy particles at the bottom of the beaker. Paste conductivity was measured by immersing the conductivity probe into the soil suspension to sit lightly

on the slurry and allowing the reading on the meter to stabilize. The reading was recorded on a data sheet with the sample ID. Paste pH was measured in a similar manner after the paste conductivity and recorded.

3.3.2 Acid-Base Accounting (ABA)

The acid-base accounting (ABA) procedure consists of two separate tests: the acid potential (AP) test and the neutralization potential (NP) test. Both tests were performed on powdered (minus no. 60 mesh) samples. The standard Sobek method (Sobek et al., 1978) was used for NP and the hydrogen peroxide method (Smith et al., 1974) was used for AP determination. The procedures for the tests are described below.

Acid Potential (AP) Test

The AP test was performed to quantify the acid producing potential of a sample. Three grams of sample was placed in a filter paper-fitted funnel on a conical flask and leached with 300 mL of 40% HCl solution in funnel-full increments to remove all reactive neutralizing minerals such as carbonates from the sample. Ample amount of DI water was used to leach the sample again to remove the chloride introduced by the HCl leaching. Complete removal of the chloride was insured by checking with a 10% silver nitrate ($AgNO_3$) solution. In the presence of chloride, silver forms a cloudy precipitate of silver chloride ($AgCl_2$). After leaching with DI water, the sample was left to air-dry for at least 24 hours.

The dried sample was scraped off the filter paper and 2.00 g of sample were weighed into a 150-mL beaker. Twenty-four milliliters of 30% hydrogen peroxide (H_2O_2) was added to the sample and heated on a hot plate to 40^{o}C. The sample was removed from

heat and allowed to react to completion or for 30 minutes. Additional 12 mL of H_2O_2 was added and left to stand for 30 minutes and then the sample was placed on heat at 90 to 95^oC for 30 minutes to remove any unreacted peroxide. More DI water was added to make a total volume of 100 mL and the sample was heated slightly to boil off dissolved CO_2. The sample was then left to cool to room temperature and titrated against standardized 0.1 N solution of sodium hydroxide (NaOH) to pH 7.0. Usually, the titration went beyond pH 7 so a titration curve was used to estimate the actual volume titrated.

The acid potential was calculated as follows:

- (mL of NaOH) * (Normality of NaOH) * 50 = meq (H^+)/100 g
- meq H^+/100 g * 0.01 = tons H^+/thousand tons of material

One ton of H^+ requires 50 tons of $CaCO_3$ equivalents to neutralize it.

- AP = tons H^+/thousand tons of material * 50 (kg of $CaCO_3$/ton of material)

Therefore
AP = mL of NaOH * Normality of NaOH * 50 * 0.01 * 50
AP = mL of NaOH * Normality of NaOH * 25 (kg of $CaCO_3$/ton)

Neutralization Potential (NP) Test

The NP test was performed to determine the quantity of acid-consuming minerals in a sample. As part of the NP test, the paste pH of the powdered sample was determined using 10 g of sample and 5 mL of DI water. The NP test itself started with a “fizz” test which was done by adding one or two drops of 25% HCl solution to about 0.5 g of sample and observing the degree of effervescence. The “fizz” test was used to rank the

Table 3.4: Volume and Concentration of HCl to be used for NP test in Standard ABA test according to "fizz" rating.

Fizz Rating	HCl	
	(ml)	(Normality)
None	20	0.1
Slight	40	0.1
Moderate	40	0.5
Strong	80	0.5

sample as none, slight, moderate or strong. Based on the fizz rating, the volume and concentration of HCl to be used was chosen as in Table 3.4.

The appropriate amount and concentration of HCl was added to 2.0 g of sample in a flask and placed on a hot plate until the sample was just beginning to boil. The flask was taken off the heat and swirled intermittently until no more effervescence was observed. More DI water was added to make a total volume of 125 mL and it was heated for one minute to drive off CO_2. The sample was left to cool to slightly above room temperature and then covered and allowed to cool to room temperature before titration. The concentration of NaOH used for titration was the same as the concentration of the HCl used to start the test based on the "fizz rating". The sample was titrated to pH 7.0.

In order to calculate the NP, a blank test was done for each pair of concentrations of HCl and NaOH used per "fizz rating". The NP was calculated as follows:

1. Constant (C) = (mL acid in blank) / (mL base in blank)
2. mL acid consumed = (mL acid added) – (mL base added * C)
3. NP (kg $CaCO_3$/ton) = (mL of acid consumed) * (25.0) * (N of acid)

Net Neutralization Potential and Neutralization Potential Ratio

The final results of the ABA tests were calculated from the AP and NP test results. The net neutralization potential (NNP) was calculated as NNP = NP – AP, and the neutralization potential ratio (NPR) as the ratio of NP to AP (NPR = NP/AP). All the ABA results are expressed in kg $CaCO_3$/t of sample.

3.3.3 Static Net Acid Generation (NAG)

The static NAG test is used to determine the net acid remaining, if any, after complete oxidation of mine rock pile material with hydrogen peroxide and allowing complete reaction of the acid formed with the neutralizing components of the material. Two hundred and fifty milliliter of 15% H_2O_2 was added to 2.5 g of sample in a conical flask and left in a fume hood to react to completion. The pH of the solution (NAG liquor) was measured and recorded as NAG pH_1. The liquor was gently heated on a hot plate for two hours and allowed to cool to room temperature. The pH was measured again and recorded as NAG pH_2. DI water was added to make a total volume of 250 mL and the liquor was titrated with standardized 0.1 N HCl if the pH was more than 2.5, or with 0.5 N HCl if the pH was less than 2.5. Titration was done to pH 4.5 and then to pH 7.0. Titration to pH 4.5 accounts for acidity due to Fe, Al and most of the hydrogen ion. Any additional acidity accounted for in titration between pH 4.5 and pH 7 is usually indicative of soluble metals such as Cu and Zn (Environmental Geochemistry International, 2004). The actual volume of HCl titrated was estimated from a titration curve and the NAG value was calculated as follows:

$$NAG = \frac{50 * V * N}{W}$$

Where:
NAG = net acid generation (kg $CaCO_3$/t)
V = volume of base NaOH titrated (mL)
N = normality of base NaOH (eq/L)
W = weight of sample reacted (g)

The NAG test evolved over the period of testing from the simple method that includes only one pH measurement and titration to pH 4.5 to the more detailed method that includes two NAG pH measurements and titration to both pH 4.5 and 7.0. Therefore, some of the samples that were tested earlier do not have NAG pH_1 and NAG at pH 7.0 values.

3.4 Mineralogy and Chemistry

To be able to compare acid generation tests to the actual chemical components of the rock pile samples, the chemistry and mineralogy of the samples were determined using X-ray fluorescence (XRF) spectrometry and modal mineralogy analysis, respectively.

3.4.1 X-ray Fluorescence

The XRF analyses were done in laboratories at the New Mexico State University (NMSU) and Washington State University (WSU). The XRF was used to determine the whole rock chemistry of the samples. These included concentrations in percentage of SiO_2, TiO_2, Al_2O_3, Fe_2O_3T, FeOT, MnO, MgO, CaO, Na_2O, K_2O, P_2O_5, and S. Also, the concentrations of the trace metals Ni, Cr, Sc, V, Ba, Rb, Sr, Zr, Y, Nb, Ga, Cu, Sn, Pb, La, Th, Nb, U, and Co were determined in parts per million (ppm).

3.4.2 Modal Mineralogy

Modal mineralogy is a procedure that combines results from various chemical and mineralogy analysis including petrography, electron microprobe, clay mineralogy, pyrite reserve estimation and chemistry from XRF to determine the major minerals present in a sample. It is a tedious and somewhat subjective procedure and although the results are reported in percentages, there could be up to 10% error in the absolute abundance of each mineral identified. However, the results are very useful when the relative values between samples are compared. Figure 3.9 is a schematic chart showing how modal mineralogy is determined using a variety of laboratory analyses.

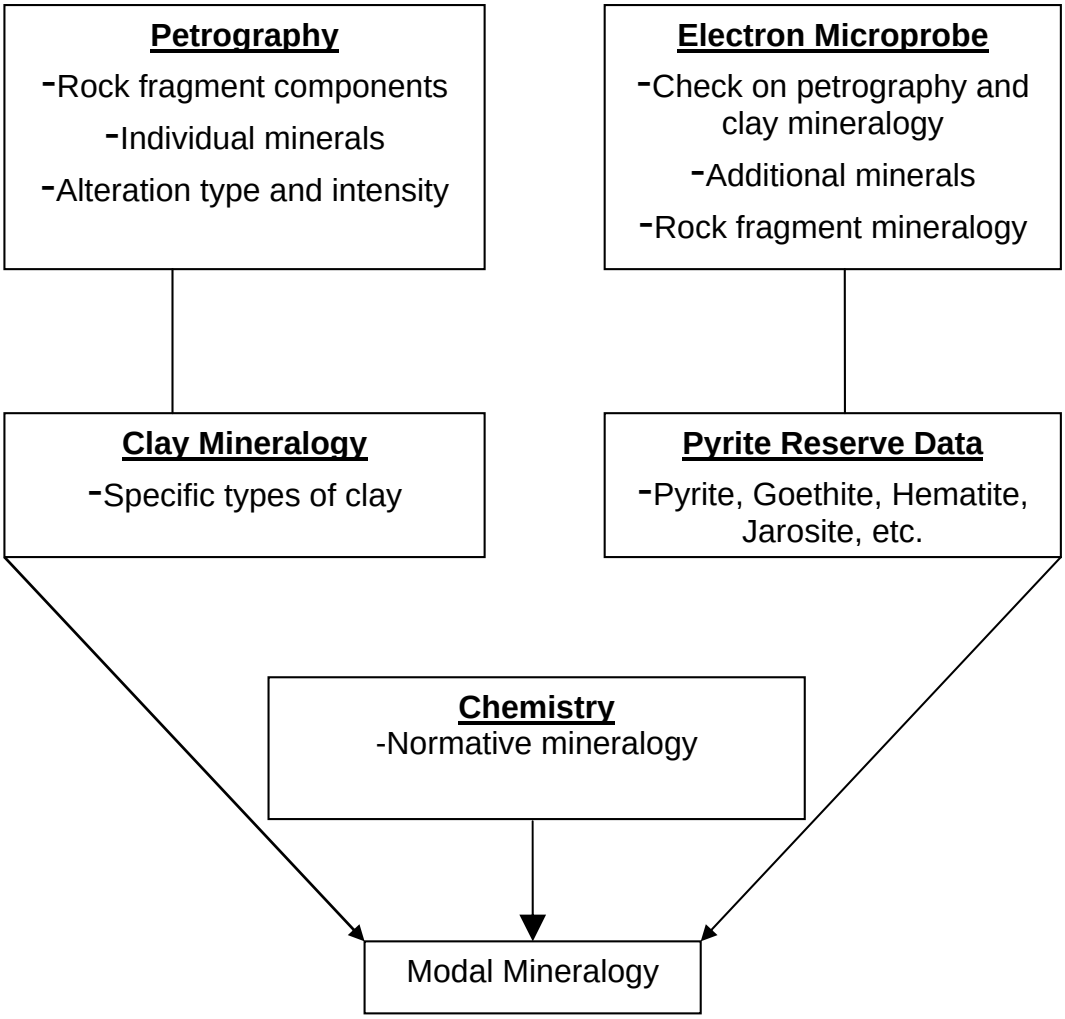

Figure 3.9: Procedure for determining modal mineralogy

4 RESULTS

The results are presented here in summary tables, and charts based on the results are presented alongside the discussions in the next chapter. The bulk of the results are presented in Appendix C.

4.1 Description of Geologic Units in GHN

The geologic units identified during trench sampling in the GHN rock pile are named and described in Table 4.1. These units were identified only in the stable portion of the rock pile. The descriptions were mostly made in the field by visual inspection. Units A through H were identified at the surface of the pile. Units I, J and N were the subsurface units closest to the surface of the pile and all the other units were deeper within the pile.

Table 4.1: Geologic units of Goathill North rock pile.

Unit	Description	Structure	Lithology	Location
A	Light brown unit with approximately 60% covered by cobbles or larger sized rocks with vegetation growing upon the surface.	Layered in some of the rills near the base.	Mixed volcanic rocks	Southern-most surface unit of the stable part
B	Massive, light brown to gray to yellow brown unit containing crusts of soluble acid salts. Approximately 65% is covered by cobbles or larger sized rocks. Consists of clayey sand with gravel and cobbles and is locally cohesive.	Shallow rills (0.2-1 m deep) of finer grained material are cut into the surface.	Quartz-sericite-pyrite (QSP) altered Amalia Tuff (70%) and andesite (30%).	Surface unit of stable portion of the GHN rock pile

Table 4.1 continued.

Unit	Description	Structure	Lithology	Location
C	Grayish brown to yellowish gray unit consisting of fine-grained materials (sand with cobbles and gravel) and approximately 15% boulders. Locally is cohesive and well cemented by clays and soluble minerals.	Massive alternating zones, up to 3 m thick.	Amalia Tuff (70%) and andesite (30%)	Surface unit of stable portion of the GHN rock pile
D	Yellow-brown gravely sand unit that differs from Unit C by a marked increase in cobbles and boulders (approximately 30-40%).	Massive	Amalia Tuff (80%) and andesite (20%).	Surface unit of unstable portion of the GHN rock pile
E	Orange brown unit with patches of gray sandy clay with approximately 15% cobbles and boulders.	Massive	70 % moderate to strong QSP altered Amalia Tuff and 30% weakly altered Amalia Tuff	Surface unit of unstable portion of the GHN rock pile
F	Similar to Unit A, consists of dark brown, silty sand with some gravel.	Massive	andesite	Surface unit of unstable portion of the GHN rock pile
G	Orange brown to yellow brown sandy gravel with some cobbles, includes colluvium material.	Massive	andesite	Surface unit of unstable portion of the GHN rock pile
H	Dark gray to red-brown V-shaped unit with oxidized orange zones and consists of poorly sorted, well graded, weakly cemented, gravel sand with some fine sand to fine sand with clay, approximately 80% cobbles or boulders.	Massive	andesite	Surface unit at the top of stable portion of the GHN rock pile
I	Light-gray, poorly sorted, well graded clayey to sandy gravel, medium hard with weak cementation, and no plasticity. The matrix is locally sandy clay with medium to high plasticity. The unit is less cemented and finer grained than the overlying unit C.	Overlain by Unit C, up to 3 m thick	andesite	Subsurface oxidized unit of stable portion of the GHN rock pile
J	Dark orange-brown, poorly sorted, well graded, coarse gravel with clay matrix and weak cementation. The top of the unit locally is a bright orange oxidized layer, 2-4 inches thick.	Overlain by unit I, 1-3.7 m thick	andesite	Subsurface oxidized unit of stable portion of the GHN rock pile

Table 4.1 continued.

Unit	Description	Structure	Lithology	Location
N	Light to dark brown moderately sorted, uniformly graded, moderately hard sandy clay with cobbles, with moderate to high plasticity and well cemented by clay, zones of bright orange to punky yellow oxidized sandy clay.	Heterogeneous with numerous coarse and fine layers, 1.5-3 m thick	andesite and Amalia Tuff	Subsurface intermediate unit of stable portion of the GHN rock pile
K	Distinctive purplish-brown gravelly sand with cobbles and is weakly cemented and very coarse, almost no clay. Cobble layer is locally overlain and underlain by finer gravelly sand layers and contacts are gradational.	grades into Unit O, 0-1.2 m thick	andesite	Subsurface unoxidized unit of stable portion of the GHN rock pile
L	Brown gray, poorly sorted, well graded gravelly sand with cobbles.	Grades into Unit O	andesite	Subsurface unoxidized unit of stable portion of the GHN rock pile
O	Brown, poorly sorted, sandy gravel matrix in coarse gravel and cobbles. Numerous coarse and fine layers at varying dips and thicknesses appear in the mass of the unit. The unit has cobbles and clay layers.	Heterogeneous, deformed layer with numerous S-shaped clay lenses and coarse layers, variable dip of individual beds	andesite	Subsurface unoxidized unit of stable portion of the GHN rock pile
M	Orange brown to brown, poorly sorted, well graded sandy gravel with boulders (up to 1 m diameter). Sandy gravel forms a matrix between boulders and cobbles. The fines are generally gritty.	Unit locally flattens with 20 degree dip	andesite and Amalia Tuff	Subsurface unoxidized unit of stable portion of the GHN rock pile
P	dark brown, poorly sorted, well graded, sandy gravel with medium hardness and no to weak cementation	Pinches out, 0-1 m thick	andesite	Subsurface unoxidized unit of stable portion of the GHN rock pile
Q	Dark brown, poorly sorted, well graded, sandy gravel with cobbles with medium hardness and no to low cementation.	Steeply dipping	andesite	Subsurface unoxidized unit of stable portion of the GHN rock pile
R	Orange gray, poorly sorted, well graded sandy gravel to gravel with cobbles with medium to weak cementation by clay.	Pinches out, 0-1 m thick	andesite	Subsurface unoxidized unit of stable portion of the GHN rock pile

Table 4.1 continued.

Unit	Description	Structure	Lithology	Location
S	Dark gray, poorly sorted, well graded sandy silt with no cementation or plasticity.	Pinches out, 0-1.2 m thick	andesite	Subsurface unoxidized unit of stable portion of the GHN rock pile
T	Dark gray, poorly sorted, well graded sandy gravel.		andesite	Subsurface unoxidized unit of stable portion of the GHN rock pile
U	Brown, poorly sorted well graded, sandy gravel with cobbles.	Pinches out, 0-0.6 thick	andesite	Subsurface unoxidized unit of stable portion of the GHN rock pile
V	Gray to brown gray poorly sorted, sandy gravel.	Pinches out, 0-3 m thick	andesite	Subsurface unoxidized unit of stable portion of the GHN rock pile
W	Olive gray clay zone, similar and possibly correlated to Unit S.		andesite	Subsurface unoxidized unit of stable portion of the GHN rock pile
Rubble zone	Orange brown, angular cobbles and large boulders (15 cm in diameter) with little sand or clay, cobble-supported rubble zone.	Unconformably on top of either soil developed on weathered andesite or colluvium that is similar to the alteration scars, up to 2.1 m thick	Andesite, Amalia	Basal subsurface unoxidized unit of stable portion of the GHN rock pile
Shear zone, alluvium, colluvium	Dark gray to brown clayey soil developed on weathered andesite or a yellow to orange brown clay to sandy clay colluvium that is similar to the alteration scars.	0.3-1 m thick	andesite	Original surface, material beneath the rubble zone
bedrock	Gray to dark gray to greenish gray, porphyritic to fine-grained andesite.	Locally fractured	andesite	Original andesite bedrock beneath the soil, alluvium, colluvium

4.2 Static Test Results

4.2.1 Paste pH and Paste Conductivity

Paste pH and paste conductivity test results are presented in Table C1, Appendix C, and summarized in Table 4.2 for the stable portion of the rock pile and Table 4.3 for the

unstable portion of the rock pile. Table 4.4 is a summary of the paste pH and paste conductivity results for the geologic units in the rock pile. The paste pH on unpowdered samples is called paste pH_1 here to differentiate it from the paste pH on powdered samples which is called paste pH_2 and presented with the ABA results. A total of 687 samples from the stable portion of the pile had an average paste pH of 4.43 and an average paste conductivity of 2.32 mS/cm. From the unstable portion of the pile, 259 samples had an average paste pH and paste conductivity of 3.86 and 1.97 mS/cm respectively. These results indicate that generally, the stable portion of the pile has higher paste pH and paste conductivity than the unstable portion. For all the 946 samples tested, the average paste pH and paste conductivity are 4.27 and 2.22 mS/cm respectively.

Table 4.2: Summary of paste pH_1 and paste conductivity results for stable portion of GHN rock pile. n = number of samples, Avg. = average, Stdv. = standard deviation.

Hole/Trench	n	Paste pH_1 (s.u.)				Paste Conductivity (mS/cm)			
		Min.	Max.	Avg.	Stdv.	Min.	Max.	Avg.	Stdv.
LFG-003	20	4.17	7.45	5.53	1.03	0.22	2.14	0.81	0.48
LFG-004	7	3.15	5.57	4.57	0.81	0.26	2.28	0.86	0.85
LFG-005	156	2.33	9.47	4.16	1.52	0.42	7.19	2.19	1.03
LFG-006	111	2.19	9.60	4.85	1.94	0.55	12.35	2.55	1.92
LFG-007	118	2.33	8.62	4.98	1.55	0.18	7.96	2.76	1.46
LFG-008	82	2.44	7.66	4.68	1.65	0.70	6.90	2.61	1.37
LFG-009	72	2.14	7.53	3.94	1.27	1.18	6.31	2.83	1.26
SI-30	16	2.65	4.13	3.26	0.36	0.88	5.30	3.02	1.36
Surface	20	2.06	5.65	3.78	1.13	0.06	4.18	1.83	1.18
TH-GN-01	32	2.36	7.11	4.10	1.34	0.42	5.21	1.68	0.85
TH-GN-06	53	2.83	7.43	3.72	0.90	0.28	2.27	1.25	0.45
Overall	687	2.06	9.60	4.43	1.58	0.06	12.35	2.32	1.42

Table 4.3: Summary of paste pH_1 and paste conductivity results for unstable portion of GHN rock pile. n = number of samples, Avg. = average, Stdv. = standard deviation.

Hole/Trench	n	Paste pH_1 (s.u.)				Paste Conductivity (mS/cm)			
		Min.	Max.	Avg.	Stdv.	Min.	Max.	Avg.	Stdv.
LFG-011	104	2.38	5.09	3.24	0.52	0.14	5.13	1.85	1.07
LFG-012	10	2.77	3.46	3.11	0.20	1.38	5.05	3.21	1.30
LFG-013	3	3.38	5.20	4.18	0.93	1.35	3.46	2.45	1.06
LFG-015	3	3.99	7.99	6.06	2.00	0.99	2.77	1.76	0.91
LFG-016	2	3.16	3.33	3.24	0.12	2.37	2.84	2.60	0.33
LFG-017	2	2.68	3.18	2.93	0.35	1.31	6.38	3.85	3.59
LFG-018	3	2.72	3.48	3.08	0.38	0.61	1.26	0.94	0.33
LFG-019	3	2.78	5.81	4.05	1.57	1.67	3.77	3.02	1.17
LFG-020	1	3.32	3.32	3.32	-	3.78	3.78	3.78	-
LFG-021	10	2.60	7.54	4.45	1.59	1.48	3.09	2.26	0.55
LFG-022	5	2.66	3.25	2.88	0.23	1.74	2.42	2.09	0.29
SI-3	16	2.51	8.39	5.23	2.08	1.02	6.73	2.54	1.40
Surface	19	2.13	6.60	3.47	1.15	0.07	3.10	1.26	1.12
TH-GN-02S	34	3.07	8.25	4.92	1.35	0.73	3.08	1.69	0.53
TH-GN-04S	20	3.06	7.35	4.71	1.03	0.40	2.46	1.70	0.59
TH-GN-07S	24	2.55	6.91	3.99	1.24	0.87	5.01	2.25	1.25
Overall	259	2.13	8.39	3.86	1.29	0.07	6.73	1.97	1.11

Table 4.4: Summary of paste pH_1 and paste conductivity results by geologic units. n = number of samples, Avg. = average, Stdv. = standard deviation.

Unit	n	Paste pH_1 (s.u.)				Paste Conductivity (mS/cm)			
		Min.	Max.	Avg.	Stdv.	Min.	Max.	Avg.	Stdv.
B	4	2.18	3.90	2.82	0.77	1.03	3.47	1.95	1.14
C	12	2.33	3.43	2.85	0.35	0.44	4.90	2.25	1.17
D	2	2.87	6.60	4.74	2.64	0.07	0.18	0.13	0.08
E	14	2.45	4.38	3.31	0.68	0.42	5.13	2.17	1.47
G	2	4.27	4.86	4.57	0.42	0.46	1.15	0.81	0.49
H	12	3.15	5.65	4.71	0.74	0.26	3.09	1.44	1.05
I	28	2.19	4.77	3.07	0.69	0.75	6.54	3.20	1.23
J	52	2.14	5.75	3.37	0.75	1.22	12.35	3.53	2.06
K	36	2.36	7.20	4.83	1.53	0.58	5.02	2.35	1.12
L	9	2.25	8.74	6.46	2.12	0.96	2.75	2.32	0.60
M	57	2.41	9.56	4.45	1.21	0.28	4.12	1.74	0.77
N	58	2.15	4.71	3.39	0.54	1.06	9.97	3.07	1.66
O	163	2.43	8.98	5.49	1.66	0.18	7.96	2.56	1.42
R	16	3.17	9.60	6.05	1.98	0.72	3.59	1.68	0.72
Rubble Z	25	2.39	8.56	3.68	1.31	0.22	6.12	1.64	1.34
S	20	2.61	9.47	6.25	1.87	0.83	3.65	2.00	0.63
T	6	3.95	4.77	4.25	0.31	0.85	2.10	1.42	0.41

Table 4.4 continued.

Unit	n	Paste pH_1 (s.u.)				Paste Conductivity (mS/cm)			
		Min.	Max.	Avg.	Stdv.	Min.	Max.	Avg.	Stdv.
Traffic Z	27	2.84	6.12	4.43	0.91	0.39	3.26	1.90	0.63
U	15	2.45	5.52	3.86	0.90	0.70	4.25	2.22	1.06
V	11	3.37	5.77	4.39	0.61	1.03	3.21	1.65	0.61
W	2	6.62	6.68	6.65	0.04	0.59	0.98	0.79	0.28

4.2.2 Acid-Base Accounting (ABA)

Results of the acid-base accounting (ABA) test are presented in Table C2 (Appendix C), and summarized in Tables 4.5 and 4.6 for the stable and unstable portions of the rock pile respectively. Paste pH_2 is the paste pH measured on powdered samples. Ninety-nine samples from the stable portion and fifteen from the unstable portion were tested. The samples from the stable portion of the pile had an average paste pH_2 of 5.30 and NNP of 5.43 kg $CaCO_3$/t. For the unstable portion, the averages for the same parameters are 4.80 and -1.26 kg $CaCO_3$/t, respectively. For all the 114 samples tested, the averages are 5.23 and 4.55 kg $CaCO_3$/t, respectively.

Table 4.5: Summary of ABA results for the stable portion of GHN rock pile. Paste pH_2 = paste pH on powdered samples; NP = neutralization potential; AP = acid potential; NNP = NP – AP; n = number of samples, Avg. = average, Stdv. = standard deviation.

Hole/ Trench	n	Paste pH_2				NNP (kg $CaCO_3$/t)			
		Min.	Max.	Avg.	Stdv	Min.	Max.	Avg.	Stdv.
LFG-005	3	3.98	7.75	5.37	2.07	-1.51	41.03	12.96	24.32
LFG-006	30	3.14	8.08	5.58	1.74	-12.92	47.78	9.23	14.71
LFG-007	3	5.47	7.81	6.47	1.21	0.32	13.33	6.55	6.52
LFG-008	13	4.14	7.69	5.77	1.16	-10.66	28.44	4..38	13.25
LFG-009	16	3.05	6.78	4.46	1.08	-12.81	51.74	2.82	14.02
Surface	2	3.72	4.09	3.91	0.26	-5.59	-5.49	-5.53	0.05
TH-GN-01	32	3.11	8.08	5.23	1.51	-18.8	29.15	3.48	10.64
Overall	99	3.05	8.08	5.30	1.53	-18.8	51.74	5.43	13.25

Table 4.6: Summary of ABA results for the unstable portion of GHN rock pile. Paste pH_2 = paste pH on powdered samples; NP = neutralization potential; AP = acid potential; NNP = NP – AP; n = number of samples, Avg. = average, Stdv. = standard deviation.

Hole/ Trench	n	Paste pH_2				NNP (kg $CaCO_3$/t)			
		Min.	Max.	Avg.	Stdv	Min.	Max.	Avg.	Stdv.
LFG-011	6	3.65	5.48	4.37	0.67	-14.47	3.27	-5.72	6.17
LFG-019	3	3.93	6.75	4.90	1.61	-9.36	14.48	-0.17	12.82
LFG-021	2	3.86	7.21	5.54	2.37	-3.85	14.78	5.47	13.17
LFG-022	1	3.98	3.98	3.98	-	-2.03	-2.03	-2.03	-
Surface	3	4.05	6.51	5.36	1.24	-3.90	11.34	2.36	7.97
Overall	15	3.65	7.21	4.80	1.19	-14.47	14.78	-1.26	8.76

4.2.3 Static Net Acid Generation (NAG)

The NAG test results are presented in bulk in Table C3, Appendix C and summarized in Tables 4.7 and 4.8. A total of 107 samples from the stable potion and 30 samples from the unstable portion were tested. Very few samples had NAG pH_1 and $NAG_{7.0}$ measured on them so the results are not included in this report. The samples from the stable portion of the pile have an average NAG pH_2 of 5.16 and $NAG_{4.5}$ of 2.68 kg $CaCO_3$/t. For the unstable portion of the pile, the averages are 3.99 and 3.73 kg $CaCO_3$/t, respectively. For all the 137 samples from the rock pile, the averages are 4.91 and 2.91 kg $CaCO_3$/t, respectively.

Table 4.7: Summary of NAG test results for the stable portion of the GHN rock pile. n = number of samples, Avg. = average, Stdv. = standard deviation.

Hole/ Trench	n	NAG pH_2				$NAG_{4.5}$ (kg $CaCO_3$/t)			
		Min.	Max.	Avg.	Stdv	Min.	Max.	Avg.	Stdv.
LFG-005	3	2.96	8.99	5.38	3.18	0.00	1.27	0.42	0.73
LFG-006	29	2.42	9.29	6.32	2.06	0.00	29.74	2.02	7.14
LFG-007	3	6.26	8.51	7.27	1.14	0.00	0.00	0.00	0.00
LFG-008	22	2.43	8.62	5.10	1.96	0.00	14.77	1.58	3.70
LFG-009	16	2.03	8.49	4.55	2.10	0.00	25.89	4.99	9.54
Surface	2	2.84	3.00	2.92	0.11	1.66	3.98	2.82	1.64
TH-GN-01	32	1.37	8.06	4.39	2.16	0.00	31.18	3.33	6.44
Overall	107	1.37	9.29	5.16	2.22	0.00	31.18	2.68	6.55

Table 4.8: Summary of NAG test results for the unstable portion of the GHN rock pile. n = number of samples, Avg. = average, Stdv. = standard deviation.

Hole/ Trench	n	NAG pH_2				$NAG_{4.5}$ (kg $CaCO_3$/t)			
		Min.	Max.	Avg.	Stdv	Min.	Max.	Avg.	Stdv.
LFG-011	20	2.29	6.35	3.31	1.03	0.00	22.42	4.79	5.51
LFG-019	3	2.44	7.89	4.65	2.87	0.00	9.83	3.62	5.40
LFG-021	3	3.45	8.77	6.18	2.66	0.00	1.22	0.41	0.71
LFG-022	1	3.86	3.86	3.86	-	0.00	0.00	0.00	-
Surface	3	2.88	8.80	5.69	2.97	0.00	4.06	1.35	2.34
Overall	30	2.29	8.80	3.99	1.88	0.00	22.42	3.73	5.03

4.3 Chemistry and Mineralogy Results

Results of X-ray fluorescence analysis are presented in Tables C4 to C7, Appendix C. Tables C4 and C5 contain concentrations of major metal oxides, sulfur, fluorine and loss on ignition (LOI) in percentages. Tables C6 and C7 contain concentrations of trace metals in parts per million (ppm). XRF analyses were done on 84 samples: 70 from the stable portion and 14 from the unstable portion of the pile.

Modal mineralogy was determined for 74 samples: 70 from the stable portion and 4 from the unstable portion of the rock pile. The results are presented in Tables C8 and C9 in Appendix C.

5 DISCUSSION

5.1 Variation of Current pH and Conductivity in GHN Rock Pile

To assess how paste pH_1 and paste conductivity (measured on unpowdered samples) vary in the rock pile, charts of paste pH_1 and paste conductivity against UTM Easting in trenches, and elevation in boreholes were plotted. UTM Easting was used for the trenches because the trenches were dug in an East-West direction across the thickness of the pile, and elevation was used for the boreholes because all the boreholes were vertical. Lower values of UTM Easting and higher values of elevation are closer to the open face (or edge) of the rock pile. The paste pH and paste conductivity plots are discussed separately for the stable and unstable portions of the pile.

5.1.1 Stable Portion of GHN

Plots of paste pH_1 and paste conductivity are presented in Figures 5.1 to 5.4 for trenches LFG-005, LFG-006, and LFG-007, and borehole TH-GN-01 respectively, in the stable portion of the rock pile. In Figure 5.1, the pH values (i.e. paste pH_1) are mostly below 4.0 for the outer units (C, I, J, K and N) and the innermost units (M, K and the rubble zone). The units in the middle have the highest pH values. The traffic zone in Bench 1, representing the compacted horizontal surface at the crest of the pile, also has high pH values.

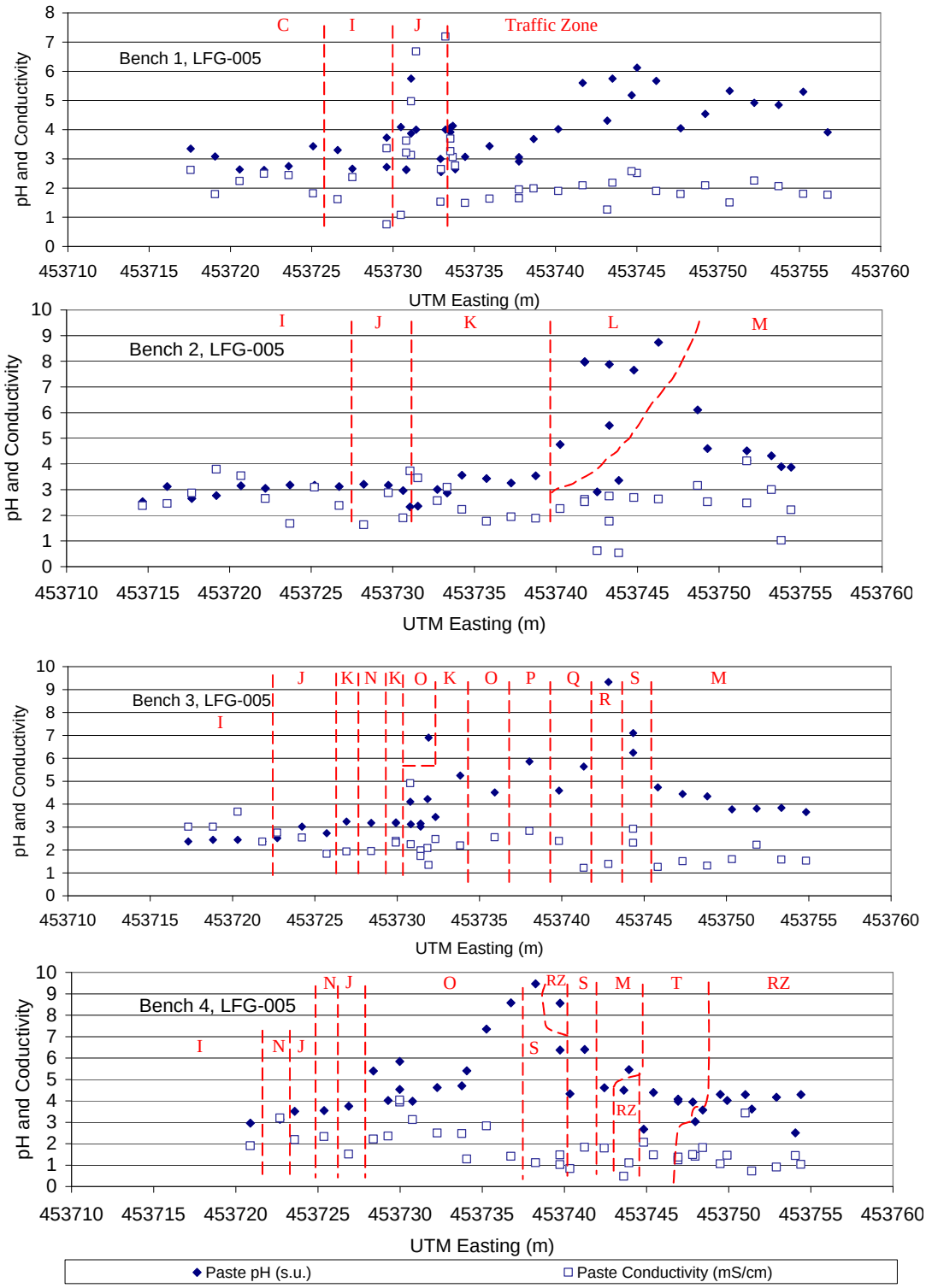

Figure 5.1: Plots of paste pH_1 and paste conductivity along benches in Trench LFG-005. The red dotted lines and labels represent geologic units. RZ = rubble zone. The outer (C, I, J, K and N) and innermost (T, M and RZ) units have the lowest pH. The middle units (e.g. L, S and O) have the highest pH, although O is quite variable. Paste conductivity is not clearly linked to the units.

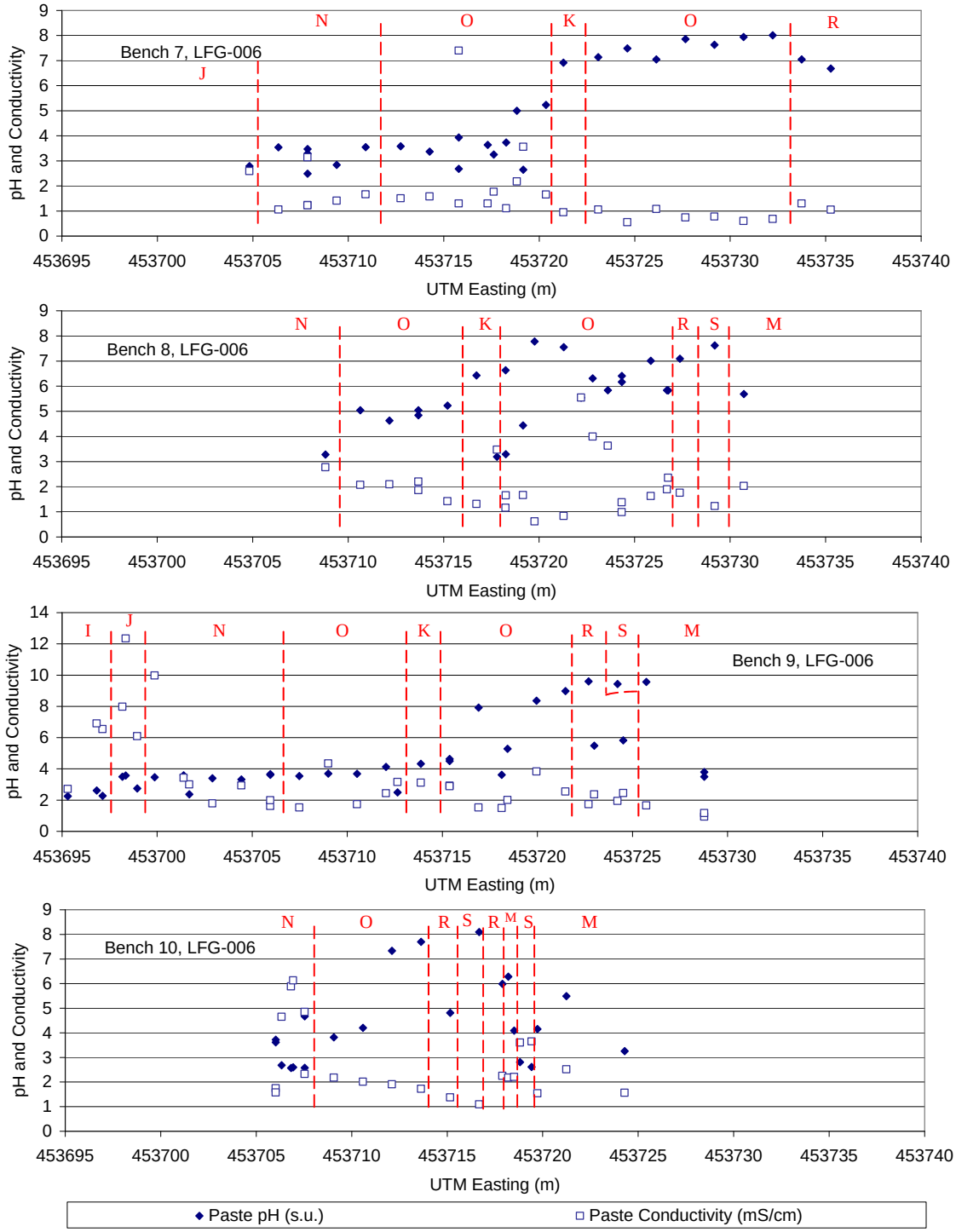

Figure 5.2: Plots of paste pH_1 and paste conductivity along benches in Trench LFG-006. The red dotted lines and labels represent geologic units. The outer units (I, J and N) have the lowest pH and the outer part of Unit O has lower pH than the inner Unit O. The innermost unit (M) also has some low pH values. The other units have variable pH. Paste conductivity is not clearly linked to the units.

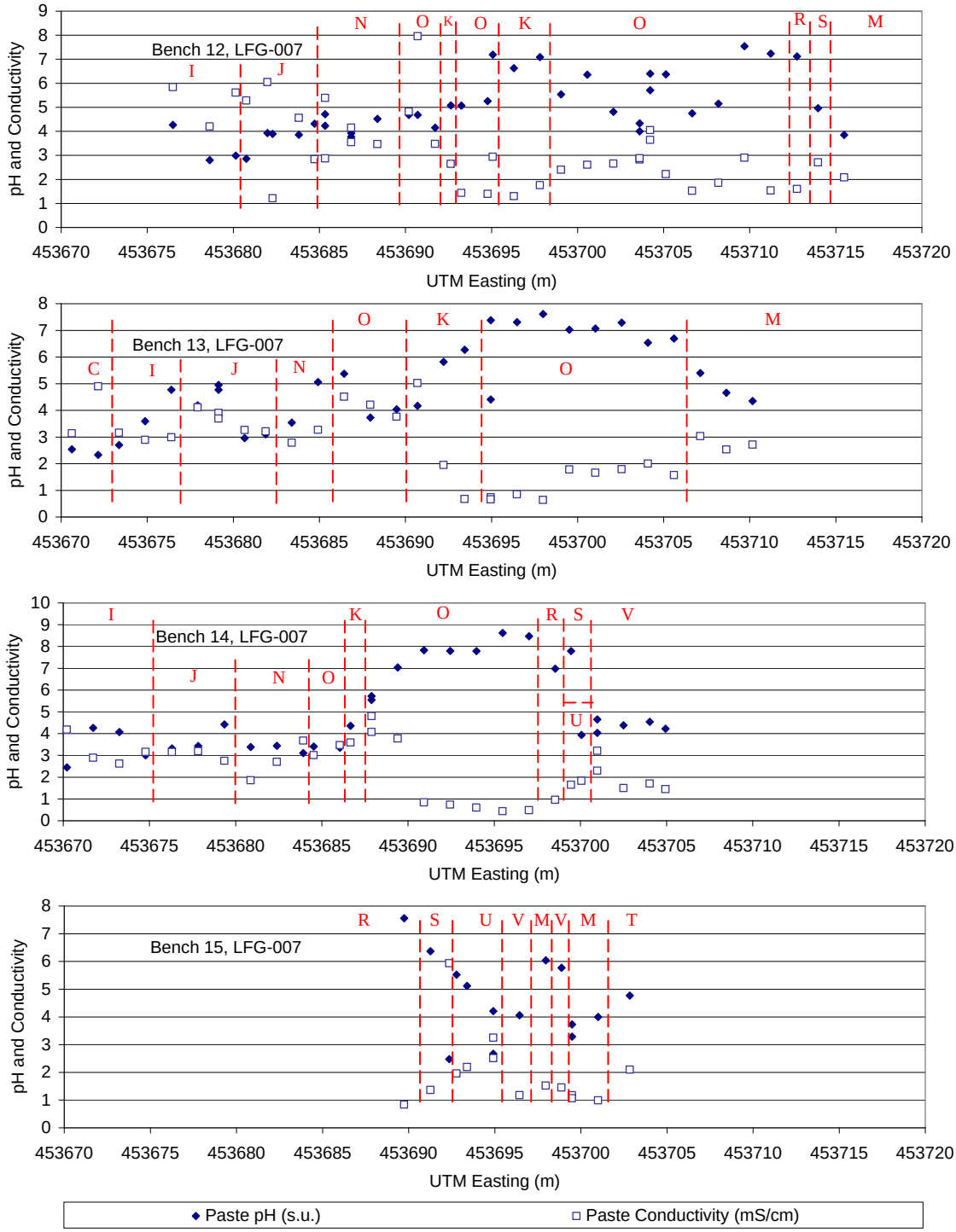

Figure 5.3: Plots of paste pH_1 and paste conductivity along benches in Trench LFG-007. The red dotted lines and labels represent geologic units. The outer units (C, I, J andN) have the lowest pH and the outer part of unit O has lower pH than the inner unit O. The innermost units (M, T and V) also have low pH values. The other units have variable, but mostly high, pH. There is a slight negative correlation between paste pH_1 and paste conductivity.

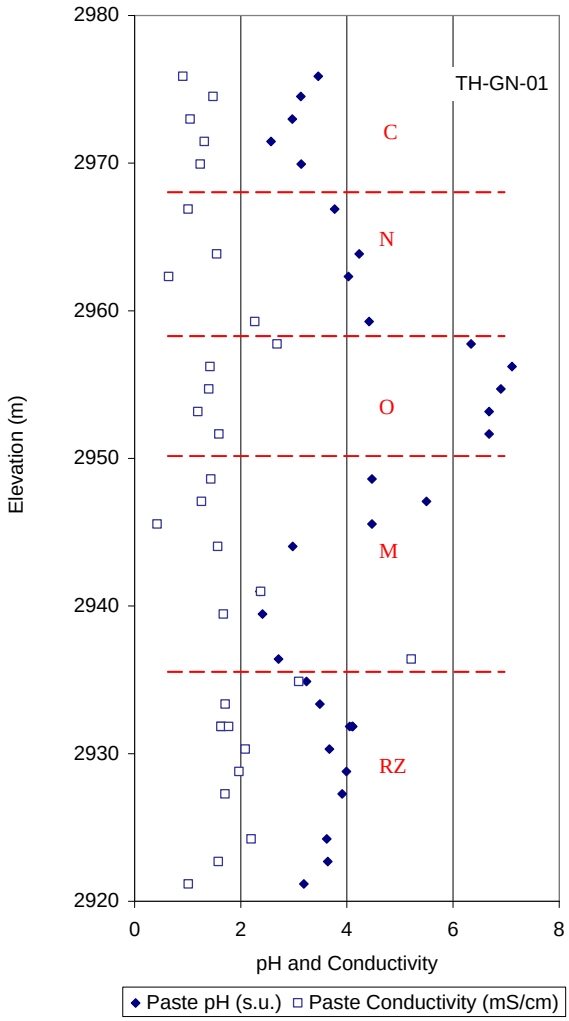

Figure 5.4: Plot of paste pH_1 and paste conductivity along borehole TH-GN-01. The red dotted lines and labels represent geologic units. RZ = rubble zone. The outer units (C and N) and innermost units (M and RZ) have the lowest pH. Unit O in the middle has the highest pH. Paste conductivity does not change much from unit to unit.

Unlike the paste pH, the paste conductivity plots do not show any clear trend along the benches. In Figure 5.2, the paste pH variation on individual benches is similar to what is observed in trench LFG-005 (Figure 5.1) in that the pH is lowest in the outermost units (I, J and N). Not all the benches cut across the whole thickness of the pile and so it is not surprising that the top three benches in Figure 5.2 have relatively high pH values in the innermost units.

The pH trends observed in the two trenches discussed above are also shared by trench LFG-007 in Figure 5.3. It is interesting to note that in Bench 15, because the samples were taken closer to the eastern end of the trench, the low pH units (I, J and N) are absent, and the pH values start from the highest in unit R and reduce towards the end of the bench. The samples in LFG-007 show a slight negative correlation between paste pH_1 and paste conductivity. In borehole TH-GN-01 (Figure 5.4), paste pH is lowest in the outer units (C and N) and the inner units (M and the rubble zone). Bearing in mind that the GHN rock pile is an end-dumped pile and inclined at approximately 20-40^o, the pH trend in the borehole can be translated to be the same as has been observed in the trenches. Again, paste conductivity values do not show any convincing trend in the borehole.

To be able to picture the variation of paste pH_1 in the stable portion of GHN rock pile better, pH values for all the samples considered for this work were plotted on a single vertical plane representing a longitudinal cross-section through the rock pile (Figure 5.5). Different colors were used to represent different pH ranges. The plot confirms the observation that paste pH_1 is lowest near the face and base of the pile. However, the highest values occur not exactly in the middle, but about a tenth to a quarter of the pile thickness from the face of the pile. It is also observed from Figure 5.5 that over half the thickness of the pile from its base has pH values below neutral and mostly less than 4.0. Values of pH above neutral are only observed within the upper half of the pile's thickness, with most of them being 5 to 30 m below the traffic surface. Also, the concentration of high pH values reduces as elevation drops towards the toe of the pile.

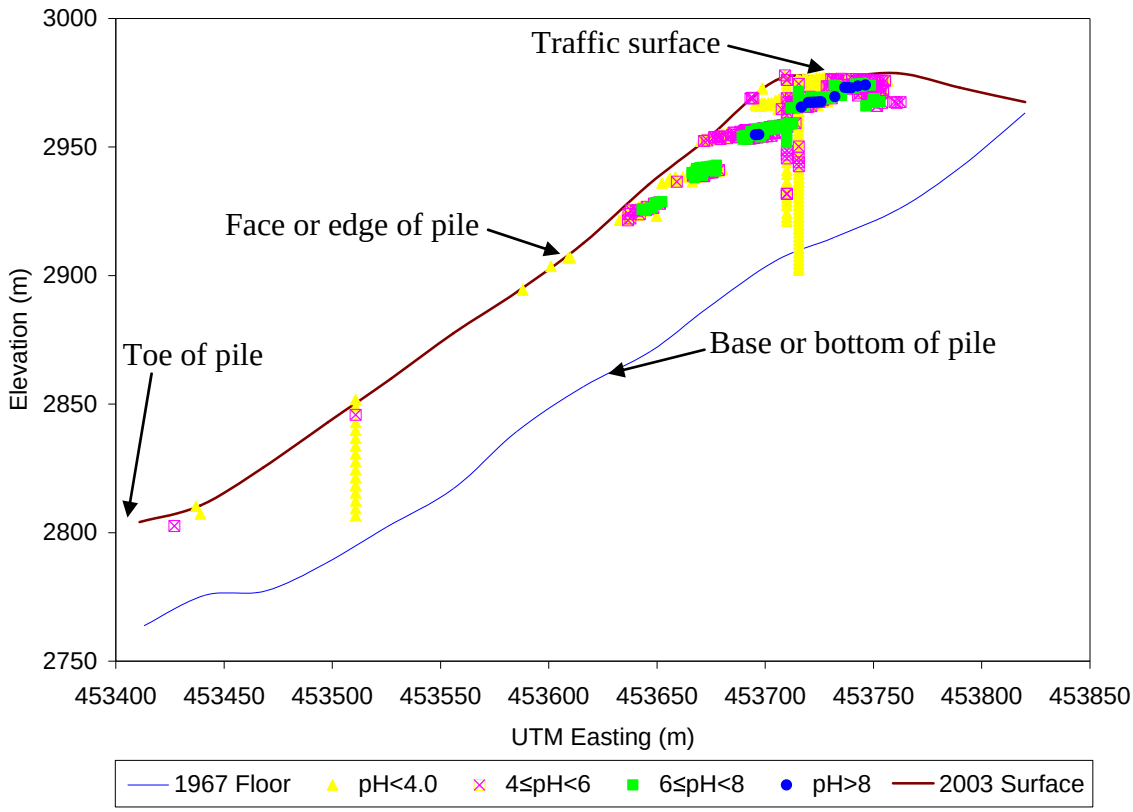

Figure 5.5: Longitudinal cross-section through the stable portion of GHN rock pile showing samples with different ranges of paste pH_1. The two continuous lines represent the surface and bottom of the stable portion of the pile as determined from 2003 and 1967 contour maps, respectively. The plot shows that there is a high pH zone below the traffic surface and subparallel to the pile face. The high pH zone is sandwiched between two low pH zones, one close to the surface and the other close to the base. The concentration of high pH samples decreases with decreasing elevation from the top of the pile down.

To explain the pH trends observed in Figures 5.1 to 5.5 so far, one needs to bear in mind the processes and factors that contribute to low pH soils as discussed in Chapter 2. The low pH samples close to the edge of the pile are most likely the results of greater exposure of that part to the atmosphere. Atmospheric oxygen and moisture from snow and rain have increased the rate of oxidation of sulfide minerals near the edge of the pile to produce the acidity and, therefore, low pH soils. This is also enhanced by the presence of microorganisms, which have been observed on the piles at Questa. The low

pH observed in samples close to the base of the pile is also thought to be the result of oxidation due to the ample supply of air by advective flow through rubble zones (rubble zones were observed near the base of the pile in Bench 4 of LFG-005, and borehole TH-GN-01), and water from perched water tables that drain along the contact between the rock pile and the original ground. However, the thickness of low pH soils close to the base is quite large and it is possible that some of the material close to the base was already oxidized before it was dumped in the pile. This will also explain why the borehole close to the toe of the pile has low pH values throughout its depth. It is worth mentioning here that in rock pile construction from an open pit, the topmost material in the pit, which is most of the time weathered overburden, becomes the base of the rock pile. Also, in end-dumped rock piles, the first materials to be dumped settle closer to the toe of the pile. Differences in rock type could also be the reason for the different pH zones in the rock pile, and this is investigated later in the chapter.

5.1.2 Unstable Portion of GHN

Mapping of geologic units could not be done on the unstable portion of the pile because the material was so jumbled up by the sliding movement that it was impossible to identify the units: the units had been folded together. Figure 5.6 compares photographs from the stable and the unstable portions of the GHN rock pile.

Figures 5.7 and 5.8 are plots of paste pH_1 and paste conductivity along two benches in trench LFG-011, and borehole TH-GN-07S, respectively, in the unstable portion of the GHN rock pile. One obvious observation is the low pH values that run through both the

Figure 5.6: Photographs of benches on the stable (left) and unstable (right) portions of the GHN rock pile. The stable portions shows well defined inclined units with different colors. The unstable portion is mixed up such that the units are not identifiable.

benches and the borehole. Except for a few neutral pH samples at about 2840 m in the borehole, all the samples have pH values less than 5.0. Also, the pH does not exhibit any trends with distance from the edge of the pile, unlike what was observed in the stable portion. Although, Bench 44 has a few higher pH samples near the middle of the trench, the differences are subtle and not shared by the other plots.

In Figure 5.8, there is a weak negative correlation between paste pH_1 and paste conductivity. Particularly, the highest paste pH_1 occurs for the same samples that have the lowest paste conductivity at about 2840 m, and the lowest paste pH_1 occurs close to the highest paste conductivity between 2820 and 2825 m. Also, the paste conductivity is lower than 2.0 mS/cm for the upper half of the borehole, and higher than 2.0 mS/cm for the lower half. The relationship between paste pH_1 and paste conductivity is looked at in detail in the next subsection with a plot of paste pH_1 against paste conductivity.

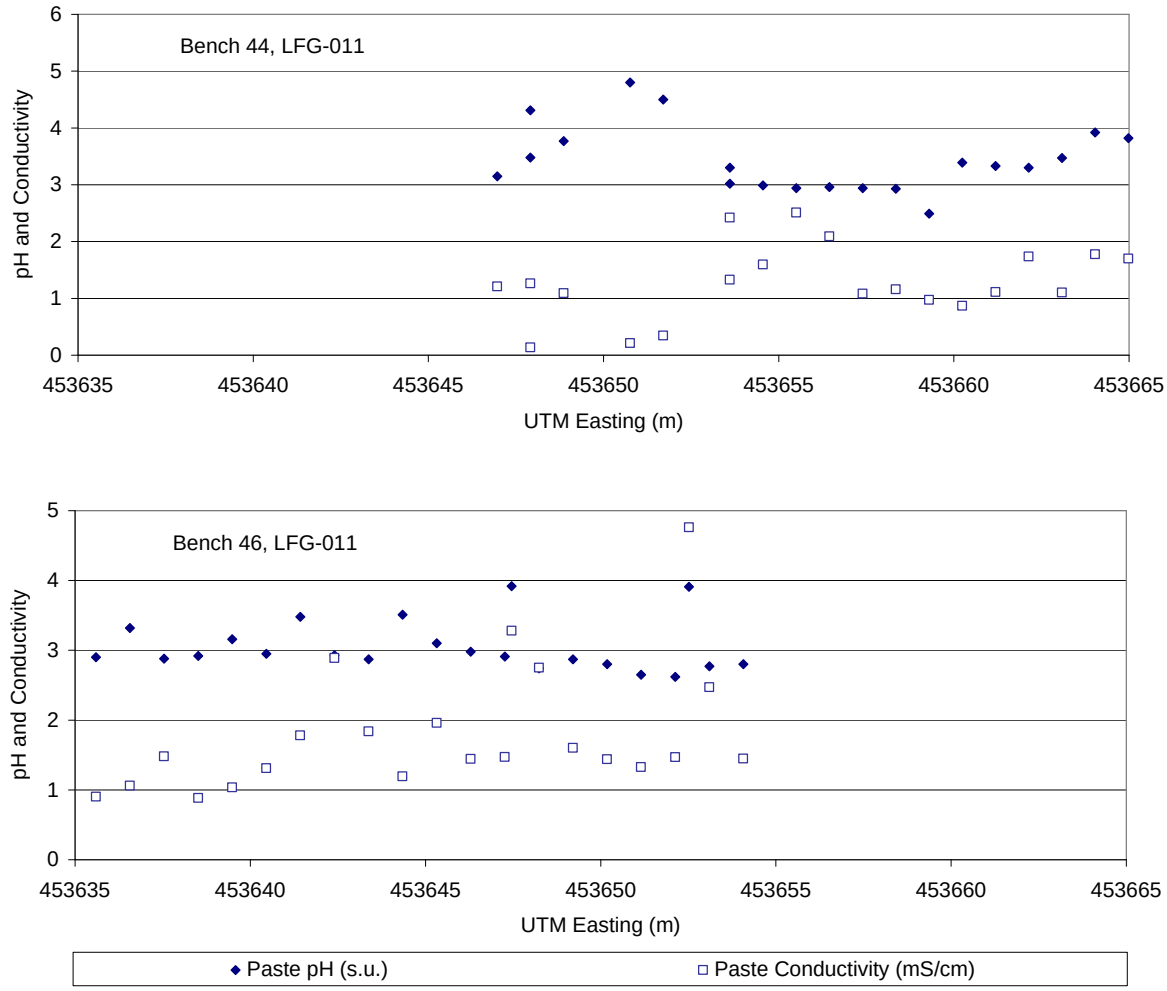

Figure 5.7: Plots of paste pH_1 and paste conductivity along benches in Trench LFG-011 in the unstable portion of GHN rock pile. The pH values are mostly less than 4.0 and do not show any correlation to distance from the edge of the pile.

A clearer picture of the variation of paste pH_1 in the unstable portion of the pile is shown in Figure 5.9, which is a plot of all the samples from the unstable portion of the pile in a single vertical plan using different colors to represent different pH ranges. The pH values in the upper part of the unstable portion of the pile are mostly below neutral (except for three samples which are all close to the edge) and do not show any trend across the thickness of the pile. However, the boreholes in the lower part of the unstable pile have quite a number of high pH samples which are mostly close to the top of the

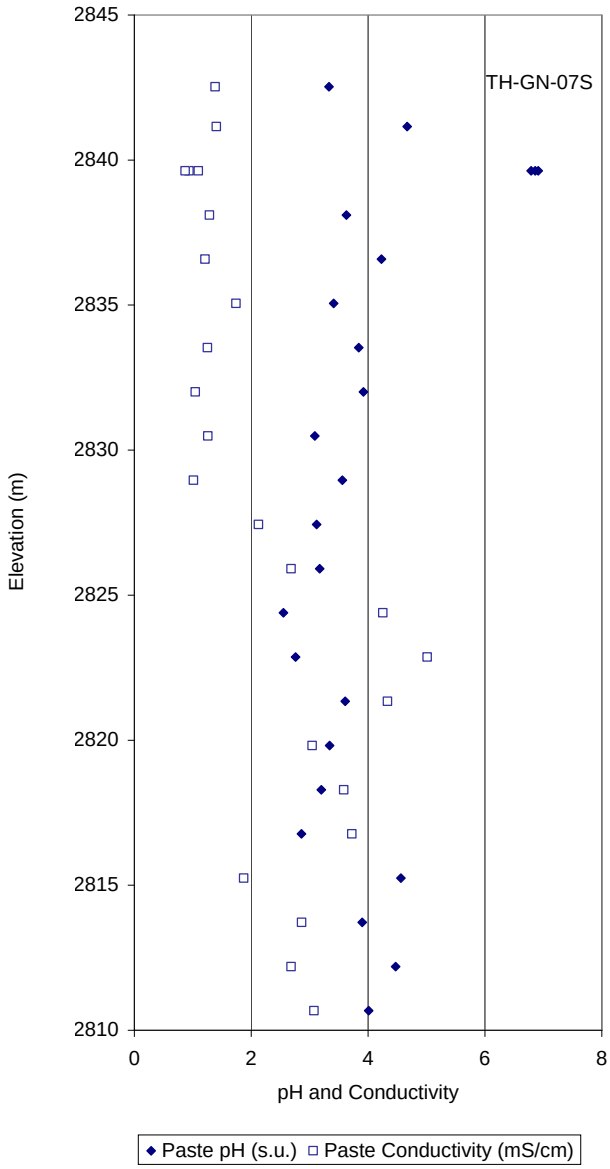

Figure 5.8: Plots of paste pH_1 and paste conductivity along borehole TH-GN-07S in the unstable portion of the GHN rock pile.

boreholes. The slow but constant movement of the pile material is likely to have altered the permeability of the soil and given it greater access to moisture and air over the years, resulting in increased oxidation to produce the lower pH values of the upper part of the unstable pile portion. It is likely that the sliding introduced several episodes of loosening the material and closing it up at different locations on the pile, resulting in a

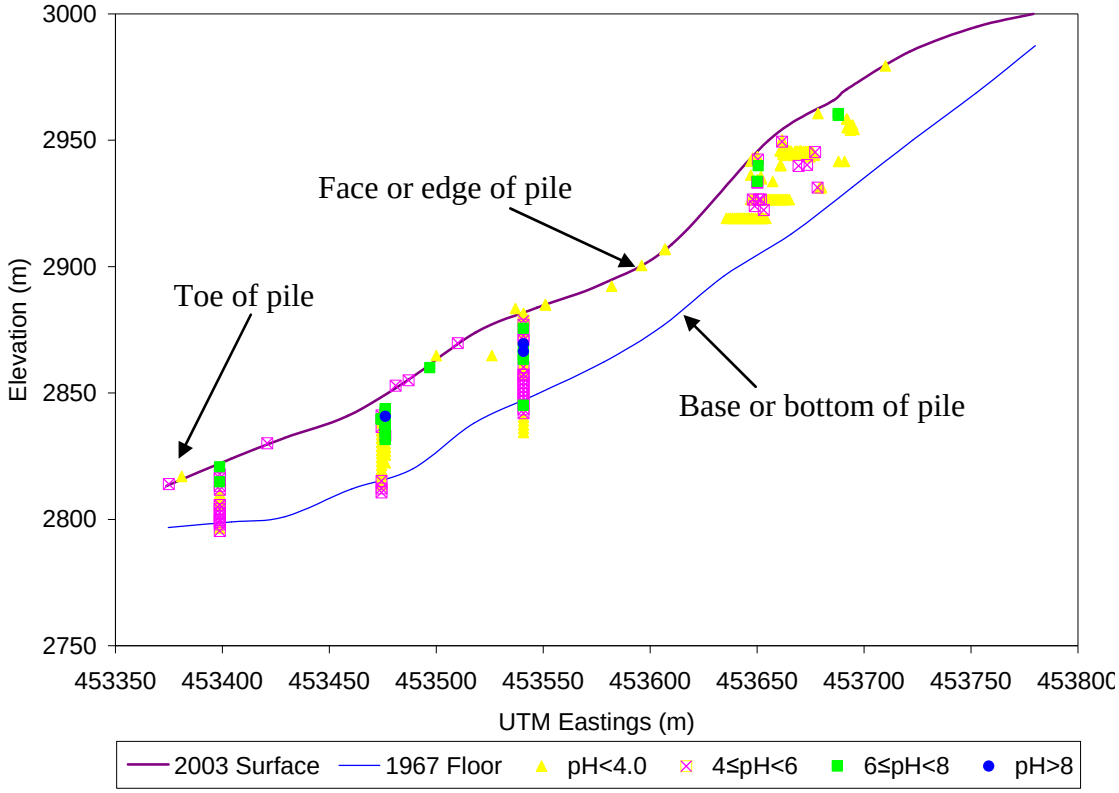

Figure 5.9: Longitudinal cross-section through unstable portion of GHN rock pile showing samples with different ranges of paste pH_1. The two continuous lines represent the surface and bottom of the unstable portion of the pile as determined from 2003 and 1967 contour maps, respectively. Generally, the samples in the upper part of the pile have lower pH values than those in the boreholes at the lower part.

net increase in permeability. With the increase in permeability of the soil, seepage of water into the pile would increase and allow more water to seep at higher elevations and less water to run off to lower elevations before seeping into the soil. This phenomenon may also account for the high pH values in the top portions of the boreholes at lower elevations.

From the foregoing discussions, at least three major differences can be identified between the stable and unstable portions of the GHN rock pile with regards to paste

pH_1: (1) paste pH_1 is generally higher in the stable portion than in the unstable portion; (2) paste pH_1 is lowest in units near the edge and base of the stable portion, but does not show any trend in the unstable portion; (3) the highest pH values are in the upper part of the stable portion, but in the unstable portion, they occur in the lower part.

5.1.3 Relationship between Paste pH_1 and Paste Conductivity

Figure 5.10 shows the relationship between paste pH_1 and paste conductivity for the stable and unstable portions of the pile. There is a slight negative correlation between the two parameters for both portions of the pile. Samples with the highest paste pH_1 have paste conductivities that are about two orders of magnitude lower than samples with the lowest paste pH_1. In the stable portion, samples from the surface (Units A through H), outer (Units I, J, K and N) and innermost (Units M, T and V) parts that were identified in Section 5.1.1 to have the lowest pH, plot mostly below pH 6.0. Samples from the middle units (e.g. O, S, R and U) have low to high pH values. The negative correlation between pH and conductivity is expected since the oxidation of sulfides to produce acidity and low pH will also release ion concentrations into solution. However, Figure 5.10 shows that the relationship is rather weak. It also suggests that not all the oxidation or dissolution products are soluble as there are many low pH samples with low paste conductivity too. There may be some secondary reaction products that have a range of solubilities. The presence of such minerals is not necessarily reflected in the measurement of bulk paste conductivity.

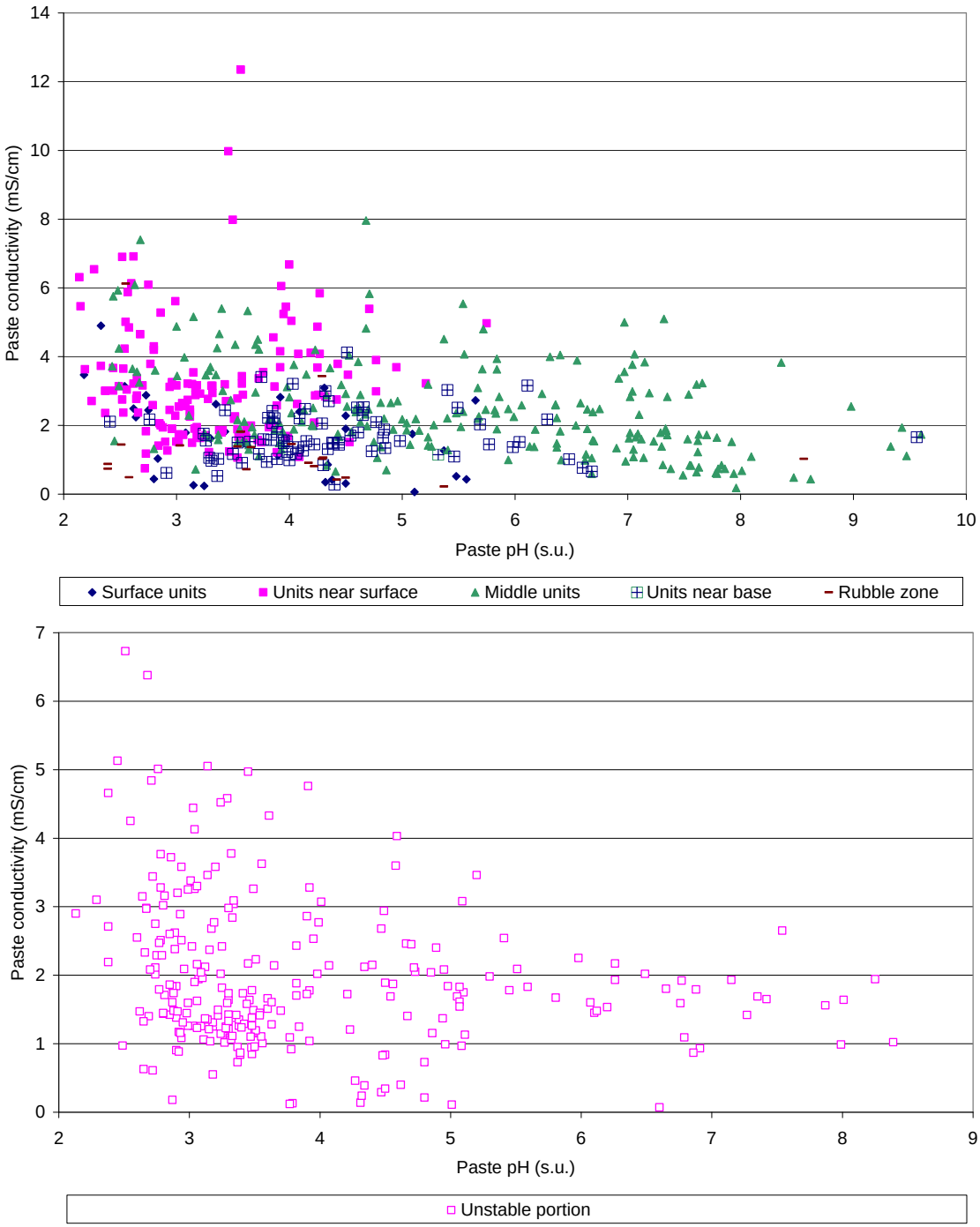

Figure 5.10: Plots of paste pH_1 against paste conductivity for the stable (top) and unstable (bottom) portions of the pile. Both charts show a slight negative correlation between paste pH_1 and paste conductivity. In the top chart, different groups of units are plotted separately. Apart from the middle units (O. R, S, U, W), which have low through high pH values, all the other units have most of their pH values less than 6.0.

5.2 Variation of predictive Test Results in GHN Rock Pile

Acid-base accounting (ABA) and net acid generation (NAG) test results were plotted along four benches and one borehole to find out how they vary in the rock pile. The ABA results are the net neutralization potential (NNP) and the paste pH_2 (pH measured on powdered samples); and the NAG results are the NAG pH_2 and $NAG_{4.5}$ (i.e. NAG measured at pH 4.5). The plots are presented in Figures 5.11 to 5.15 for Benches 9, 19, 23 and 46, and borehole TH-GN-01, respectively. Apart from Bench 46 (Figure 5.14) which is in the unstable portion of the rock pile, all the other benches and the borehole are in the stable portion. Note that not all the samples had ABA performed on them so there are some samples in the charts without NNP values.

The paste pH_2 values on Bench 9 follow the same trend along the bench as the paste pH_1 values (compare Figures 5.2 and 5.10), although the paste pH_2 values are generally higher than their respective paste pH_1 values for lower pH's and conversely for higher pH's. This trend is true for borehole TH-GN-01 (Figures 5.4 and 5.14) and Bench 46 (Figures 5.6 and 5.13). Figure 5.16 shows that if a sample's paste pH_1 is less than 7.5, it has paste pH_2 > paste pH_1, and if the paste pH_1 is greater than 7.5 it has paste pH_1 > paste pH_2. The relationship between these two paste pH data sets may be the effect of soluble carbonate minerals and the deionized water used for the test. The paste pH of a soil sample is determined by the soluble minerals that are made available to go into solution by the test procedure. So if the sample is crushed and pulverized, soluble carbonate minerals like calcite, that are other wise concealed in the uncrushed sample, will go into solution more readily and increase the pH of the solution or paste. This is why low pH soils get an increase in paste pH when they are powdered.

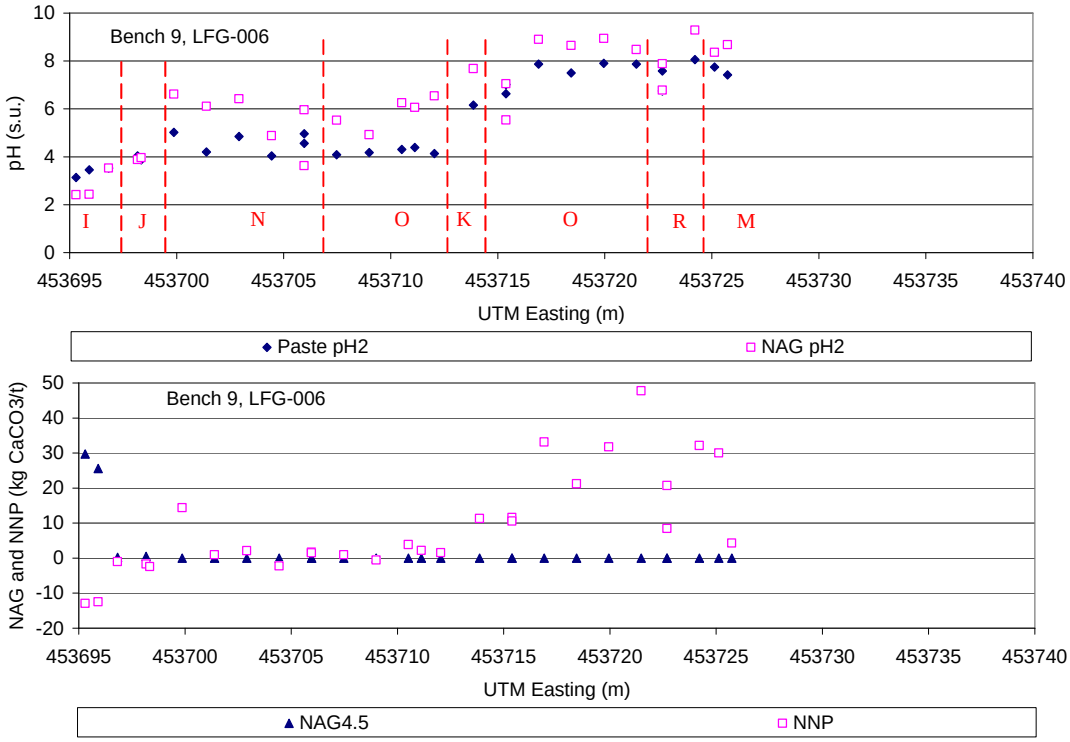

Figure 5.11: ABA and NAG results for Bench 9, Trench LFG-006. The top chart is for paste pH_2 and NAG pH_2; and the bottom chart is for $NAG_{4.5}$ and NNP. Red lines represent units

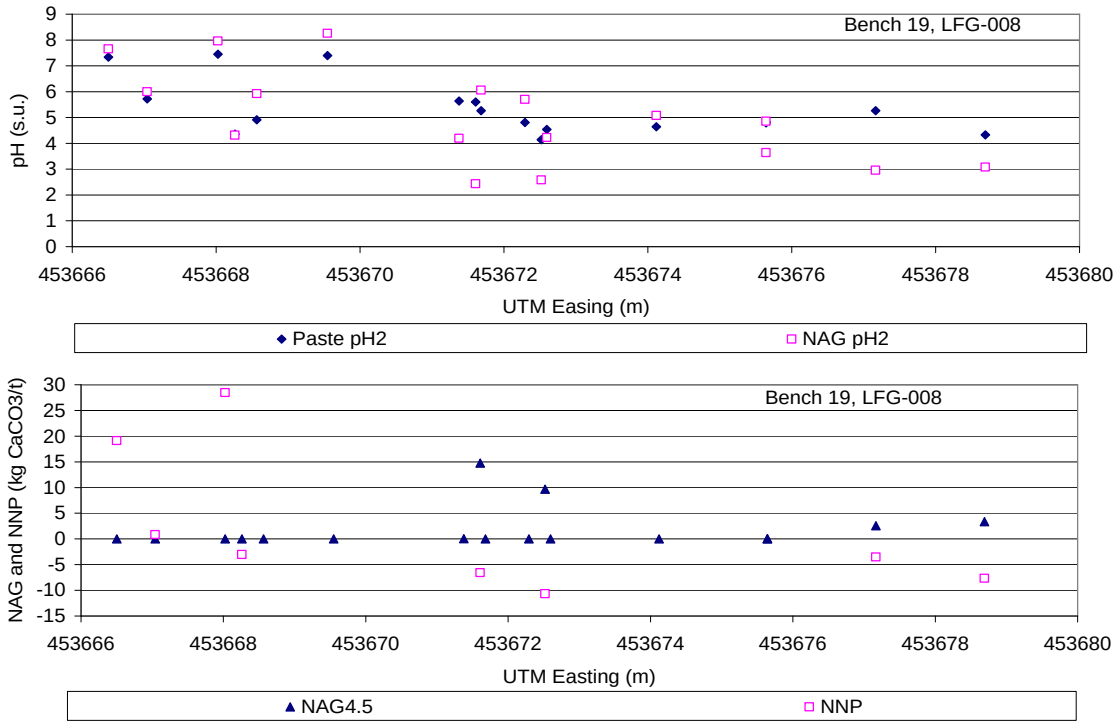

Figure 5.12: ABA and NAG results for Bench 19, Trench LFG-008. The top chart is for paste pH_2 and NAG pH_2; and the bottom chart is for $NAG_{4.5}$ and NNP.

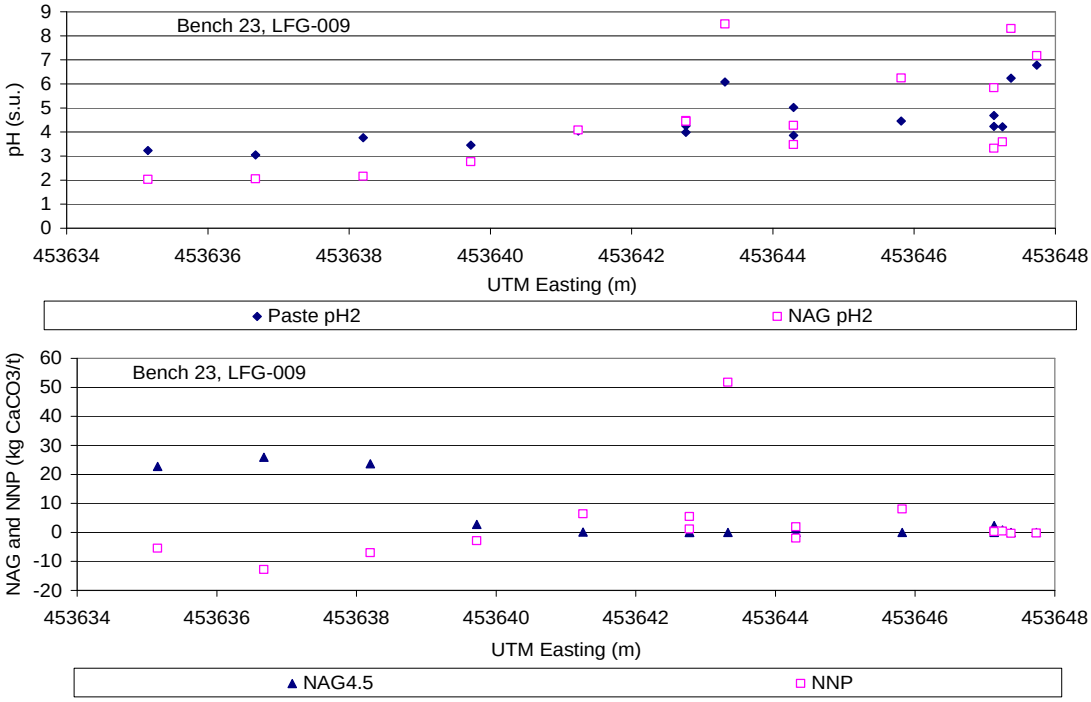

Figure 5.13: ABA and NAG results for Bench 23, Trench LFG-009. The top chart is for paste pH_2 and NAG pH_2; and the bottom chart is for $NAG_{4.5}$ and NNP.

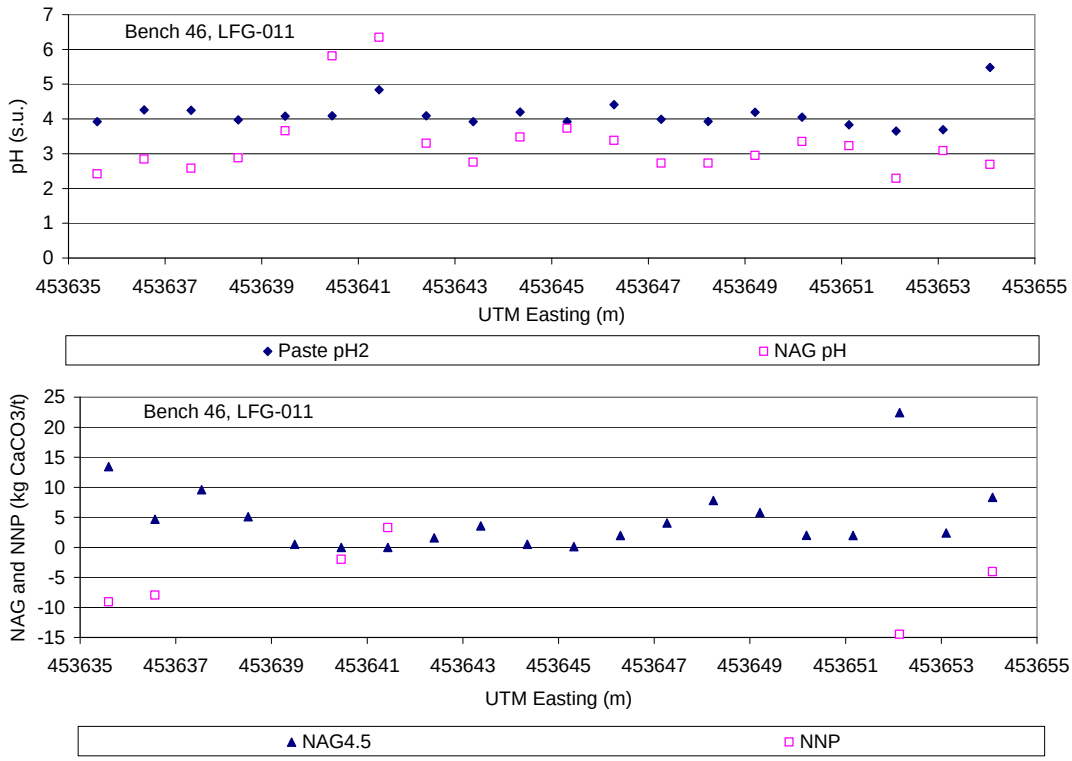

Figure 5.14: ABA and NAG results for Bench 46, Trench LFG-011. The top chart is for paste pH_2 and NAG pH_2; and the bottom chart is for $NAG_{4.5}$ and NNP.

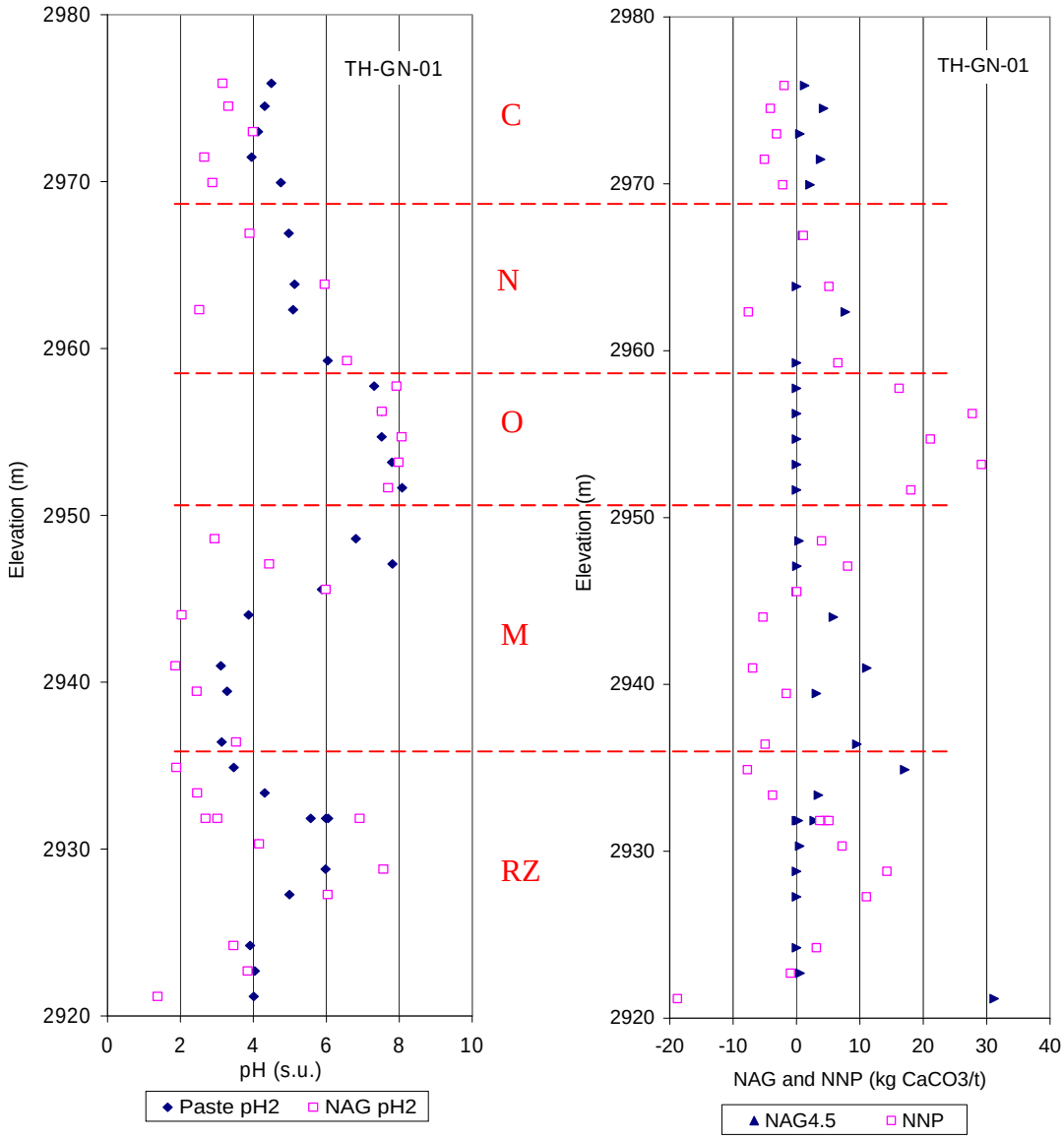

Figure 5.15: ABA and NAG results for borehole TH-GN-01. The left chart is for paste pH_2 and NAG pH_2; and the right chart is for $NAG_{4.5}$ and NNP. The red dotted lines represent different geologic units.

Robertson GeoConsultants Inc.(2000) made a similar observation when they tested samples from other rock piles at the Questa mine. However, high pH soils do not behave the same way, not because they have no soluble carbonates, but because the deionized water used for the test has a pH of about 5.8, which is significantly lower than pHs above 7.5 and therefore overcomes the effect of dissolved carbonates and reduces

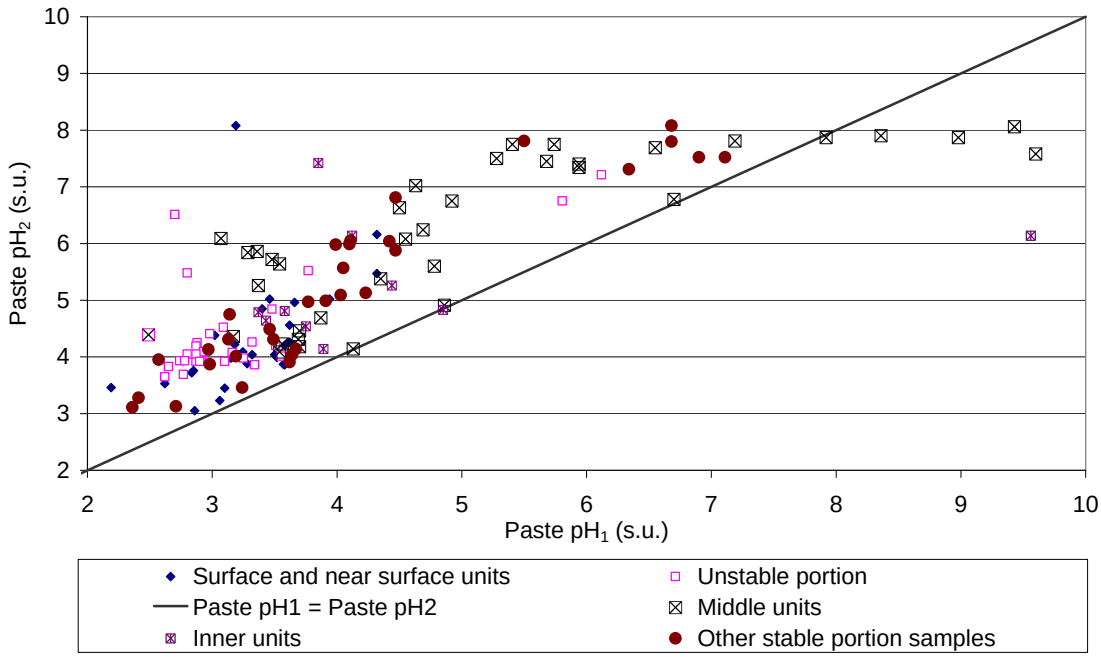

Figure 5.16: Plot of paste pH_1 versus paste pH_2. Samples with paste pH_1 less than 7.5 have lower paste pH_1 than paste pH_2. The opposite is true for samples with paste pH_1 greater than 7.5.

the pH of the entire paste. As will be expected, the samples from the unstable portion of the pile and the low pH units of the stable portion all plot above the equal line in Figure 5.16. Only samples from the middle units which have high pH plot below the equal line.

NAG pH values also follow a similar trend as paste pH_1 and paste pH_2 values: that is samples with higher paste pH values also have higher NAG pH values. High pH samples have NAG pH's that are higher than their paste pH's and low pH samples have NAG pH's that are lower than their paste pH's. This is further illustrated in Figure 5.17. The relationship between paste pH and NAG pH suggests that samples with low paste pH have higher acid producing potential and those with high paste pH have lower acid producing potential. This is an indication that samples with low paste pH values have less neutralization capacity remaining in them. Better understanding of the relationship

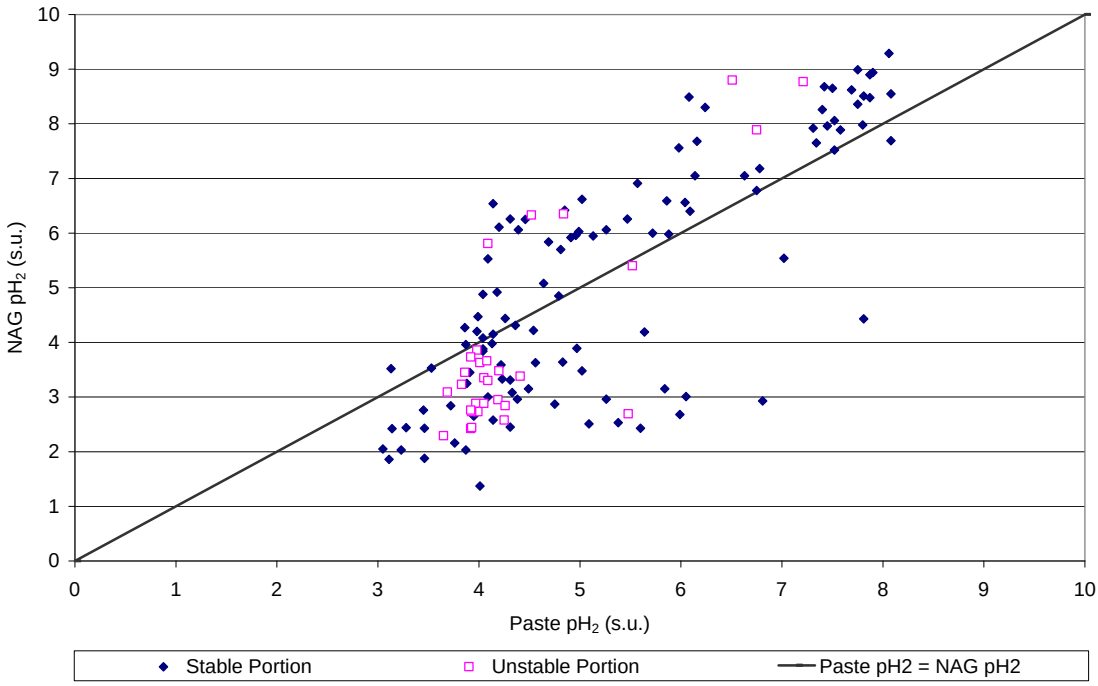

Figure 5.17: Relationship between paste pH_2 and NAG pH_2. Samples with low paste pH_2 have low NAG pH_2.

between the current soil pH and the potential for future acid generation or neutralization is gained from the discussion of $NAG_{4.5}$ and NNP results below. Since the fact has been established that in the stable portion of the pile the outermost and innermost units have the lowest paste pHs, it is inferable that they also have the lowest NAG pH_2.

In Figures 5.11 to 5.15, $NAG_{4.5}$ and NNP show a trend that is related to the paste pH values along the benches: samples with lower paste pHs have higher $NAG_{4.5}$ and lower NNP values, whereas samples with higher paste pH's have lower $NAG_{4.5}$ and higher NNP values. Specifically, most of the samples with paste pH_2 less than 4.5 have positive $NAG_{4.5}$ and negative NNP, and most of the samples with paste pH_2 greater than 4.5 have zero NAG and positive NNP. In Figure 5.14, because almost all the samples on Bench 46 have low paste pH_2 (less that 4.5), almost all the NAG values are positive.

The observed relationship between $NAG_{4.5}$ and NNP versus paste pH_2 is made clearer in Figure 5.18. Remember that unlike the ABA test which can give both positive and negative values of NNP, the NAG test has a lower detection limit of zero for $NAG_{4.5}$, and so it will assign a zero value to most samples with positive net neutralization potentials (NNP).

5.2.1 Summary of Discussions on Static Test Results

Comparisons made so far between paste pH, ABA and NAG results indicate that samples that have low paste pH values have higher net acid producing potentials or lower net acid neutralization potentials. From the earlier argument that samples with lower paste pH values have been oxidized more, it follows that the oxidation has not

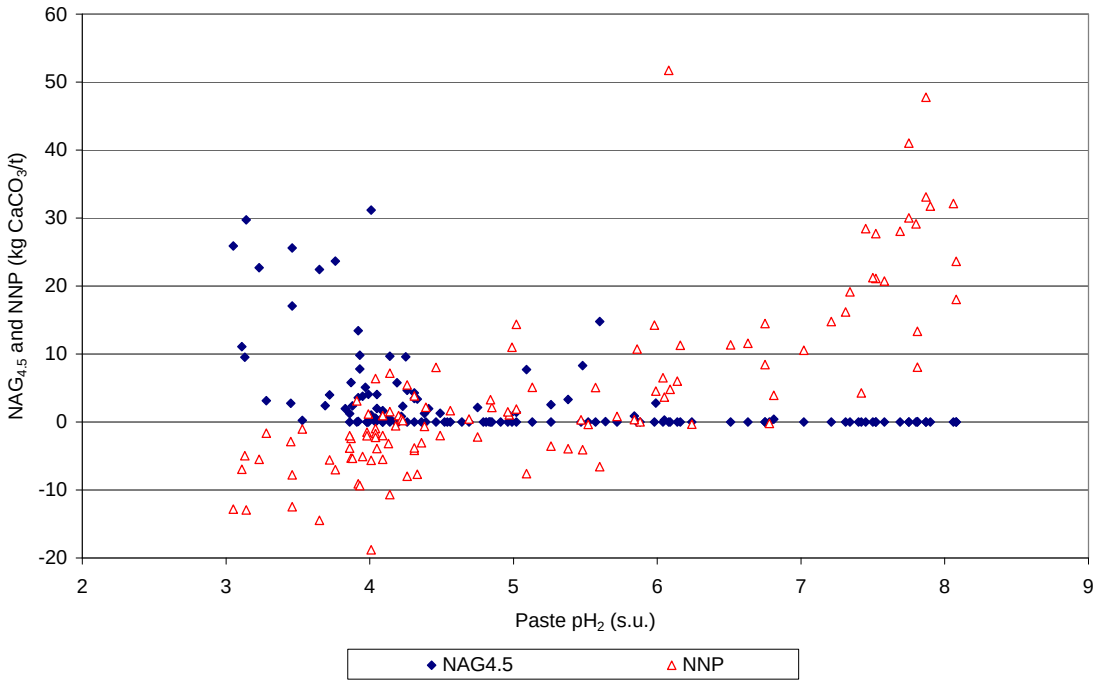

Figure 5.18: Plot of paste pH_2 versus $NAG_{4.5}$ and NNP. NNP covaries positively with paste pH_2. $NAG_{4.5}$ covaries negatively with paste pH_2 only below pH 5, since $NAG_{4.5}$ is mostly zero above pH 5.

only resulted in the generation of acid (the source of the low pH) but the acid it generated has consumed some, probably most, of the neutralizing capacity that might have been in the soil originally. Samples with high paste pH values have higher NNP values because either they have less reactive sulfides that can oxidize to produce acid to consume the neutralizers, or they have not yet been exposed much to oxidizing environments or both. For the stable portion of the rock pile, the geologic units near the edge and base of the pile have the lowest paste pH, NAG pH and NNP, and the highest $NAG_{4.5}$ as observed in Figure 5.11 and 5.15.

5.3 Relationships between acid producing characteristics, and lithology, mineralogy and chemistry of GHN samples

The GHN rock pile consists of two major lithologic units that were mined from the Questa open pit: andesite (including latite and quartz latite) and Amalia Tuff. Both lithologies have undergone hydrothermal quartz–sericite-pyrite (QSP) alteration, which is more intense in the Amalia Tuff than the andesite (Carpenter, 1968). Therefore, one major compositional difference between these two rock types is that Amalia Tuff has higher silica and pyrite content. Some of the andesites have undergone propylitic alteration. The samples collected from the rock pile have varying proportions of andesite and Amalia Tuff. This section explores the effect of the lithologic units and their mineralogical and chemical compositions on the acid-producing characteristics of the GHN samples.

5.3.1 Effects of Rock Type on NNP

Comparing the description of the GHN geologic units in Table 4.1 to the plots of paste test, ABA and NAG results along benches and boreholes (Figures 5.1 – 5.4, 5.11 and

5.15), it is clear that the units that contain appreciable amounts of Amalia Tuff such as C (70% Amalia), M, N and the rubble zones have the samples with low paste pH and NNP. This is an indication that samples with higher percentage of Amalia have higher acid-producing potential. In Figure 5.19 samples with high quartz (more than 40%) and SiO_2 (more than 65%) proportions represent Amalia-rich samples and they have low NNP values (less than 20 kg $CaCO_3$/t). Conversely, samples with low quartz and SiO_2 contents, representing andesite-rich samples, have low to high NNP values. In Figure 5.20, epidote, CaO and NaO_2 have positive correlations with NNP. Epidote is a propylitic alteration mineral more abundant in andesite-rich samples, and Ca and Na are also more abundant in the Questa andesites because of the greater percentage of feldspars (before alteration) in andesites. In the Questa rocks, the feldspars have been altered to minerals such as epidote, smectite, albite, gypsum and calcite, which contain Na and Ca. Thus, Figure 5.20 is another proof of the dependence of NNP on rock type. There is, therefore, enough evidence to confirm that the acid-producing potential of the GHN samples is partly determined by the relative proportions of Amalia Tuff and andesite. Samples with higher proportions of Amalia Tuff are more likely to generate acid and at a faster rate.

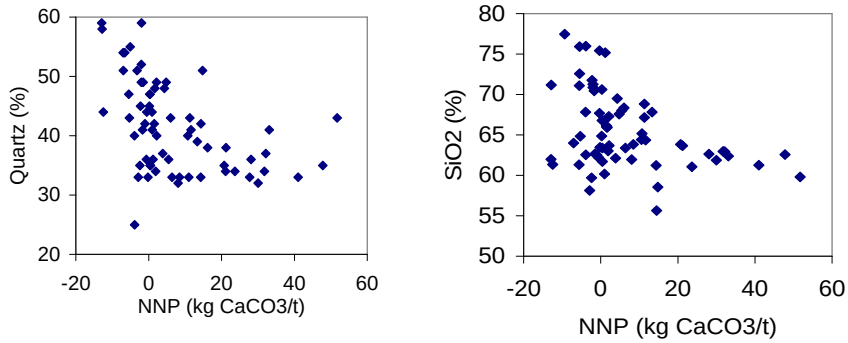

Figure 5.19: Plots of quartz (left) and SiO_2 (right) versus NNP. Both quartz and SiO_2 have negative correlation with NNP.

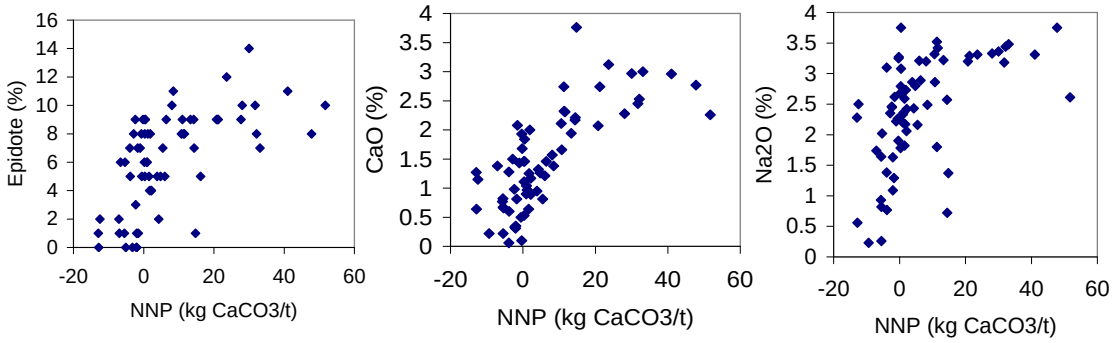

Figure 5.20: Plots of CaO (left) and NaO_2 (right) versus NNP. Both CaO and NaO_2 show a positive correlation with NNP.

5.3.2 Acid-Generating and Acid-Consuming Minerals

In Figure 5.21 NNP is plotted against pyrite concentrations determined with two different methods: the Rietveld method and modal mineralogy. There are some differences between the plots obviously because of the different degrees of accuracy in using the two methods for determining the pyrite content. However, the plots are similar in that they both show a slight negative correlation between NNP and pyrite content. In both charts, samples with more than 1.5% pyrite have NNP less than -5 kg $CaCO_3$/t and samples with less than 1.5% pyrite have NNP ranging between about -5 and 60 kg $CaCO_3$/t. A stronger correlation would have been expected between NNP and pyrite content since pyrite oxidation is directly related to acid production. The weak correlation is probably due to the inclusion of neutralization potential in the calculation of NNP, because NP is independent of pyrite content.

In Figure 5.22, the silicates (epidote, plagioclase and K-feldspar) and calcite, which are acid-consuming minerals, all show a positive correlation with NNP, although not very strong. This relationship is expected since the acid-consuming minerals contribute to

positive NNP. The CaO-NNP chart in Figure 5.20 complements the correlation between calcite and NNP, Ca being a major element in calcite.

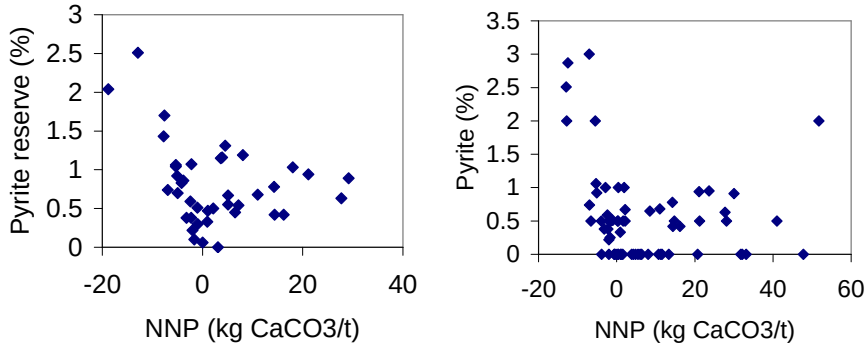

Figure 5.21: Plots of NNP versus pyrite reserve (left) determined with the Rietveld method and percentage pyrite (right) determined from modal mineralogy. Both plots show a very slight negative correlation between pyrite and NNP.

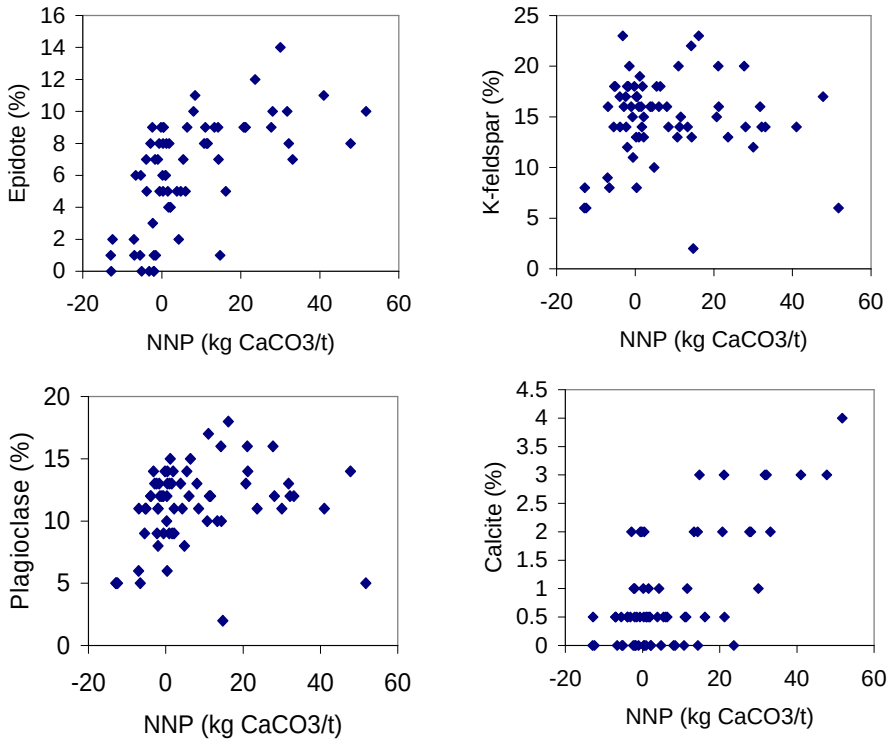

Figure 5.22: Plots of epidote (top left), K-feldspar (top right), plagioclase (bottom left) and calcite (bottom right) versus NNP. All the four minerals are acid-consuming and have positive correlations with NNP.

Figure 5.23 shows that both detrital gypsum (formed during hydrothermal alteration) and authigenic gypsum (formed in the rock pile) correlate negatively with NNP. Authigenic Gypsum is a product of the acid-consuming reaction between sulfuric acid and calcite. As was observed earlier in the chapter, low pH samples have lower NNP. The authigenic gypsum correlates inversely with NNP because some acid has already been generated in the samples with low NNP and calcite has reacted with the acid to produce the gypsum.

5.4 Implications for Future Weathering of GHN Rock Pile Material

The discussions so far in the chapter have revealed that although the rock pile material contains a number of acid-consuming minerals, silicates and carbonates, acid generation has been going on and has the potential to continue in the pile. The processes that generate acid have been enhanced by the availability of moisture and air close to the surface of the pile from the atmosphere, and the base of the pile from rubble zones and perched water tables at the contact between the pile and the bedrock. The movement of the unstable portion of the rock pile has also been a factor in reducing the pH of

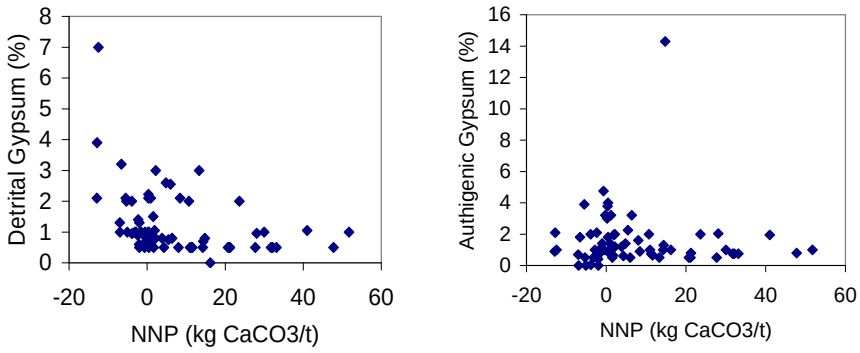

Figure 5.23: Plots of NNP versus detrital gypsum (left) and authigenic gypsum (right). Both types of gypsum have a slight negative correlation with NNP.

materials in that portion.

Because the rock pile was disturbed (on purpose) during the remediation construction (see Section 1.6.2), it is expected that acid generating processes will be increased to some degree. However, since silicate minerals form the bulk of the rocks in the pile, it is expected that over a long term period, the acid generated will be consumed by the silicates. This can eventually result in weathering of the silicates. Considering the current distribution of acidity in the pile, it is likely that the weathering rates will be higher near the face and the base of the pile, where the pH is already low.

6 CONCLUSIONS AND RECOMMENDATIONS

6.1 Conclusions

The current distribution of acidity in the Goathill North rock pile varies between the stable and unstable portions of the pile. In the stable portion, there is a recognizable zone of high pH parallel to and within about a tenth to a quarter of the pile's thickness from the face of the upper part of the pile. This zone represents geologic units that were identified in the middle of the trenches (e.g. units L, O, P, Q, R and S). The lowest pH values are found in units A to H at the surface; units I, J, and N, near the face; and units M, T and V near the base of the pile. In the unstable portion, the pH is generally lower and persists throughout the whole thickness of the pile except for the lower part where there are a few high pH values. The sliding movement of the pile has produced a more homogeneous oxidation and flow system, which has increased the chances of oxidation any where in the upper part of the unstable portion.

Portions of the rock pile still have the potential to produce acid, and even though there are acid-consuming minerals in abundance in the pile, the more reactive carbonates are consumed by the acid very quickly and are not enough to neutralize all of the acid that could be produced. It is expected that the less reactive silicate minerals will react slowly with the acid over the long term to mitigate the low pH (Plumlee, 1999). This will

eventually result in weathering of the pile material. Judging from the current distribution of acidity in the pile, it is likely that the material closer to the face and base of the pile will weather faster than the material in between, because weathering is faster at low pH than at high pH.

The acid generating characteristics of the pile are influenced by the rock types present in the pile. Samples rich in Amalia Tuff generate acid faster and have lower net neutralization potential than andesite-rich samples. This is because the Amalia Tuff has higher pyrite content and lower concentrations of fast-reacting neutralizing minerals.

6.2 Recommendations

It is recommended that kinetic tests be continued on the rock pile samples to gain better understanding of the rates at which acid-generating and acid-consuming processes are occurring. The kinetic tests will also help in identifying the weathering products and assessing how they will affect the strength of the rock pile in the long term. It is also recommended that DI leach chemistry tests should be done on both uncrushed and powdered splits of the GHN samples and the results compared to aid in explaining the difference between paste pH on powdered and unpowdered specimens. The kinetic and DI leach tests may also produce more information about the relationship between the paste pH and paste conductivity of the GHN materials.

REFERENCES

American Geological Institute, 1997, Dictionary of Mining, Mineral, and Related Terms: Alexandria, American Geological Institute, 646 p.

American Society for Testing and Materials, 1980, Natural Building Stones; Soil and Rock, Annual Book of ASTM Standards, Part 19: Philadelphia, ASTM, 634 p.

Andrina, J., Miller, S., and Neale, A., 2003, The design, construction, instrumentation and performance of a full-scale overburden stockpile trial for mitigation of acid rock drainage, Grasberg Mine, Papua Province, Indonesia, Proceedings of the 6th International Conference on Acid Rock Drainage: Cairns, Queensland, Australia, p. 123-132.

Barton-Bridges, J. P., and Robertson, A. M., 1989a, Design and Reclamation of Mine Waste Facilities to Control Acid Mine Drainage.

Barton-Bridges, J. P., and Robertson, A. M., 1989b, Geotechnical Considerations in the Control of Acid Mine Drainage.

Beedlow, P. A., 1984, Design of Vegetation Covers for Long-Term Stabilization of Uranium Tailings: BPNW, NUREG/CR-3674.

Beedlow, P. A., and Parker, G. B., 1985, Designing Protective Covers for Uranium Mill tailings Piles, NUREG/CR-4075, PNL-5323.

Bergholm, A., 1955, Oxidation of Pyrite: Jernkontorets Annallen, v. 139, p. 531-549.

Bethune, K. J., Lochington, D. A., and Williams, D. J., 1997, Acid Mine Drainage: Comparison of Laboratory Testing to Mine Site Conditions, Fourth International Conference on Acid Rock Drainage: Vancouver, p. 305-318.

Blight, G. E., 1969, Foundation Failures of Four Rockfill Slopes: Journal Soil Mechanics and Foundations Division, American Society of Civil Engineers, v. 95, no. SM3.

Blight, G. E., and Fourie, A. B., 2005, Catastrophe revisited - disastrous flows failures of mine and municipal solid waste: Geotechnical and Geological Engineering, v. 2005, no. 23, p. 219-248.

Blowes, D. W., and Jambor, J. L., 1990, The pore-water geochemistry and mineralogy of the vadose zone of sulfide tailings, Waite Amulet, Quebec, Canada: Applied Geochemistry, v. 5, p. 327-346.

Boyle, D. R., 1994, Oxidation of massive sulfide deposits in the Bathurst mining camp, New Brunswick - natural analogues of acid drainage in temperate climates, *in* Alpers, C. N., and Blowes, D. W., eds., Environmental Geochemistry of Sulfide Oxidation: American Chemical Society Symposium Series 550, p. 535-550.

Brady, K. B. C., and Hornberger, R. H., 1990, The prediction of mine drainage quality in Pennsylvania: Water Pollution Control Association Pa. Magazine, v. 23, no. 5, p. 8-15.

British Columbia AMD Task Force, 1989, Acid Rock Drainage Draft Technical Guide, Volumes I
and II, Report 66002/2. Prepared for the British Columbia AMD Task Force by SRK, Inc.

Brodie, M. J., Broughton, L. M., and Roberston, A. M., 1991, A conceptual rock classification system for waste management and a laboratory method for ARD prediction from rock piles, Proceedings of the 2nd International Conference on the Abatement of Acidic Drainage, Sept. 16-18, 1991: Montreal, Canada, p. 119-135.

Broughton, L. M., and Robertson, A., 1991, Modelling of Leachate Quality from Acid Generating Waste Rock Dumps, Second International Conference on the Abatement of Acidic Drainage: Montreal, Mine Environment Neutral Drainage, p. 341-361.

Bruynesteyn, A., and Duncan, D. W., 1979, Determination of acid production potential of waste materials, Met. Soc. AIME, paper A-79-29: Littleton, CO., AIME, 10 p.

Bruynesteyn, A., and Hackl, R., 1982, Evaluation of Acid Production Potential of Mining Waste Materials: Minerals and the Environment, v. 4, no. 1.

Busenberg, E., and Clemency, C., 1976, The dissolution kinetics of feldspars at 25^{o}C and 1 atmosphere CO_2 partial pressure: Geochimica et Cosmochimica Acta, v. 40, p. 41-49.

Caine, J. S., 2003, Questa baseline and pre-mining ground-water quality investigation 6: Preliminary brittle structural geologic data, Questa mining district, southern Sangre de Cristo Mountains, New Mexico: U.S. Geological Survey, Open-file Report 02-0280.

Caldwell, J. A., and Moss, A. S. E., 1981, The Simplified Analysis of Mine Waste Embankments, AIME Fall Meeting 1981, *in* Symposium on Design of Non-Impounding Mine Waste Embankments, Denver, CO, USA.

Carpenter, R. H., 1968, Geology and Ore Deposits of the Questa Molybdenum Mine Area, Taos County, New Mexico., Ore Deposits of the United States, 1933-1967, AIME

Graton-Sales, American Institute of Mining, Metallurgical and Petroleum Engineers, p. 1328-1350.

Carpentor, L. V., and Herndon, L. K., 1933, Acid mine drainage form bituminous coal mines, West Virginia University Engineering Exploration Station Research Bulletin No. 19, 38 p.

Caruccio, F. T., Geidel, G., and Pelletier, M., 1981, Occurrence and prediction of acid mine drainage: J. Energy Div. Am. Soc. Civ. Eng., v. 107, p. 167–178.

Clarke, F. W., 1966, Oxidation of coal mine pyrite: Journal of Sanitary Engineering Division, Proceedings of American Society of Civil Engineers, v. 92, p. 127-145.

Coastech Research Inc., 1989, Investigation of prediction techniques for acid mine drainage: MEND Project 1.16.1a., Canada Centre for Mineral and Energy Technology, Energy, Mines and Resources, Canada, 61 p.

Colmer, A. R., and Hinkle, M. E., 1947, The role of microorganisms in acid mine drainage: Science, v. 106, p. 253-256.

Colmer, A. R., Temple, K. L., and Hinkle, M. E., 1950, An iron-oxidizing bacterium from the acid drainage of some bituminous coal mines: Journal of Bacteriology, v. 59, p. 317-328.

Cravotta, C. A. I., Brady, K. B. C., Smith, M. W., and Beam, R. L., 1990, Effectiveness of alkaline addition at surface mines in preventing or abating acid mine drainage: part 1, geochemical considerations, Proceedings of the 1990 Mining and Reclamation Conference and Exhibition: Charleston, West Virginia, West Virginia University, p. 221-226.

Cruywagen, L. M., Usher, B. H., Hodgson, F. D. I., and de Necker, E., 2003, Towards a standardized static testing methodology for opencast collieries in South Africa, 6th International Conference on Acid Rock Drainage: Cairns, Queensland, Australia, p. 203-210.

Dawson, R. F., Morgenstern, N. R., and Stokes, A. W., 1998, Liquefaction flowslides in Rocky Mountains coal mine waste dumps: Canadian Geotechnical Journal, v. 35, no. 2, p. 328-343.

Day, S., 1989, Comments after presentation of - A practical approach to testing for acid mine drainage in the mine planning and approval process, *in* 13th Annual British Columbia Mine Reclamation Symposium, June 7-8, 1989, Vernon, B.C.

Day, S., Sexsmith, K., and Millard, J., 2003, Acidic drainage from calcereous coarse kimberlite reject, Ekati Diamond Mine, Northwest Territories, Canada, Proceedings of the 6th International Conference on Acid Rock Drainage: Cairns, Queensland, Australia, p. 587-600.

Drever, J. I., 1997, The geochemistry of natural waters - Surface and groundwater environments: Upper Saddle River, NJ, Prentice Hall, 436 p.

Duncan, D. W., and Walden, C. C., 1975, Prediction of acid generation potential: Environment Canada, Nov. 1975, 18 pp., Report to Water Pollution Control Directorate, Environmental Protection Service.

Edgar, A., and Lapakko, K., 1985, Heavy Metal Study Progress Report on the Field Leaching and Reclamation Program: 1977-1983: MN Dept. Nat. Res., Division of Minerals.

Environmental Geochemistry International, 2004, Net Acid Generation (NAG) Test Procedures.

EPA and Hardrock Mining, 2003, A Source Book for Industry in the Northwest and Alaska, Appendix C: Characterization of Ore, Waste Rock, and Tailings.

Evangelou, V. P., 1995, Pyrite oxidation and its control: Boca Raton, Fla, CRC Press, 285 p.

Ferguson, K. D., and Erickson, P. M., 1988, Pre-Mine Prediction of Acid Mine Drainage, *in* Salomons, W., and Forstner, U., eds., Dredged Material and Mine Tailings, Springer-Verlag Berlin Heidelberg.

Ferguson, K. D., and Morin, K., 1991, The prediction of acid rock drainage - Lessons from the data base, Proceedings of the 2nd International Conference on the Abatement of Acidic Drainage, Sept. 16-18: Montreal, Canada, p. 83-106.

Ferguson, K. D., and Robertson, J., 1994, Assessing the risk of ARD, International Land Reclamation and Mine Drainage Conference and Third International Conference on the Abatement of Acidic Drainage: U. S. Bureau of Mines Special Publication SP 06A-94, p. 2-11.

Filipek, L., Gormley, J., Ewing, R., and Ellsworth, D., 1991, Kinetic acid-prediction studies as aids to waste rock and water management during advanced exploration of a massive sulfide deposit, Proceedings Second International Conference on the Abatement of Acidic Drainage: Ottowa, Ontario, CANMET, p. 191-208.

Fines, P., Wilson, G. W., Williams, D. J., Tran, A. B., and Miller, S., 2003, Field Characterisation of Two Full-Scale Waste Rock Piles, *in* Sixth International Conference ACID ROCK DRAINAGE, Cairns, Queensland, Australia, p. 903-909.

Finkleman, R. B., and Giffin, D. E., 1986, Hydrogen peroxide oxidation: an improved method for rapidly assessing acid-generating potential of sediments and sedimentary rocks: Reclamation and Reveg. Res., v. 5, p. 521-534.

Gale, V. G., and Thompson, A. J. B., 2001, Reconnaissance study of waste rock mineralogy: Questa New Mexico, petrography, PIMA spectral analysis and Rietveld analysis: PetraScience Consultants, Inc.

Garrels, R. M., and Mackenzie, F. T., 1967, Origin of the chemical compositions of some springs and lakes, *in* Gould, R. F., ed., Equilibrium Concepts in Natural Water Systems: Advances in Chemistry Series: Washington, DC, American Chemical Society, p. 222-242.

Garrels, R. M., and Thompson, M. E., 1960, Oxidation of pyrite by iron sulfate solutions: American Journal of Science, v. 258A, p. 57-67.

Gerard, F., Ranger, J., Menetrier, C., and Bonnaud, P., 2003, Silicate weathering mechanisms determined using soil solutions held at high matric potential: Chemical Geology, v. 202, p. 443-460.

Ghomshei, M., Holmes, A., Denholm, E., R., L., and Carriou, T., 1997, Acid Rock Drainage from the Samatosum Waste Dump, British Columbia, Canada, Fourth International Conference on Acid Rock Drainage: Vancouver, p. 351-366.

Gibbs, R. J., 1967, The geochemistry of the Amazon River system: I. The factors that control the salinity and the composition and concentration of the suspended solids: Geological Society of America, v. 78, p. 1203-1232.

Gibbs, R. J., 1970, Mechanisms controlling world water chemistry: Science, v. 170, p. 1088-1090.

Gibbs, R. J., 1972, Water chemistry of the Amazon river: Geochimica et Cosmochimica Acta, v. 36, p. 1061-1066.

Goldhaber, M. B., 1983, Experimental Study of Metastable sulfur oxyanion formation during pyrite oxidation at pH 6-9 and 30^{o}C: American Journal of Science, v. 283, p. 193-217.

Granger, H. C., and Warren, C. G., 1969, Unstable sulfur compounds and the origin of roll-type uranium deposits: Economic Geology, v. 64, p. 160-171.

Halbert, B., Scharer, J., Knapp, R., and Gorber, D., 1983, Determination of Acid Generation Rates in Pyritic
Mine Tailings. Presented at the 56th Annual Conference of Water Pollution Control Federation,
October 2-7, 1983.

Hem, J. D., 1970, Study and interpretation of the chemical characteristics of natural water, U.S. Geological Survey Water-Supply Paper 1473: Washington, D.C., 363 p.

Higgs, T. W., Murphy, F. M., and Stewart, C. J., 1997, ARD Assessment Program from Exploration to Operation: Case Studies from the Eskay Creek Mine, Fourth International Conference on Acid Rock Drainage: Vancouver, p. 385-398.

Hood, W., and Oertel, A., 1984, A Leaching Column Method for Predicting Effluent Quality From Surface Mines, Proc. Symp. on Surface Mining Hydrology, Sedimentology and Reclamation., University of Kentucky.

Hutchinson, J. N., 1988, General Report. Morphological and geotechnical parameters of landslides in relation to geology and hydrogeology, 5th International Symposium on Landslides: Switzerland, p. 3-35.

Jackson, M. L., 1958, Soil chemical analysis: Englewood Cliffs, NJ, Prentice Hall.

Johnes, M., and McLean, I., 1999, The Aberfan Disaster.

Kim, A. G., Heisey, B., Kleinmann, R., and Duel, M., 1982, Acid Mine Drainage: Control and Abatement Research: U.S. DOI, Bureau of Mines, IC 8905.

King, T. V. V., 1995, Environmental Considerations of Active and Abandoned Mine Lands: Lessons from Summitville, Colorado, U.S. Geological Survey Bulletin: Denver, U.S. Geological Survey, 38 p.

Kleinmann, R., 2001, The ADTI Manual on Predicting Water Quality at Surface Coal Mines: Acid Drainage Technology Initiative.

Kleinmann, R. L. P., 1989, Acid mine drainage in the United States - Controlling the impact on streams and rivers, 4th World Congress on the Conservation of the Built and Natural Environments: University of Toronto, Canada, p. 1-10.

Knight, P. J., 1990, The flora of the Sangre de Cristo Mountains, New Mexico, *in* Bauer, P. W., Lucas, S. G., Mawer, C. K., and McIntosh, W. C., eds., Tectonic Development of the Southern Sangre de Cristo Mountains, New Mexico: New Mexico Geological Society Forty-First Annual Field Conference, September 12-15: Socorro, NM, New Mexico Geological Society, p. 94-95.

Lapakko, K., 1988, Prediction of acid mine drainage from Duluth Complex mining wastes in northeastern Minnesota, Mine Drainage and Surface Mine Reclamation: Mine Water and Mine Waste. Proceedings of the 1988 Mine Drainage and Surface Mine Reclamation Conference, Bureau of Mines IC 9183, p. 180-190.

Lapakko, K., 1992, Recent literature on static predictive tests, *in* Chander, S., ed., Emerging Process Technologies for a Cleaner Environment: Proceedings of the Symposium on Emerging Processing Technologies for a Cleaner Environment, Feb. 24-27, Phoenix, AZ.: Littleton, CO., Society for Mining, Metallurgy, and Exploration, Inc., p. 109-119.

Lapakko, K., 1993, Mine Waste Drainage Quality Prediction: A Literature Review: St. Paul, MN, Minnesota Department of Natural Resources, Division of Minerals.

Lapakko, K., 2002, Metal Mine Rock and Waste Characterization Tools: An Overview, International Institute for Environment and Development.

Lapakko, K., and Wessels, J. N., 1995, Release of acid from hydrothermal quartz-carbonate hosted gold-mine tailings, Conference on Mining and the Environment: Sudbury, Ontario, p. 139-148.

Lawrence, R. W., 1990, Prediction of the behavior of mining and processing wastes in the environment, *in* Doyle, F., ed., Proceedings of the Western Regional Symposium on Mining and Mineral Processing Wastes: Littleton, CO., Society for Mining, Metallurgy, and Exploration, Inc., p. 115-121.

Lefebvre, R., Lamontagne, A., Wels, C., and Robertson, A., 2002, ARD Production and Water Vapor Transport at the Questa Mine, Tailings and Mine Waste '02: Proceedings of the Tailings & Mine Waste '02 Conference, January 27-30: Fort Collins, A.A.Balkema, p. 479-488.

Lewis, H. S., Susteyo, W., Miller, S. D., and Jeffery, J. J., 1997, Waste Rock Management Planning and Implementation at P.T. Freeport Indonesia Company's Mining Operations in Irian Jaya., Fourth International Conference on Acid Rock Drainage: Vancouver, p. 1361-1376.

Li, C. T., Elmore, M. R., and Hartley, J. N., 1983, A review of fugitive dust control for uranium mill tailings: BPNW.

Lipman, P. W., 1981, Volcano-tectonic setting of tertiary ore deposits, southern Rocky Mountains: Arizona Geological Society Digest, v. 14, p. 199-213.

Lipman, P. W., and Reed, J. C., Jr., 1989, Geologic map of the Latir volcanic field and adjacent areas, northern New Mexico: U.S. Geological Survey, scale 1:48,000.

Lowson, R. T., 1982, Aqueous oxidation of pyrite by molecular oxygen: Chemical Reviews, v. 82, p. 461-497.

Ludington, S., Plumlee, G. S., Jonathan, C., Bove, D., Holloway, J., and Livo, E., 2004, Questa baseline and pre-mining ground-water quality investigation. 10. Geologic influences on ground and surface waters in the lower Red River watershed, New Mexico: United States Geological Survey, Scientific Investigations Report 2004-5245.

Mattson, B., and Carreau, R., 2003, Acid rock drainage prediction and waste rock segregation plan for ankerite-containing mine waste - Restigouche mine case study, Proceedings of the 6th International Conference on Acid Rock Drainage: Cairns, Queensland, Australia, p. 71-80.

McKibben, M. A., and Barnes, H. L., 1986, Oxidation of pyrite in low-temperature acidic solutions - Rate laws and surface textures: Geochimica et Cosmochimica Acta, v. 50, p. 1509-1520.

McLemore, V. T., Donahue, K., Phillips, E., Dunbar, N., Walsh, P., Gutierrez, L., Tachie-Menson, S., Shannon, H. R., Wilson, G. W., and Walker, B., 2006, Characterization of Goathill North mine rock pile, Questa molybdenum mine, Questa, New Mexico, *in* 2006 International Conference of Acid Rock Drainage (ICARD). In press, St. Louis, MS.

McLemore, V. T., Hoffman, G. K., and Jones, G. R., 2004, Use of the New Mexico mine rock pile database in characterization at mine sites, Tailings and Mine Waste '04, A. A. Balkema, p. 11-14.

McLemore, V. T., Walsh, P., Donahue, K., Gutierrez, L., Tachie-Menson, S., Shannon, H. R., and Wilson, G. W., 2005, Preliminary Status Report On Molycorp Goathill North Trenches, Questa, New Mexico, *in* 2005 National Meeting of the American Society of Mining and Reclamation, Breckenridge, Colorado, p. 26.

Meyer, J. W., and Leonardson, R. W., 1990, Tectonic, hydrothermal and geomorphic controls on alteration scar formation near Questa, New Mexico: Guidebook - New Mexico Geological Society, v. 41, p. 417-422.

Meyer, J. W., and Leonardson, R. W., 1997, Geology of the Questa mining district: Volcanic, plutonic, tectonic and hydrothermal history, New Mexico Bureau of Mines and Mineral Resources Bulletin, Open File Report 431: Socorro, 187 p.

Miller, R. A., and Hertel, T. M., 1997, Mine Rock Characterization - Zortman and Landusky Mines, Little Rocky Mountains, Phillips County, North-Central Montana, Fourth International Conference on Acid Rock Drainage: Vancouver, p. 515-532.

Miller, S., Andrina, J., and Richards, D., 2003, Overburden geochemistry and acid rock drainage scale-up investigations at the Grasberg mine, Papua Province, Indonesia, Proceedings of the 6th International Conference on Acid Rock Drainage: Cairns, Queensland, Australia, p. 111-121.

Miller, S. D., 1999, Predicting acid drainage: Groundwork, v. 2, p. 8-9.

Miller, S. D., and Murray, G. S. C., 1988, Application of acid base analysis to wastes from base metal and precious metal mines, Proceedings Mine Drainage and Surface Mine Reclamation: US Bureau of Mines IC 9183: Mine Water and Mine Waste, p. 29-32.

Mills, A. L., 1999, The role of bacteria in environmental geochemistry, *in* Plumlee, G. S., and Logsdon, M. J., eds., The Environmental Geochemistry of Mineral Deposits: Littleton, CO, Society of Economic Geologists, p. 125-132.

Molycorp Inc., 2002, Request for Letters of Intent, Questa, NM. http://www.infomine.com/consultants/doc/mcrliaun.pdf

Molycorp Project Team, 2004, General Work Plan for Molycorp/Questa Phase 1 Weathering Study.

Morin, K., and Hutt, N., 1994, Observed preferential depletion of neutralization potential over sulfide minerals in kinetic tests - Site specific criteria for safe NP/AP ratios, Proceedings of the International Land Reclamation and Mine Drainage Conference on the Abatement of Acidic Drainage: Pittsburgh, PA, p. 148-156.

Moses, C. O., and Herman, J. S., 1991, Pyrite oxidation at circumneutral pH: Geochimica et Cosmochimica Acta, v. 55, p. 471-482.

Moses, C. O., Nordstrom, D. K., Herman, J. S., and Mills, A. L., 1987, Aqueous pyrite oxidation by dissolved oxygen and by ferric iron: Geochimica et Cosmochimica Acta, v. 51, p. 1561-1571.

Mutschler, F. E., Wright, E. G., Ludington, S. D., and Abbott, J. T., 1981, Granitic molybdenite systems: Economic Geology, v. 76, p. 874-897.

NCE, 1982, Liberian Slip Kills 200: New Civil Engineer, no. October 14.

Nelson, J. D., R.L., V., R.E., W., S.A., S., and W., S., 1983, Design Considerations for Long-Term Stabilization of Uranium Mill Tailings Impoundments: BPNW, NUREG/CR-3397.

Nichols, R. S., 1987, Rock segregation in waste dumps, *in* Flow-through rock drains: Proceedings of the International symposium convened at the Inn of the South, Cranbrook, B. C.

Nordstrom, D. K., 1982, Aqueous pyrite oxidation and the consequent formation of secondary iron minerals, *in* Kittrick, J. A., Fanning, D. S., and Hossner, L. R., eds., Acid sulfate weathering: Soil Science Society of America Special Publication No. 10, Soil Science Society of America, p. 37-56.

Nordstrom, D. K., 1991, Chemical modeling of acid mine waters in the western United States, *in* Mallard, G. E., and Aronson, D. A., eds., Proceedings, U.S. Geological Survey Toxic Substances Hydrology Program: U.S. Geological Survey Water-Resources Investigations Report 91-4034, p. 534-538.

Nordstrom, D. K., and Alpers, C. N., 1999, Geochemistry of Acid Mine Waters, *in* Plumlee, G. S., and Logsdon, M. J., eds., The Environmental Geochemistry of Mineral Deposits. Part A: Processes, Techniques and Health Issues: Reviews in Economic Geology: Littleton, CO, Society of Economic Geologists, p. 133-160.

Nordstrom, D. K., McCleskey, R. B., Hunt, A. G., and Naus, C. A., 2005, Questa baseline and pre-mining ground-water quality investigation. 14. Interpretation of

ground-water geochemistry in catchments other than the Straight Creek catchment, Red River Valley, Taos County, New Mexico, 2002-2003: U.S. Geological Survey, Scientific Investigations Report 2005-5050.

Norwest Corporation, 2003, Goathill North Mine Rock Pile Evaluation and Conceptual Mitigation Plan: Molycorp Inc.

Norwest Corporation, 2004, Goathill North Slide Investigation, Evaluation and Mitigation Report: Molycorp Inc.

Patterson, R. J., and Ferguson, K. D., 1994, The Gibraltar North Project assessing acid rock drainage, International Land Reclamation and Mine Drainage Conference and Third International Conference on the Abatement of Acidic Drainage: U. S. Bureau of Mines Special Publication SP 06B-94, p. 12-21.

Peech, M., 1965, Hydrogen-ion activity, *in* Black, C. A., ed., Methods of soil analysis: Agronomy: Madison, Wis., Am. Soc. of Agron., p. 914-920.

Perry, E. F., 1998, Interpretation of Acid-Base Accounting. Chapter 11, Coal Mine Drainage Prediction and Pollution Prevention in Pennsylvania: Harrisburg, PA, PA Department of Environmental Protection.

Plumlee, G. S., 1999, The Environmental Geology of Mineral Deposits, *in* Plumlee, G. S., and Logsdon, M. J., eds., The Environmental Geochemistry of Mineral Deposits. Part A: Processes, Techniques, and Health Issues: Littleton, CO, Society of Economic Geologists, p. 71-116.

Powell, A. R., and Parr, S. W., 1919, Forms in which sulfur occurs in coal, Bulletin of the American Institute of Mining and Metallurgical Engineering, p. 2041-2049.

Quine, R. L., 1993, Stability and deformation of mine waste dumps in north-central Nevada [M. S. thesis]: University of Nevada, 402 p.

Reeder, S. W., Hitchon, B., and Levinson, A. A., 1972, Hydrogeochemistry of the surface waters of the Mackenzie River drainage basin, Canada: I. Factors controlling inorganic composition: Geochimica et Cosmochimica Acta, v. 36, p. 825-865.

Rehrig, W. A., 1969, Fracturing and its effects on molybdenum mineralization at Questa, New Mexico [PhD Dissertation thesis]: University of Arizona, 194 p.

Robertson, A., and Skermer, N. A., 1988, Design Considerations for the Long Term Stability of Mine Wastes, *in* First International Environmental Workshop, Darwin.

Robertson, A. M., 1982, Deformation and Monitoring of Waste Dump Slopes, p. 16.

Robertson, A. M., 1985, Mine Waste Disposal: An Update on Geotechnical and Geohydrological Aspects.

Robertson GeoConsultants Inc., 1999a, Interim Report: Questa Waste Rock Pile Drilling, Instrumentation and Characterization Study: Robertson GeoConsultants, Report 052007/1 Prepared for Molycorp Inc.

Robertson GeoConsultants Inc., 1999b, Progress Report on Questa Waste Rock Investigation: Workplans for Geochemical and Physical Characterization: Robertson GeoConsultants, Report 052007/2 Prepared for Molycorp Inc.

Robertson GeoConsultants Inc., 2000, Progress Report: Questa Mine Rock Pile Monitoring and Characterization Study: Robertson Geo Consultants Inc., Report No. 052007/3 For Molycorp Inc.

Robinson, G., Skaftfeld, K., Aslund, R., and Copland, H., 2005, Landslide dams and creeks stabilization at the former Clinton Creek asbestos mine: Northern Latitudes.

Rumble, C., Miller, S., Kundapen, H., and Bolton, B., 2003, Evaluation of the sulfide and carbonate distribution in waste rock dumps and development of operational guidelines for acid rock drainage control at the Ok Tedi mine, Papua New Guinea, Proceedings of the 6th International Conference on Acid Rock Drainage: Cairns, Queensland, Australia, p. 173-180.

Runnells, D. D., Shepard, T. A., and Angino, E. E., 1992, Metals in water - Determining natural background concentrations in mineralized areas: Environmental Science and Technology, v. 26, p. 2316-2322.

Schilling, J. H., 1956, Geology of the Questa Molybdenum (Moly) Mine Area, Taos County, New Mexico: State Bureau of Mines and Mineral Resources Bulletin, v. 51, no. 87.

Schwendiman, L. C., Schmel, G. A., Horst, T. W., Thomson, C. W., and Perkins, R. W., 1980, A field and model study of windblown particulates from a uranium mill tailings pile: Battelle-Pacific BPNW Northwest Laboratory, NUREG/CR-1407, PNL-3345.

Shaw, S. C., 2000, Geochemical Characterization and Water Quality Prediction for the Zortman/Landusky Reclamation Project, *in* Mine Design, operations and Closure Conference 2000.

Shaw, S. C., Robertson, A. M., and Maehl, W. C., 2000, Material Characterization and Prioritization of Remediation Measures at the Zortman/Landusky Mine Sites, *in* 2000 Billings Land Reclamation Symposium, Billings, Montana, p. 346-358.

Shaw, S. C., Wels, C., Robertson, A., Fortin, S., and Walker, B., 2003, Background Characterization Study of Naturally Occurring Acid Rock Drainage in the Sangre De Cristo Mountains, Taos County, New Mexico, *in* 6th International Conference on Acid Rock Drainage, Cairns, QLD, p. 605-616.

Shaw, S. C., Wels, C., Robertson, A., and Lorinczi, G., 2002, Physical and Geochemical Characterization of Mine Rock Piles at the Questa Mine, New Mexico:

An Overview, 9th International Conference on Tailings and Mine Waste '02: Rotterdam, Balkema.

Shum, M. G. W., 1999, Characterization and dissolution of secondary weathering products from the Gibraltar mine site [M. S. thesis]: University of British Columbia, 310 p.

Singer, P. C., and Stumm, W., 1968, Kinetics of the oxidation of ferrous iron, 2nd Symposium on Coal Mine Drainage Research, National Coal Association/Bituminous Coal Research, p. 12-34.

Singer, P. C., and Stumm, W., 1970a, Acid Mine Drainage: the rate-determining step: Science, v. 167, p. 1121-1123.

Singer, P. C., and Stumm, W., 1970b, Oxygenation of ferrous iron, Federal Water Quality Administration Report 14010-06/69, 198 p.

Singleton, G. A., and Lavkulich, L. M., 1978, Adaption of the Soxhelet Extractor for Pedologic Studies: Soil Science Society of America Journal, v. 42, p. 984-986.

Skousen, J., Sencindiver, J. C., and Smith, R., 1987, A Review of Procedures For Surface Mining And Reclamation In Areas With Acid-Producing Materials, West Virginia University Energy and Water Research Center, in cooperation with the West Virginia Mining and Reclamation Association and West Virginia Surface Mine Drainage Task Force, 39 p.

Smith, R., Sobek, A., Arkle, T., Sencindiver, J. C., and Freeman, J. R., 1976, Extensive Overburden Potentials for Soil and Water Quality: U.S. Environmental Protection Agency, EPA-600/2-76-184.

Smith, R. M., Grube, W. E., Arkle, T. A., and Sobek, A. A., 1974, Mine Spoil Potentials for Soil and Water Quality: U.S. Environmental Protection Agency, EPA-670/2-74-070.

Sobek, A. A., Schuller, W. A., Freeman, J. R., and Smith, R. M., 1978, Field and Laboratory Methods Applicable to Overburdens and Minesoils: US Environmental Protection Agency, EPA-600/2-78-054.

Sonner, S., 2005, Huge rock slide at gold mine dump near Carlin under investigation, Las Vegas Sun.

Sracek, O., Choquette, M., Gelinas, P., Lefebvre, R., and Nicholson, R. V., 2004, Geochemical Characterization of Acid Mine Drainage from a Waste Rock Pile, Mine Doyon, Quebec, Canada: Journal of Contaminant Hydrology, v. 69, p. 45-71.

Stallard, R. F., 1985, River chemistry, geology, geomorphology, and soils in the Amazon and Orinoco Basins, *in* Drever, J. I., ed., The Chemistry of Weathering: Dordrecht, Netherlands, Reidel, p. 293-316.

Stallard, R. F., and Edmond, J. M., 1981, Geochemistry of the Amazon: 1. Precipitation chemistry and the marine contribution to the dissolved load at the time of peak discharge: J. Geophys. Res., v. 86, p. 9844-9858.

Stallard, R. F., and Edmond, J. M., 1983, Geochemistry of the Amazon: 2. The influence of the geology and weathering environment on the dissolved load: J. Geophys. Res., v. 88, p. 9671-9688.

Stallard, R. F., and Edmond, J. M., 1987, Geochemistry of the Amazon: 3. Weathering chemistry and limits to dissolved inputs: J. Geophys. Res., v. 92, p. 8293-8302.

Steger, H. F., and Desjardins, L. E., 1978, Oxidation of sulfide minerals, IV. Pyrite, chalcopyrite and pyrrhotite: Chemical Geology, v. 23, p. 225-237.

Stokes, H. N., 1901, On pyrite and marcasite, U.S. Geological Survey Bulletin 186, 50 p.

Stormont, J. C., and Farfan, E., 2005, Stability evaluation of a mine waste pile: Environmental and Engineering Geoscience, v. 11, no. 1, p. 43-52.

Stumm, W., and Morgan, J. J., 1981, Aquatic Chemistry - An Introduction Emphasizing Chemical Equilibria in Natural Waters, John Wiley & Sons, Inc., 470 p.

Sullivan, P. J., and Sobek, A., 1982, Laboratory Weathering Studies of Coal Refuse: Minerals and the Environment, v. 4, no. 1.

Surface Mine Drainage Task Force, 1979, Suggested guidelines for methods of operation in surface mining of areas with potentially acid-producing materials: Green Lands, v. 9, p. 21-40.

Temple, K. L., and Colmer, A. R., 1951, The autotrophic oxidation of iron by a new bacterium - Thiobacillus ferrooxidans: Journal of Bacteriology, v. 62, p. 605-611.

Temple, K. L., and Delchamps, E. W., 1953, Autotrophic bacteria and the formation of acid in bituminous coal mines: Applied Microbiology, v. 1, p. 255-258.

Thomson, D. G., Manly, J. K., Kitchin, R. F., Eenkooren, N. E., Davies, M. P., Gibson, G. G., and Dawson, B. B., 1997, Mark Creek Improvement Project, Control of ARD in the Lower Mine Yard, Kimberley, British Columbia, Fourth International Conference on Acid Rock Drainage: Vancouver, p. 65-79.

Tran, A. B., 2003, Geochemistry of Acid Generating Waste Rock Dumps: Investigations Aimed at Improving Laboratory Analysis Techniques, Dump Construction and Operation, and Closure [MPhil thesis]: University of Queensland, 217 p.

Tran, A. B., Fines, P., Miller, S., Williams, D., and Wilson, W., 2003a, Hydrologic and Geochemical Characterization of Two Full-Scale Waste Rock Piles - A Joint

University/Industry Research Program Sponsored by INAP: Geotechnical News, no. September 2003, p. 36-42.

Tran, A. B., Miller, S., Williams, D. J., Fines, P., and Wilson, G. W., 2003b, Geochemical and Mineralogical Characterisation of Two Contrasting Waste Rock Dumps - The INAP Waste Rock Dump Characterisation Project, *in* Sixth International Conference Acid Rock Drainage, Cairns, Queensland, Australia, p. 939-947.

U.S. EPA, 1994, Technical Document - Acid Mine Drainage Prediction: Office of Solid Waste, Special Waste Branch, EPA530-R-94-036.

URS Corporation, 2000, Interim Mine Rock Pile Erosion and Stability Evaluations, Questa Mine, Molycorp Inc.

USDA Forest Service, 1993, Acid Mine Drainage From Mines in the National Forests, A Management Challenge, Program Aid 1505.

Usher, B. H., Cruywagen, L. M., de Necker, E., and Hodgson, F. D. I., 2003, Comparing different prediction techniques, and field results from South African opencast collieries, 6th International Conference on Acid Rock Drainage: Cairns, Queensland, Australia, p. 627-638.

Van Zyl, D., Sassoon, M., Digby, C., Fleury, A. M., and Kyeyune, S., 2002, Mining for the Future: Appendix A, Large Volume Waste Working Paper: International Institute for Environment and Development, 31.

Wagner, A., 2005, The history and operating practices of Molycorp's Questa mine: Questa.

Wagner, A. M., and Harrington, J. T., 1995, Revegetation report for Molycorp, Inc. Questa mine site, Unpublished report for Vail Engineering.

Walters, M. H., 1983, Overland erosion of uranium mill tailings impoundments: Physical processes and computational methods: BPNW, NUREG/CR-3027, PNL-4523.

Wels, C., Loudon, S., and Fortin, S., 2002, Factors Influencing Net Infiltration into Mine Rock Piles at Questa Mine, New Mexico, Tailings and Mine Waste '02: Proceedings of the Tailings & Mine Waste '02 Conference, January 27-30: Fort Collins, CO., A. A. Balkema, p. 469-478.

Western Regional Climate Center, 2003, Historical climate information: New Mexico climate summaries, Red River, New Mexico (297323).

White, W. W., III, and Jeffers, T. H., 1994, Chemical predictive modeling of acid mine drainage from metallic sulfide-bearing waste rock, Environmental Geochemistry of Sulfide Oxidation: ACS Symposium Series 550: Washington, D.C., American Chemical Society, p. 608-630.

White, W. W., III, Lapakko, K., and Cox, R. L., 1999, Static-Test Methods Most Commonly Used To Predict Acid-Mine Drainage: Practical Guidelines for Use and Interpretation, *in* Plumlee, G. S., and Logsdon, M. J., eds., The Environmental Geochemistry of Mineral Deposits. Part A: Processes, Techniques, and Health Issues: Littleton, CO, Society of Economic Geologists, Inc., p. 325-338.

Williams, D. J., Jeffrey, J., Gilbert, L., Wilson, G. W., Panidis, C., and Perry, B., 2003, A review of the acid rock drainage potential and hydrological implications of selectively-placed waste rock at a gold mine in NSW, Australia, 6th International Conference on Acid Rock Drainage: Cairns, Queensland, Australia, p. 949-956.

Williamson, M. A., and Rimstidt, J. D., 1993, The rate of decomposition of the ferric-thiosulfate complex in acidic aqueous solutions: Geochimica et Cosmochimica Acta, v. 57, p. 3555-3561.

Zahl, E. G., Biggs, F., Boldt, C. M. K., Connolly, R. E., Gertsch, L., and Lambeth, R. H., 1992, Waste Disposal and Contaminant Control, *in* Hartman, H. L., ed., SME Mining Engineering Handbook: Littleton, CO, Society for Mining, Metallurgy and Exploration Inc., p. 1170-1180.

APPENDIX A SAMPLE LOCATIONS

Table A1: Samples and their locations on the GHN rock pile

Sample ID	Pile Portion	Hole/Pit ID	Bench	UTM Easting m	UTM Northing m	Elevation m (ft)
GHN-ACT-0001	Stable	TH-GN-01		453709.91	4062157.70	2975.88 (9763)
GHN-ACT-0002	Stable	TH-GN-01		453709.91	4062157.70	2974.51 (9758)
GHN-ACT-0003	Stable	TH-GN-01		453709.91	4062157.70	2972.98 (9753)
GHN-ACT-0004	Stable	TH-GN-01		453709.91	4062157.70	2971.46 (9748)
GHN-ACT-0005	Stable	TH-GN-01		453709.91	4062157.70	2969.94 (9743)
GHN-ACT-0006	Stable	TH-GN-01		453709.91	4062157.70	2966.89 (9733)
GHN-ACT-0007	Stable	TH-GN-01		453709.91	4062157.70	2963.84 (9723)
GHN-ACT-0008	Stable	TH-GN-01		453709.91	4062157.70	2962.32 (9718)
GHN-ACT-0010	Stable	TH-GN-01		453709.91	4062157.70	2959.27 (9708)
GHN-ACT-0011	Stable	TH-GN-01		453709.91	4062157.70	2957.74 (9703)
GHN-ACT-0012	Stable	TH-GN-01		453709.91	4062157.70	2956.22 (9698)
GHN-ACT-0013	Stable	TH-GN-01		453709.91	4062157.70	2954.70 (9693)
GHN-ACT-0014	Stable	TH-GN-01		453709.91	4062157.70	2953.17 (9688)
GHN-ACT-0015	Stable	TH-GN-01		453709.91	4062157.70	2951.65 (9683)
GHN-ACT-0016	Stable	TH-GN-01		453709.91	4062157.70	2948.60 (9673)
GHN-ACT-0017	Stable	TH-GN-01		453709.91	4062157.70	2947.08 (9668)
GHN-ACT-0018	Stable	TH-GN-01		453709.91	4062157.70	2945.55 (9663)
GHN-ACT-0019	Stable	TH-GN-01		453709.91	4062157.70	2944.03 (9658)
GHN-ACT-0020	Stable	TH-GN-01		453709.91	4062157.70	2940.98 (9648)
GHN-ACT-0021	Stable	TH-GN-01		453709.91	4062157.70	2939.46 (9643)
GHN-ACT-0022	Stable	TH-GN-01		453709.91	4062157.70	2936.41 (9633)
GHN-ACT-0023	Stable	TH-GN-01		453709.91	4062157.70	2934.88 (9628)
GHN-ACT-0024	Stable	TH-GN-01		453709.91	4062157.70	2933.36 (9623)
GHN-ACT-0025	Stable	TH-GN-01		453709.91	4062157.70	2931.84 (9618)
GHN-ACT-0026	Stable	TH-GN-01		453709.91	4062157.70	2931.84 (9618)
GHN-ACT-0027	Stable	TH-GN-01		453709.91	4062157.70	2931.84 (9618)
GHN-ACT-0028	Stable	TH-GN-01		453709.91	4062157.70	2930.31 (9613)
GHN-ACT-0029	Stable	TH-GN-01		453709.91	4062157.70	2928.79 (9608)
GHN-ACT-0030	Stable	TH-GN-01		453709.91	4062157.70	2927.26 (9603)
GHN-ACT-0031	Stable	TH-GN-01		453709.91	4062157.70	2924.22 (9593)
GHN-ACT-0032	Stable	TH-GN-01		453709.91	4062157.70	2922.69 (9588)
GHN-ACT-0033	Stable	TH-GN-01		453709.91	4062157.70	2921.17 (9583)
GHN-ACT-0037	Unstable	TH-GN-02S		453540.76	4062249.20	2881.48 (9453)
GHN-ACT-0038	Unstable	TH-GN-02S		453540.76	4062249.20	2880.11 (9449)
GHN-ACT-0039	Unstable	TH-GN-02S		453540.76	4062249.20	2878.59 (9444)
GHN-ACT-0040	Unstable	TH-GN-02S		453540.76	4062249.20	2877.06 (9439)

Table A1 continued.

Sample ID	Pile Portion	Hole/Pit ID	Bench	UTM Easting m	UTM Northing m	Elevation m (ft)
GHN-ACT-0041	Unstable	TH-GN-02S		453540.76	4062249.20	2875.54 (9434)
GHN-ACT-0042	Unstable	TH-GN-02S		453540.76	4062249.20	2874.02 (9429)
GHN-ACT-0043	Unstable	TH-GN-02S		453540.76	4062249.20	2872.49 (9424)
GHN-ACT-0044	Unstable	TH-GN-02S		453540.76	4062249.20	2870.97 (9419)
GHN-ACT-0045	Unstable	TH-GN-02S		453540.76	4062249.20	2869.44 (9414)
GHN-ACT-0046	Unstable	TH-GN-02S		453540.76	4062249.20	2867.92 (9409)
GHN-ACT-0047	Unstable	TH-GN-02S		453540.76	4062249.20	2866.40 (9404)
GHN-ACT-0048	Unstable	TH-GN-02S		453540.76	4062249.20	2864.87 (9399)
GHN-ACT-0049	Unstable	TH-GN-02S		453540.76	4062249.20	2863.35 (9394)
GHN-ACT-0050	Unstable	TH-GN-02S		453540.76	4062249.20	2861.82 (9389)
GHN-ACT-0051	Unstable	TH-GN-02S		453540.76	4062249.20	2860.30 (9384)
GHN-ACT-0052	Unstable	TH-GN-02S		453540.76	4062249.20	2858.78 (9379)
GHN-ACT-0053	Unstable	TH-GN-02S		453540.76	4062249.20	2857.25 (9374)
GHN-ACT-0054	Unstable	TH-GN-02S		453540.76	4062249.20	2857.25 (9374)
GHN-ACT-0055	Unstable	TH-GN-02S		453540.76	4062249.20	2857.25 (9374)
GHN-ACT-0056	Unstable	TH-GN-02S		453540.76	4062249.20	2855.73 (9369)
GHN-ACT-0057	Unstable	TH-GN-02S		453540.76	4062249.20	2854.20 (9364)
GHN-ACT-0058	Unstable	TH-GN-02S		453540.76	4062249.20	2852.68 (9359)
GHN-ACT-0059	Unstable	TH-GN-02S		453540.76	4062249.20	2851.16 (9354)
GHN-ACT-0060	Unstable	TH-GN-02S		453540.76	4062249.20	2849.63 (9349)
GHN-ACT-0061	Unstable	TH-GN-02S		453540.76	4062249.20	2848.11 (9344)
GHN-ACT-0062	Unstable	TH-GN-02S		453540.76	4062249.20	2846.58 (9339)
GHN-ACT-0063	Unstable	TH-GN-02S		453540.76	4062249.20	2845.06 (9334)
GHN-ACT-0064	Unstable	TH-GN-02S		453540.76	4062249.20	2843.54 (9329)
GHN-ACT-0065	Unstable	TH-GN-02S		453540.76	4062249.20	2842.01 (9324)
GHN-ACT-0066	Unstable	TH-GN-02S		453540.76	4062249.20	2840.49 (9319)
GHN-ACT-0067	Unstable	TH-GN-02S		453540.76	4062249.20	2838.96 (9314)
GHN-ACT-0068	Unstable	TH-GN-02S		453540.76	4062249.20	2837.44 (9309)
GHN-ACT-0069	Unstable	TH-GN-02S		453540.76	4062249.20	2835.92 (9304)
GHN-ACT-0070	Unstable	TH-GN-02S		453540.76	4062249.20	2834.39 (9299)
GHN-ACT-0071	Unstable	TH-GN-04S		453398.70	4062174.87	2820.74 (9254)
GHN-ACT-0073	Unstable	TH-GN-04S		453398.70	4062174.87	2817.84 (9244)
GHN-ACT-0074	Unstable	TH-GN-04S		453398.70	4062174.87	2816.32 (9239)
GHN-ACT-0075	Unstable	TH-GN-04S		453398.70	4062174.87	2814.79 (9234)
GHN-ACT-0076	Unstable	TH-GN-04S		453398.70	4062174.87	2813.27 (9229)
GHN-ACT-0077	Unstable	TH-GN-04S		453398.70	4062174.87	2811.74 (9224)
GHN-ACT-0078	Unstable	TH-GN-04S		453398.70	4062174.87	2810.22 (9219)
GHN-ACT-0079	Unstable	TH-GN-04S		453398.70	4062174.87	2808.70 (9214)
GHN-ACT-0080	Unstable	TH-GN-04S		453398.70	4062174.87	2807.17 (9209)
GHN-ACT-0081	Unstable	TH-GN-04S		453398.70	4062174.87	2805.65 (9204)
GHN-ACT-0082	Unstable	TH-GN-04S		453398.70	4062174.87	2805.65 (9204)
GHN-ACT-0083	Unstable	TH-GN-04S		453398.70	4062174.87	2805.65 (9204)
GHN-ACT-0084	Unstable	TH-GN-04S		453398.70	4062174.87	2804.12 (9199)
GHN-ACT-0085	Unstable	TH-GN-04S		453398.70	4062174.87	2802.60 (9194)
GHN-ACT-0086	Unstable	TH-GN-04S		453398.70	4062174.87	2801.08 (9189)
GHN-ACT-0087	Unstable	TH-GN-04S		453398.70	4062174.87	2799.86 (9185)
GHN-ACT-0088	Unstable	TH-GN-04S		453398.70	4062174.87	2799.10 (9183)

Table A1 continued.

Sample ID	Pile Portion	Hole/Pit ID	Bench	UTM Easting m	UTM Northing m	Elevation m (ft)
GHN-ACT-0089	Unstable	TH-GN-04S		453398.70	4062174.87	2798.03 (9179)
GHN-ACT-0090	Unstable	TH-GN-04S		453398.70	4062174.87	2796.50 (9174)
GHN-ACT-0091	Unstable	TH-GN-04S		453398.70	4062174.87	2795.44 (9171)
GHN-ACT-0108	Stable	TH-GN-06		453715.48	4062117.41	2975.97 (9763)
GHN-ACT-0109	Stable	TH-GN-06		453715.48	4062117.41	2974.60 (9759)
GHN-ACT-0111	Stable	TH-GN-06		453715.48	4062117.41	2971.55 (9749)
GHN-ACT-0112	Stable	TH-GN-06		453715.48	4062117.41	2970.03 (9744)
GHN-ACT-0113	Stable	TH-GN-06		453715.48	4062117.41	2968.50 (9739)
GHN-ACT-0114	Stable	TH-GN-06		453715.48	4062117.41	2966.98 (9734)
GHN-ACT-0115	Stable	TH-GN-06		453715.48	4062117.41	2966.98 (9734)
GHN-ACT-0116	Stable	TH-GN-06		453715.48	4062117.41	2966.98 (9734)
GHN-ACT-0117	Stable	TH-GN-06		453715.48	4062117.41	2965.46 (9729)
GHN-ACT-0118	Stable	TH-GN-06		453715.48	4062117.41	2963.93 (9724)
GHN-ACT-0119	Stable	TH-GN-06		453715.48	4062117.41	2962.41 (9719)
GHN-ACT-0120	Stable	TH-GN-06		453715.48	4062117.41	2960.88 (9714)
GHN-ACT-0121	Stable	TH-GN-06		453715.48	4062117.41	2959.36 (9709)
GHN-ACT-0122	Stable	TH-GN-06		453715.48	4062117.41	2957.84 (9704)
GHN-ACT-0123	Stable	TH-GN-06		453715.48	4062117.41	2956.31 (9699)
GHN-ACT-0124	Stable	TH-GN-06		453715.48	4062117.41	2954.79 (9694)
GHN-ACT-0125	Stable	TH-GN-06		453715.48	4062117.41	2953.26 (9689)
GHN-ACT-0126	Stable	TH-GN-06		453715.48	4062117.41	2951.74 (9684)
GHN-ACT-0127	Stable	TH-GN-06		453715.48	4062117.41	2950.22 (9679)
GHN-ACT-0128	Stable	TH-GN-06		453715.48	4062117.41	2948.69 (9674)
GHN-ACT-0129	Stable	TH-GN-06		453715.48	4062117.41	2947.17 (9669)
GHN-ACT-0130	Stable	TH-GN-06		453715.48	4062117.41	2945.64 (9664)
GHN-ACT-0131	Stable	TH-GN-06		453715.48	4062117.41	2944.12 (9659)
GHN-ACT-0132	Stable	TH-GN-06		453715.48	4062117.41	2942.60 (9654)
GHN-ACT-0133	Stable	TH-GN-06		453715.48	4062117.41	2941.07 (9649)
GHN-ACT-0134	Stable	TH-GN-06		453715.48	4062117.41	2939.55 (9644)
GHN-ACT-0135	Stable	TH-GN-06		453715.48	4062117.41	2938.02 (9639)
GHN-ACT-0136	Stable	TH-GN-06		453715.48	4062117.41	2936.50 (9634)
GHN-ACT-0137	Stable	TH-GN-06		453715.48	4062117.41	2936.50 (9634)
GHN-ACT-0138	Stable	TH-GN-06		453715.48	4062117.41	2936.50 (9634)
GHN-ACT-0139	Stable	TH-GN-06		453715.48	4062117.41	2934.98 (9629)
GHN-ACT-0140	Stable	TH-GN-06		453715.48	4062117.41	2933.45 (9624)
GHN-ACT-0141	Stable	TH-GN-06		453715.48	4062117.41	2931.93 (9619)
GHN-ACT-0142	Stable	TH-GN-06		453715.48	4062117.41	2930.40 (9614)
GHN-ACT-0143	Stable	TH-GN-06		453715.48	4062117.41	2928.88 (9609)
GHN-ACT-0144	Stable	TH-GN-06		453715.48	4062117.41	2927.36 (9604)
GHN-ACT-0145	Stable	TH-GN-06		453715.48	4062117.41	2925.83 (9599)
GHN-ACT-0146	Stable	TH-GN-06		453715.48	4062117.41	2924.31 (9594)
GHN-ACT-0147	Stable	TH-GN-06		453715.48	4062117.41	2922.78 (9589)
GHN-ACT-0148	Stable	TH-GN-06		453715.48	4062117.41	2921.26 (9584)
GHN-ACT-0149	Stable	TH-GN-06		453715.48	4062117.41	2919.74 (9579)
GHN-ACT-0150	Stable	TH-GN-06		453715.48	4062117.41	2918.21 (9574)
GHN-ACT-0151	Stable	TH-GN-06		453715.48	4062117.41	2916.69 (9569)
GHN-ACT-0152	Stable	TH-GN-06		453715.48	4062117.41	2915.16 (9564)

Table A1 continued.

Sample ID	Pile Portion	Hole/Pit ID	Bench	UTM Easting m	UTM Northing m	Elevation m (ft)
GHN-ACT-0153	Stable	TH-GN-06		453715.48	4062117.41	2913.64 (9559)
GHN-ACT-0154	Stable	TH-GN-06		453715.48	4062117.41	2912.12 (9554)
GHN-ACT-0155	Stable	TH-GN-06		453715.48	4062117.41	2910.59 (9549)
GHN-ACT-0156	Stable	TH-GN-06		453715.48	4062117.41	2909.07 (9544)
GHN-ACT-0157	Stable	TH-GN-06		453715.48	4062117.41	2907.54 (9539)
GHN-ACT-0158	Stable	TH-GN-06		453715.48	4062117.41	2906.02 (9534)
GHN-ACT-0159	Stable	TH-GN-06		453715.48	4062117.41	2904.50 (9529)
GHN-ACT-0160	Stable	TH-GN-06		453715.48	4062117.41	2902.97 (9524)
GHN-ACT-0161	Stable	TH-GN-06		453715.48	4062117.41	2902.06 (9521)
GHN-ACT-0162	Unstable	TH-GN-07S		453474.41	4062185.16	2842.52 (9325)
GHN-ACT-0163	Unstable	TH-GN-07S		453474.41	4062185.16	2841.15 (9321)
GHN-ACT-0164	Unstable	TH-GN-07S		453474.41	4062185.16	2839.62 (9316)
GHN-ACT-0165	Unstable	TH-GN-07S		453474.41	4062185.16	2839.62 (9316)
GHN-ACT-0166	Unstable	TH-GN-07S		453474.41	4062185.16	2839.62 (9316)
GHN-ACT-0167	Unstable	TH-GN-07S		453474.41	4062185.16	2838.10 (9311)
GHN-ACT-0168	Unstable	TH-GN-07S		453474.41	4062185.16	2836.58 (9306)
GHN-ACT-0169	Unstable	TH-GN-07S		453474.41	4062185.16	2835.05 (9301)
GHN-ACT-0170	Unstable	TH-GN-07S		453474.41	4062185.16	2833.53 (9296)
GHN-ACT-0171	Unstable	TH-GN-07S		453474.41	4062185.16	2832.00 (9291)
GHN-ACT-0172	Unstable	TH-GN-07S		453474.41	4062185.16	2830.48 (9286)
GHN-ACT-0173	Unstable	TH-GN-07S		453474.41	4062185.16	2828.96 (9281)
GHN-ACT-0174	Unstable	TH-GN-07S		453474.41	4062185.16	2827.43 (9276)
GHN-ACT-0175	Unstable	TH-GN-07S		453474.41	4062185.16	2825.91 (9271)
GHN-ACT-0176	Unstable	TH-GN-07S		453474.41	4062185.16	2824.38 (9266)
GHN-ACT-0177	Unstable	TH-GN-07S		453474.41	4062185.16	2822.86 (9261)
GHN-ACT-0178	Unstable	TH-GN-07S		453474.41	4062185.16	2821.34 (9256)
GHN-ACT-0179	Unstable	TH-GN-07S		453474.41	4062185.16	2819.81 (9251)
GHN-ACT-0180	Unstable	TH-GN-07S		453474.41	4062185.16	2818.29 (9246)
GHN-ACT-0181	Unstable	TH-GN-07S		453474.41	4062185.16	2816.76 (9241)
GHN-ACT-0182	Unstable	TH-GN-07S		453474.41	4062185.16	2815.24 (9236)
GHN-ACT-0183	Unstable	TH-GN-07S		453474.41	4062185.16	2813.72 (9231)
GHN-ACT-0184	Unstable	TH-GN-07S		453474.41	4062185.16	2812.19 (9226)
GHN-ACT-0185	Unstable	TH-GN-07S		453474.41	4062185.16	2810.67 (9221)
GHN-ACT-0234	Unstable	SI-3		453476.16	4062179.04	2843.61 (9329)
GHN-ACT-0235	Unstable	SI-3		453476.16	4062179.04	2842.23 (9324)
GHN-ACT-0236	Unstable	SI-3		453476.16	4062179.04	2840.71 (9319)
GHN-ACT-0237	Unstable	SI-3		453476.16	4062179.04	2839.19 (9314)
GHN-ACT-0238	Unstable	SI-3		453476.16	4062179.04	2837.66 (9309)
GHN-ACT-0239	Unstable	SI-3		453476.16	4062179.04	2836.14 (9304)
GHN-ACT-0240	Unstable	SI-3		453476.16	4062179.04	2834.61 (9299)
GHN-ACT-0241	Unstable	SI-3		453476.16	4062179.04	2833.09 (9294)
GHN-ACT-0242	Unstable	SI-3		453476.16	4062179.04	2831.57 (9289)
GHN-ACT-0243	Unstable	SI-3		453476.16	4062179.04	2830.04 (9284)
GHN-ACT-0244	Unstable	SI-3		453476.16	4062179.04	2828.52 (9279)
GHN-ACT-0245	Unstable	SI-3		453476.16	4062179.04	2826.99 (9274)
GHN-ACT-0246	Unstable	SI-3		453476.16	4062179.04	2826.99 (9274)
GHN-ACT-0247	Unstable	SI-3		453476.16	4062179.04	2826.99 (9274)

Table A1 continued.

Sample ID	Pile Portion	Hole/Pit ID	Bench	UTM Easting m	UTM Northing m	Elevation m (ft)
GHN-ACT-0248	Unstable	SI-3		453476.16	4062179.04	2825.47 (9269)
GHN-ACT-0249	Unstable	SI-3		453476.16	4062179.04	2822.42 (9259)
GHN-EHP-0001	Unstable	LFG-017	40	453688.05	4062313.28	2941.67 (9651)
GHN-EHP-0002	Unstable	LFG-017	40	453690.88	4062314.54	2941.67 (9651)
GHN-EHP-0003	Unstable	LFG-011	32	453678.43	4062414.81	2960.55 (9713)
GHN-HRS-0001	Stable	LFG-003	4	453746.69	4062149.98	2966.00 (9730)
GHN-HRS-0002	Stable	LFG-003	4	453751.63	4062148.42	2966.00 (9730)
GHN-HRS-0007	Stable	Surface		453735.00	4062089.00	2976.58 (9765)
GHN-HRS-0009	Unstable	Surface		453375.00	4062236.00	2813.96 (9232)
GHN-HRS-0010	Unstable	Surface		453381.00	4062236.00	2816.96 (9241)
GHN-HRS-0011	Unstable	Surface		453421.00	4062231.00	2830.06 (9284)
GHN-HRS-0012	Unstable	Surface		453481.00	4062186.00	2852.92 (9359)
GHN-HRS-0015	Stable	Surface		453588.00	4062106.00	2894.38 (9495)
GHN-HRS-0016	Stable	Surface		453588.00	4062113.00	2894.38 (9495)
GHN-HRS-0017	Stable	Surface		453610.00	4062121.00	2906.87 (9536)
GHN-HRS-0018	Unstable	Surface		453607.00	4062179.00	2906.87 (9536)
GHN-HRS-0019	Unstable	Surface		453607.00	4062187.00	2906.87 (9536)
GHN-HRS-0020	Unstable	Surface		453607.00	4062203.00	2906.87 (9536)
GHN-HRS-0021	Unstable	Surface		453526.00	4062282.00	2864.81 (9398)
GHN-HRS-0022	Unstable	Surface		453500.00	4062314.00	2864.81 (9398)
GHN-HRS-0023	Unstable	Surface		453710.00	4062418.00	2979.42 (9774)
GHN-HRS-0024	Stable	Surface		453698.75	4062049.00	2972.58 (9752)
GHN-HRS-0025	Stable	Surface		453698.58	4062050.11	2972.88 (9753)
GHN-HRS-0026	Stable	LFG-005	4	453744.83	4062138.18	2972.10 (9750)
GHN-HRS-0085	Stable	Surface		453694.45	4062089.79	2968.96 (9740)
GHN-HRS-0086	Stable	Surface		453693.82	4062091.45	2969.16 (9741)
GHN-HRS-0087	Stable	Surface		453693.15	4062088.37	2968.92 (9740)
GHN-HRS-0088	Unstable	LFG-011	29	453662.60	4062329.33	2945.62 (9664)
GHN-HRS-0089	Unstable	LFG-011	29	453663.91	4062330.77	2945.62 (9664)
GHN-HRS-0090	Unstable	LFG-011	29	453665.92	4062333.00	2945.62 (9664)
GHN-HRS-0091	Unstable	LFG-011	29	453664.11	4062331.00	2945.62 (9664)
GHN-HRS-0092	Unstable	LFG-011	29	453675.16	4062343.25	2945.62 (9664)
GHN-HRS-0093	Unstable	LFG-011	29	453664.31	4062331.22	2945.62 (9664)
GHN-HRS-0094	Unstable	LFG-011	29	453661.70	4062328.32	2945.62 (9664)
GHN-HRS-0095	Unstable	LFG-012	31	453692.03	4062353.25	2955.09 (9695)
GHN-HRS-0096	Unstable	LFG-012	31	453693.06	4062353.67	2954.94 (9694)
GHN-HRS-0098	Unstable	LFG-018	41	453679.32	4062296.16	2931.32 (9617)
GHN-HRS-0099	Unstable	LFG-013	41	453679.85	4062296.42	2931.32 (9617)
GHN-HRS-0100	Unstable	LFG-013	41	453679.32	4062296.16	2931.32 (9617)
GHN-HRS-0101	Unstable	LFG-013	41	453678.26	4062295.62	2931.32 (9617)
GHN-HRS-0102	Unstable	LFG-011	37	453673.37	4062330.02	2940.31 (9646)
GHN-HRS-0103	Unstable	LFG-011	37	453669.31	4062325.23	2939.85 (9645)
GHN-HRS-0104	Unstable	LFG-011	46	453647.46	4062268.53	2919.13 (9577)
GHN-HRS-0105	Unstable	LFG-011	46	453652.52	4062274.49	2919.13 (9577)
GHN-JMS-0001	Stable	Surface		453710.00	4062089.00	2976.06 (9763)
GHN-JMS-0002	Stable	Surface		453710.00	4062089.00	2976.06 (9763)
GHN-JMS-0003	Stable	Surface		453709.00	4062086.00	2977.89 (9769)

Table A1 continued.

Sample ID	Pile Portion	Hole/Pit ID	Bench	UTM Easting m	UTM Northing m	Elevation m (ft)
GHN-JMS-0004	Stable	Surface		453709.00	4062086.00	2977.89 (9769)
GHN-JRM-0001	Stable	LFG-009	22	453642.21	4062136.81	2926.67 (9601)
GHN-JRM-0002	Stable	LFG-009	22	453642.36	4062136.82	2926.40 (9600)
GHN-JRM-0003	Stable	LFG-009	23	453642.56	4062133.02	2925.07 (9596)
GHN-JRM-0004	Stable	LFG-009	23	453642.77	4062133.03	2925.10 (9596)
GHN-JRM-0005	Stable	LFG-009	23	453642.46	4062133.02	2925.05 (9596)
GHN-JRM-0006	Stable	LFG-009	24	453642.10	4062129.64	2923.90 (9592)
GHN-JRM-0007	Stable	LFG-009	24	453641.49	4062129.58	2923.51 (9591)
GHN-JRM-0008	Stable	LFG-009	25	453637.65	4062123.30	2922.30 (9587)
GHN-JRM-0009	Stable	LFG-009	25	453634.16	4062122.93	2921.75 (9585)
GHN-JRM-0010	Stable	LFG-009	24	453636.73	4062117.58	2923.92 (9592)
GHN-JRM-0011	Stable	LFG-009	24	453636.73	4062117.58	2924.53 (9594)
GHN-JRM-0012	Stable	LFG-009	23	453640.17	4062114.68	2925.25 (9597)
GHN-JRM-0013	Stable	LFG-009	23	453640.48	4062114.72	2925.90 (9599)
GHN-JRM-0014	Stable	LFG-009	22	453649.80	4062137.47	2923.14 (9590)
GHN-JRM-0015	Stable	LFG-009	22	453649.80	4062137.47	2923.14 (9590)
GHN-JRM-0019	Stable	LFG-009	22	453651.32	4062137.60	2927.92 (9605)
GHN-JRM-0020	Stable	LFG-009	22	453645.24	4062137.07	2926.78 (9602)
GHN-JRM-0021	Stable	LFG-009	22	453637.95	4062136.44	2925.41 (9597)
GHN-JRM-0022	Stable	LFG-009	22	453649.80	4062137.47	2927.64 (9605)
GHN-JRM-0024	Stable	LFG-009	24	453641.49	4062129.58	2923.82 (9592)
GHN-JRM-0025	Stable	LFG-009	24	453636.03	4062129.04	2922.47 (9588)
GHN-JRM-0026	Stable	LFG-009	25	453636.59	4062123.19	2921.52 (9584)
GHN-JRM-0027	Stable	LFG-009	23	453644.71	4062115.25	2925.87 (9599)
GHN-JRM-0028	Stable	LFG-009	22	453645.24	4062137.07	2926.78 (9602)
GHN-JRM-0029	Stable	LFG-009	22	453637.95	4062136.44	2925.41 (9597)
GHN-JRM-0030	Stable	LFG-009	23	453645.01	4062115.29	2925.30 (9597)
GHN-JRM-0031	Stable	LFG-009	23	453645.01	4062115.29	2925.61 (9598)
GHN-JRM-0033	Unstable	LFG-011	29	453677.09	4062345.39	2945.32 (9663)
GHN-JRM-0034	Unstable	LFG-011	29	453668.33	4062335.68	2945.62 (9664)
GHN-JRM-0035	Unstable	LFG-011	30	453664.33	4062326.42	2944.06 (9658)
GHN-JRM-0036	Unstable	LFG-011	30	453676.89	4062341.76	2944.06 (9658)
GHN-JRM-0037	Unstable	LFG-011	28	453664.78	4062334.15	2945.74 (9664)
GHN-JRM-0038	Unstable	LFG-011	28	453670.12	4062340.01	2945.74 (9664)
GHN-JRM-0039	Unstable	LFG-011	30	453670.80	4062334.32	2944.37 (9659)
GHN-JRM-0040	Unstable	LFG-011	30	453670.04	4062333.39	2944.52 (9660)
GHN-JRM-0041	Unstable	LFG-011	30	453666.24	4062328.74	2944.06 (9658)
GHN-JRM-0042	Unstable	LFG-012	31	453693.83	4062353.98	2954.33 (9692)
GHN-JRM-0043	Unstable	LFG-012	31	453695.37	4062354.61	2954.33 (9692)
GHN-JRM-0044	Unstable	LFG-012	31	453693.83	4062353.98	2955.85 (9697)
GHN-JRM-0045	Unstable	LFG-012	31	453694.60	4062354.30	2954.94 (9694)
GHN-JRM-0046	Unstable	LFG-012	31	453694.60	4062354.30	2956.01 (9698)
GHN-JRM-0047	Unstable	LFG-011	29	453669.39	4062334.79	2944.71 (9661)
GHN-JRM-0048	Unstable	LFG-012	28	453670.12	4062340.01	2945.74 (9664)
GHN-JRM-0049	Unstable	LFG-012	28	453664.78	4062334.15	2945.74 (9664)
GHN-JRM-0050	Unstable	LFG-011	30	453674.70	4062336.88	2943.45 (9656)
GHN-JRM-0051	Unstable	LFG-012	31	453693.57	4062353.88	2954.03 (9691)

Table A1 continued.

Sample ID	Pile Portion	Hole/Pit ID	Bench	UTM Easting m	UTM Northing m	Elevation m (ft)
GHN-KMD-0001	Stable	LFG-006	7	453717.61	4062127.74	2968.85 (9740)
GHN-KMD-0002	Stable	LFG-006	7	453715.78	4062147.53	2969.33 (9741)
GHN-KMD-0003	Stable	LFG-006	8	453718.25	4062130.64	2968.33 (9738)
GHN-KMD-0004	Stable	LFG-006	7	453718.27	4062133.73	2966.71 (9733)
GHN-KMD-0005	Stable	LFG-006	9	453715.66	4062134.27	2967.65 (9736)
GHN-KMD-0006	Stable	LFG-006	10	453718.81	4062141.05	2965.98 (9730)
GHN-KMD-0007	Stable	LFG-006	9	453719.34	4062141.71	2965.66 (9729)
GHN-KMD-0008	Stable	LFG-006	10	453706.83	4062138.79	2964.53 (9726)
GHN-KMD-0009	Stable	LFG-006	8	453719.16	4062144.50	2967.94 (9737)
GHN-KMD-0010	Stable	LFG-006	8	453726.76	4062144.01	2968.35 (9738)
GHN-KMD-0011	Stable	LFG-006	7	453719.16	4062147.27	2968.96 (9740)
GHN-KMD-0012	Stable	LFG-006	10	453706.32	4062141.66	2964.69 (9726)
GHN-KMD-0013	Stable	LFG-006	9	453711.13	4062142.23	2966.95 (9733)
GHN-KMD-0014	Stable	LFG-006	8	453717.79	4062144.54	2967.88 (9737)
GHN-KMD-0015	Stable	LFG-006	9	453722.69	4062141.51	2967.45 (9735)
GHN-KMD-0016	Stable	LFG-006	9	453725.12	4062141.35	2967.56 (9735)
GHN-KMD-0017	Stable	LFG-006	9	453695.91	4062143.17	2965.99 (9730)
GHN-KMD-0018	Stable	LFG-006	9	453698.17	4062143.15	2965.86 (9730)
GHN-KMD-0019	Stable	LFG-006	8	453726.70	4062144.12	2968.31 (9738)
GHN-KMD-0020	Stable	LFG-006	8	453722.20	4062144.30	2968.41 (9738)
GHN-KMD-0021	Stable	LFG-006	8	453723.60	4062144.37	2968.22 (9738)
GHN-KMD-0022	Stable	LFG-006	10	453707.54	4062141.60	2964.79 (9726)
GHN-KMD-0023	Stable	LFG-006	10	453717.90	4062141.09	2965.75 (9730)
GHN-KMD-0024	Stable	LFG-006	10	453719.42	4062141.02	2965.87 (9730)
GHN-KMD-0025	Stable	LFG-006	10	453724.29	4062140.78	2966.25 (9731)
GHN-KMD-0026	Stable	LFG-006	9	453728.78	4062141.13	2967.57 (9736)
GHN-KMD-0027	Stable	LFG-006	7	453707.87	4062147.95	2968.30 (9738)
GHN-KMD-0028	Stable	LFG-006	10	453706.93	4062141.63	2964.74 (9726)
GHN-KMD-0036	Stable	LFG-006	9	453697.13	4062143.10	2966.04 (9731)
GHN-KMD-0037	Stable	LFG-006	9	453698.95	4062142.98	2966.12 (9731)
GHN-KMD-0038	Stable	LFG-006	9	453701.69	4062142.81	2966.24 (9731)
GHN-KMD-0039	Stable	LFG-006	9	453712.65	4062142.13	2966.71 (9733)
GHN-KMD-0040	Stable	LFG-006	9	453718.13	4062141.79	2966.95 (9733)
GHN-KMD-0041	Stable	LFG-006	9	453722.99	4062141.49	2967.47 (9735)
GHN-KMD-0042	Stable	LFG-006	9	453724.52	4062141.39	2967.53 (9735)
GHN-KMD-0043	Stable	LFG-006	9	453728.78	4062141.13	2967.72 (9736)
GHN-KMD-0044	Stable	LFG-007	12	453690.71	4062145.29	2956.61 (9700)
GHN-KMD-0045	Stable	LFG-007	13	453690.94	4062141.93	2955.44 (9696)
GHN-KMD-0046	Stable	LFG-007	13	453678.23	4062143.57	2953.95 (9691)
GHN-KMD-0047	Stable	LFG-007	14	453690.82	4062139.41	2954.37 (9692)
GHN-KMD-0048	Stable	LFG-007	15	453691.79	4062131.53	2953.02 (9688)
GHN-KMD-0049	Stable	LFG-007	15	453692.36	4062129.29	2953.01 (9688)
GHN-KMD-0050	Stable	LFG-007	12	453704.22	4062145.44	2957.41 (9702)
GHN-KMD-0051	Stable	LFG-007	12	453695.08	4062145.80	2955.95 (9697)
GHN-KMD-0052	Stable	LFG-007	12	453692.64	4062145.89	2955.64 (9696)
GHN-KMD-0053	Stable	LFG-007	12	453684.72	4062146.20	2954.64 (9693)
GHN-KMD-0054	Stable	LFG-007	12	453681.98	4062146.31	2954.30 (9692)

Table A1 continued.

Sample ID	Pile Portion	Hole/Pit ID	Bench	UTM Easting m	UTM Northing m	Elevation m (ft)
GHN-KMD-0055	Stable	LFG-007	12	453676.49	4062146.52	2953.91 (9691)
GHN-KMD-0056	Stable	LFG-007	14	453704.94	4062139.52	2955.62 (9696)
GHN-KMD-0057	Stable	LFG-007	14	453695.80	4062139.90	2954.74 (9693)
GHN-KMD-0062	Stable	LFG-007	14	453682.40	4062140.46	2953.44 (9689)
GHN-KMD-0063	Stable	LFG-007	14	453677.22	4062140.67	2952.94 (9688)
GHN-KMD-0064	Stable	LFG-007	15	453694.92	4062131.91	2953.53 (9689)
GHN-KMD-0065	Stable	LFG-007	15	453698.88	4062131.75	2953.96 (9691)
GHN-KMD-0066	Stable	LFG-007	12	453704.22	4062145.44	2958.02 (9704)
GHN-KMD-0067	Stable	LFG-008	17	453670.47	4062141.29	2941.87 (9651)
GHN-KMD-0068	Stable	LFG-008	18	453670.75	4062137.43	2940.04 (9645)
GHN-KMD-0069	Stable	LFG-008	19	453671.07	4062134.12	2938.91 (9641)
GHN-KMD-0070	Stable	LFG-008	20	453671.82	4062129.19	2938.70 (9641)
GHN-KMD-0071	Stable	LFG-008	18	453678.68	4062137.53	2941.06 (9649)
GHN-KMD-0072	Stable	LFG-008	18	453671.36	4062137.44	2940.11 (9645)
GHN-KMD-0073	Stable	LFG-008	18	453666.79	4062137.39	2939.52 (9643)
GHN-KMD-0074	Stable	LFG-008	18	453680.20	4062137.54	2941.26 (9649)
GHN-KMD-0075	Stable	LFG-008	19	453667.11	4062133.99	2938.98 (9642)
GHN-KMD-0076	Stable	LFG-008	19	453671.68	4062134.14	2939.60 (9644)
GHN-KMD-0077	Stable	LFG-008	19	453670.16	4062134.09	2939.40 (9643)
GHN-KMD-0078	Stable	LFG-008	19	453671.68	4062134.14	2939.60 (9644)
GHN-KMD-0079	Stable	LFG-008	18	453679.29	4062137.53	2941.91 (9651)
GHN-KMD-0080	Stable	LFG-008	18	453677.46	4062137.51	2941.52 (9650)
GHN-KMD-0081	Stable	LFG-008	18	453675.93	4062137.49	2941.32 (9649)
GHN-KMD-0082	Stable	LFG-008	20	453659.07	4062126.45	2936.84 (9635)
GHN-KMD-0083	Stable	LFG-008	20	453659.07	4062126.45	2936.53 (9634)
GHN-KMD-0084	Stable	LFG-008	20	453658.66	4062127.16	2936.43 (9633)
GHN-KMD-0085	Stable	LFG-008	20	453658.66	4062127.16	2937.04 (9635)
GHN-KMD-0086	Stable	LFG-008	20	453658.66	4062127.16	2937.04 (9635)
GHN-KMD-0087	Stable	LFG-008	20	453658.66	4062127.16	2937.04 (9635)
GHN-KMD-0088	Stable	LFG-008	20	453657.44	4062127.08	2936.87 (9635)
GHN-KMD-0089	Stable	LFG-008	20	453657.75	4062127.10	2936.30 (9633)
GHN-KMD-0090	Stable	LFG-008	20	453655.01	4062126.94	2936.51 (9634)
GHN-KMD-0091	Stable	LFG-008	20	453652.27	4062126.79	2935.96 (9632)
GHN-KMD-0092	Stable	LFG-008	19	453661.93	4062133.82	2938.28 (9639)
GHN-KMD-0093	Stable	LFG-008	19	453658.88	4062133.72	2937.86 (9638)
GHN-KMD-0095	Stable	LFG-008	18	453656.02	4062118.60	2937.84 (9638)
GHN-KMD-0096	Stable	LFG-008	18	453658.45	4062118.83	2938.36 (9640)
GHN-KMD-0098	Stable	LFG-008	17	453670.47	4062141.29	2941.26 (9649)
GHN-KMD-0099	Stable	LFG-008	18	453679.59	4062137.54	2941.18 (9649)
GHN-KMD-0100	Stable	LFG-008	19	453666.26	4062133.40	2936.45 (9633)
GHN-LFG-0015	Unstable	Surface		453551.00	4062310.00	2884.93 (9464)
GHN-LFG-0016	Unstable	Surface		453551.00	4062310.00	2884.93 (9464)
GHN-LFG-0017	Unstable	Surface		453551.00	4062310.00	2884.93 (9464)
GHN-LFG-0018	Stable	LFG-003	1	453747.00	4062150.00	2970.58 (9745)
GHN-LFG-0019	Stable	LFG-003	1	453747.00	4062150.00	2970.58 (9745)
GHN-LFG-0020	Stable	LFG-003	1	453747.00	4062150.00	2970.58 (9745)
GHN-LFG-0021	Stable	LFG-003	2	453750.61	4062150.39	2968.63 (9739)

Table A1 continued.

Sample ID	Pile Portion	Hole/Pit ID	Bench	UTM Easting m	UTM Northing m	Elevation m (ft)
GHN-LFG-0022	Stable	LFG-003	2	453750.04	4062150.59	2968.63 (9739)
GHN-LFG-0023	Stable	LFG-003	2	453749.75	4062150.69	2968.78 (9739)
GHN-LFG-0024	Stable	LFG-003	2	453748.89	4062150.99	2968.93 (9740)
GHN-LFG-0025	Stable	LFG-003	2	453746.87	4062151.69	2969.39 (9741)
GHN-LFG-0027	Stable	LFG-003	3	453753.96	4062148.71	2967.22 (9734)
GHN-LFG-0028	Stable	LFG-003	3	453753.08	4062148.98	2967.53 (9735)
GHN-LFG-0029	Stable	LFG-003	3	453748.43	4062150.46	2967.83 (9736)
GHN-LFG-0030	Stable	LFG-003	3	453750.18	4062149.90	2967.83 (9736)
GHN-LFG-0031	Stable	LFG-003	3	453749.89	4062150.00	2967.22 (9734)
GHN-LFG-0032	Stable	LFG-003	4	453751.63	4062148.42	2966.00 (9730)
GHN-LFG-0033	Stable	LFG-003	4	453746.69	4062149.98	2966.00 (9730)
GHN-LFG-0034	Stable	LFG-004	1	453713.08	4062099.07	2969.05 (9740)
GHN-LFG-0035	Stable	LFG-004	1	453711.90	4062099.07	2969.05 (9740)
GHN-LFG-0036	Stable	LFG-004	1	453709.86	4062099.07	2969.05 (9740)
GHN-LFG-0037	Stable	LFG-004	1	453742.79	4062149.01	2970.04 (9744)
GHN-LFG-0038	Stable	LFG-004	2	453716.05	4062098.47	2967.53 (9735)
GHN-LFG-0039	Stable	LFG-004	2	453714.68	4062098.47	2967.53 (9735)
GHN-LFG-0040	Stable	LFG-004	2	453712.85	4062098.47	2967.53 (9735)
GHN-LFG-0041	Stable	LFG-003	3	453759.65	4062146.91	2967.53 (9735)
GHN-LFG-0042	Stable	LFG-003	3	453760.64	4062146.59	2967.22 (9734)
GHN-LFG-0043	Stable	LFG-003	3	453762.50	4062146.00	2967.53 (9735)
GHN-LFG-0044	Stable	LFG-005	1	453730.49	4062148.09	2976.49 (9765)
GHN-LFG-0045	Stable	LFG-005	1	453731.42	4062146.33	2976.15 (9764)
GHN-LFG-0046	Stable	LFG-005	1	453731.12	4062146.37	2976.16 (9764)
GHN-LFG-0047	Stable	LFG-005	1	453733.68	4062147.57	2975.81 (9763)
GHN-LFG-0048	Stable	LFG-005	1	453733.23	4062146.06	2976.10 (9763)
GHN-LFG-0049	Stable	LFG-005	1	453733.53	4062146.01	2976.24 (9764)
GHN-LFG-0050	Stable	LFG-005	1	453733.53	4062146.01	2976.55 (9765)
GHN-LFG-0051	Stable	LFG-005	1	453731.12	4062146.37	2976.16 (9764)
GHN-LFG-0052	Stable	LFG-005	1	453729.61	4062146.60	2976.66 (9765)
GHN-LFG-0053	Stable	LFG-005	1	453743.50	4062146.15	2974.91 (9760)
GHN-LFG-0054	Stable	LFG-005	1	453745.02	4062145.97	2974.68 (9759)
GHN-LFG-0057	Stable	LFG-005	1	453733.83	4062145.97	2976.38 (9764)
GHN-LFG-0058	Stable	LFG-005	1	453732.96	4062146.06	2975.59 (9762)
GHN-LFG-0059	Stable	LFG-005	2	453731.53	4062143.23	2974.86 (9759)
GHN-LFG-0060	Stable	LFG-005	4	453747.96	4062141.02	2971.77 (9749)
GHN-LFG-0061	Stable	LFG-005	2	453733.34	4062144.76	2975.29 (9761)
GHN-LFG-0062	Stable	LFG-005	2	453731.06	4062145.05	2975.56 (9762)
GHN-LFG-0063	Stable	LFG-005	3	453730.80	4062142.34	2973.74 (9756)
GHN-LFG-0064	Stable	LFG-005	3	453731.85	4062142.16	2973.62 (9755)
GHN-LFG-0065	Stable	LFG-005	4	453729.98	4062140.02	2972.28 (9751)
GHN-LFG-0066	Stable	LFG-005	4	453729.98	4062140.02	2972.28 (9751)
GHN-LFG-0067	Stable	LFG-005	4	453743.61	4062132.22	2970.90 (9746)
GHN-LFG-0068	Stable	LFG-005	4	453749.48	4062141.02	2972.73 (9752)
GHN-LFG-0069	Stable	LFG-005	4	453751.01	4062141.02	2973.94 (9756)
GHN-LFG-0070	Stable	LFG-005	4	453754.06	4062141.02	2973.48 (9755)
GHN-LFG-0071	Stable	LFG-005	2	453743.86	4062126.53	2973.79 (9756)

Table A1 continued.

Sample ID	Pile Portion	Hole/Pit ID	Bench	UTM Easting m	UTM Northing m	Elevation m (ft)
GHN-LFG-0072	Stable	LFG-005	2	453742.53	4062126.78	2970.96 (9747)
GHN-LFG-0075	Stable	LFG-005	5	453755.62	4062133.60	2970.84 (9746)
GHN-LFG-0076	Stable	LFG-005	5	453755.02	4062133.71	2970.78 (9746)
GHN-LFG-0077	Stable	LFG-005	5	453754.42	4062133.82	2971.10 (9747)
GHN-LFG-0084	Stable	LFG-005	3	453731.91	4062143.59	2974.01 (9757)
GHN-LFG-0085	Stable	LFG-005	3	453731.42	4062143.33	2974.75 (9759)
GHN-LFG-0086	Stable	LFG-005	3	453731.42	4062143.33	2974.75 (9759)
GHN-LFG-0088	Stable	LFG-005	4	453734.05	4062140.29	2973.33 (9754)
GHN-PXW-0001	Stable	SI-30		453510.71	4062092.39	2851.83 (9356)
GHN-PXW-0002	Stable	SI-30		453510.71	4062092.39	2848.93 (9346)
GHN-PXW-0003	Stable	SI-30		453510.71	4062092.39	2845.88 (9336)
GHN-PXW-0004	Stable	SI-30		453510.71	4062092.39	2842.83 (9326)
GHN-PXW-0005	Stable	SI-30		453510.71	4062092.39	2839.79 (9316)
GHN-PXW-0006	Stable	SI-30		453510.71	4062092.39	2836.74 (9306)
GHN-PXW-0007	Stable	SI-30		453510.71	4062092.39	2833.69 (9296)
GHN-PXW-0008	Stable	SI-30		453510.71	4062092.39	2830.64 (9286)
GHN-PXW-0009	Stable	SI-30		453510.71	4062092.39	2827.59 (9276)
GHN-PXW-0010	Stable	SI-30		453510.71	4062092.39	2824.55 (9266)
GHN-PXW-0011	Stable	SI-30		453510.71	4062092.39	2821.50 (9256)
GHN-PXW-0012	Stable	SI-30		453510.71	4062092.39	2818.45 (9246)
GHN-PXW-0013	Stable	SI-30		453510.71	4062092.39	2815.40 (9236)
GHN-PXW-0014	Stable	SI-30		453510.71	4062092.39	2812.35 (9226)
GHN-PXW-0015	Stable	SI-30		453510.71	4062092.39	2809.31 (9216)
GHN-PXW-0016	Stable	SI-30		453510.71	4062092.39	2806.56 (9207)
GHN-SAW-0001	Unstable	LFG-018	41	453680.11	4062296.56	2931.32 (9617)
GHN-SAW-0002	Unstable	LFG-018	41	453680.11	4062296.56	2931.32 (9617)
GHN-SAW-0004	Unstable	LFG-011	43	453657.30	4062290.29	2933.73 (9624)
GHN-SAW-0200	Unstable	LFG-021	51	453650.52	4062394.34	2939.92 (9645)
GHN-SAW-0201	Unstable	LFG-022	53	453647.00	4062393.80	2941.69 (9651)
GHN-STM-0001	Stable	Surface		453601.00	4062104.00	2903.52 (9525)
GHN-STM-0002	Stable	Surface		453602.00	4062110.00	2906.87 (9536)
GHN-STM-0003	Unstable	Surface		453596.00	4062188.00	2900.47 (9515)
GHN-STM-0004	Unstable	Surface		453582.00	4062213.00	2892.24 (9488)
GHN-STM-0005	Unstable	Surface		453537.00	4062293.00	2883.40 (9459)
GHN-STM-0006	Unstable	Surface		453497.00	4062157.00	2859.93 (9382)
GHN-STM-0007	Unstable	Surface		453510.00	4062202.00	2869.69 (9414)
GHN-STM-0008	Unstable	Surface		453487.00	4062249.00	2855.06 (9366)
GHN-STM-0009	Stable	Surface		453427.00	4062085.00	2802.63 (9194)
GHN-STM-0010	Stable	Surface		453439.00	4062097.00	2807.20 (9209)
GHN-STM-0011	Stable	Surface		453437.00	4062103.00	2810.25 (9219)
GHN-STM-0012	Stable	Surface		453382.00	4062098.00	2841.65 (9322)
GHN-STM-0013	Stable	Surface		453382.00	4062098.00	2841.65 (9322)
GHN-VTM-0030	Stable	LFG-005	1	453717.55	4062148.41	2976.54 (9765)
GHN-VTM-0031	Stable	LFG-005	1	453719.06	4062148.19	2976.50 (9765)
GHN-VTM-0032	Stable	LFG-005	1	453720.56	4062147.96	2976.46 (9765)
GHN-VTM-0033	Stable	LFG-005	1	453722.07	4062147.73	2976.42 (9765)
GHN-VTM-0034	Stable	LFG-005	1	453723.58	4062147.51	2976.98 (9766)

Table A1 continued.

Sample ID	Pile Portion	Hole/Pit ID	Bench	UTM Easting m	UTM Northing m	Elevation m (ft)
GHN-VTM-0035	Stable	LFG-005	1	453725.09	4062147.28	2976.94 (9766)
GHN-VTM-0036	Stable	LFG-005	1	453726.59	4062147.05	2976.90 (9766)
GHN-VTM-0037	Stable	LFG-005	1	453727.50	4062146.92	2976.87 (9766)
GHN-VTM-0038	Stable	LFG-005	1	453729.61	4062146.60	2976.81 (9766)
GHN-VTM-0039	Stable	LFG-005	1	453730.81	4062146.42	2976.78 (9766)
GHN-VTM-0040	Stable	LFG-005	1	453732.93	4062146.10	2976.71 (9766)
GHN-VTM-0041	Stable	LFG-005	1	453734.43	4062145.88	2976.67 (9765)
GHN-VTM-0042	Stable	LFG-005	1	453735.94	4062145.65	2976.63 (9765)
GHN-VTM-0043	Stable	LFG-005	1	453737.75	4062145.38	2976.58 (9765)
GHN-VTM-0044	Stable	LFG-005	1	453738.65	4062145.24	2976.55 (9765)
GHN-VTM-0045	Stable	LFG-005	1	453740.16	4062145.01	2976.51 (9765)
GHN-VTM-0046	Stable	LFG-005	1	453741.67	4062144.79	2976.47 (9765)
GHN-VTM-0047	Stable	LFG-005	1	453743.18	4062144.56	2976.42 (9765)
GHN-VTM-0048	Stable	LFG-005	1	453744.68	4062144.34	2976.38 (9764)
GHN-VTM-0049	Stable	LFG-005	1	453746.19	4062144.11	2976.34 (9764)
GHN-VTM-0050	Stable	LFG-005	1	453747.70	4062143.88	2976.29 (9764)
GHN-VTM-0051	Stable	LFG-005	1	453749.21	4062143.66	2975.95 (9763)
GHN-VTM-0052	Stable	LFG-005	1	453750.71	4062143.43	2975.90 (9763)
GHN-VTM-0053	Stable	LFG-005	1	453752.22	4062143.20	2975.86 (9763)
GHN-VTM-0054	Stable	LFG-005	1	453753.73	4062142.98	2975.82 (9763)
GHN-VTM-0055	Stable	LFG-005	1	453755.24	4062142.75	2975.77 (9762)
GHN-VTM-0056	Stable	LFG-005	1	453756.74	4062142.52	2975.73 (9762)
GHN-VTM-0057	Stable	LFG-005	2	453714.67	4062147.76	2976.20 (9764)
GHN-VTM-0058	Stable	LFG-005	2	453716.17	4062147.52	2975.81 (9763)
GHN-VTM-0059	Stable	LFG-005	2	453717.68	4062147.29	2975.73 (9762)
GHN-VTM-0060	Stable	LFG-005	2	453719.18	4062147.05	2975.64 (9762)
GHN-VTM-0061	Stable	LFG-005	2	453720.69	4062146.81	2975.56 (9762)
GHN-VTM-0062	Stable	LFG-005	2	453722.19	4062146.58	2975.48 (9761)
GHN-VTM-0063	Stable	LFG-005	2	453723.70	4062146.34	2975.39 (9761)
GHN-VTM-0064	Stable	LFG-005	2	453725.21	4062146.10	2975.31 (9761)
GHN-VTM-0065	Stable	LFG-005	2	453726.71	4062145.86	2975.23 (9761)
GHN-VTM-0066	Stable	LFG-005	2	453728.22	4062145.63	2975.14 (9760)
GHN-VTM-0067	Stable	LFG-005	2	453729.72	4062145.39	2975.06 (9760)
GHN-VTM-0068	Stable	LFG-005	2	453730.63	4062145.25	2975.01 (9760)
GHN-VTM-0069	Stable	LFG-005	2	453732.74	4062144.92	2974.89 (9760)
GHN-VTM-0070	Stable	LFG-005	2	453734.24	4062144.68	2974.81 (9759)
GHN-VTM-0071	Stable	LFG-005	2	453735.75	4062144.44	2974.72 (9759)
GHN-VTM-0072	Stable	LFG-005	2	453737.25	4062144.21	2974.64 (9759)
GHN-VTM-0073	Stable	LFG-005	2	453738.76	4062143.97	2974.56 (9758)
GHN-VTM-0074	Stable	LFG-005	2	453740.26	4062143.73	2974.47 (9758)
GHN-VTM-0075	Stable	LFG-005	2	453741.77	4062143.49	2974.39 (9758)
GHN-VTM-0076	Stable	LFG-005	2	453743.28	4062143.26	2974.31 (9758)
GHN-VTM-0077	Stable	LFG-005	2	453744.78	4062143.02	2974.22 (9757)
GHN-VTM-0078	Stable	LFG-005	2	453746.29	4062142.78	2974.14 (9757)
GHN-VTM-0079	Stable	LFG-005	1	453730.81	4062146.42	2976.78 (9766)
GHN-VTM-0080	Stable	LFG-005	1	453737.75	4062145.38	2976.58 (9765)
GHN-VTM-0081	Stable	LFG-005	2	453741.77	4062143.49	2974.39 (9758)

Table A1 continued.

Sample ID	Pile Portion	Hole/Pit ID	Bench	UTM Easting m	UTM Northing m	Elevation m (ft)
GHN-VTM-0082	Stable	LFG-005	2	453748.70	4062142.40	2974.01 (9757)
GHN-VTM-0083	Stable	LFG-005	2	453749.30	4062142.31	2973.97 (9757)
GHN-VTM-0084	Stable	LFG-005	2	453751.71	4062141.93	2973.84 (9756)
GHN-VTM-0085	Stable	LFG-005	2	453751.71	4062141.93	2973.84 (9756)
GHN-VTM-0086	Stable	LFG-005	2	453753.22	4062141.69	2973.76 (9756)
GHN-VTM-0087	Stable	LFG-005	2	453754.42	4062141.50	2973.69 (9756)
GHN-VTM-0088	Stable	LFG-005	3	453717.31	4062145.83	2975.26 (9761)
GHN-VTM-0089	Stable	LFG-005	3	453718.81	4062145.56	2975.18 (9760)
GHN-VTM-0090	Stable	LFG-005	3	453720.32	4062145.30	2975.09 (9760)
GHN-VTM-0091	Stable	LFG-005	3	453721.82	4062145.03	2975.00 (9760)
GHN-VTM-0092	Stable	LFG-005	3	453722.72	4062144.87	2974.95 (9760)
GHN-VTM-0093	Stable	LFG-005	3	453724.22	4062144.61	2974.86 (9759)
GHN-VTM-0094	Stable	LFG-005	3	453725.72	4062144.34	2974.77 (9759)
GHN-VTM-0095	Stable	LFG-005	3	453726.92	4062144.13	2974.70 (9759)
GHN-VTM-0096	Stable	LFG-005	3	453728.42	4062143.86	2974.62 (9759)
GHN-VTM-0097	Stable	LFG-005	3	453729.92	4062143.60	2974.53 (9758)
GHN-VTM-0098	Stable	LFG-005	3	453729.92	4062143.60	2974.53 (9758)
GHN-VTM-0099	Stable	LFG-005	3	453730.82	4062143.44	2974.48 (9758)
GHN-VTM-0100	Stable	LFG-005	3	453732.32	4062143.17	2974.39 (9758)
GHN-VTM-0101	Stable	LFG-005	3	453733.83	4062142.91	2974.30 (9758)
GHN-VTM-0102	Stable	LFG-005	3	453735.93	4062142.53	2974.18 (9757)
GHN-VTM-0103	Stable	LFG-005	3	453738.03	4062142.16	2974.05 (9757)
GHN-VTM-0104	Stable	LFG-005	3	453739.83	4062141.84	2973.95 (9756)
GHN-VTM-0105	Stable	LFG-005	3	453741.33	4062141.58	2973.86 (9756)
GHN-VTM-0106	Stable	LFG-005	3	453742.83	4062141.31	2973.77 (9756)
GHN-VTM-0107	Stable	LFG-005	3	453744.33	4062141.05	2973.69 (9756)
GHN-VTM-0108	Stable	LFG-005	3	453744.33	4062141.05	2973.69 (9756)
GHN-VTM-0109	Stable	LFG-005	3	453745.83	4062140.78	2973.60 (9755)
GHN-VTM-0110	Stable	LFG-005	3	453747.33	4062140.52	2973.51 (9755)
GHN-VTM-0111	Stable	LFG-005	3	453748.84	4062140.25	2973.42 (9755)
GHN-VTM-0112	Stable	LFG-005	3	453750.34	4062139.99	2973.34 (9754)
GHN-VTM-0113	Stable	LFG-005	3	453751.84	4062139.72	2973.25 (9754)
GHN-VTM-0114	Stable	LFG-005	3	453753.34	4062139.45	2973.16 (9754)
GHN-VTM-0115	Stable	LFG-005	3	453754.84	4062139.19	2973.07 (9754)
GHN-VTM-0116	Stable	LFG-005	4	453720.89	4062142.86	2973.79 (9756)
GHN-VTM-0117	Stable	LFG-005	4	453722.68	4062142.51	2973.68 (9756)
GHN-VTM-0118	Stable	LFG-005	4	453723.58	4062142.33	2973.94 (9756)
GHN-VTM-0119	Stable	LFG-005	4	453725.38	4062141.98	2973.83 (9756)
GHN-VTM-0120	Stable	LFG-005	4	453726.87	4062141.69	2973.75 (9756)
GHN-VTM-0121	Stable	LFG-005	4	453728.37	4062141.40	2973.66 (9756)
GHN-VTM-0122	Stable	LFG-005	4	453729.27	4062141.22	2973.61 (9755)
GHN-VTM-0123	Stable	LFG-005	4	453730.76	4062140.93	2973.52 (9755)
GHN-VTM-0124	Stable	LFG-005	4	453732.26	4062140.64	2973.44 (9755)
GHN-VTM-0125	Stable	LFG-005	4	453733.75	4062140.34	2973.35 (9754)
GHN-VTM-0126	Stable	LFG-005	4	453735.25	4062140.05	2973.26 (9754)
GHN-VTM-0127	Stable	LFG-005	4	453736.75	4062139.76	2973.18 (9754)
GHN-VTM-0128	Stable	LFG-005	4	453738.24	4062139.47	2973.09 (9754)

Table A1 continued.

Sample ID	Pile Portion	Hole/Pit ID	Bench	UTM Easting m	UTM Northing m	Elevation m (ft)
GHN-VTM-0129	Stable	LFG-005	4	453739.74	4062139.18	2973.00 (9753)
GHN-VTM-0130	Stable	LFG-005	4	453741.23	4062138.88	2972.92 (9753)
GHN-VTM-0131	Stable	LFG-005	4	453742.43	4062138.65	2972.85 (9753)
GHN-VTM-0132	Stable	LFG-005	4	453743.93	4062138.36	2972.76 (9753)
GHN-VTM-0133	Stable	LFG-005	4	453745.42	4062138.06	2972.68 (9752)
GHN-VTM-0134	Stable	LFG-005	4	453746.92	4062137.77	2972.59 (9752)
GHN-VTM-0135	Stable	LFG-005	4	453739.74	4062139.18	2973.00 (9753)
GHN-VTM-0136	Stable	LFG-005	4	453746.92	4062137.77	2972.59 (9752)
GHN-VTM-0137	Stable	LFG-005	4	453748.42	4062137.48	2972.50 (9752)
GHN-VTM-0138	Stable	LFG-005	4	453749.91	4062137.19	2972.42 (9751)
GHN-VTM-0139	Stable	LFG-005	4	453751.41	4062136.90	2972.33 (9751)
GHN-VTM-0140	Stable	LFG-005	4	453752.90	4062136.60	2972.24 (9751)
GHN-VTM-0141	Stable	LFG-005	4	453754.40	4062136.31	2972.16 (9751)
GHN-VTM-0143	Stable	LFG-005	5	453748.13	4062134.98	2970.13 (9744)
GHN-VTM-0144	Stable	LFG-005	5	453749.62	4062134.70	2970.29 (9744)
GHN-VTM-0145	Stable	LFG-005	5	453751.12	4062134.43	2970.44 (9745)
GHN-VTM-0146	Stable	LFG-005	5	453752.92	4062134.10	2970.62 (9746)
GHN-VTM-0147	Stable	LFG-005	5	453754.42	4062133.82	2971.39 (9748)
GHN-VTM-0152	Stable	LFG-005	2	453743.28	4062143.26	2974.61 (9759)
GHN-VTM-0153	Stable	LFG-005	2	453753.82	4062141.60	2973.72 (9756)
GHN-VTM-0154	Stable	LFG-005	4	453740.34	4062139.06	2972.66 (9752)
GHN-VTM-0155	Stable	LFG-005	4	453747.82	4062137.60	2972.23 (9751)
GHN-VTM-0156	Stable	LFG-006	7	453704.82	4062148.11	2968.14 (9737)
GHN-VTM-0157	Stable	LFG-006	7	453706.34	4062148.03	2968.52 (9739)
GHN-VTM-0158	Stable	LFG-006	7	453707.87	4062147.95	2968.60 (9739)
GHN-VTM-0159	Stable	LFG-006	7	453707.87	4062147.95	2968.60 (9739)
GHN-VTM-0160	Stable	LFG-006	7	453709.39	4062147.87	2968.53 (9739)
GHN-VTM-0161	Stable	LFG-006	7	453710.91	4062147.79	2968.61 (9739)
GHN-VTM-0162	Stable	LFG-006	7	453712.74	4062147.69	2968.86 (9740)
GHN-VTM-0163	Stable	LFG-006	7	453714.26	4062147.61	2968.94 (9740)
GHN-VTM-0164	Stable	LFG-006	7	453715.78	4062147.53	2969.02 (9740)
GHN-VTM-0165	Stable	LFG-006	7	453717.30	4062147.45	2969.41 (9742)
GHN-VTM-0166	Stable	LFG-006	7	453718.83	4062147.37	2969.19 (9741)
GHN-VTM-0167	Stable	LFG-006	7	453720.35	4062147.29	2969.57 (9742)
GHN-VTM-0168	Stable	LFG-006	7	453721.26	4062147.24	2969.32 (9741)
GHN-VTM-0169	Stable	LFG-006	7	453723.09	4062147.15	2969.26 (9741)
GHN-VTM-0170	Stable	LFG-006	7	453724.61	4062147.07	2969.34 (9741)
GHN-VTM-0171	Stable	LFG-006	7	453726.13	4062146.99	2969.27 (9741)
GHN-VTM-0172	Stable	LFG-006	7	453727.66	4062146.91	2969.35 (9741)
GHN-VTM-0173	Stable	LFG-006	7	453729.18	4062146.83	2969.43 (9742)
GHN-VTM-0174	Stable	LFG-006	7	453730.70	4062146.75	2969.51 (9742)
GHN-VTM-0175	Stable	LFG-006	7	453732.22	4062146.67	2969.59 (9742)
GHN-VTM-0176	Stable	LFG-006	7	453733.75	4062146.59	2969.98 (9743)
GHN-VTM-0177	Stable	LFG-006	7	453735.27	4062146.51	2970.06 (9744)
GHN-VTM-0178	Stable	LFG-006	8	453710.64	4062145.06	2967.47 (9735)
GHN-VTM-0179	Stable	LFG-006	8	453712.16	4062144.96	2967.55 (9735)
GHN-VTM-0180	Stable	LFG-006	8	453713.68	4062144.86	2967.64 (9736)

Table A1 continued.

Sample ID	Pile Portion	Hole/Pit ID	Bench	UTM Easting m	UTM Northing m	Elevation m (ft)
GHN-VTM-0181	Stable	LFG-006	8	453713.68	4062144.86	2967.64 (9736)
GHN-VTM-0182	Stable	LFG-006	8	453715.20	4062144.76	2968.02 (9737)
GHN-VTM-0183	Stable	LFG-006	8	453716.72	4062144.66	2967.96 (9737)
GHN-VTM-0184	Stable	LFG-006	8	453718.24	4062144.56	2968.04 (9737)
GHN-VTM-0185	Stable	LFG-006	8	453719.76	4062144.46	2968.12 (9737)
GHN-VTM-0186	Stable	LFG-006	8	453721.28	4062144.36	2968.21 (9738)
GHN-VTM-0187	Stable	LFG-006	8	453722.81	4062144.27	2968.44 (9738)
GHN-VTM-0188	Stable	LFG-006	8	453724.33	4062144.17	2968.52 (9739)
GHN-VTM-0189	Stable	LFG-006	8	453724.33	4062144.17	2968.52 (9739)
GHN-VTM-0190	Stable	LFG-006	8	453725.85	4062144.07	2968.61 (9739)
GHN-VTM-0191	Stable	LFG-006	8	453727.37	4062143.97	2968.69 (9739)
GHN-VTM-0192	Stable	LFG-006	8	453729.19	4062143.85	2968.79 (9740)
GHN-VTM-0193	Stable	LFG-006	8	453730.72	4062143.75	2968.87 (9740)
GHN-VTM-0194	Stable	LFG-006	9	453695.30	4062143.21	2966.57 (9732)
GHN-VTM-0195	Stable	LFG-006	9	453696.82	4062143.12	2966.94 (9733)
GHN-VTM-0196	Stable	LFG-006	9	453698.35	4062143.02	2967.01 (9734)
GHN-VTM-0197	Stable	LFG-006	9	453699.87	4062142.93	2967.07 (9734)
GHN-VTM-0198	Stable	LFG-006	9	453701.39	4062142.83	2967.14 (9734)
GHN-VTM-0199	Stable	LFG-006	9	453702.91	4062142.74	2967.21 (9734)
GHN-VTM-0200	Stable	LFG-006	9	453704.43	4062142.64	2967.27 (9735)
GHN-VTM-0201	Stable	LFG-006	8	453708.81	4062145.18	2967.37 (9735)
GHN-VTM-0202	Stable	LFG-006	9	453705.95	4062142.55	2967.34 (9735)
GHN-VTM-0203	Stable	LFG-006	9	453705.95	4062142.55	2967.34 (9735)
GHN-VTM-0204	Stable	LFG-006	9	453707.47	4062142.45	2967.40 (9735)
GHN-VTM-0205	Stable	LFG-006	9	453709.00	4062142.36	2966.86 (9733)
GHN-VTM-0206	Stable	LFG-006	9	453710.52	4062142.26	2966.93 (9733)
GHN-VTM-0207	Stable	LFG-006	9	453712.04	4062142.17	2966.99 (9734)
GHN-VTM-0208	Stable	LFG-006	9	453713.87	4062142.06	2967.07 (9734)
GHN-VTM-0209	Stable	LFG-006	9	453715.39	4062141.96	2967.14 (9734)
GHN-VTM-0210	Stable	LFG-006	9	453715.39	4062141.96	2967.14 (9734)
GHN-VTM-0211	Stable	LFG-006	9	453716.91	4062141.87	2967.20 (9734)
GHN-VTM-0212	Stable	LFG-006	9	453718.43	4062141.77	2967.27 (9735)
GHN-VTM-0213	Stable	LFG-006	9	453719.95	4062141.68	2967.34 (9735)
GHN-VTM-0214	Stable	LFG-006	9	453721.47	4062141.58	2967.40 (9735)
GHN-VTM-0215	Stable	LFG-006	9	453722.69	4062141.51	2967.45 (9735)
GHN-VTM-0216	Stable	LFG-006	9	453724.21	4062141.41	2967.52 (9735)
GHN-VTM-0217	Stable	LFG-006	9	453725.73	4062141.32	2967.59 (9736)
GHN-VTM-0218	Stable	LFG-006	10	453706.02	4062141.67	2964.97 (9727)
GHN-VTM-0219	Stable	LFG-006	10	453706.02	4062141.67	2964.67 (9726)
GHN-VTM-0220	Stable	LFG-006	10	453707.54	4062141.60	2964.79 (9726)
GHN-VTM-0221	Stable	LFG-006	10	453709.07	4062141.52	2964.90 (9727)
GHN-VTM-0222	Stable	LFG-006	10	453710.59	4062141.45	2965.02 (9727)
GHN-VTM-0223	Stable	LFG-006	10	453712.11	4062141.38	2965.14 (9728)
GHN-VTM-0224	Stable	LFG-006	10	453713.63	4062141.30	2965.26 (9728)
GHN-VTM-0225	Stable	LFG-006	10	453715.16	4062141.23	2965.38 (9728)
GHN-VTM-0226	Stable	LFG-006	10	453716.68	4062141.15	2965.50 (9729)
GHN-VTM-0227	Stable	LFG-006	10	453718.20	4062141.08	2965.62 (9729)

Table A1 continued.

Sample ID	Pile Portion	Hole/Pit ID	Bench	UTM Easting m	UTM Northing m	Elevation m (ft)
GHN-VTM-0228	Stable	LFG-006	10	453718.51	4062141.06	2965.65 (9729)
GHN-VTM-0229	Stable	LFG-006	10	453719.72	4062141.00	2965.74 (9730)
GHN-VTM-0230	Stable	LFG-006	10	453721.25	4062140.93	2965.86 (9730)
GHN-VTM-0231	Stable	LFG-007	12	453678.63	4062146.44	2954.79 (9694)
GHN-VTM-0232	Stable	LFG-007	12	453680.15	4062146.38	2954.98 (9694)
GHN-VTM-0233	Stable	LFG-007	12	453680.76	4062146.36	2955.06 (9694)
GHN-VTM-0234	Stable	LFG-007	12	453682.28	4062146.30	2955.25 (9695)
GHN-VTM-0235	Stable	LFG-007	12	453683.80	4062146.24	2955.44 (9696)
GHN-VTM-0236	Stable	LFG-007	12	453685.33	4062146.18	2955.63 (9696)
GHN-VTM-0237	Stable	LFG-007	12	453685.33	4062146.18	2955.63 (9696)
GHN-VTM-0238	Stable	LFG-007	12	453686.85	4062146.12	2955.83 (9697)
GHN-VTM-0239	Stable	LFG-007	12	453686.85	4062146.12	2955.83 (9697)
GHN-VTM-0240	Stable	LFG-007	12	453690.20	4062145.99	2956.25 (9698)
GHN-VTM-0241	Stable	LFG-007	12	453691.73	4062145.93	2956.44 (9699)
GHN-VTM-0242	Stable	LFG-007	12	453693.25	4062145.87	2956.64 (9700)
GHN-VTM-0243	Stable	LFG-007	12	453694.77	4062145.81	2956.83 (9700)
GHN-VTM-0244	Stable	LFG-007	12	453696.30	4062145.75	2957.02 (9701)
GHN-VTM-0245	Stable	LFG-007	12	453697.82	4062145.69	2957.21 (9702)
GHN-VTM-0246	Stable	LFG-007	12	453699.04	4062145.65	2957.37 (9702)
GHN-VTM-0247	Stable	LFG-007	12	453700.56	4062145.59	2957.56 (9703)
GHN-VTM-0248	Stable	LFG-007	12	453702.08	4062145.53	2957.75 (9703)
GHN-VTM-0249	Stable	LFG-007	12	453703.61	4062145.47	2957.95 (9704)
GHN-VTM-0250	Stable	LFG-007	12	453703.61	4062145.47	2957.95 (9704)
GHN-VTM-0251	Stable	LFG-007	12	453705.13	4062145.41	2958.14 (9705)
GHN-VTM-0252	Stable	LFG-007	12	453706.65	4062145.35	2958.33 (9705)
GHN-VTM-0253	Stable	LFG-007	12	453708.18	4062145.29	2958.52 (9706)
GHN-VTM-0254	Stable	LFG-007	12	453709.70	4062145.23	2958.72 (9706)
GHN-VTM-0255	Stable	LFG-007	12	453711.22	4062145.17	2958.91 (9707)
GHN-VTM-0256	Stable	LFG-007	12	453712.75	4062145.11	2959.10 (9708)
GHN-VTM-0257	Stable	LFG-007	12	453713.96	4062145.06	2959.26 (9708)
GHN-VTM-0258	Stable	LFG-007	12	453715.49	4062145.00	2959.45 (9709)
GHN-VTM-0260	Stable	LFG-007	12	453688.37	4062146.06	2956.02 (9698)
GHN-VTM-0261	Stable	LFG-007	13	453670.62	4062144.09	2953.04 (9688)
GHN-VTM-0262	Stable	LFG-007	13	453672.14	4062143.98	2953.22 (9688)
GHN-VTM-0263	Stable	LFG-007	13	453673.36	4062143.90	2953.37 (9689)
GHN-VTM-0264	Stable	LFG-007	13	453674.88	4062143.80	2953.55 (9690)
GHN-VTM-0265	Stable	LFG-007	13	453676.40	4062143.69	2953.73 (9690)
GHN-VTM-0266	Stable	LFG-007	13	453677.92	4062143.59	2953.91 (9691)
GHN-VTM-0267	Stable	LFG-007	13	453679.14	4062143.51	2954.06 (9691)
GHN-VTM-0268	Stable	LFG-007	13	453679.14	4062143.51	2954.06 (9691)
GHN-VTM-0269	Stable	LFG-007	13	453680.66	4062143.40	2954.24 (9692)
GHN-VTM-0270	Stable	LFG-007	13	453681.88	4062143.32	2954.38 (9692)
GHN-VTM-0271	Stable	LFG-007	13	453683.40	4062143.22	2954.56 (9693)
GHN-VTM-0272	Stable	LFG-007	13	453684.92	4062143.11	2954.74 (9693)
GHN-VTM-0273	Stable	LFG-007	13	453686.44	4062143.01	2954.93 (9694)
GHN-VTM-0274	Stable	LFG-007	13	453687.96	4062142.91	2955.11 (9695)
GHN-VTM-0275	Stable	LFG-007	13	453689.48	4062142.80	2955.29 (9695)

Table A1 continued.

Sample ID	Pile Portion	Hole/Pit ID	Bench	UTM Easting m	UTM Northing m	Elevation m (ft)
GHN-VTM-0276	Stable	LFG-007	13	453690.70	4062142.72	2955.43 (9696)
GHN-VTM-0277	Stable	LFG-007	13	453692.22	4062142.62	2955.61 (9696)
GHN-VTM-0278	Stable	LFG-007	13	453693.44	4062142.53	2955.76 (9697)
GHN-VTM-0279	Stable	LFG-007	13	453694.96	4062142.43	2955.94 (9697)
GHN-VTM-0280	Stable	LFG-007	13	453694.96	4062142.43	2955.94 (9697)
GHN-VTM-0281	Stable	LFG-007	13	453696.48	4062142.33	2956.12 (9698)
GHN-VTM-0282	Stable	LFG-007	13	453698.00	4062142.22	2956.30 (9699)
GHN-VTM-0283	Stable	LFG-007	13	453699.52	4062142.12	2956.48 (9699)
GHN-VTM-0284	Stable	LFG-007	13	453701.04	4062142.01	2956.66 (9700)
GHN-VTM-0285	Stable	LFG-007	13	453702.56	4062141.91	2956.84 (9700)
GHN-VTM-0286	Stable	LFG-007	13	453704.08	4062141.81	2957.02 (9701)
GHN-VTM-0287	Stable	LFG-007	13	453705.60	4062141.70	2957.21 (9702)
GHN-VTM-0288	Stable	LFG-007	13	453707.12	4062141.60	2957.39 (9702)
GHN-VTM-0289	Stable	LFG-007	13	453708.64	4062141.50	2957.57 (9703)
GHN-VTM-0290	Stable	LFG-007	13	453710.17	4062141.39	2957.75 (9703)
GHN-VTM-0291	Stable	LFG-007	14	453670.21	4062140.96	2952.26 (9685)
GHN-VTM-0292	Stable	LFG-007	14	453671.73	4062140.90	2952.41 (9686)
GHN-VTM-0293	Stable	LFG-007	14	453673.26	4062140.84	2952.56 (9686)
GHN-VTM-0294	Stable	LFG-007	14	453674.78	4062140.77	2952.70 (9687)
GHN-VTM-0295	Stable	LFG-007	14	453676.30	4062140.71	2952.85 (9687)
GHN-VTM-0296	Stable	LFG-007	14	453677.83	4062140.65	2953.00 (9688)
GHN-VTM-0297	Stable	LFG-007	14	453679.35	4062140.58	2953.15 (9688)
GHN-VTM-0298	Stable	LFG-007	14	453680.87	4062140.52	2953.29 (9689)
GHN-VTM-0299	Stable	LFG-007	14	453682.40	4062140.46	2953.44 (9689)
GHN-VTM-0300	Stable	LFG-007	14	453683.92	4062140.39	2953.59 (9690)
GHN-VTM-0301	Stable	LFG-007	14	453684.53	4062140.37	2953.65 (9690)
GHN-VTM-0302	Stable	LFG-007	14	453686.05	4062140.30	2953.79 (9690)
GHN-VTM-0303	Stable	LFG-007	14	453686.66	4062140.28	2953.85 (9691)
GHN-VTM-0304	Stable	LFG-007	14	453687.88	4062140.23	2953.97 (9691)
GHN-VTM-0305	Stable	LFG-007	14	453687.88	4062140.23	2953.97 (9691)
GHN-VTM-0306	Stable	LFG-007	14	453689.40	4062140.17	2954.12 (9691)
GHN-VTM-0307	Stable	LFG-007	14	453690.92	4062140.10	2954.27 (9692)
GHN-VTM-0308	Stable	LFG-007	14	453692.45	4062140.04	2954.41 (9692)
GHN-VTM-0309	Stable	LFG-007	14	453693.97	4062139.98	2954.56 (9693)
GHN-VTM-0310	Stable	LFG-007	14	453695.49	4062139.91	2954.71 (9693)
GHN-VTM-0311	Stable	LFG-007	14	453697.02	4062139.85	2954.86 (9694)
GHN-VTM-0312	Stable	LFG-007	14	453698.54	4062139.79	2955.00 (9694)
GHN-VTM-0313	Stable	LFG-007	14	453699.45	4062139.75	2955.09 (9695)
GHN-VTM-0314	Stable	LFG-007	14	453700.06	4062139.72	2955.15 (9695)
GHN-VTM-0315	Stable	LFG-007	14	453700.98	4062139.68	2955.24 (9695)
GHN-VTM-0316	Stable	LFG-007	14	453700.98	4062139.68	2955.24 (9695)
GHN-VTM-0317	Stable	LFG-007	14	453702.50	4062139.62	2955.39 (9696)
GHN-VTM-0318	Stable	LFG-007	14	453704.02	4062139.56	2955.53 (9696)
GHN-VTM-0319	Stable	LFG-007	14	453704.94	4062139.52	2955.62 (9696)
GHN-VTM-0340	Stable	LFG-007	15	453689.74	4062132.12	2952.97 (9688)
GHN-VTM-0341	Stable	LFG-007	15	453691.26	4062132.05	2953.14 (9688)
GHN-VTM-0342	Stable	LFG-007	15	453692.78	4062131.99	2953.30 (9689)

Table A1 continued.

Sample ID	Pile Portion	Hole/Pit ID	Bench	UTM Easting m	UTM Northing m	Elevation m (ft)
GHN-VTM-0343	Stable	LFG-007	15	453693.39	4062131.97	2953.37 (9689)
GHN-VTM-0344	Stable	LFG-007	15	453694.92	4062131.91	2953.53 (9689)
GHN-VTM-0345	Stable	LFG-007	15	453696.44	4062131.85	2953.70 (9690)
GHN-VTM-0346	Stable	LFG-007	15	453697.96	4062131.78	2953.86 (9691)
GHN-VTM-0347	Stable	LFG-007	15	453699.48	4062131.72	2954.03 (9691)
GHN-VTM-0348	Stable	LFG-007	15	453699.48	4062131.72	2954.03 (9691)
GHN-VTM-0349	Stable	LFG-007	15	453701.01	4062131.66	2954.19 (9692)
GHN-VTM-0350	Stable	LFG-007	15	453702.84	4062131.59	2954.39 (9692)
GHN-VTM-0351	Stable	LFG-008	17	453665.90	4062141.16	2941.25 (9649)
GHN-VTM-0352	Stable	LFG-008	17	453667.43	4062141.20	2941.45 (9650)
GHN-VTM-0353	Stable	LFG-008	17	453668.34	4062141.23	2941.58 (9650)
GHN-VTM-0354	Stable	LFG-008	17	453669.87	4062141.27	2941.79 (9651)
GHN-VTM-0355	Stable	LFG-008	17	453669.87	4062141.27	2941.79 (9651)
GHN-VTM-0356	Stable	LFG-008	17	453671.39	4062141.31	2941.99 (9652)
GHN-VTM-0357	Stable	LFG-008	17	453672.91	4062141.36	2942.20 (9652)
GHN-VTM-0358	Stable	LFG-008	17	453674.44	4062141.40	2942.41 (9653)
GHN-VTM-0359	Stable	LFG-008	17	453675.96	4062141.44	2942.62 (9654)
GHN-VTM-0360	Stable	LFG-008	17	453677.48	4062141.49	2942.83 (9654)
GHN-VTM-0361	Stable	LFG-008	18	453666.18	4062137.38	2940.05 (9645)
GHN-VTM-0362	Stable	LFG-008	18	453667.70	4062137.40	2940.25 (9646)
GHN-VTM-0363	Stable	LFG-008	18	453669.23	4062137.41	2940.45 (9647)
GHN-VTM-0364	Stable	LFG-008	18	453669.23	4062137.41	2940.45 (9647)
GHN-VTM-0365	Stable	LFG-008	18	453670.75	4062137.43	2940.65 (9647)
GHN-VTM-0366	Stable	LFG-008	18	453672.27	4062137.45	2940.84 (9648)
GHN-VTM-0368	Stable	LFG-008	18	453673.49	4062137.46	2941.00 (9648)
GHN-VTM-0369	Stable	LFG-008	18	453674.10	4062137.47	2941.08 (9649)
GHN-VTM-0370	Stable	LFG-008	18	453675.32	4062137.49	2941.24 (9649)
GHN-VTM-0371	Stable	LFG-008	18	453676.24	4062137.50	2941.36 (9650)
GHN-VTM-0372	Stable	LFG-008	18	453677.76	4062137.52	2941.56 (9650)
GHN-VTM-0373	Stable	LFG-008	18	453678.98	4062137.53	2941.71 (9651)
GHN-VTM-0374	Stable	LFG-008	18	453679.90	4062137.54	2941.83 (9651)
GHN-VTM-0375	Stable	LFG-008	19	453666.50	4062133.97	2938.90 (9641)
GHN-VTM-0377	Stable	LFG-008	19	453668.03	4062134.02	2939.11 (9642)
GHN-VTM-0378	Stable	LFG-008	19	453669.55	4062134.07	2939.31 (9643)
GHN-VTM-0379	Stable	LFG-008	19	453671.38	4062134.13	2939.56 (9644)
GHN-VTM-0380	Stable	LFG-008	19	453671.68	4062134.14	2939.60 (9644)
GHN-VTM-0381	Stable	LFG-008	19	453672.29	4062134.16	2939.69 (9644)
GHN-VTM-0382	Stable	LFG-008	19	453672.60	4062134.17	2939.42 (9643)
GHN-VTM-0383	Stable	LFG-008	19	453674.12	4062134.22	2939.94 (9645)
GHN-VTM-0384	Stable	LFG-008	19	453675.64	4062134.27	2940.14 (9646)
GHN-VTM-0385	Stable	LFG-008	19	453675.64	4062134.27	2940.14 (9646)
GHN-VTM-0386	Stable	LFG-008	19	453677.17	4062134.32	2940.35 (9646)
GHN-VTM-0387	Stable	LFG-008	19	453678.69	4062134.38	2940.56 (9647)
GHN-VTM-0388	Stable	LFG-008	20	453667.26	4062128.90	2938.03 (9639)
GHN-VTM-0389	Stable	LFG-008	20	453667.87	4062128.94	2938.12 (9639)
GHN-VTM-0390	Stable	LFG-008	20	453668.48	4062128.98	2938.21 (9639)
GHN-VTM-0391	Stable	LFG-008	20	453670.00	4062129.07	2938.43 (9640)

Table A1 continued.

Sample ID	Pile Portion	Hole/Pit ID	Bench	UTM Easting m	UTM Northing m	Elevation m (ft)
GHN-VTM-0392	Stable	LFG-008	20	453671.52	4062129.17	2938.65 (9641)
GHN-VTM-0393	Stable	LFG-008	20	453671.52	4062129.17	2938.65 (9641)
GHN-VTM-0394	Stable	LFG-008	19	453667.04	4062122.46	2939.10 (9642)
GHN-VTM-0395	Stable	LFG-008	19	453668.26	4062122.53	2939.28 (9643)
GHN-VTM-0396	Stable	LFG-008	19	453668.56	4062122.55	2939.32 (9643)
GHN-VTM-0398	Stable	LFG-008	19	453671.61	4062122.74	2939.77 (9644)
GHN-VTM-0399	Stable	LFG-008	19	453672.52	4062122.80	2939.90 (9645)
GHN-VTM-0400	Stable	LFG-008	19	453674.04	4062122.89	2940.12 (9645)
GHN-VTM-0401	Stable	LFG-008	19	453674.04	4062122.89	2940.12 (9645)
GHN-VTM-0402	Stable	LFG-008	19	453675.56	4062122.98	2940.34 (9646)
GHN-VTM-0403	Stable	LFG-008	19	453677.08	4062123.08	2940.57 (9647)
GHN-VTM-0404	Stable	LFG-009	22	453637.04	4062136.36	2925.85 (9599)
GHN-VTM-0405	Stable	LFG-009	22	453638.56	4062136.49	2926.14 (9600)
GHN-VTM-0406	Stable	LFG-009	22	453640.08	4062136.62	2926.42 (9601)
GHN-VTM-0407	Stable	LFG-009	22	453641.60	4062136.75	2926.71 (9601)
GHN-VTM-0408	Stable	LFG-009	22	453643.12	4062136.89	2926.99 (9602)
GHN-VTM-0409	Stable	LFG-009	22	453644.64	4062137.02	2927.28 (9603)
GHN-VTM-0410	Stable	LFG-009	22	453646.15	4062137.15	2927.56 (9604)
GHN-VTM-0411	Stable	LFG-009	22	453647.67	4062137.28	2927.85 (9605)
GHN-VTM-0412	Stable	LFG-009	22	453648.58	4062137.36	2928.02 (9606)
GHN-VTM-0413	Stable	LFG-009	22	453649.19	4062137.41	2928.13 (9606)
GHN-VTM-0414	Stable	LFG-009	22	453649.80	4062137.47	2928.25 (9607)
GHN-VTM-0415	Stable	LFG-009	22	453650.71	4062137.55	2928.42 (9607)
GHN-VTM-0416	Stable	LFG-009	22	453652.23	4062137.68	2928.70 (9608)
GHN-VTM-0417	Stable	LFG-009	23	453635.15	4062132.76	2924.27 (9593)
GHN-VTM-0418	Stable	LFG-009	23	453636.68	4062132.81	2924.50 (9594)
GHN-VTM-0419	Stable	LFG-009	23	453638.20	4062132.87	2924.72 (9595)
GHN-VTM-0420	Stable	LFG-009	23	453639.72	4062132.92	2924.95 (9596)
GHN-VTM-0421	Stable	LFG-009	23	453641.25	4062132.97	2925.18 (9596)
GHN-VTM-0422	Stable	LFG-009	23	453642.77	4062133.03	2925.40 (9597)
GHN-VTM-0423	Stable	LFG-009	23	453642.77	4062133.03	2925.40 (9597)
GHN-VTM-0424	Stable	LFG-009	23	453644.29	4062133.08	2925.63 (9598)
GHN-VTM-0425	Stable	LFG-009	23	453644.29	4062133.08	2925.32 (9597)
GHN-VTM-0426	Stable	LFG-009	23	453645.82	4062133.14	2925.85 (9599)
GHN-VTM-0427	Stable	LFG-009	22	453651.01	4062137.57	2928.48 (9607)
GHN-VTM-0428	Stable	LFG-009	22	453641.60	4062136.75	2926.71 (9601)
GHN-VTM-0434	Stable	LFG-009	24	453639.98	4062129.43	2923.61 (9591)
GHN-VTM-0435	Stable	LFG-009	24	453641.19	4062129.55	2923.78 (9592)
GHN-VTM-0436	Stable	LFG-009	25	453632.65	4062122.77	2921.51 (9584)
GHN-VTM-0437	Stable	LFG-009	25	453634.16	4062122.93	2921.75 (9585)
GHN-VTM-0438	Stable	LFG-009	25	453635.68	4062123.09	2921.99 (9586)
GHN-VTM-0440	Stable	LFG-009	23	453636.55	4062114.22	2924.76 (9595)
GHN-VTM-0441	Stable	LFG-009	23	453639.57	4062114.60	2925.17 (9596)
GHN-VTM-0442	Stable	LFG-009	23	453641.08	4062114.79	2925.37 (9597)
GHN-VTM-0444	Stable	LFG-009	23	453643.20	4062115.06	2925.66 (9598)
GHN-VTM-0445	Stable	LFG-009	23	453644.11	4062115.18	2925.79 (9598)
GHN-VTM-0446	Stable	LFG-009	23	453645.62	4062115.37	2925.99 (9599)

Table A1 continued.

Sample ID	Pile Portion	Hole/Pit ID	Bench	UTM Easting m	UTM Northing m	Elevation m (ft)
GHN-VTM-0447	Stable	LFG-009	23	453646.83	4062115.52	2926.16 (9600)
GHN-VTM-0448	Stable	LFG-009	23	453648.34	4062115.72	2926.36 (9600)
GHN-VTM-0449	Stable	LFG-009	23	453639.57	4062114.60	2925.17 (9596)
GHN-VTM-0450	Stable	LFG-009	23	453647.74	4062115.64	2926.28 (9600)
GHN-VTM-0451	Stable	LFG-009	23	453647.13	4062115.56	2926.20 (9600)
GHN-VTM-0452	Stable	LFG-009	23	453647.25	4062115.58	2926.21 (9600)
GHN-VTM-0453	Stable	LFG-009	23	453643.32	4062115.08	2925.68 (9598)
GHN-VTM-0454	Stable	LFG-009	23	453647.13	4062115.56	2926.20 (9600)
GHN-VTM-0455	Stable	LFG-009	23	453647.37	4062115.59	2926.23 (9600)
GHN-VTM-0511	Unstable	LFG-011	29	453660.70	4062327.21	2945.77 (9664)
GHN-VTM-0512	Unstable	LFG-011	29	453661.70	4062328.32	2945.77 (9664)
GHN-VTM-0513	Unstable	LFG-011	29	453662.71	4062329.44	2945.77 (9664)
GHN-VTM-0514	Unstable	LFG-011	29	453663.71	4062330.55	2945.77 (9664)
GHN-VTM-0515	Unstable	LFG-011	29	453664.71	4062331.67	2945.62 (9664)
GHN-VTM-0516	Unstable	LFG-011	29	453665.72	4062332.78	2945.62 (9664)
GHN-VTM-0518	Unstable	LFG-011	29	453667.73	4062335.01	2945.62 (9664)
GHN-VTM-0519	Unstable	LFG-011	29	453668.73	4062336.12	2945.62 (9664)
GHN-VTM-0520	Unstable	LFG-011	29	453669.74	4062337.24	2945.62 (9664)
GHN-VTM-0521	Unstable	LFG-011	29	453670.74	4062338.35	2945.62 (9664)
GHN-VTM-0522	Unstable	LFG-011	29	453671.75	4062339.46	2945.62 (9664)
GHN-VTM-0523	Unstable	LFG-011	29	453672.75	4062340.58	2945.62 (9664)
GHN-VTM-0524	Unstable	LFG-011	29	453673.75	4062341.69	2945.62 (9664)
GHN-VTM-0525	Unstable	LFG-011	29	453674.76	4062342.81	2945.62 (9664)
GHN-VTM-0526	Unstable	LFG-011	29	453675.76	4062343.92	2945.62 (9664)
GHN-VTM-0527	Unstable	LFG-011	29	453665.72	4062332.78	2945.62 (9664)
GHN-VTM-0528	Unstable	LFG-011	29	453673.75	4062341.69	2945.62 (9664)
GHN-VTM-0529	Unstable	LFG-011	30	453662.05	4062323.63	2944.37 (9659)
GHN-VTM-0530	Unstable	LFG-011	30	453663.00	4062324.79	2944.37 (9659)
GHN-VTM-0531	Unstable	LFG-011	30	453663.95	4062325.95	2944.37 (9659)
GHN-VTM-0532	Unstable	LFG-011	30	453664.90	4062327.12	2944.37 (9659)
GHN-VTM-0533	Unstable	LFG-011	30	453665.85	4062328.28	2944.37 (9659)
GHN-VTM-0534	Unstable	LFG-011	30	453666.81	4062329.44	2944.37 (9659)
GHN-VTM-0535	Unstable	LFG-011	30	453667.76	4062330.60	2944.37 (9659)
GHN-VTM-0536	Unstable	LFG-011	30	453668.71	4062331.77	2944.37 (9659)
GHN-VTM-0537	Unstable	LFG-011	30	453669.66	4062332.93	2944.37 (9659)
GHN-VTM-0538	Unstable	LFG-011	30	453670.61	4062334.09	2944.37 (9659)
GHN-VTM-0539	Unstable	LFG-011	30	453671.56	4062335.25	2944.37 (9659)
GHN-VTM-0540	Unstable	LFG-011	30	453672.51	4062336.42	2944.37 (9659)
GHN-VTM-0541	Unstable	LFG-011	30	453673.47	4062337.58	2944.37 (9659)
GHN-VTM-0542	Unstable	LFG-011	30	453674.42	4062338.74	2944.37 (9659)
GHN-VTM-0543	Unstable	LFG-011	30	453675.37	4062339.90	2944.37 (9659)
GHN-VTM-0544	Unstable	LFG-011	30	453676.32	4062341.07	2944.37 (9659)
GHN-VTM-0545	Unstable	LFG-011	30	453670.61	4062334.09	2944.37 (9659)
GHN-VTM-0546	Unstable	LFG-011	30	453675.37	4062339.90	2944.37 (9659)
GHN-VTM-0548	Unstable	LFG-011	37	453660.88	4062315.28	2940.23 (9646)
GHN-VTM-0549	Unstable	LFG-011	37	453660.99	4062315.42	2940.00 (9645)
GHN-VTM-0550	Unstable	LFG-011	37	453661.09	4062315.53	2940.00 (9645)

Table A1 continued.

Sample ID	Pile Portion	Hole/Pit ID	Bench	UTM Easting m	UTM Northing m	Elevation m (ft)
GHN-VTM-0551	Unstable	LFG-016	35	453691.91	4062371.57	2958.42 (9706)
GHN-VTM-0552	Unstable	LFG-016	35	453691.91	4062371.57	2958.42 (9706)
GHN-VTM-0553	Unstable	LFG-015	34	453688.05	4062390.20	2960.44 (9712)
GHN-VTM-0554	Unstable	LFG-015	34	453688.05	4062390.20	2959.83 (9710)
GHN-VTM-0555	Unstable	LFG-015	34	453688.05	4062390.20	2960.44 (9712)
GHN-VTM-0556	Unstable	LFG-011	46	453635.59	4062254.55	2919.13 (9577)
GHN-VTM-0557	Unstable	LFG-011	46	453636.57	4062255.70	2919.13 (9577)
GHN-VTM-0558	Unstable	LFG-011	46	453637.54	4062256.84	2919.13 (9577)
GHN-VTM-0559	Unstable	LFG-011	46	453638.51	4062257.99	2919.13 (9577)
GHN-VTM-0560	Unstable	LFG-011	46	453639.48	4062259.13	2919.13 (9577)
GHN-VTM-0561	Unstable	LFG-011	46	453640.46	4062260.28	2919.13 (9577)
GHN-VTM-0562	Unstable	LFG-011	46	453641.43	4062261.43	2919.13 (9577)
GHN-VTM-0563	Unstable	LFG-011	46	453642.40	4062262.57	2919.13 (9577)
GHN-VTM-0564	Unstable	LFG-011	46	453643.37	4062263.72	2919.13 (9577)
GHN-VTM-0565	Unstable	LFG-011	46	453644.35	4062264.86	2919.13 (9577)
GHN-VTM-0566	Unstable	LFG-011	46	453645.32	4062266.01	2919.13 (9577)
GHN-VTM-0567	Unstable	LFG-011	46	453646.29	4062267.15	2919.13 (9577)
GHN-VTM-0568	Unstable	LFG-011	46	453647.27	4062268.30	2919.13 (9577)
GHN-VTM-0569	Unstable	LFG-011	46	453648.24	4062269.45	2919.13 (9577)
GHN-VTM-0570	Unstable	LFG-011	46	453649.21	4062270.59	2919.13 (9577)
GHN-VTM-0571	Unstable	LFG-011	46	453650.18	4062271.74	2919.13 (9577)
GHN-VTM-0572	Unstable	LFG-011	46	453651.16	4062272.88	2919.13 (9577)
GHN-VTM-0573	Unstable	LFG-011	46	453652.13	4062274.03	2919.13 (9577)
GHN-VTM-0574	Unstable	LFG-011	46	453653.10	4062275.18	2919.13 (9577)
GHN-VTM-0575	Unstable	LFG-011	46	453654.07	4062276.32	2919.13 (9577)
GHN-VTM-0576	Unstable	LFG-011	44	453646.97	4062276.00	2926.50 (9601)
GHN-VTM-0577	Unstable	LFG-011	44	453647.91	4062277.16	2926.50 (9601)
GHN-VTM-0578	Unstable	LFG-011	44	453648.86	4062278.32	2926.50 (9601)
GHN-VTM-0579	Unstable	LFG-011	44	453647.91	4062277.16	2926.50 (9601)
GHN-VTM-0580	Unstable	LFG-011	44	453650.76	4062280.65	2926.50 (9601)
GHN-VTM-0581	Unstable	LFG-011	44	453651.71	4062281.81	2926.50 (9601)
GHN-VTM-0582	Unstable	LFG-011	44	453653.60	4062284.14	2926.50 (9601)
GHN-VTM-0583	Unstable	LFG-011	44	453653.60	4062284.14	2926.50 (9601)
GHN-VTM-0584	Unstable	LFG-011	44	453654.55	4062285.30	2926.50 (9601)
GHN-VTM-0585	Unstable	LFG-011	44	453655.50	4062286.46	2926.50 (9601)
GHN-VTM-0586	Unstable	LFG-011	44	453656.45	4062287.63	2926.50 (9601)
GHN-VTM-0587	Unstable	LFG-011	44	453657.40	4062288.79	2926.50 (9601)
GHN-VTM-0588	Unstable	LFG-011	44	453658.34	4062289.95	2926.50 (9601)
GHN-VTM-0589	Unstable	LFG-011	44	453659.29	4062291.12	2926.50 (9601)
GHN-VTM-0590	Unstable	LFG-011	44	453660.24	4062292.28	2926.50 (9601)
GHN-VTM-0591	Unstable	LFG-011	44	453661.19	4062293.44	2926.50 (9601)
GHN-VTM-0592	Unstable	LFG-011	44	453662.14	4062294.60	2926.50 (9601)
GHN-VTM-0593	Unstable	LFG-011	44	453663.08	4062295.77	2926.50 (9601)
GHN-VTM-0594	Unstable	LFG-011	44	453664.03	4062296.93	2926.50 (9601)
GHN-VTM-0595	Unstable	LFG-011	44	453664.98	4062298.09	2926.50 (9601)
GHN-VTM-0596	Unstable	LFG-011	45	453648.85	4062274.25	2923.90 (9592)
GHN-VTM-0597	Unstable	LFG-011	47	453653.11	4062271.19	2922.36 (9587)

Table A1 continued.

Sample ID	Pile Portion	Hole/Pit ID	Bench	UTM Easting m	UTM Northing m	Elevation m (ft)
GHN-VTM-0598	Unstable	LFG-019	49	453661.57	4062434.77	2950.19 (9679)
GHN-VTM-0602	Unstable	LFG-019	49	453661.57	4062434.77	2949.43 (9676)
GHN-VTM-0603	Unstable	LFG-019	49	453661.57	4062434.77	2949.73 (9677)
GHN-VTM-0605	Unstable	LFG-020	50	453662.23	4062392.60	2945.00 (9661)
GHN-VTM-0606	Unstable	LFG-022	53	453647.99	4062394.79	2942.91 (9655)
GHN-VTM-0607	Unstable	LFG-022	54	453647.00	4062393.80	2936.20 (9633)
GHN-VTM-0612	Unstable	LFG-021	52	453650.15	4062391.26	2933.66 (9624)
GHN-VTM-0614	Unstable	LFG-021	52	453652.01	4062391.67	2934.73 (9628)
GHN-VTM-0615	Unstable	LFG-021	52	453650.15	4062391.26	2934.42 (9627)
GHN-VTM-0616	Unstable	LFG-021	52	453650.15	4062391.26	2933.51 (9624)
GHN-VTM-0618	Unstable	LFG-021	52	453650.15	4062391.26	2933.20 (9623)
GHN-VTM-0619	Unstable	LFG-021	51	453650.27	4062394.28	2943.43 (9656)
GHN-VTM-0620	Unstable	LFG-021	51	453650.27	4062394.28	2943.28 (9656)
GHN-VTM-0621	Unstable	LFG-021	51	453650.40	4062394.31	2942.36 (9653)
GHN-VTM-0622	Unstable	LFG-022	54	453651.74	4062420.00	2935.59 (9631)
GHN-VTM-0623	Unstable	LFG-022	53	453647.99	4062394.79	2942.91 (9655)
GHN-VTM-0624	Unstable	LFG-021	51	453650.02	4062394.23	2943.28 (9656)

APPENDIX B TEST PROCEDURES

Appendix B1: Paste pH and Paste Conductivity

Introduction

Water is added to the sample to form a paste or slurry thus mobilizing secondary mineral phases and providing a medium accessible to the pH and conductivity or TDS probes. The probe is placed in the paste or slurry and the pH or conductivity value is read directly from the meter.

Equipment and Reagents

- The following materials are required for conducting paste pH and conductivity tests.
- A pH meter with a combination pH electrode
- pH 4 and pH 7 calibration standards
- A conductivity meter with standard calibration solution(s)
- Stirring rod
- 50 mL glass beaker
- Deionized water
- Paste tests data sheet (Form 1)

Procedure

1. Calibrate pH and conductivity meters using the standard solutions and following the instructions provided with the meters. Record the calibration data on the laboratory test data sheet(s).

2. Obtain approximately 25 grams of fines (particles smaller than 2 mm if possible) from the soil or rock sample to be tested, and place in a fresh or decontaminated beaker. Reseal the bag from which the paste test sample was obtained.
3. Add approximately 25 mL of distilled water to sample. (More water may be required if the sample is extremely fine).
4. Stir sample with a cleaned spatula to form a paste or slurry. Paste should slide off spatula easily.
5. Let stand for 10 minutes. The soil-water mixture will segregate into water, slurry and sandy soil from top to bottom of the beaker.
6. Dip the probe into the slurry, allow the meter reading to stabilize, and record the data. The conductivity reading should be taken first, as electrolyte from the combination pH probe may affect the conductivity of the solution.
7. Decontaminate probes and containers by rinsing them with deionized water.
8. Record the measurements on the laboratory data sheet with the sample ID, date and your initials. Transfer the data to the Project Database after completing a batch of tests.

Quality Assurance/Quality Control

Verify the accuracy of the pH and conductivity meters using standard solutions after testing not more than 20 samples in a row. If readings on the standard solutions have drifted by more than 5 percent, recalibrate the probe, record the calibration data, and retest all the samples tested after the previous calibration. If the pH probe cannot be re-calibrated, clean and rejuvenate the electrode according to the manufacturer's instructions.

Table B1: Data sheet for paste pH and paste conductivity tests.

Paste Tests Data Sheet

Date	Sample ID	Paste Conductivity	Paste TDS	Temp	Paste pH	Temp	Initials	Comments
		mS/cm	g/L	^{o}C		^{o}C		
	1							
	2							
	3							
	4							
	5							
	6							
	7							
	8							
	9							
	10							
	11							
	12							

Appendix B2: Acid Potential Test with Peroxide

Introduction

Reduced sulfur in a soil sample is directly oxidized to acid with hydrogen peroxide and titrated with a standard base to evaluate the acid potential of the soil. Before treating with hydrogen peroxide, the sample is leached with hydrochloric acid to remove any neutralizing compounds from it and then rinsed with excess deionized water to remove any traces of acid that is introduced by the acid leaching.

Equipment

- A pH meter with combination pH electrode
- pH 4 and pH 7 calibration standards
- Acid Potential Test Data sheet (Form B, Appendix 1)

- 250 mL wide mouth conical flask or equivalent
- Watch glass
- Weighing paper or aluminum foil
- Magnetic stirrer
- Fume hood
- Hot plate
- Burette (50 mL), with stand and clamp
- Chemical balance reading to at least 2 decimal places in grams
- Helium water-degassing apparatus
- Ascarite tube
- Wash bottles for DI water
- Parafilm
- Funnel
- Filter paper (11.0 cm, Whatman No. 41)
- Spatula
- 150 mL tall form beaker
- Burette, (25 mL or bigger)
- Thermometer reading in degrees Celsius
- Other glass and plastic beakers as may be needed

Reagents

- Deionized (DI) water
- 40% Aqueous HCl solution: Dilute 400 mL of concentrated HCl with 600 mL of DI water.

- 10% silver nitrate solution (w/v). Dissolve 100g of silver nitrate ($AgNO_3$) crystals in 1L of DI water.
- Hydrogen Peroxide, Reagent Grade 30% H_2O_2
- Approximately 0.1 N sodium hydroxide, standardized: Dilute 200 mL of 0.5 N NaOH with carbon dioxide-free water to a volume of 1 liter. Or dissolve 4.0g of NaOH pellets in carbon dioxide-free water and dilute to 1 liter. Protect from CO_2 in air with ascarite tube. Standardize solution by placing 20 mL of certified 0.1 N HCl in a beaker and titrating with the prepared 0.1 N NaOH until a pH of 7.00 is obtained. Calculate the normality of the NaOH using the equation above.

Procedure

1. Place 3.0 grams of pulverized sample into a funnel fitted with filter paper. Leach sample with 300 mL of 40% HCl solution in funnel-full increments, followed by DI water (also in funnel-full increments) until effluent is free from chloride. Use 10% silver nitrate solution to test for presence of chloride in effluent by watching for white cloudy coloration as you put drops of silver nitrate in effluent. Absence of white coloration indicates that there is no chloride.
2. Air-dry filter paper and sample overnight.
3. Carefully scrape dried sample from paper surface and mix.
4. Weigh out accurately 2.00 grams of sample into a 150 mL tall form beaker. Add 24 mL of 30% H_2O_2 and heat beaker on a hotplate until the solution is approximately 40^oC. Remove beaker from hotplate and allow reaction to go to completion or for 30 minutes which ever comes first. Caution: Initial reaction may be quite turbulent when samples contain 0.1% or greater sulfur.

5. Add an additional 12 mL of 30% H_2O_2 to sample and allow to react for 30 minutes, then place beaker on hotplate at approximately 90 to 95^oC, solution temperature, for 30 minutes to destroy any unreacted H_2O_2 left in beaker. Do not allow to go to dryness.
6. Wash down the sides of the beaker with DI water and make the volume of solution to approximately 100 mL.
7. Place beaker on the hotplate and heat the solution to boiling to drive off any dissolved CO_2, then cool the solution to room temperature.
8. Titrate the solution with 0.1 N NaOH that is free of CO_2 and protected from the atmosphere, to pH 7.0 using a pH meter.

Documentation

Complete an Acid Potential Test Data Sheet (Table B2) for each sample tested, noting any deviations from the SOP. Plot the data from the data sheet on a graph sheet and estimate the actual volume of NaOH titrated at pH 7.0. Calculate the AP value with the equation below and record the results in the ABA Table in the Project Database

Calculations

- (mL of NaOH) * (Normality of NaOH) * 50 = meq (H^+)/100 g
- meq H^+/100 g * 0.01 = tons H^+/thousand tons of material

One ton of H^+ requires 50 tons of $CaCO_3$ equivalents to neutralize it.

- AP = tons H^+/thousand tons of material * 50 (kg of $CaCO_3$/ton of material)

Therefore, Acid Potential

AP = mL of NaOH * Normality of NaOH * 50 * 0.01 * 50

AP = mL of NaOH * Normality of NaOH * 25 (kg of $CaCO_3$/t)

Quality Assurance/Quality Control

Calibrate the pH meter according to the manufacturer's instructions before each titration. If in the course of titration the pH meter is suspected to be reading inaccurately, check with the pH 7.0 buffer and recalibrate if it is off by more than 0.05 units. Run one duplicate sample for every 5 samples tested within a batch. Also, run between batch duplicates: test a duplicate of one sample in each batch during the next batch of tests. A duplicate of this sample should have been tested when testing its own batch. Test one specimen of the Standard ABA material for every 20 samples tested.

Table B2: Acid Potential Test Data Sheet

Acid Potential Test Data Sheet

Sample ID	
Date Started	
Date Titrated	
Volume of Solution (mL)	
Initial Burette Reading (mL)	
Initial pH of solution	
Concentration of NaOH (N)	
Initials of Technician	
Titration Points	
Volume (mL)	pH
Comments End Point (mL) =	
Volume Titrated (mL) =	

Appendix B3: Neutralization Potential Test

Introduction

The amount of neutralizing bases, including carbonates, present in waste rock material is found by treating a sample with a known excess of standardized hydrochloric acid. The sample and acid are heated to insure that the reaction between the acid and the neutralizers goes to completion. The calcium carbonate equivalent of the sample is obtained by determining the amount of unconsumed acid by titration with standardized sodium hydroxide.

Equipment

- Appropriate sample containers with weatherproof labels pens
- A pH meter with a combination pH electrode
- pH 4 and pH 7 calibration standards
- Neutralization Potential Test Data Sheet (Table B4)
- 250 mL wide mouth conical flask or equivalent
- 30 mL glass beaker
- Watch glasses
- Weighing paper or aluminum foil
- Magnetic stirrer
- Fume hood
- Hot plate
- Burette (50 mL), stand and clamp
- Chemical balance reading to at least 2 decimal places in grams
- Helium water-degassing apparatus

- Ascarite tube
- Wash bottles for DI water
- Parafilm
- Other glass and plastic beakers as may be needed

Reagents

- Carbon dioxide-free DI water: Use the helium water-degassing apparatus to bubble out gasses from the DI water, then pour the degassed water into a container equipped with an ascarite tube.
- Certified grade, 0.1 Normal (N) hydrochloric acid, for standardization of bases.
- Approximately 0.5 N sodium hydroxide, standardized: Dissolve 20.0g of NaOH pellets in carbon dioxide-free water and dilute to 1 liter. Protect from CO_2 in the air with ascarite tube. Standardize solution by placing 50 mL of certified 0.1 N HCl in a beaker and titrating with the prepared 0.5 N NaOH until a pH of 7.00 is obtained. Calculate the Normality of the NaOH using the following equation:

  $N_2 = \frac{N_1 V_1}{V_2}$ Where:

  V_1 = Volume of HCl used
  N_1 = Normality of HCl used
  V_2 = Volume of NaOH used
  N_2 = Calculated normality of NaOH
- Approximately 0.1 N sodium hydroxide, standardized: Dilute 200 mL of 0.5 N NaOH with carbon dioxide-free water to a volume of 1 liter. Or dissolve 4.0g of NaOH pellets in carbon dioxide-free water and dilute to 1 liter. Protect from CO_2 in air with ascarite tube. Standardize solution by placing 20 mL of certified 0.1 N HCl

in a beaker and titrating with the prepared 0.1 N NaOH until a pH of 7.00 is obtained. Calculate the normality of the NaOH using the equation above.

- Approximately 0.5 N hydrochloric acid, standardized: Dilute 42 mL of concentrated HCL to a volume of 1 liter with DI water. Standardize solution by placing 20 of the standardized 0.5 N NaOH solution in a beaker and titrating with prepared HCl until a pH of 7.00 is obtained. Calculate the normality of the HCl using the following equation:

$$N_1 = \frac{N_2 V_2}{V_1}$$ Where:

V_2 = Volume of NaOH used
N_2 – Normality of NaOH used
V_1 = Volume of HCl used
N_1 = Calculated normality of HCl.

- Approximately 0.1 N hydrochloric acid, standardized: Dilute 200 mL of 0.5 N HCl to a volume of 1 L with DI water. Or dilute 8.4 mL of concentrated HCl with DI water to 1 L. Standardize solution by placing 20 mL of the standardized 0.1 N NaOH solution in a beaker and titrating with prepared HCl until a pH of 7.00 is obtained. Calculate the normality of the HCl using the equation above.
- Approximately 25% strength hydrochloric acid, for the $CaCO_2$ fizz test: Dilute 250 mL of concentrated HCl with 750 mL of DI water.
- Certified Acid-Base Accounting Standard.

Procedure

1. Determine paste pH of pulverized sample using 10 g of sample and 5 mL of water to make paste in a 30 mL glass beaker.

2. Add one or two drops of 25% HCl to 0.5 g of pulverized sample on a watch glass or piece of aluminum foil. A bubbling or audible “fizz” indicates the presence of $CaCO_2$. Observe the degree of reaction and assign a fizz rating as "none, slight, moderate, or strong fizz" (as indicated in Table B3). Record the fizz rating.

Table B1: Fizz ratings and their respective volumes and concentrations of HCl.

Observation	Fizz Rating	HCl	
		(mL)	(Normality)
Not audible nor visible	None	20	0.1
Audible but not visible	Slight	40	0.1
Audible and visible	Moderate	40	0.5
Very audible and visible	Strong	80	0.5

3. Weigh 2.00 g of sample into a 250 mL wide mouth conical flask.
4. Carefully add HCl indicated by Table B3 into the flask containing the sample.
5. Put the flask on a hot plate and heat until the sample just begins to boil.
6. Remove the flask from the hot plate and swirl every 5 minutes until the reaction is complete. Note: Reaction is complete when no gas evolution is visible and particles settle evenly over the bottom of the flask.
7. Add DI water to make a total volume of 125 mL.
8. Boil contents of flask for one minute and cool to slightly above room temperature. Cover tightly with parafilm and cool to room temperature. Caution: do not place parafilm on hot flask as it may implode upon cooling.
9. Titrate using standardized 0.1 N or 0.5 N NaOH to pH 7.0. The concentration of NaOH used in the titration should correspond to the concentration of the HCl used in Step 4.
10. If less than 3 mL of the NaOH is required to obtain a pH of 7.0, it is likely that the HCl added was not sufficient to neutralize the entire base present in the 2.00-g

sample. A duplicate sample should be run using the next higher volume or concentration of acid as indicated in Table B3.

11. Run a blank for each fizz rating that is obtained in a batch of samples using Steps 4, 7, 8, 9, and 10.

Documentation

Complete a Neutralization Potential Test Data Sheet (Table B4) for each sample tested. Note any deviation from the SOP. Plot the data from the data sheet on a graph sheet and estimate the actual volume of NaOH titrated at pH 7.0. Calculate the NP value with the equation below and record the results in the ABA Table in the Project Database.

Calculations

- Constant (C) = (mL acid in blank) / (mL base in blank)
- mL acid consumed = (mL acid added) – (mL base added * C)
- NP (kg $CaCO_3$/t) = (mL of acid consumed) * (25.0) * (N of acid)

Quality Assurance/Quality Control

Calibrate the pH meter according to the manufacturer's instructions before each titration. If in the course of titration the pH meter is suspected to be reading inaccurately, check with the pH 7.0 buffer and recalibrate if it is off by more than 0.05 units. Run one duplicate sample for every 5 samples tested within a batch. Also, run between batch duplicates: test a duplicate of one sample in each batch during the next batch of tests. A duplicate of this sample should have been tested when testing its own batch. Test one specimen of the Standard ABA material for every 20 samples tested.

Table B4: Neutralization Potential Test Data Sheet

Neutralization Potential Test Data Sheet	
Sample ID	
Date Started	
Fizz Rating	
Normality of HCl (N)	
Volume of HCL (mL)	
Titration	
Date Titrated	
Volume of Solution in Flask (mL)	
Initial Burrete Reading (mL)	
Initial pH of solution	
Concentration of NaOH (N)	
Initials of Technician	
Titration Points	
Volume (mL)	pH
Comments	
End Point (mL) =	
Volume Titrated (mL) =	

Appendix B4: Net Acid Generation Test

Introduction

The Net Acid Generation (NAG) test is used to determine the net acid remaining, if any, after complete oxidation of mine rock pile material with hydrogen peroxide and allowing complete reaction of the acid formed with the neutralizing components of the material. The test provides a direct assessment of the potential for a material to produce acid after a period of exposure and weathering and is used to refine the results of the theoretical acid-base accounting (ABA) predictions.

After hydrogen peroxide oxidation and subsequent neutralization is complete, the remaining sulfuric acid (H_2SO_4), if any, is titrated with sodium hydroxide (NaOH). The amount of NaOH needed is equivalent to the NAG of the material (expressed in kg $CaCO_3$/tonne material).

Equipment List

- A pH meter with combination pH electrode
- pH 4 and pH 7 calibration standards
- Deionized (DI) water
- Net Acid Generation Test Data sheet (Table B6)
- 500 mL wide mouth conical flask or equivalent
- Watch glass
- Weighing paper or aluminum foil
- Magnetic stirrer
- Fume hood
- Hot plate

- Thermometer
- Burette (25 mL or bigger), stand and clamp
- Chemical balance reading to at least 2 decimal places in grams
- Helium water-degassing apparatus
- Ascarite tube
- Wash bottles for DI water
- Other glass and plastic beakers as may be needed

Reagents

- 15% Hydrogen Peroxide (H_2O_2) solution: dilute Hydrogen Peroxide Reagent Grade 30% with DI water at a ratio of 1:1 to 15%. Make sure the pH is between 5 and 6.
- Certified grade, 0.1 N hydrochloric acid, for standardization of bases.
- Carbon dioxide-free DI water. Use the helium water-degassing apparatus to bubble out gasses from the DI water, and then pour degassed water into a container equipped with an ascarite tube.
- Approximately 0.5 N sodium hydroxide solution, standardized: Dissolve 20.0g of NaOH pellets in carbon dioxide-free water and dilute to 1 liter. Protect from CO_2 in the air with an ascarite tube. Standardize the solution by placing 50 mL of certified 0.1 N HCl in a beaker and titrating with the prepared 0.5 N NaOH until a pH of 7.00 is obtained. Calculate the Normality of the NaOH using the following equation:

$$N_2 = \frac{N_1 V_1}{V_2}$$ Where:

V_1 = Volume of HCl used
N_1 = Normality of HCl used
V_2 = Volume of NaOH used
N_2 = Calculated normality of NaOH

- Approximately 0.1 N sodium hydroxide solution, standardized: Dilute 200 mL of 0.5 N NaOH with carbon dioxide-free DI water to a volume of 1 liter. Or dissolve 4.0g of NaOH pellets in carbon dioxide-free water and dilute to 1 liter. Protect from CO_2 in air with the ascarite tube. Standardize the solution by placing 20 mL of certified 0.1 N HCl in a beaker and titrating with the prepared 0.1 N NaOH until a pH of 7.00 is obtained. Calculate the normality of the NaOH using the equation above.

Procedures

1. Weigh 2.50g of pulverized sample into a 500 mL wide mouth conical flask.
2. Add 250 mL of 15% H_2O_2 to the sample. Cover the flask with a watch glass and place it in a fume hood or well-ventilated area. The H_2O_2 should be at room temperature before commencing the test.
3. Allow the sample to react until 'boiling' or effervescing ceases. This may take days to a week. The NAG reaction can be vigorous and sample solutions can 'boil' at temperatures of up to 120^{o}C. Great care must be taken to place samples in a well-ventilated area or fume hood.
4. Measure and record the pH of the solution as NAG pH_1.
5. Heat the sample on a hot plate and gently boil for 2 hours. Do not allow sample to boil dry – add DI water if necessary.
6. Allow the solution to cool to room temperature, then measure and record the pH as NAG pH_2.
7. Rinse the sample that has adhered to the sides of the flask down into the solution with DI water. Add DI water to give a final volume of 250 mL.

8. Measure the pH of the final NAG solution. If the pH is greater than or equal to 7.0, end the test there. If the pH is less than 7.0, titrate the solution to pH 4.5 and then to pH 7.0 with NaOH solution of the appropriate concentration based on final NAG solution pH as in Table 1 below.

Table B2: Concentration of NaOH Solution to use for Titration.

NAG Solution pH	Reagent	NaOH Concentration
>2.5	5	0.10 N
<2.5	4	0.50 N

Calculations

The NAG capacity is determined as follows:

$$NAG = \frac{50 * V * N}{W}$$

Where:

NAG = net acid generation (kg $CaCO_3$/t)
V = volume of base NaOH titrated (mL)
N = normality of base NaOH (eq/L)
W = weight of sample reacted (g)

Documentation

Complete a Net Acid Generation Test Data Sheet (Table B6) for each sample tested, noting any deviations from the SOP. Plot the data from the Data Sheet on a graph sheet and estimate the actual volume of NaOH titrated at pH 4.5 and pH 7.0, respectively. Calculate the NAG values with the equation in 8.0 and record the results in the NAG Table in the Project Database.

Quality Assurance/Quality Control

The pH of the H_2O_2 used in the NAG test should be checked to ensure it is approximately 5.5. If the pH is less than 5, then add dilute NaOH (use a solution made by adding 1 g NaOH to 100 mL DI water) until the pH is greater than 5 (aim for a pH

between 5 and 6). The pH is adjusted to greater than pH 5 to ensure that the phosphoric acid, used to stabilize H_2O_2 in some brands, is neutralized. The pH of the 15% H_2O_2 should always be checked to ensure that any stabilizing acid is neutralized; otherwise, false positive results may be obtained.

Calibrate the pH meter according to the manufacturer's instructions before each titration. If, in the course of titration, the pH meter is suspected to be reading inaccurately, check with the pH 7.0 buffer and recalibrate the meter if it is off by more than 0.05 units. Run one duplicate sample for every 5 samples tested within a batch. Also, run between batch duplicates: test a duplicate of one sample in each batch during the next batch of tests. A duplicate of this sample should have been tested when testing its own batch.

Table B3: Net Acid Generation Test Data Sheet.

Net Acid Generation Test Data Sheet	
Sample ID	
Date Started	
Mass of Specimen (g)	
NAG pH_1	
NAG pH_2	
pH at 250 mL	
Date Titrated	
Volume of Solution (mL)	
Initial Burette Reading (mL)	
Initial pH of solution	
Concentration of NaOH (N)	
Initials of Technician	
Titration Points	
Volume (mL)	pH
Comments	
At pH 4.5 End Point (mL) =	
Volume Titrated (mL) =	
At pH 7.0 End Point (mL) =	
Volume Titrated (mL) =	

APPENDIX C TEST RESULTS

Table C1: Results of paste pH and paste conductivity tests on unpowdered samples.

Sample ID	Paste pH_1 (s.u.)	Paste Conductivity (mS/cm)	Sample ID	Paste pH_1 (s.u.)	Paste Conductivity (mS/cm)
GHN-ACT-0001	3.46	0.91	GHN-VTM-0050	4.05	1.79
GHN-ACT-0002	3.13	1.47	GHN-VTM-0051	4.54	2.09
GHN-ACT-0003	2.97	1.04	GHN-VTM-0052	5.33	1.51
GHN-ACT-0004	2.57	1.31	GHN-VTM-0053	4.92	2.25
GHN-ACT-0005	3.14	1.23	GHN-VTM-0054	4.85	2.06
GHN-ACT-0006	3.77	1.00	GHN-VTM-0055	5.30	1.80
GHN-ACT-0007	4.23	1.54	GHN-VTM-0056	3.91	1.77
GHN-ACT-0008	4.03	0.64	GHN-VTM-0057	2.53	2.37
GHN-ACT-0010	4.42	2.26	GHN-VTM-0058	3.12	2.46
GHN-ACT-0011	6.34	2.68	GHN-VTM-0059	2.65	2.87
GHN-ACT-0012	7.11	1.42	GHN-VTM-0060	2.77	3.79
GHN-ACT-0013	6.90	1.39	GHN-VTM-0061	3.15	3.54
GHN-ACT-0014	6.68	1.19	GHN-VTM-0062	3.05	2.65
GHN-ACT-0015	6.68	1.59	GHN-VTM-0063	3.18	1.68
GHN-ACT-0016	4.47	1.43	GHN-VTM-0064	3.17	3.09
GHN-ACT-0017	5.50	1.26	GHN-VTM-0065	3.12	2.38
GHN-ACT-0018	4.47	0.42	GHN-VTM-0066	3.21	1.63
GHN-ACT-0019	2.98	1.56	GHN-VTM-0067	3.17	2.88
GHN-ACT-0020	2.36	2.37	GHN-VTM-0068	2.96	1.90
GHN-ACT-0021	2.41	1.67	GHN-VTM-0069	3.01	2.57
GHN-ACT-0022	2.71	5.21	GHN-VTM-0070	3.56	2.23
GHN-ACT-0023	3.24	3.09	GHN-VTM-0071	3.43	1.76
GHN-ACT-0024	3.49	1.70	GHN-VTM-0072	3.26	1.94
GHN-ACT-0025	4.10	1.62	GHN-VTM-0073	3.54	1.88
GHN-ACT-0026	4.05	1.62	GHN-VTM-0074	4.76	2.26
GHN-ACT-0027	4.11	1.77	GHN-VTM-0075	7.99	2.62
GHN-ACT-0028	3.67	2.08	GHN-VTM-0076	7.88	2.75
GHN-ACT-0029	3.99	1.96	GHN-VTM-0077	7.66	2.69
GHN-ACT-0030	3.91	1.70	GHN-VTM-0078	8.74	2.63
GHN-ACT-0031	3.62	2.19	GHN-VTM-0079	2.64	3.62
GHN-ACT-0032	3.64	1.57	GHN-VTM-0080	2.91	1.65
GHN-ACT-0033	3.19	1.01	GHN-VTM-0081	7.97	2.52
GHN-ACT-0037	3.50	1.15	GHN-VTM-0082	6.11	3.16
GHN-ACT-0038	3.60	1.66	GHN-VTM-0083	4.60	2.52
GHN-ACT-0039	4.50	0.84	GHN-VTM-0084	4.51	4.12

Table C1 continued.

Sample ID	Paste pH_1 (s.u.)	Paste Conductivity (mS/cm)	Sample ID	Paste pH_1 (s.u.)	Paste Conductivity (mS/cm)
GHN-ACT-0040	4.80	0.73	GHN-VTM-0085	4.14	2.48
GHN-ACT-0041	6.10	1.45	GHN-VTM-0086	4.32	3.00
GHN-ACT-0042	3.60	1.51	GHN-VTM-0087	3.87	2.21
GHN-ACT-0043	5.10	1.75	GHN-VTM-0088	2.37	3.01
GHN-ACT-0044	5.30	1.98	GHN-VTM-0089	2.44	3.01
GHN-ACT-0045	8.25	1.94	GHN-VTM-0090	2.44	3.67
GHN-ACT-0046	7.42	1.65	GHN-VTM-0091	2.37	2.36
GHN-ACT-0047	8.01	1.64	GHN-VTM-0092	2.52	2.75
GHN-ACT-0048	6.77	1.92	GHN-VTM-0093	3.02	2.54
GHN-ACT-0049	6.07	1.60	GHN-VTM-0094	2.73	1.83
GHN-ACT-0050	3.78	0.92	GHN-VTM-0095	3.24	1.93
GHN-ACT-0051	5.45	1.78	GHN-VTM-0096	3.18	1.95
GHN-ACT-0052	3.38	1.26	GHN-VTM-0097	3.17	2.39
GHN-ACT-0053	5.05	1.69	GHN-VTM-0098	3.20	2.32
GHN-ACT-0054	3.70	1.48	GHN-VTM-0099	3.12	2.25
GHN-ACT-0055	5.07	1.61	GHN-VTM-0100	3.44	2.47
GHN-ACT-0056	4.85	2.04	GHN-VTM-0101	5.25	2.19
GHN-ACT-0057	5.09	3.08	GHN-VTM-0102	4.51	2.55
GHN-ACT-0058	4.89	2.40	GHN-VTM-0103	5.86	2.83
GHN-ACT-0059	4.94	1.37	GHN-VTM-0104	4.59	2.39
GHN-ACT-0060	4.54	1.69	GHN-VTM-0105	5.64	1.22
GHN-ACT-0061	4.73	2.05	GHN-VTM-0106	9.33	1.39
GHN-ACT-0062	4.49	2.94	GHN-VTM-0107	7.10	2.31
GHN-ACT-0063	6.76	1.59	GHN-VTM-0108	6.24	2.92
GHN-ACT-0064	5.41	2.54	GHN-VTM-0109	4.73	1.25
GHN-ACT-0065	5.07	1.54	GHN-VTM-0110	4.44	1.50
GHN-ACT-0066	3.51	1.17	GHN-VTM-0111	4.34	1.31
GHN-ACT-0067	3.07	1.94	GHN-VTM-0112	3.77	1.59
GHN-ACT-0068	3.37	0.95	GHN-VTM-0113	3.81	2.22
GHN-ACT-0069	3.49	1.49	GHN-VTM-0114	3.84	1.58
GHN-ACT-0070	3.45	2.17	GHN-VTM-0115	3.65	1.53
GHN-ACT-0071	7.35	1.69	GHN-VTM-0116	2.96	1.91
GHN-ACT-0073	5.59	1.83	GHN-VTM-0117	3.14	3.20
GHN-ACT-0074	4.62	0.40	GHN-VTM-0118	3.51	2.19
GHN-ACT-0075	6.26	1.93	GHN-VTM-0119	3.55	2.33
GHN-ACT-0076	4.72	2.11	GHN-VTM-0120	3.75	1.51
GHN-ACT-0077	4.07	2.14	GHN-VTM-0121	5.40	2.21
GHN-ACT-0078	3.65	2.14	GHN-VTM-0122	4.02	2.36
GHN-ACT-0079	3.82	1.88	GHN-VTM-0123	3.98	3.12
GHN-ACT-0080	3.18	1.25	GHN-VTM-0124	4.62	2.50
GHN-ACT-0081	3.48	0.85	GHN-VTM-0125	4.70	2.47
GHN-ACT-0082	5.11	1.13	GHN-VTM-0126	7.35	2.83
GHN-ACT-0083	4.96	0.99	GHN-VTM-0127	8.58	1.42
GHN-ACT-0084	4.48	0.83	GHN-VTM-0128	9.47	1.11
GHN-ACT-0085	4.66	2.46	GHN-VTM-0129	6.37	1.48
GHN-ACT-0086	4.70	2.45	GHN-VTM-0130	6.40	1.83

Table C1 continued.

Sample ID	Paste pH_1 (s.u.)	Paste Conductivity (mS/cm)	Sample ID	Paste pH_1 (s.u.)	Paste Conductivity (mS/cm)
GHN-ACT-0087	5.51	2.09	GHN-VTM-0131	4.61	1.79
GHN-ACT-0088	4.95	2.08	GHN-VTM-0132	5.46	1.10
GHN-ACT-0089	4.98	1.84	GHN-VTM-0133	4.39	1.48
GHN-ACT-0090	3.06	2.16	GHN-VTM-0134	3.98	1.23
GHN-ACT-0091	5.07	1.83	GHN-VTM-0135	8.56	1.03
GHN-ACT-0108	3.78	1.17	GHN-VTM-0136	4.08	1.37
GHN-ACT-0109	4.17	1.30	GHN-VTM-0137	3.57	1.81
GHN-ACT-0111	6.23	1.45	GHN-VTM-0138	4.02	1.46
GHN-ACT-0112	6.45	1.31	GHN-VTM-0139	3.62	0.72
GHN-ACT-0113	7.43	0.55	GHN-VTM-0140	4.17	0.91
GHN-ACT-0114	4.96	1.41	GHN-VTM-0141	4.29	1.03
GHN-ACT-0115	4.56	1.83	GHN-VTM-0143	4.30	0.85
GHN-ACT-0116	4.57	1.67	GHN-VTM-0144	3.54	1.39
GHN-ACT-0117	3.58	1.80	GHN-VTM-0145	3.66	1.37
GHN-ACT-0118	3.59	1.24	GHN-VTM-0146	4.22	0.81
GHN-ACT-0119	3.41	1.16	GHN-VTM-0147	4.42	0.42
GHN-ACT-0120	3.41	0.81	GHN-VTM-0152	5.50	1.77
GHN-ACT-0121	3.52	1.05	GHN-VTM-0153	3.89	1.03
GHN-ACT-0122	3.56	1.05	GHN-VTM-0154	4.33	0.83
GHN-ACT-0123	3.54	1.35	GHN-VTM-0155	3.95	1.49
GHN-ACT-0124	3.56	1.44	GHN-VTM-0156	2.79	2.59
GHN-ACT-0125	3.59	1.24	GHN-VTM-0157	3.54	1.06
GHN-ACT-0126	3.75	1.11	GHN-VTM-0158	3.47	1.24
GHN-ACT-0127	4.02	0.63	GHN-VTM-0159	3.29	1.22
GHN-ACT-0128	3.88	0.62	GHN-VTM-0160	2.84	1.41
GHN-ACT-0129	3.89	1.12	GHN-VTM-0161	3.55	1.66
GHN-ACT-0130	5.37	1.15	GHN-VTM-0162	3.58	1.51
GHN-ACT-0131	4.11	1.18	GHN-VTM-0163	3.37	1.58
GHN-ACT-0132	4.05	0.46	GHN-VTM-0164	3.93	1.30
GHN-ACT-0133	3.67	1.67	GHN-VTM-0165	3.64	1.30
GHN-ACT-0134	3.55	0.75	GHN-VTM-0166	5.00	2.18
GHN-ACT-0135	3.04	1.01	GHN-VTM-0167	5.23	1.66
GHN-ACT-0136	3.16	1.41	GHN-VTM-0168	6.92	0.95
GHN-ACT-0137	3.16	1.42	GHN-VTM-0169	7.14	1.06
GHN-ACT-0138	3.23	1.32	GHN-VTM-0170	7.49	0.55
GHN-ACT-0139	3.16	1.48	GHN-VTM-0171	7.05	1.08
GHN-ACT-0140	3.22	1.34	GHN-VTM-0172	7.86	0.74
GHN-ACT-0141	3.49	1.29	GHN-VTM-0173	7.63	0.78
GHN-ACT-0142	3.51	1.38	GHN-VTM-0174	7.94	0.60
GHN-ACT-0143	3.41	1.40	GHN-VTM-0175	8.01	0.68
GHN-ACT-0144	2.88	1.84	GHN-VTM-0176	7.05	1.30
GHN-ACT-0145	3.17	2.27	GHN-VTM-0177	6.68	1.05
GHN-ACT-0146	3.39	1.69	GHN-VTM-0178	5.04	2.07
GHN-ACT-0147	3.38	1.39	GHN-VTM-0179	4.63	2.09
GHN-ACT-0148	3.27	1.66	GHN-VTM-0180	5.04	1.86
GHN-ACT-0149	2.83	2.22	GHN-VTM-0181	4.84	2.20

Table C1 continued.

Sample ID	Paste pH_1 (s.u.)	Paste Conductivity (mS/cm)	Sample ID	Paste pH_1 (s.u.)	Paste Conductivity (mS/cm)
GHN-ACT-0150	2.87	2.26	GHN-VTM-0182	5.23	1.42
GHN-ACT-0151	2.84	1.51	GHN-VTM-0183	6.43	1.31
GHN-ACT-0152	3.06	1.35	GHN-VTM-0184	6.63	1.16
GHN-ACT-0153	3.18	1.09	GHN-VTM-0185	7.78	0.62
GHN-ACT-0154	3.14	1.07	GHN-VTM-0186	7.55	0.84
GHN-ACT-0155	3.52	0.75	GHN-VTM-0187	6.31	4.00
GHN-ACT-0156	3.14	1.19	GHN-VTM-0188	6.41	0.99
GHN-ACT-0157	3.34	0.73	GHN-VTM-0189	6.17	1.38
GHN-ACT-0158	3.39	0.28	GHN-VTM-0190	7.01	1.63
GHN-ACT-0159	3.41	1.46	GHN-VTM-0191	7.09	1.76
GHN-ACT-0160	2.98	0.61	GHN-VTM-0192	7.62	1.23
GHN-ACT-0161	3.55	0.32	GHN-VTM-0193	5.69	2.03
GHN-ACT-0162	3.33	1.38	GHN-VTM-0194	2.25	2.71
GHN-ACT-0163	4.67	1.40	GHN-VTM-0195	2.62	6.91
GHN-ACT-0164	6.79	1.09	GHN-VTM-0196	3.57	12.35
GHN-ACT-0165	6.91	0.93	GHN-VTM-0197	3.46	9.97
GHN-ACT-0166	6.86	0.87	GHN-VTM-0198	3.58	3.43
GHN-ACT-0167	3.63	1.28	GHN-VTM-0199	3.40	1.79
GHN-ACT-0168	4.23	1.21	GHN-VTM-0200	3.32	2.94
GHN-ACT-0169	3.41	1.74	GHN-VTM-0201	3.28	2.77
GHN-ACT-0170	3.84	1.25	GHN-VTM-0202	3.62	1.62
GHN-ACT-0171	3.92	1.04	GHN-VTM-0203	3.66	1.99
GHN-ACT-0172	3.09	1.26	GHN-VTM-0204	3.54	1.52
GHN-ACT-0173	3.56	1.01	GHN-VTM-0205	3.70	4.35
GHN-ACT-0174	3.12	2.12	GHN-VTM-0206	3.69	1.73
GHN-ACT-0175	3.17	2.68	GHN-VTM-0207	4.13	2.44
GHN-ACT-0176	2.55	4.25	GHN-VTM-0208	4.32	3.11
GHN-ACT-0177	2.76	5.01	GHN-VTM-0209	4.50	2.92
GHN-ACT-0178	3.61	4.33	GHN-VTM-0210	4.63	2.89
GHN-ACT-0179	3.34	3.04	GHN-VTM-0211	7.92	1.52
GHN-ACT-0180	3.20	3.58	GHN-VTM-0212	5.28	2.01
GHN-ACT-0181	2.86	3.72	GHN-VTM-0213	8.36	3.83
GHN-ACT-0182	4.56	1.87	GHN-VTM-0214	8.98	2.55
GHN-ACT-0183	3.90	2.86	GHN-VTM-0215	9.60	1.73
GHN-ACT-0184	4.47	2.68	GHN-VTM-0216	9.43	1.94
GHN-ACT-0185	4.01	3.07	GHN-VTM-0217	9.56	1.66
GHN-ACT-0234	7.87	1.56	GHN-VTM-0218	3.62	1.74
GHN-ACT-0235	7.27	1.42	GHN-VTM-0219	3.72	1.58
GHN-ACT-0236	8.39	1.02	GHN-VTM-0220	4.68	2.33
GHN-ACT-0237	6.88	1.79	GHN-VTM-0221	3.82	2.18
GHN-ACT-0238	6.26	2.17	GHN-VTM-0222	4.20	2.01
GHN-ACT-0239	7.15	1.93	GHN-VTM-0223	7.34	1.91
GHN-ACT-0240	6.49	2.02	GHN-VTM-0224	7.70	1.73
GHN-ACT-0241	4.50	1.89	GHN-VTM-0225	4.81	1.37
GHN-ACT-0242	6.65	1.80	GHN-VTM-0226	8.10	1.09
GHN-ACT-0243	3.98	2.02	GHN-VTM-0227	6.29	2.18

Table C1 continued.

Sample ID	Paste pH_1 (s.u.)	Paste Conductivity (mS/cm)	Sample ID	Paste pH_1 (s.u.)	Paste Conductivity (mS/cm)
GHN-ACT-0244	3.82	2.43	GHN-VTM-0228	4.09	2.21
GHN-ACT-0245	2.67	2.98	GHN-VTM-0229	4.15	1.54
GHN-ACT-0246	2.51	6.73	GHN-VTM-0230	5.49	2.52
GHN-ACT-0247	2.64	3.15	GHN-VTM-0231	2.80	4.20
GHN-ACT-0248	3.03	4.44	GHN-VTM-0232	2.99	5.61
GHN-ACT-0249	3.49	3.26	GHN-VTM-0233	2.86	5.28
GHN-EHP-0001	2.68	6.38	GHN-VTM-0234	3.89	1.22
GHN-EHP-0002	3.18	1.31	GHN-VTM-0235	3.86	4.56
GHN-EHP-0003	3.04	3.26	GHN-VTM-0236	4.71	5.39
GHN-HRS-0001	6.51	2.14	GHN-VTM-0237	4.23	2.87
GHN-HRS-0002	5.32	1.15	GHN-VTM-0238	3.77	3.55
GHN-HRS-0007	4.44	2.24	GHN-VTM-0239	3.92	4.15
GHN-HRS-0009	4.34	0.39	GHN-VTM-0240	4.68	4.82
GHN-HRS-0010	3.79	0.13	GHN-VTM-0241	4.15	3.48
GHN-HRS-0011	5.01	0.11	GHN-VTM-0242	5.07	1.44
GHN-HRS-0012	4.47	0.29	GHN-VTM-0243	5.26	1.39
GHN-HRS-0015	2.18	3.47	GHN-VTM-0244	6.63	1.30
GHN-HRS-0016	2.80	0.44	GHN-VTM-0245	7.09	1.76
GHN-HRS-0017	2.53	0.87	GHN-VTM-0246	5.54	2.40
GHN-HRS-0018	2.65	0.63	GHN-VTM-0247	6.36	2.61
GHN-HRS-0019	2.29	3.10	GHN-VTM-0248	4.81	2.66
GHN-HRS-0020	3.18	0.55	GHN-VTM-0249	4.00	2.82
GHN-HRS-0021	2.38	2.71	GHN-VTM-0250	4.33	2.88
GHN-HRS-0022	2.38	2.19	GHN-VTM-0251	6.37	2.22
GHN-HRS-0023	2.13	2.90	GHN-VTM-0252	4.75	1.52
GHN-HRS-0024	2.12	4.18	GHN-VTM-0253	5.15	1.85
GHN-HRS-0025	2.06	2.91	GHN-VTM-0254	7.54	2.90
GHN-HRS-0026	2.68	2.06	GHN-VTM-0255	7.23	1.54
GHN-HRS-0085	5.65	2.73	GHN-VTM-0256	7.12	1.60
GHN-HRS-0086	5.09	1.75	GHN-VTM-0257	4.96	2.71
GHN-HRS-0087	4.31	3.09	GHN-VTM-0258	3.85	2.08
GHN-HRS-0088	2.72	3.44	GHN-VTM-0260	4.52	3.47
GHN-HRS-0089	2.90	1.84	GHN-VTM-0261	2.54	3.14
GHN-HRS-0090	2.89	2.62	GHN-VTM-0262	2.33	4.90
GHN-HRS-0091	3.04	1.90	GHN-VTM-0263	2.70	3.16
GHN-HRS-0092	2.80	3.02	GHN-VTM-0264	3.59	2.89
GHN-HRS-0093	3.45	4.97	GHN-VTM-0265	4.77	2.99
GHN-HRS-0094	2.71	4.84	GHN-VTM-0266	4.19	4.11
GHN-HRS-0095	3.14	5.05	GHN-VTM-0267	4.77	3.90
GHN-HRS-0096	3.29	4.58	GHN-VTM-0268	4.95	3.69
GHN-HRS-0098	3.03	1.26	GHN-VTM-0269	2.96	3.26
GHN-HRS-0099	3.38	1.35	GHN-VTM-0270	3.10	3.21
GHN-HRS-0100	3.95	2.53	GHN-VTM-0271	3.54	2.78
GHN-HRS-0101	5.20	3.46	GHN-VTM-0272	5.06	3.27
GHN-HRS-0102	4.58	3.60	GHN-VTM-0273	5.37	4.51
GHN-HRS-0103	4.59	4.03	GHN-VTM-0274	3.73	4.21

Table C1 continued.

Sample ID	Paste pH_1 (s.u.)	Paste Conductivity (mS/cm)	Sample ID	Paste pH_1 (s.u.)	Paste Conductivity (mS/cm)
GHN-HRS-0104	3.92	3.28	GHN-VTM-0275	4.04	3.76
GHN-HRS-0105	3.91	4.76	GHN-VTM-0276	4.17	5.02
GHN-JMS-0001	4.09	2.40	GHN-VTM-0277	5.82	1.95
GHN-JMS-0002	5.37	1.27	GHN-VTM-0278	6.27	0.68
GHN-JMS-0003	2.84	2.38	GHN-VTM-0279	7.38	0.74
GHN-JMS-0004	4.33	2.26	GHN-VTM-0280	4.41	0.66
GHN-JRM-0001	2.14	6.31	GHN-VTM-0281	7.31	0.85
GHN-JRM-0002	2.15	5.46	GHN-VTM-0282	7.61	0.64
GHN-JRM-0003	2.53	3.65	GHN-VTM-0283	7.02	1.78
GHN-JRM-0004	2.54	4.23	GHN-VTM-0284	7.07	1.66
GHN-JRM-0005	2.94	3.12	GHN-VTM-0285	7.29	1.79
GHN-JRM-0006	4.71	5.83	GHN-VTM-0286	6.54	2.00
GHN-JRM-0007	3.38	4.66	GHN-VTM-0287	6.69	1.57
GHN-JRM-0008	4.25	4.87	GHN-VTM-0288	5.40	3.03
GHN-JRM-0009	3.97	5.45	GHN-VTM-0289	4.66	2.53
GHN-JRM-0010	4.02	5.04	GHN-VTM-0290	4.35	2.71
GHN-JRM-0011	3.99	1.69	GHN-VTM-0291	2.45	4.18
GHN-JRM-0012	4.08	4.08	GHN-VTM-0292	4.26	2.89
GHN-JRM-0013	2.65	3.38	GHN-VTM-0293	4.07	2.62
GHN-JRM-0014	2.43	3.72	GHN-VTM-0294	3.00	3.16
GHN-JRM-0015	2.41	2.11	GHN-VTM-0295	3.32	3.15
GHN-JRM-0019	5.67	3.09	GHN-VTM-0296	3.43	3.19
GHN-JRM-0020	3.31	3.15	GHN-VTM-0297	4.42	2.75
GHN-JRM-0021	2.80	4.30	GHN-VTM-0298	3.38	1.86
GHN-JRM-0022	6.20	4.42	GHN-VTM-0299	3.44	2.70
GHN-JRM-0024	3.00	4.88	GHN-VTM-0300	3.11	3.68
GHN-JRM-0025	2.55	6.12	GHN-VTM-0301	3.41	3.01
GHN-JRM-0026	4.25	3.68	GHN-VTM-0302	3.35	3.47
GHN-JRM-0027	6.48	4.00	GHN-VTM-0303	4.36	3.59
GHN-JRM-0028	4.19	2.53	GHN-VTM-0304	5.72	4.80
GHN-JRM-0029	5.21	3.22	GHN-VTM-0305	5.55	4.07
GHN-JRM-0030	6.06	2.59	GHN-VTM-0306	7.04	3.77
GHN-JRM-0031	4.46	3.18	GHN-VTM-0307	7.83	0.84
GHN-JRM-0033	5.09	0.97	GHN-VTM-0308	7.80	0.74
GHN-JRM-0034	2.78	2.51	GHN-VTM-0309	7.79	0.60
GHN-JRM-0035	2.81	1.71	GHN-VTM-0310	8.62	0.44
GHN-JRM-0036	2.69	1.40	GHN-VTM-0311	8.47	0.49
GHN-JRM-0037	2.91	3.20	GHN-VTM-0312	6.98	0.96
GHN-JRM-0038	2.99	1.26	GHN-VTM-0313	7.79	1.65
GHN-JRM-0039	3.06	1.23	GHN-VTM-0314	3.94	1.83
GHN-JRM-0040	3.37	0.73	GHN-VTM-0315	4.65	2.30
GHN-JRM-0041	3.01	3.38	GHN-VTM-0316	4.03	3.21
GHN-JRM-0042	3.06	3.30	GHN-VTM-0317	4.38	1.50
GHN-JRM-0043	2.90	1.38	GHN-VTM-0318	4.54	1.70
GHN-JRM-0044	3.24	4.52	GHN-VTM-0319	4.22	1.45
GHN-JRM-0045	3.19	2.77	GHN-VTM-0340	7.56	0.83

Table C1 continued.

Sample ID	Paste pH_1 (s.u.)	Paste Conductivity (mS/cm)	Sample ID	Paste pH_1 (s.u.)	Paste Conductivity (mS/cm)
GHN-JRM-0046	3.14	3.46	GHN-VTM-0341	6.37	1.36
GHN-JRM-0047	2.99	3.25	GHN-VTM-0342	5.52	1.96
GHN-JRM-0048	2.77	1.79	GHN-VTM-0343	5.12	2.19
GHN-JRM-0049	2.94	3.58	GHN-VTM-0344	4.21	2.51
GHN-JRM-0050	3.04	4.13	GHN-VTM-0345	4.06	1.17
GHN-JRM-0051	3.46	1.64	GHN-VTM-0346	6.04	1.52
GHN-KMD-0001	3.25	1.77	GHN-VTM-0347	3.73	1.17
GHN-KMD-0002	2.68	7.40	GHN-VTM-0348	3.29	1.06
GHN-KMD-0003	3.29	1.65	GHN-VTM-0349	4.00	0.99
GHN-KMD-0004	3.73	1.11	GHN-VTM-0350	4.77	2.10
GHN-KMD-0005	3.11	2.29	GHN-VTM-0351	3.54	1.88
GHN-KMD-0006	2.81	3.60	GHN-VTM-0352	3.91	2.08
GHN-KMD-0007	4.23	4.20	GHN-VTM-0353	6.34	2.28
GHN-KMD-0008	2.57	5.88	GHN-VTM-0354	6.58	2.65
GHN-KMD-0009	4.44	1.67	GHN-VTM-0355	7.06	4.07
GHN-KMD-0010	5.83	2.35	GHN-VTM-0356	6.97	3.56
GHN-KMD-0011	2.65	3.56	GHN-VTM-0357	7.04	2.99
GHN-KMD-0012	2.68	4.65	GHN-VTM-0358	7.63	1.74
GHN-KMD-0013	2.49	4.24	GHN-VTM-0359	7.62	1.55
GHN-KMD-0014	3.19	3.47	GHN-VTM-0360	6.64	1.90
GHN-KMD-0015	4.92	1.88	GHN-VTM-0361	7.20	2.94
GHN-KMD-0016	5.74	2.46	GHN-VTM-0362	6.92	3.37
GHN-KMD-0017	2.19	3.63	GHN-VTM-0363	7.34	1.85
GHN-KMD-0018	3.50	7.98	GHN-VTM-0364	7.35	1.72
GHN-KMD-0019	5.84	1.89	GHN-VTM-0365	7.66	3.23
GHN-KMD-0020	5.54	5.54	GHN-VTM-0366	7.61	3.19
GHN-KMD-0021	5.84	3.63	GHN-VTM-0368	4.21	1.98
GHN-KMD-0022	2.58	4.85	GHN-VTM-0369	3.94	1.43
GHN-KMD-0023	5.99	2.25	GHN-VTM-0370	7.30	1.39
GHN-KMD-0024	2.61	3.65	GHN-VTM-0371	3.91	1.49
GHN-KMD-0025	3.26	1.56	GHN-VTM-0372	3.64	1.43
GHN-KMD-0026	3.80	0.94	GHN-VTM-0373	3.98	1.54
GHN-KMD-0027	2.49	3.14	GHN-VTM-0374	3.95	1.57
GHN-KMD-0028	2.60	6.13	GHN-VTM-0375	5.94	2.48
GHN-KMD-0036	2.27	6.54	GHN-VTM-0377	5.68	2.26
GHN-KMD-0037	2.75	6.09	GHN-VTM-0378	5.94	1.00
GHN-KMD-0038	2.37	3.00	GHN-VTM-0379	3.54	2.16
GHN-KMD-0039	2.49	3.15	GHN-VTM-0380	3.37	1.73
GHN-KMD-0040	3.62	1.49	GHN-VTM-0381	3.37	1.03
GHN-KMD-0041	5.48	2.36	GHN-VTM-0382	3.58	0.91
GHN-KMD-0042	5.82	2.45	GHN-VTM-0383	3.89	1.81
GHN-KMD-0043	3.50	1.17	GHN-VTM-0384	4.12	1.27
GHN-KMD-0044	4.68	7.96	GHN-VTM-0385	3.85	2.42
GHN-KMD-0045	4.61	3.85	GHN-VTM-0386	3.75	3.41
GHN-KMD-0046	4.27	4.08	GHN-VTM-0387	3.43	2.44
GHN-KMD-0047	7.32	5.10	GHN-VTM-0388	6.13	1.39

Table C1 continued.

Sample ID	Paste pH_1 (s.u.)	Paste Conductivity (mS/cm)	Sample ID	Paste pH_1 (s.u.)	Paste Conductivity (mS/cm)
GHN-KMD-0048	6.18	1.88	GHN-VTM-0389	3.67	1.95
GHN-KMD-0049	2.48	5.93	GHN-VTM-0390	3.54	1.50
GHN-KMD-0050	5.71	3.64	GHN-VTM-0391	3.31	0.97
GHN-KMD-0051	7.19	2.94	GHN-VTM-0392	3.24	1.76
GHN-KMD-0052	5.08	2.64	GHN-VTM-0393	4.84	1.88
GHN-KMD-0053	4.32	2.84	GHN-VTM-0394	3.48	2.74
GHN-KMD-0054	3.93	6.05	GHN-VTM-0395	3.17	0.72
GHN-KMD-0055	4.27	5.84	GHN-VTM-0396	4.86	0.70
GHN-KMD-0056	4.85	1.34	GHN-VTM-0398	4.78	1.06
GHN-KMD-0057	7.96	0.18	GHN-VTM-0399	4.44	1.44
GHN-KMD-0062	4.43	3.79	GHN-VTM-0400	4.83	1.64
GHN-KMD-0063	3.95	5.24	GHN-VTM-0401	4.98	1.55
GHN-KMD-0064	2.67	3.25	GHN-VTM-0402	5.98	1.37
GHN-KMD-0065	5.77	1.45	GHN-VTM-0403	6.48	1.02
GHN-KMD-0066	6.40	4.05	GHN-VTM-0404	3.14	1.49
GHN-KMD-0067	6.97	5.00	GHN-VTM-0405	2.90	1.52
GHN-KMD-0068	7.02	2.83	GHN-VTM-0406	3.26	1.71
GHN-KMD-0069	6.75	2.48	GHN-VTM-0407	2.94	2.45
GHN-KMD-0070	4.29	2.06	GHN-VTM-0408	3.41	1.86
GHN-KMD-0071	4.35	1.44	GHN-VTM-0409	3.90	1.98
GHN-KMD-0072	7.15	3.84	GHN-VTM-0410	3.82	1.94
GHN-KMD-0073	6.55	3.89	GHN-VTM-0411	3.89	2.58
GHN-KMD-0074	3.36	4.25	GHN-VTM-0412	4.18	2.41
GHN-KMD-0075	5.23	3.19	GHN-VTM-0413	6.63	1.82
GHN-KMD-0076	4.43	1.75	GHN-VTM-0414	4.59	2.48
GHN-KMD-0077	2.45	1.55	GHN-VTM-0415	6.64	2.47
GHN-KMD-0078	3.26	3.46	GHN-VTM-0416	6.69	2.39
GHN-KMD-0079	3.07	3.98	GHN-VTM-0417	3.06	1.72
GHN-KMD-0080	6.36	2.59	GHN-VTM-0418	2.86	2.00
GHN-KMD-0081	3.29	3.59	GHN-VTM-0419	2.85	2.06
GHN-KMD-0082	3.30	3.70	GHN-VTM-0420	3.10	2.74
GHN-KMD-0083	4.36	3.67	GHN-VTM-0421	3.21	2.92
GHN-KMD-0084	3.15	5.16	GHN-VTM-0422	3.52	2.26
GHN-KMD-0085	3.01	3.44	GHN-VTM-0423	3.62	1.95
GHN-KMD-0086	3.63	5.33	GHN-VTM-0424	3.58	3.21
GHN-KMD-0087	3.52	4.35	GHN-VTM-0425	3.94	3.91
GHN-KMD-0088	2.63	6.09	GHN-VTM-0426	3.70	2.96
GHN-KMD-0089	3.40	5.40	GHN-VTM-0427	4.90	2.66
GHN-KMD-0090	2.44	5.76	GHN-VTM-0428	2.99	2.28
GHN-KMD-0091	2.55	5.01	GHN-VTM-0434	3.60	2.11
GHN-KMD-0092	3.72	4.50	GHN-VTM-0435	3.85	2.17
GHN-KMD-0093	2.52	6.90	GHN-VTM-0436	3.02	1.51
GHN-KMD-0095	2.73	2.88	GHN-VTM-0437	3.16	1.90
GHN-KMD-0096	2.56	3.04	GHN-VTM-0438	3.08	2.56
GHN-KMD-0098	2.80	1.32	GHN-VTM-0440	2.73	1.18
GHN-KMD-0099	2.76	2.18	GHN-VTM-0441	2.88	1.94

Table C1 continued.

Sample ID	Paste pH_1 (s.u.)	Paste Conductivity (mS/cm)	Sample ID	Paste pH_1 (s.u.)	Paste Conductivity (mS/cm)
GHN-KMD-0100	3.42	3.25	GHN-VTM-0442	4.54	1.51
GHN-LFG-0015	2.74	2.01	GHN-VTM-0444	6.36	1.32
GHN-LFG-0016	3.14	1.35	GHN-VTM-0445	5.67	2.20
GHN-LFG-0017	2.85	2.60	GHN-VTM-0446	4.11	2.10
GHN-LFG-0018	4.19	1.19	GHN-VTM-0447	7.53	1.60
GHN-LFG-0019	4.65	0.51	GHN-VTM-0448	4.04	1.89
GHN-LFG-0020	4.45	1.75	GHN-VTM-0449	2.92	1.27
GHN-LFG-0021	6.60	0.77	GHN-VTM-0450	6.70	1.55
GHN-LFG-0022	6.62	0.98	GHN-VTM-0451	3.87	1.85
GHN-LFG-0023	5.35	0.96	GHN-VTM-0452	3.18	3.16
GHN-LFG-0024	5.25	0.96	GHN-VTM-0453	4.55	1.81
GHN-LFG-0025	5.17	0.39	GHN-VTM-0454	3.56	1.90
GHN-LFG-0027	5.73	0.24	GHN-VTM-0455	4.69	1.98
GHN-LFG-0028	7.45	0.75	GHN-VTM-0511	3.22	1.41
GHN-LFG-0029	4.17	0.58	GHN-VTM-0512	3.55	1.10
GHN-LFG-0030	6.68	0.59	GHN-VTM-0513	3.54	1.45
GHN-LFG-0031	6.68	0.66	GHN-VTM-0514	3.63	1.61
GHN-LFG-0032	4.40	0.28	GHN-VTM-0515	3.31	1.09
GHN-LFG-0033	6.77	0.65	GHN-VTM-0516	3.31	1.08
GHN-LFG-0034	3.15	0.26	GHN-VTM-0518	3.06	1.62
GHN-LFG-0035	4.50	0.31	GHN-VTM-0519	3.11	1.06
GHN-LFG-0036	4.50	1.90	GHN-VTM-0520	2.85	1.42
GHN-LFG-0037	4.50	2.28	GHN-VTM-0521	3.24	2.02
GHN-LFG-0038	4.32	0.35	GHN-VTM-0522	3.30	1.64
GHN-LFG-0039	5.57	0.43	GHN-VTM-0523	3.51	2.23
GHN-LFG-0040	5.48	0.52	GHN-VTM-0524	3.30	1.21
GHN-LFG-0041	5.37	0.22	GHN-VTM-0525	3.22	1.50
GHN-LFG-0042	4.66	0.71	GHN-VTM-0526	3.30	1.42
GHN-LFG-0043	4.54	0.72	GHN-VTM-0527	3.28	1.25
GHN-LFG-0044	4.09	1.08	GHN-VTM-0528	3.12	1.37
GHN-LFG-0045	4.00	6.68	GHN-VTM-0529	2.89	2.38
GHN-LFG-0046	5.75	4.97	GHN-VTM-0530	3.24	1.14
GHN-LFG-0047	4.13	3.06	GHN-VTM-0531	2.75	2.29
GHN-LFG-0048	4.00	7.19	GHN-VTM-0532	2.79	2.29
GHN-LFG-0049	4.07	3.26	GHN-VTM-0533	2.92	1.17
GHN-LFG-0050	3.92	3.69	GHN-VTM-0534	3.29	1.59
GHN-LFG-0051	3.87	3.13	GHN-VTM-0535	3.39	0.84
GHN-LFG-0052	3.73	3.36	GHN-VTM-0536	3.28	1.23
GHN-LFG-0053	5.75	2.18	GHN-VTM-0537	3.27	1.02
GHN-LFG-0054	6.12	2.51	GHN-VTM-0538	3.25	1.82
GHN-LFG-0057	2.65	2.77	GHN-VTM-0539	3.48	1.38
GHN-LFG-0058	2.55	2.65	GHN-VTM-0540	3.36	1.42
GHN-LFG-0059	2.36	3.45	GHN-VTM-0541	3.42	1.29
GHN-LFG-0060	3.03	1.41	GHN-VTM-0542	3.44	1.58
GHN-LFG-0061	2.87	3.09	GHN-VTM-0543	3.54	1.41
GHN-LFG-0062	2.33	3.73	GHN-VTM-0544	2.81	3.16

Table C1 continued.

Sample ID	Paste pH_1 (s.u.)	Paste Conductivity (mS/cm)	Sample ID	Paste pH_1 (s.u.)	Paste Conductivity (mS/cm)
GHN-LFG-0063	4.10	4.91	GHN-VTM-0545	3.50	0.96
GHN-LFG-0064	4.22	2.08	GHN-VTM-0546	3.40	1.24
GHN-LFG-0065	5.84	3.94	GHN-VTM-0548	2.67	2.97
GHN-LFG-0066	4.53	4.04	GHN-VTM-0549	2.78	3.28
GHN-LFG-0067	4.50	0.48	GHN-VTM-0550	2.45	5.13
GHN-LFG-0068	4.30	1.06	GHN-VTM-0551	3.33	2.84
GHN-LFG-0069	4.29	3.43	GHN-VTM-0552	3.16	2.37
GHN-LFG-0070	2.51	1.44	GHN-VTM-0553	3.99	2.77
GHN-LFG-0071	3.36	0.53	GHN-VTM-0554	6.20	1.53
GHN-LFG-0072	2.91	0.62	GHN-VTM-0555	7.99	0.99
GHN-LFG-0075	2.39	0.74	GHN-VTM-0556	2.90	0.90
GHN-LFG-0076	2.58	0.49	GHN-VTM-0557	3.32	1.06
GHN-LFG-0077	2.39	0.88	GHN-VTM-0558	2.88	1.48
GHN-LFG-0084	6.90	1.34	GHN-VTM-0559	2.92	0.88
GHN-LFG-0085	3.15	1.98	GHN-VTM-0560	3.16	1.04
GHN-LFG-0086	3.02	1.74	GHN-VTM-0561	2.95	1.31
GHN-LFG-0088	5.41	1.28	GHN-VTM-0562	3.48	1.78
GHN-PXW-0001	3.54	3.15	GHN-VTM-0563	2.93	2.89
GHN-PXW-0002	3.72	4.00	GHN-VTM-0564	2.87	1.84
GHN-PXW-0003	4.13	3.17	GHN-VTM-0565	3.51	1.19
GHN-PXW-0004	3.04	4.38	GHN-VTM-0566	3.10	1.96
GHN-PXW-0005	2.65	5.30	GHN-VTM-0567	2.98	1.45
GHN-PXW-0006	2.92	3.96	GHN-VTM-0568	2.91	1.47
GHN-PXW-0007	3.15	2.91	GHN-VTM-0569	2.74	2.75
GHN-PXW-0008	2.96	5.02	GHN-VTM-0570	2.87	1.60
GHN-PXW-0009	2.96	3.87	GHN-VTM-0571	2.80	1.44
GHN-PXW-0010	3.14	2.98	GHN-VTM-0572	2.65	1.33
GHN-PXW-0011	3.43	2.69	GHN-VTM-0573	2.62	1.47
GHN-PXW-0012	3.40	1.34	GHN-VTM-0574	2.77	2.47
GHN-PXW-0013	3.30	1.89	GHN-VTM-0575	2.80	1.45
GHN-PXW-0014	3.26	1.64	GHN-VTM-0576	3.15	1.21
GHN-PXW-0015	3.46	0.88	GHN-VTM-0577	3.48	1.26
GHN-PXW-0016	3.06	1.18	GHN-VTM-0578	3.77	1.09
GHN-SAW-0001	2.72	0.61	GHN-VTM-0579	4.31	0.14
GHN-SAW-0002	3.48	0.94	GHN-VTM-0580	4.80	0.21
GHN-SAW-0004	2.38	4.66	GHN-VTM-0581	4.50	0.34
GHN-SAW-0200	7.54	2.65	GHN-VTM-0582	3.30	1.33
GHN-SAW-0201	2.74	2.11	GHN-VTM-0583	3.02	2.42
GHN-STM-0001	2.84	1.03	GHN-VTM-0584	2.99	1.60
GHN-STM-0002	3.25	0.24	GHN-VTM-0585	2.94	2.51
GHN-STM-0003	2.87	0.18	GHN-VTM-0586	2.96	2.09
GHN-STM-0004	2.70	2.08	GHN-VTM-0587	2.94	1.08
GHN-STM-0005	3.77	0.12	GHN-VTM-0588	2.93	1.16
GHN-STM-0006	6.60	0.07	GHN-VTM-0589	2.49	0.97
GHN-STM-0007	4.34	2.12	GHN-VTM-0590	3.39	0.87
GHN-STM-0008	4.27	0.46	GHN-VTM-0591	3.33	1.11

Table C1 continued.

Sample ID	Paste pH_1 (s.u.)	Paste Conductivity (mS/cm)	Sample ID	Paste pH_1 (s.u.)	Paste Conductivity (mS/cm)
GHN-STM-0009	5.11	0.06	GHN-VTM-0592	3.30	1.74
GHN-STM-0010	3.90	1.12	GHN-VTM-0593	3.47	1.10
GHN-STM-0011	3.92	2.82	GHN-VTM-0594	3.92	1.78
GHN-STM-0012	4.38	0.42	GHN-VTM-0595	3.82	1.70
GHN-STM-0013	4.34	0.86	GHN-VTM-0596	4.32	0.24
GHN-VTM-0030	3.35	2.62	GHN-VTM-0597	4.86	1.15
GHN-VTM-0031	3.08	1.79	GHN-VTM-0598	2.78	3.77
GHN-VTM-0032	2.64	2.24	GHN-VTM-0602	5.81	1.67
GHN-VTM-0033	2.62	2.49	GHN-VTM-0603	3.56	3.63
GHN-VTM-0034	2.75	2.44	GHN-VTM-0605	3.32	3.78
GHN-VTM-0035	3.43	1.82	GHN-VTM-0606	3.25	2.42
GHN-VTM-0036	3.30	1.62	GHN-VTM-0607	2.66	2.33
GHN-VTM-0037	2.66	2.37	GHN-VTM-0612	6.12	1.48
GHN-VTM-0038	2.72	0.75	GHN-VTM-0614	3.09	2.04
GHN-VTM-0039	2.62	3.21	GHN-VTM-0615	3.90	1.73
GHN-VTM-0040	3.00	1.53	GHN-VTM-0616	4.40	2.15
GHN-VTM-0041	3.07	1.49	GHN-VTM-0618	4.21	1.72
GHN-VTM-0042	3.44	1.64	GHN-VTM-0619	2.60	2.55
GHN-VTM-0043	3.06	1.95	GHN-VTM-0620	3.30	2.98
GHN-VTM-0044	3.68	1.99	GHN-VTM-0621	5.98	2.25
GHN-VTM-0045	4.02	1.90	GHN-VTM-0622	2.85	1.86
GHN-VTM-0046	5.60	2.09	GHN-VTM-0623	2.88	1.74
GHN-VTM-0047	4.31	1.26	GHN-VTM-0624	3.34	3.09
GHN-VTM-0048	5.18	2.57			
GHN-VTM-0049	5.67	1.90			

Table C2: Acid-base accounting results. Paste pH2 is paste pH measured on powdered samples.

Sample ID	Paste pH_2 (s.u.)	AP (kg $CaCO_3$/t)	NP (kg $CaCO_3$/t)	NNP (kg $CaCO_3$/t)	NP/AP
GHN-ACT-0001	4.49	3.03	1.05	-1.98	0.35
GHN-ACT-0002	4.31	4.63	0.47	-4.16	0.10
GHN-ACT-0003	4.13	4.09	0.91	-3.18	0.22
GHN-ACT-0004	3.95	5.08	0.00	-5.08	0.00
GHN-ACT-0005	4.75	6.01	3.81	-2.20	0.63
GHN-ACT-0006	4.97	1.15	2.21	1.06	1.92
GHN-ACT-0007	5.13	1.64	6.73	5.09	4.11
GHN-ACT-0008	5.09	8.23	0.63	-7.60	0.08
GHN-ACT-0010	6.04	3.35	9.87	6.52	2.95
GHN-ACT-0011	7.31	1.79	17.97	16.18	10.04
GHN-ACT-0012	7.52	1.49	29.21	27.72	19.60
GHN-ACT-0013	7.52	1.46	22.57	21.11	15.46
GHN-ACT-0014	7.80	0.77	29.92	29.15	38.85
GHN-ACT-0015	8.08	3.08	21.11	18.03	6.85
GHN-ACT-0016	6.81	4.38	8.30	3.92	1.89
GHN-ACT-0017	7.81	2.82	10.88	8.06	3.86
GHN-ACT-0018	5.88	1.28	1.32	0.04	1.03
GHN-ACT-0019	3.87	5.31	0.00	-5.31	0.00
GHN-ACT-0020	3.11	6.94	0.00	-6.94	0.00
GHN-ACT-0021	3.28	1.65	0.00	-1.65	0.00
GHN-ACT-0022	3.13	4.96	0.00	-4.96	0.00
GHN-ACT-0023	3.46	7.77	0.00	-7.77	0.00
GHN-ACT-0024	4.31	3.82	0.00	-3.82	0.00
GHN-ACT-0025	5.99	4.22	8.76	4.54	2.08
GHN-ACT-0026	5.57	3.28	8.36	5.08	2.55
GHN-ACT-0027	6.05	4.00	7.66	3.66	1.91
GHN-ACT-0028	4.14	1.99	9.16	7.17	4.60
GHN-ACT-0029	5.98	1.27	15.53	14.26	12.23
GHN-ACT-0030	4.99	1.78	12.79	11.01	7.18
GHN-ACT-0031	3.91	1.37	4.47	3.10	3.26
GHN-ACT-0032	4.04	0.96	0.00	-0.96	0.00
GHN-ACT-0033	4.01	18.80	0.00	-18.80	0.00
GHN-KMD-0013	4.39	3.29	5.47	2.18	1.66
GHN-KMD-0014	8.08	0.27	23.91	23.64	88.54
GHN-KMD-0015	6.75	2.47	10.93	8.46	4.43
GHN-KMD-0016	7.75	1.82	31.84	30.02	17.49
GHN-KMD-0017	3.46	13.20	0.73	-12.47	0.06
GHN-KMD-0018	4.04	1.71	0.00	-1.71	0.00
GHN-KMD-0051	7.81	1.83	15.16	13.33	8.29
GHN-KMD-0053	5.47	3.04	3.36	0.32	1.11
GHN-KMD-0056	6.14	1.83	7.84	6.01	4.28
GHN-KMD-0071	5.38	7.75	3.83	-3.92	0.49
GHN-KMD-0073	7.69	3.58	31.66	28.08	8.84
GHN-KMD-0074	5.86	3.77	14.49	10.72	3.84
GHN-KMD-0079	6.09	4.79	9.60	4.81	2.00
GHN-KMD-0081	5.84	6.30	6.64	0.34	1.05
GHN-LFG-0085	3.98	1.51	0.00	-1.51	0.00

Table C2 continued.

Sample ID	Paste pH_2 (s.u.)	AP (kg $CaCO_3$/t)	NP (kg $CaCO_3$/t)	NNP (kg $CaCO_3$/t)	NP/AP
GHN-LFG-0086	4.38	5.15	4.50	-0.65	0.87
GHN-LFG-0088	7.75	2.24	43.27	41.03	19.32
GHN-STM-0001	3.72	6.19	0.63	-5.56	0.10
GHN-STM-0002	4.09	5.49	0.00	-5.49	0.00
GHN-STM-0003	4.05	3.90	0.00	-3.90	0.00
GHN-STM-0004	6.51	2.88	14.22	11.34	4.94
GHN-STM-0005	5.52	1.75	1.40	-0.36	0.80
GHN-VTM-0194	3.14	12.92	0.00	-12.92	0.00
GHN-VTM-0195	3.53	1.03	0.00	-1.03	0.00
GHN-VTM-0196	3.87	2.40	0.00	-2.40	0.00
GHN-VTM-0197	5.02	2.13	16.49	14.36	7.74
GHN-VTM-0198	4.20	2.54	3.48	0.94	1.37
GHN-VTM-0199	4.85	2.75	4.88	2.13	1.77
GHN-VTM-0200	4.04	2.59	0.32	-2.27	0.12
GHN-VTM-0201	3.88	5.98	0.65	-5.33	0.11
GHN-VTM-0202	4.56	4.26	5.95	1.69	1.40
GHN-VTM-0203	4.96	2.77	4.26	1.49	1.54
GHN-VTM-0204	4.09	2.69	3.64	0.95	1.35
GHN-VTM-0205	4.18	2.08	1.53	-0.55	0.73
GHN-VTM-0206	4.31	1.87	5.72	3.85	3.06
GHN-VTM-0207	4.14	1.56	3.09	1.53	1.98
GHN-VTM-0208	6.16	0.59	11.89	11.30	20.15
GHN-VTM-0209	6.63	0.64	12.24	11.60	19.12
GHN-VTM-0210	7.02	0.80	11.37	10.57	14.21
GHN-VTM-0211	7.87	1.36	34.48	33.12	25.35
GHN-VTM-0212	7.50	0.82	22.04	21.22	26.88
GHN-VTM-0213	7.90	1.56	33.31	31.75	21.35
GHN-VTM-0214	7.87	1.03	48.81	47.78	47.38
GHN-VTM-0215	7.58	1.34	22.07	20.73	16.47
GHN-VTM-0216	8.06	1.39	33.54	32.15	24.13
GHN-VTM-0217	7.42	0.26	4.55	4.29	17.49
GHN-VTM-0375	7.34	4.30	23.44	19.14	5.45
GHN-VTM-0377	7.45	3.92	32.36	28.44	8.26
GHN-VTM-0386	5.26	5.97	2.43	-3.54	0.41
GHN-VTM-0387	4.33	7.67	0.00	-7.67	0.00
GHN-VTM-0394	5.72	3.09	3.92	0.83	1.27
GHN-VTM-0395	4.36	3.04	0.00	-3.04	0.00
GHN-VTM-0398	5.60	14.60	8.03	-6.57	0.55
GHN-VTM-0399	4.14	10.66	0.00	-10.66	0.00
GHN-VTM-0417	3.23	5.48	0.00	-5.48	0.00
GHN-VTM-0418	3.05	12.81	0.00	-12.81	0.00
GHN-VTM-0419	3.76	7.74	0.72	-7.02	0.09
GHN-VTM-0420	3.45	2.86	0.00	-2.86	0.00
GHN-VTM-0421	4.04	1.85	8.25	6.40	4.46
GHN-VTM-0422	3.99	3.01	4.18	1.17	1.39
GHN-VTM-0423	4.26	0.57	6.03	5.46	10.57
GHN-VTM-0424	3.86	2.01	0.00	-2.01	0.00
GHN-VTM-0425	5.02	2.11	4.00	1.89	1.90

Table C2 continued.

Sample ID	Paste pH_2 (s.u.)	AP (kg $CaCO_3$/t)	NP (kg $CaCO_3$/t)	NNP (kg $CaCO_3$/t)	NP/AP
GHN-VTM-0426	4.46	1.44	9.49	8.05	6.59
GHN-VTM-0450	6.78	2.13	1.93	-0.21	0.90
GHN-VTM-0451	4.69	2.78	3.22	0.44	1.16
GHN-VTM-0452	4.22	1.83	2.27	0.44	1.24
GHN-VTM-0453	6.08	1.54	53.28	51.74	34.60
GHN-VTM-0454	4.23	0.86	1.08	0.22	1.25
GHN-VTM-0455	6.24	1.05	0.73	-0.32	0.70
GHN-VTM-0556	3.92	9.08	0.00	-9.08	0.00
GHN-VTM-0557	4.26	7.97	0.00	-7.97	0.00
GHN-VTM-0561	4.09	2.00	0.00	-2.00	0.00
GHN-VTM-0562	4.84	0.68	3.95	3.27	5.81
GHN-VTM-0573	3.65	14.47	0.00	-14.47	0.00
GHN-VTM-0575	5.48	4.07	0.00	-4.07	0.00
GHN-VTM-0598	3.93	9.36	0.00	-9.36	0.00
GHN-VTM-0602	6.75	4.88	19.36	14.48	3.97
GHN-VTM-0603	4.01	5.64	0.00	-5.64	0.00
GHN-VTM-0606	3.98	2.03	0.00	-2.03	0.00
GHN-VTM-0612	7.21	3.85	18.63	14.78	4.84
GHN-VTM-0624	3.86	3.85	0.00	-3.85	0.00

Table C3: Net acid generation test results.

Sample ID	NAG pH_2	$NAG_{4.5}$ (kg $CaCO_3$/t)
GHN-ACT-0001	3.15	1.28
GHN-ACT-0002	3.31	4.28
GHN-ACT-0003	3.98	0.54
GHN-ACT-0004	2.65	3.79
GHN-ACT-0005	2.87	2.15
GHN-ACT-0006	3.89	0.99
GHN-ACT-0007	5.95	0.00
GHN-ACT-0008	2.51	7.72
GHN-ACT-0010	6.56	0.00
GHN-ACT-0011	7.92	0.00
GHN-ACT-0012	7.52	0.00
GHN-ACT-0013	8.06	0.00
GHN-ACT-0014	7.98	0.00
GHN-ACT-0015	7.69	0.00
GHN-ACT-0016	2.93	0.41
GHN-ACT-0017	4.43	0.06
GHN-ACT-0018	5.98	0.00
GHN-ACT-0019	2.03	5.82
GHN-ACT-0020	1.86	11.09
GHN-ACT-0021	2.44	3.13
GHN-ACT-0022	3.52	9.53
GHN-ACT-0023	1.88	17.08
GHN-ACT-0024	2.45	3.46
GHN-ACT-0025	2.68	2.80
GHN-ACT-0026	6.91	0.00
GHN-ACT-0027	3.01	0.29
GHN-ACT-0028	4.15	0.49
GHN-ACT-0029	7.56	0.00
GHN-ACT-0030	6.03	0.00
GHN-ACT-0031	3.45	0.00
GHN-ACT-0032	3.84	0.56
GHN-ACT-0033	1.37	31.18
GHN-KMD-0013	6.06	0.00
GHN-KMD-0014	8.55	0.00
GHN-KMD-0015	6.78	0.00
GHN-KMD-0016	8.36	0.00
GHN-KMD-0017	2.43	25.60
GHN-KMD-0018	3.88	0.50
GHN-KMD-0051	8.51	0.00
GHN-KMD-0053	6.26	0.00
GHN-KMD-0056	7.05	0.00
GHN-KMD-0071	2.53	3.32
GHN-KMD-0073	8.62	0.00
GHN-KMD-0074	6.59	0.00
GHN-KMD-0079	6.40	0.00
GHN-KMD-0081	3.15	0.88
GHN-LFG-0085	4.20	0.00
GHN-LFG-0086	2.96	1.27

Table C3 continued.

Sample ID	NAG pH_2	$NAG_{4.5}$ (kg $CaCO_3$/t)
GHN-LFG-0088	8.99	0.00
GHN-STM-0001	2.84	3.98
GHN-STM-0002	3.00	1.66
GHN-STM-0003	2.88	4.06
GHN-STM-0004	8.80	0.00
GHN-STM-0005	5.40	0.00
GHN-VTM-0194	2.42	29.74
GHN-VTM-0195	3.53	0.24
GHN-VTM-0197	6.62	0.00
GHN-VTM-0198	6.11	0.00
GHN-VTM-0199	6.42	0.00
GHN-VTM-0200	4.88	0.00
GHN-VTM-0201	3.25	2.37
GHN-VTM-0202	3.63	0.00
GHN-VTM-0203	5.96	0.00
GHN-VTM-0204	5.53	0.00
GHN-VTM-0205	4.92	0.00
GHN-VTM-0206	6.26	0.00
GHN-VTM-0207	6.54	0.00
GHN-VTM-0208	7.68	0.00
GHN-VTM-0209	7.05	0.00
GHN-VTM-0210	5.54	0.00
GHN-VTM-0211	8.90	0.00
GHN-VTM-0212	8.65	0.00
GHN-VTM-0213	8.94	0.00
GHN-VTM-0214	8.48	0.00
GHN-VTM-0215	7.89	0.00
GHN-VTM-0216	9.29	0.00
GHN-VTM-0217	8.68	0.00
GHN-VTM-0375	7.65	0.00
GHN-VTM-0377	7.96	0.00
GHN-VTM-0378	8.26	0.00
GHN-VTM-0379	4.19	0.06
GHN-VTM-0380	6.06	0.00
GHN-VTM-0381	5.70	0.00
GHN-VTM-0382	4.22	0.00
GHN-VTM-0383	5.08	0.00
GHN-VTM-0384	3.64	0.04
GHN-VTM-0385	4.85	0.00
GHN-VTM-0386	2.96	2.56
GHN-VTM-0387	3.08	3.37
GHN-VTM-0394	6.00	0.00
GHN-VTM-0395	4.31	0.00
GHN-VTM-0396	5.92	0.00
GHN-VTM-0398	2.43	14.77
GHN-VTM-0399	2.58	9.67
GHN-VTM-0417	2.03	22.71
GHN-VTM-0418	2.05	25.89

Table C3 continued.

Sample ID	NAG pH_2	$NAG_{4.5}$ (kg $CaCO_3$/t)
GHN-VTM-0419	2.16	23.67
GHN-VTM-0420	2.76	2.76
GHN-VTM-0421	4.08	0.14
GHN-VTM-0422	4.47	0.00
GHN-VTM-0423	4.44	0.00
GHN-VTM-0424	4.27	0.00
GHN-VTM-0425	3.48	1.44
GHN-VTM-0426	6.25	0.00
GHN-VTM-0450	7.18	0.00
GHN-VTM-0451	5.84	0.00
GHN-VTM-0452	3.59	0.83
GHN-VTM-0453	8.49	0.00
GHN-VTM-0454	3.33	2.33
GHN-VTM-0455	8.30	0.00
GHN-VTM-0556	2.42	13.44
GHN-VTM-0557	2.84	4.66
GHN-VTM-0558	2.58	9.60
GHN-VTM-0559	2.88	5.09
GHN-VTM-0560	3.66	0.49
GHN-VTM-0561	5.81	0.00
GHN-VTM-0562	6.35	0.00
GHN-VTM-0563	3.30	1.58
GHN-VTM-0564	2.76	3.57
GHN-VTM-0565	3.48	0.51
GHN-VTM-0566	3.73	0.10
GHN-VTM-0567	3.38	1.96
GHN-VTM-0568	2.73	4.07
GHN-VTM-0569	2.73	7.81
GHN-VTM-0570	2.95	5.77
GHN-VTM-0571	3.35	2.00
GHN-VTM-0572	3.23	1.96
GHN-VTM-0573	2.29	22.42
GHN-VTM-0574	3.09	2.40
GHN-VTM-0575	2.69	8.31
GHN-VTM-0598	2.44	9.83
GHN-VTM-0602	7.89	0.00
GHN-VTM-0603	3.63	1.03
GHN-VTM-0606	3.86	0.00
GHN-VTM-0612	8.77	0.00
GHN-VTM-0614	6.33	0.00
GHN-VTM-0624	3.45	1.23

Table C4: Part 1 of concentrations (in percentage) of major metal oxides, sulfur, fluorine and loss on ignition (LOI). BD = below detection limit.

Sample ID	SiO_2	TiO_2	Al_2O_3	Fe_2O_3T	FeOT	FeO	Fe_2O_3	MnO	MgO
GHN-EHP-0001	67.14	0.47	13.71	3.62	3.29	1.78	1.66	0.11	1.23
GHN-JRM-0001	61.64	0.53	13.65	5.24	4.76	2.86	2.09	0.08	1.28
GHN-JRM-0039	66.64	0.60	15.10	2.58	2.34	1.03	1.45	0.02	0.50
GHN-KMD-0013	63.68	0.60	14.59	6.23	BD	3.48	2.40	0.07	1.46
GHN-KMD-0014	61.05	0.82	14.79	5.10	BD	2.72	2.11	0.22	2.74
GHN-KMD-0015	63.83	0.70	14.36	5.72	BD	3.15	2.25	0.37	2.05
GHN-KMD-0016	61.88	0.79	14.44	5.51	BD	3.00	2.21	0.31	2.83
GHN-KMD-0017	61.34	0.61	14.37	6.03	BD	3.35	2.35	0.08	1.51
GHN-KMD-0018	70.45	0.36	12.95	3.48	BD	1.73	1.58	0.22	1.23
GHN-KMD-0019	61.78	0.81	14.94	5.35	BD	2.88	2.18	0.32	3.14
GHN-KMD-0026	69.83	0.32	12.81	3.86	3.52	1.98	1.68	0.15	0.76
GHN-KMD-0027	68.03	0.43	12.93	4.57	4.15	2.45	1.88	0.21	1.05
GHN-KMD-0051	67.83	0.59	14.44	4.32	BD	2.22	1.88	0.29	1.80
GHN-KMD-0052	61.82	0.60	14.16	5.34	4.85	2.90	2.15	0.37	2.23
GHN-KMD-0053	70.62	0.33	12.82	3.73	BD	1.90	1.64	0.30	0.91
GHN-KMD-0054	62.74	0.73	14.19	5.21	4.74	2.82	2.11	0.24	2.33
GHN-KMD-0055	71.86	0.27	12.19	3.49	3.17	1.77	1.54	0.06	0.63
GHN-KMD-0056	68.34	0.59	14.53	4.31	BD	2.20	1.89	0.22	1.64
GHN-KMD-0065	66.82	0.66	14.69	6.12	BD	3.40	2.38	0.52	2.15
GHN-KMD-0071	67.81	0.49	14.77	3.85	BD	1.89	1.77	0.13	1.35
GHN-KMD-0072	63.63	0.65	14.26	5.25	4.77	2.84	2.13	0.40	2.25
GHN-KMD-0073	62.63	0.72	14.38	5.14	BD	2.76	2.10	0.34	2.65
GHN-KMD-0074	65.16	0.71	14.68	5.70	BD	3.12	2.27	0.33	2.26
GHN-KMD-0079	67.58	0.55	14.22	4.56	BD	2.38	1.94	0.23	1.49
GHN-KMD-0081	66.80	0.43	14.17	3.82	3.47	1.90	1.73	0.13	1.32
GHN-KMD-0082	60.30	0.74	14.32	5.31	4.83	2.88	2.14	0.64	2.74
GHN-KMD-0088	64.35	0.49	14.19	4.19	3.81	2.14	1.84	0.16	1.51
GHN-LFG-0037	61.32	0.50	13.88	5.10	4.64	2.76	2.06	0.28	1.87
GHN-LFG-0085	62.66	0.69	14.68	6.13	BD	3.41	2.38	0.28	2.48
GHN-LFG-0088	61.25	0.77	14.44	5.04	BD	2.69	2.08	0.30	2.77
GHN-STM-0001	71.09	0.47	13.03	3.63	BD	1.82	1.63	0.09	1.09
GHN-STM-0002	75.91	0.18	12.06	1.64	BD	0.55	1.04	0.03	0.40
GHN-STM-0003	75.97	0.19	12.05	2.07	BD	0.83	1.16	0.02	0.38
GHN-STM-0004	68.83	0.29	12.04	3.17	BD	1.56	1.45	0.10	0.82
GHN-STM-0005	75.43	0.15	11.63	2.15	BD	0.90	1.16	0.06	0.28
GHN-VTM-0194	61.99	0.55	13.18	5.09	4.81	2.78	2.03	0.13	1.51
GHN-VTM-0195	62.50	0.60	13.42	5.66	5.10	3.15	2.20	0.23	2.16
GHN-VTM-0196	59.70	0.80	14.09	7.43	6.69	4.29	2.71	0.47	2.44
GHN-VTM-0197	61.22	0.71	14.47	5.43	4.91	2.95	2.18	0.37	2.44
GHN-VTM-0198	66.79	0.43	13.39	4.50	4.09	2.38	1.88	0.28	1.22
GHN-VTM-0199	67.28	0.43	13.37	4.74	4.31	2.54	1.95	0.28	1.23
GHN-VTM-0200	71.77	0.28	14.04	3.18	2.72	1.48	1.55	0.15	0.54
GHN-VTM-0201	64.84	0.44	13.72	4.90	4.45	2.63	2.01	0.20	1.34
GHN-VTM-0202	65.92	0.51	13.30	5.29	4.64	2.91	2.09	0.24	1.56
GHN-VTM-0203	66.12	0.49	13.21	5.28	4.70	2.91	2.08	0.37	1.42
GHN-VTM-0204	60.17	0.72	14.77	6.72	6.11	3.79	2.55	0.59	2.28

Table C4 continued.

Sample ID	SiO_2	TiO_2	Al_2O_3	Fe_2O_3T	FeOT	FeO	Fe_2O_3	MnO	MgO
GHN-VTM-0205	62.20	0.67	14.25	7.30	6.49	4.20	2.68	0.38	1.90
GHN-VTM-0206	62.13	0.71	14.64	6.82	6.18	3.86	2.57	0.85	2.13
GHN-VTM-0207	65.97	0.55	13.84	5.36	4.79	2.93	2.14	0.57	1.58
GHN-VTM-0208	67.14	0.72	14.56	5.19	BD	2.79	2.12	0.29	2.48
GHN-VTM-0209	64.37	0.72	14.41	5.53	4.90	3.02	2.21	0.43	2.30
GHN-VTM-0210	64.40	0.70	14.26	5.18	4.60	2.79	2.11	0.45	2.14
GHN-VTM-0211	62.37	0.73	14.65	5.15	4.56	2.76	2.11	0.37	2.60
GHN-VTM-0212	63.65	0.73	14.56	5.36	4.86	2.90	2.17	0.47	2.62
GHN-VTM-0213	62.95	0.73	14.66	5.30	4.82	2.86	2.15	0.47	2.45
GHN-VTM-0214	62.57	0.80	15.24	5.66	5.16	3.07	2.28	0.41	2.73
GHN-VTM-0215	63.84	0.73	14.46	5.55	5.11	3.03	2.22	0.57	2.39
GHN-VTM-0216	62.94	0.74	14.52	5.32	4.85	2.88	2.15	0.44	2.53
GHN-VTM-0217	69.51	0.41	12.92	4.07	3.67	2.12	1.74	0.16	0.94
GHN-VTM-0417	72.57	0.31	12.17	3.91	BD	2.05	1.66	0.06	0.76
GHN-VTM-0418	71.17	0.37	13.17	3.52	BD	1.74	1.61	0.05	0.75
GHN-VTM-0419	63.99	0.54	14.33	6.43	BD	3.62	2.45	0.09	1.29
GHN-VTM-0420	58.12	0.84	14.38	9.91	BD	5.93	3.39	0.50	2.97
GHN-VTM-0421	63.38	0.73	14.42	6.39	BD	3.59	2.44	0.34	2.22
GHN-VTM-0422	75.18	0.55	15.38	5.57	BD	3.00	2.27	0.33	1.63
GHN-VTM-0423	68.03	0.51	13.36	4.94	BD	2.68	1.99	0.25	1.62
GHN-VTM-0424	70.87	0.29	12.57	4.13	BD	2.17	1.74	0.16	0.73
GHN-VTM-0425	63.01	0.60	15.50	5.29	BD	2.81	2.20	0.32	2.06
GHN-VTM-0426	61.95	0.75	15.06	6.00	BD	3.30	2.37	0.77	2.41
GHN-VTM-0450	63.45	0.77	14.62	6.38	BD	3.57	2.45	0.36	2.60
GHN-VTM-0451	61.69	0.74	14.62	5.15	BD	2.76	2.11	0.41	2.42
GHN-VTM-0452	63.39	0.65	14.13	5.34	BD	2.91	2.14	0.28	2.07
GHN-VTM-0453	59.80	0.71	14.49	6.18	5.47	3.45	2.38	0.46	2.57
GHN-VTM-0454	64.87	0.48	15.32	4.11	BD	2.04	1.87	0.19	1.61
GHN-VTM-0455	67.69	0.56	13.73	4.00	BD	2.04	1.76	0.17	1.94
GHN-VTM-0598	77.46	0.23	12.60	1.92	BD	0.71	1.14	0.05	0.54
GHN-VTM-0602	55.65	0.62	18.20	6.63	BD	3.58	2.69	0.25	2.03
GHN-VTM-0603	61.31	0.68	15.99	5.33	4.74	2.82	2.23	0.10	1.75
GHN-VTM-0605	67.75	0.62	14.77	4.97	BD	2.63	2.08	0.12	1.57
GHN-VTM-0606	71.25	0.35	12.09	3.63	3.27	1.86	1.58	0.06	0.67
GHN-VTM-0607	68.88	0.50	14.32	4.05	BD	2.04	1.81	0.16	1.21
GHN-VTM-0612	58.55	0.44	13.70	2.58	2.25	1.09	1.38	0.25	1.60
GHN-VTM-0614	63.72	0.71	18.09	4.14	BD	1.93	2.02	0.05	1.23
GHN-VTM-0624	62.55	0.68	15.68	4.93	BD	2.56	2.11	0.08	1.56

Table C5: Part 2 of concentrations (in percentage) of major metal oxides, sulfur, fluorine and loss on ignition (LOI). BD = below detection limit.

Sample ID	CaO	Na_2O	K_2O	P_2O_5	S	F	LOI	Total
GHN-EHP-0001	0.81	2.22	3.97	0.19	BD	BD	4.55	104.75
GHN-JRM-0001	0.98	1.87	3.91	0.19	0.00	BD	8.81	107.89
GHN-JRM-0039	0.08	0.15	3.65	0.23	BD	BD	6.28	100.65
GHN-KMD-0013	1.17	2.42	3.68	0.23	0.24	0.0112	4.81	99.19
GHN-KMD-0014	3.12	3.31	4.65	0.29	0.08	0.0081	2.34	98.52
GHN-KMD-0015	1.38	2.49	4.07	0.25	0.18	0.0138	3.70	99.11
GHN-KMD-0016	2.97	3.36	3.12	0.29	0.13	0.0099	3.42	99.06
GHN-KMD-0017	1.15	2.50	3.49	0.23	3.06	0.0151	7.40	101.79
GHN-KMD-0018	0.81	1.29	4.81	0.08	0.80	0.0122	4.20	100.69
GHN-KMD-0019	3.59	3.48	2.92	0.26	0.00	0.0103	4.30	100.90
GHN-KMD-0026	0.50	2.59	4.26	0.13	0.17	0.0075	3.53	98.92
GHN-KMD-0027	0.56	2.03	4.15	0.19	0.00	0.0000	4.48	98.63
GHN-KMD-0051	1.94	3.22	3.96	0.16	0.00	0.0071	2.72	101.28
GHN-KMD-0052	2.32	2.48	3.44	0.27	0.00	0.0000	4.49	97.52
GHN-KMD-0053	0.53	1.78	4.54	0.06	0.00	0.0096	3.65	99.28
GHN-KMD-0054	2.19	2.70	3.64	0.32	0.00	0.0000	4.20	98.49
GHN-KMD-0055	0.76	0.38	3.88	0.10	0.00	0.0000	5.04	98.66
GHN-KMD-0056	1.21	3.21	3.80	0.16	0.00	0.0088	3.09	101.11
GHN-KMD-0065	1.29	2.76	3.73	0.20	0.11	0.0121	3.59	102.65
GHN-KMD-0071	1.28	3.10	3.75	0.13	0.29	0.0127	3.35	100.31
GHN-KMD-0072	2.10	3.09	3.57	0.29	0.00	0.0000	3.60	99.09
GHN-KMD-0073	2.28	3.33	3.37	0.26	0.04	0.0093	3.17	98.32
GHN-KMD-0074	1.66	2.86	3.53	0.22	0.16	0.0091	3.23	100.51
GHN-KMD-0079	1.26	2.80	3.82	0.16	0.12	0.0113	3.21	100.01
GHN-KMD-0081	1.11	2.79	3.87	0.19	0.13	0.0087	3.16	97.93
GHN-KMD-0082	2.74	3.46	3.05	0.34	0.00	0.0000	4.60	98.24
GHN-KMD-0088	1.13	2.92	3.80	0.21	0.00	0.0000	5.14	98.09
GHN-LFG-0037	1.39	2.05	3.57	0.24	0.00	0.0000	5.50	95.70
GHN-LFG-0085	2.08	2.62	3.56	0.24	0.37	0.0109	4.94	100.74
GHN-LFG-0088	2.96	3.31	3.41	0.27	0.14	0.0084	6.03	100.70
GHN-STM-0001	0.82	1.64	3.72	0.11	1.45	0.0139	4.30	101.45
GHN-STM-0002	0.22	0.82	5.06	0.00	0.26	0.0084	2.96	99.55
GHN-STM-0003	0.06	1.38	5.21	0.00	0.28	0.0078	2.72	100.34
GHN-STM-0004	2.32	1.80	4.36	0.06	2.14	0.0085	4.22	100.16
GHN-STM-0005	0.10	1.90	5.05	0.00	0.17	0.0059	2.06	98.99
GHN-VTM-0194	1.27	2.28	3.52	0.27	3.05	0.0151	8.05	100.91
GHN-VTM-0195	1.43	2.22	3.93	0.29	0.00	0.0097	5.23	97.68
GHN-VTM-0196	0.98	2.46	3.48	0.34	0.00	0.0000	5.71	97.90
GHN-VTM-0197	2.17	2.57	3.59	0.27	0.54	0.0104	5.35	99.14
GHN-VTM-0198	0.90	2.20	4.34	0.18	0.27	0.0103	4.01	98.52
GHN-VTM-0199	0.89	2.06	4.02	0.19	0.19	0.0108	4.11	98.80
GHN-VTM-0200	0.33	2.45	4.81	0.07	0.20	0.0077	2.68	100.51
GHN-VTM-0201	0.66	2.02	4.02	0.21	0.62	0.0111	5.06	98.04
GHN-VTM-0202	1.25	2.17	3.84	0.19	0.51	0.0097	4.47	99.26
GHN-VTM-0203	0.95	1.82	4.31	0.19	0.44	0.0116	4.43	99.04
GHN-VTM-0204	1.04	2.33	3.54	0.34	0.32	0.0131	5.47	98.30

Table C5 continued.

Sample ID	CaO	Na_2O	K_2O	P_2O_5	S	F	LOI	Total
GHN-VTM-0205	0.50	2.26	3.30	0.26	0.32	0.0144	5.59	98.94
GHN-VTM-0206	0.95	2.86	3.33	0.29	0.21	0.0132	4.88	99.81
GHN-VTM-0207	0.64	2.59	3.90	0.22	0.16	0.0096	4.12	99.51
GHN-VTM-0208	2.74	3.52	3.68	0.25	0.22	0.0100	2.87	103.67
GHN-VTM-0209	2.31	3.42	3.34	0.29	0.00	0.0103	3.23	100.36
GHN-VTM-0210	2.11	3.32	3.54	0.27	0.16	BD	3.30	109.33
GHN-VTM-0211	3.00	3.48	3.27	0.30	0.00	0.0089	3.54	99.47
GHN-VTM-0212	2.74	3.29	3.32	0.30	0.00	0.0107	3.34	100.39
GHN-VTM-0213	2.45	3.18	3.57	0.30	0.00	0.0091	3.70	99.77
GHN-VTM-0214	2.77	3.75	3.11	0.31	0.00	0.0084	3.69	101.05
GHN-VTM-0215	2.07	3.20	3.29	0.29	0.00	0.0078	3.60	100.00
GHN-VTM-0216	2.53	3.44	3.33	0.30	0.00	0.0106	3.52	99.62
GHN-VTM-0217	1.32	2.43	4.32	0.16	0.00	0.0079	2.52	98.77
GHN-VTM-0417	0.67	0.26	4.22	0.03	0.00	0.0126	5.01	99.98
GHN-VTM-0418	0.64	0.56	4.22	0.02	0.00	0.0149	5.25	99.73
GHN-VTM-0419	1.38	1.74	3.85	0.16	0.00	0.0175	6.40	100.22
GHN-VTM-0420	1.50	2.35	3.23	0.30	0.00	0.0131	6.09	100.20
GHN-VTM-0421	1.46	2.89	3.63	0.25	0.00	0.0095	4.43	100.15
GHN-VTM-0422	0.97	2.36	4.53	0.15	0.00	0.0106	4.25	110.91
GHN-VTM-0423	0.81	2.16	4.44	0.14	0.36	0.0098	3.59	100.22
GHN-VTM-0424	0.35	1.63	4.49	0.06	0.36	0.0106	4.32	99.97
GHN-VTM-0425	2.00	2.73	3.51	0.19	0.89	0.0170	5.03	101.15
GHN-VTM-0426	1.57	3.20	3.34	0.26	0.25	0.0124	4.82	100.39
GHN-VTM-0450	1.68	3.27	3.30	0.25	0.19	0.0091	3.19	100.07
GHN-VTM-0451	1.84	3.75	3.20	0.26	0.59	0.0101	3.82	98.50
GHN-VTM-0452	1.46	3.08	3.32	0.21	0.51	0.0093	4.05	98.50
GHN-VTM-0453	2.26	2.61	3.53	0.29	1.46	0.0134	5.13	99.50
GHN-VTM-0454	1.46	2.68	3.68	0.13	0.96	0.0953	4.90	100.49
GHN-VTM-0455	1.93	3.25	3.53	0.16	0.00	0.0079	2.33	99.30
GHN-VTM-0598	0.22	0.23	3.73	0.01	0.00	0.0117	4.10	101.10
GHN-VTM-0602	2.21	0.72	4.22	0.18	0.00	0.0153	8.28	99.01
GHN-VTM-0603	0.77	0.93	3.64	0.15	0.00	0.0113	8.37	99.03
GHN-VTM-0605	0.68	0.93	3.55	0.17	0.00	0.0147	5.66	100.80
GHN-VTM-0606	0.31	1.09	4.27	0.16	0.00	0.0075	5.32	99.21
GHN-VTM-0607	0.57	1.45	3.81	0.14	0.00	0.0112	5.25	100.35
GHN-VTM-0612	3.76	1.37	3.72	0.12	0.00	0.0122	7.67	93.77
GHN-VTM-0614	4.11	0.21	5.36	0.06	0.00	0.0101	9.28	106.97
GHN-VTM-0624	0.60	0.77	3.61	0.21	0.00	0.0107	8.36	99.04

Table C6: Part 1 of concentrations of trace metals in parts per million (ppm). BD = below detection limit.

Sample ID	Ba	Rb	Sr	Pb	Th	U	Zr	Nb	Y
GHN-EHP-0001	794.3	129.5	223	59.9	11.6	5	190.8	20.1	28.7
GHN-JRM-0001	832	134	136	153	11	5	163	16	25
GHN-JRM-0039	1060	97	739	72	14	4	211	14	42
GHN-KMD-0013	1015	99	367	158.5	9.82	3.59	176	17	27.4
GHN-KMD-0014	1629	93	719	67	6.68	0.37	182	14	17.3
GHN-KMD-0015	1564	102	421	117.4	10.34	1.65	160	14	20.7
GHN-KMD-0016	1174	76	579	186.2	7.82	2.52	164	15	16.3
GHN-KMD-0017	1186	118	183	125.2	13.39	3.98	132	13	15.3
GHN-KMD-0018	712	149	197	154	10.45	4.31	240	32	38
GHN-KMD-0019	1065	73	668	154	8	3	182	13	17
GHN-KMD-0026	609	127	191	81	13	5	242	26	49
GHN-KMD-0027	726	130	221	103	13	4	238	24	40
GHN-KMD-0051	963	99	436	150.5	9.02	3.22	204	23	33.5
GHN-KMD-0052	1217	106	386	99	9	4	170	12	20
GHN-KMD-0053	583	136	165	67.1	15.87	4.31	264	33	56.4
GHN-KMD-0054	1180	98	496	242	9	4	181	14	23
GHN-KMD-0055	237.9	127.4	50.5	101.7	14.8	4	255.4	26.2	50.5
GHN-KMD-0056	935	100	324	102	9.64	3.88	206	23	28.1
GHN-KMD-0065	1124	99	376	121.8	9.9	2.91	194	20	35.6
GHN-KMD-0071	1102	101	399	132.2	9.61	5.66	185	19	33
GHN-KMD-0072	1036.9	89.6	475	89.6	10.9	2	198	16.5	35.5
GHN-KMD-0073	1338	88	549	175.9	7.45	1.47	151	13	15.3
GHN-KMD-0074	1180	88	412	112.9	8.79	3.47	180	18	25.7
GHN-KMD-0079	1027	109	305	52.4	12.81	2.62	215	22	30.7
GHN-KMD-0081	813.2	105	339	129	11	4.75	208	21	42.5
GHN-KMD-0082	1139	74	552	239	9	3	179	12	31
GHN-KMD-0088	1216	102	374	60	7	4	176	13	25.6
GHN-LFG-0037	1066	121	286	53	7	4	172	12	25
GHN-LFG-0085	1279	BD	BD	BD	BD	BD	BD	BD	BD
GHN-LFG-0088	1161	BD	BD	BD	BD	BD	BD	BD	BD
GHN-STM-0001	1013	138	141	161.8	7.2	2.29	173	18	20.1
GHN-STM-0002	222	163	54	96.9	10.46	6.15	302	42	50.6
GHN-STM-0003	223	163	62	67.3	10.62	5.02	296	39	47.2
GHN-STM-0004	551	131	165	125.2	8.59	4.34	230	31	39
GHN-STM-0005	142	143	65	43.5	10.85	5.33	303	41	50
GHN-VTM-0194	778	112	161	93	12	4	149	12	17
GHN-VTM-0195	1030	112	401	115	10	3	202.5	16.6	25.5
GHN-VTM-0196	1278	104	359	93	10	1	177	13	20.5
GHN-VTM-0197	1057	98	411	79	8	3	184	14	30
GHN-VTM-0198	712	129	275	100	13	4	236	24	45
GHN-VTM-0199	853	128	246	145	13	3	216	21	43
GHN-VTM-0200	429	138	117	68	14	5	255	29	52
GHN-VTM-0201	953	126	229	85	11	5	198	18	37
GHN-VTM-0202	858	122	279	134	11	4	206	19	32
GHN-VTM-0203	927	144	221	163	12	2	205	18	31
GHN-VTM-0204	1245	111	351	198	12	4	175	13	24

Table C6 continued.

Sample ID	Ba	Rb	Sr	Pb	Th	U	Zr	Nb	Y
GHN-VTM-0205	1031	107	259	236	10	5	178	15	28
GHN-VTM-0206	1125	100	380	115	10	3	184	13	30
GHN-VTM-0207	938	106	291	160	12	4	209	19	38
GHN-VTM-0208	1294	BD	BD	BD	BD	BD	BD	BD	BD
GHN-VTM-0209	1117	84	553	128	9	4	187	14	43
GHN-VTM-0210	1118	88	544	133	9	4	187	15	46
GHN-VTM-0211	1173	83	619	180	9	4	180	12	22
GHN-VTM-0212	1137	85	600	153	8	2	178	12	24
GHN-VTM-0213	1206	86	588	141	9	3	175	12	28
GHN-VTM-0214	1123	73	653	88	9	3	187	13	25
GHN-VTM-0215	1148	79	538	106	9	1	183	13	28
GHN-VTM-0216	1091	79	565	241	9	2	183	13	44
GHN-VTM-0217	705	127	278	60.5	11	5	234.5	24	44
GHN-VTM-0417	501	BD	BD	BD	BD	BD	BD	BD	BD
GHN-VTM-0418	641	BD	BD	BD	BD	BD	BD	BD	BD
GHN-VTM-0419	728	BD	BD	BD	BD	BD	BD	BD	BD
GHN-VTM-0420	1092	BD	BD	BD	BD	BD	BD	BD	BD
GHN-VTM-0421	1198	BD	BD	BD	BD	BD	BD	BD	BD
GHN-VTM-0422	935	BD	BD	BD	BD	BD	BD	BD	BD
GHN-VTM-0423	866	BD	BD	BD	BD	BD	BD	BD	BD
GHN-VTM-0424	599	BD	BD	BD	BD	BD	BD	BD	BD
GHN-VTM-0425	1206	BD	BD	BD	BD	BD	BD	BD	BD
GHN-VTM-0426	1140	BD	BD	BD	BD	BD	BD	BD	BD
GHN-VTM-0450	1229	81	456	103.9	7.97	1.43	381	16	19.7
GHN-VTM-0451	1229	75	468	209	7.18	3	169	16	28.7
GHN-VTM-0452	1169	83	404	125.6	9.25	1.97	168	16	28.9
GHN-VTM-0453	1333	96	393	108	8	3	173	12	51
GHN-VTM-0454	969	99	317	182.5	9.66	5.85	178	20	38.9
GHN-VTM-0455	934	93	466	70	8.48	4.47	223	23	45.2
GHN-VTM-0598	192	BD	BD	BD	BD	BD	BD	BD	BD
GHN-VTM-0602	1009	BD	BD	BD	BD	BD	BD	BD	BD
GHN-VTM-0603	1008	98	150	56	7	2	180	10	26
GHN-VTM-0605	691	BD	BD	BD	BD	BD	BD	BD	BD
GHN-VTM-0606	426	143	110.5	106	12	6	303	26.5	41
GHN-VTM-0607	992	134	158	231	11	3	198	18	45.5
GHN-VTM-0612	770	87	165	37	12	6	195	22	31
GHN-VTM-0614	1276	112	184	9	6	3	131	7	18
GHN-VTM-0624	797	87	101	63	7	3	168	10	26

Table C7: Part 2 of concentrations of trace metals in parts per million (ppm). BD = below detection limit.

Sample ID	Sc	V	Ni	Cu	Zn	Ga	Cr	Co
GHN-EHP-0001	6.4	55	26.6	26.7	162	20.1	37	BD
GHN-JRM-0001	9	74	30	172	92	21	57	BD
GHN-JRM-0039	9	80	12	23	40	21	53	BD
GHN-KMD-0013	BD	110	21	133	486	37.3	92	50
GHN-KMD-0014	BD	102	39	19	438	34.4	111	46
GHN-KMD-0015	BD	106	25	95	387	31.7	116	39
GHN-KMD-0016	BD	126	49	59	451	35.1	88	39
GHN-KMD-0017	9.5	116	4	92	109	21.2	86	32
GHN-KMD-0018	BD	51	0	105	502	39	76	58
GHN-KMD-0019	10	91	59	54	320	20	81	BD
GHN-KMD-0026	4	36	19	40	180	23	27	BD
GHN-KMD-0027	5	42	25	78	160	23	36	BD
GHN-KMD-0051	BD	80	14	54	403	33.8	78	47
GHN-KMD-0052	8	76	38	87	357	19	55	BD
GHN-KMD-0053	BD	42	0	86	416	37.1	34	46
GHN-KMD-0054	9	87	48	61	374	20	71	BD
GHN-KMD-0055	3.9	37	18	146.1	137.2	19	23.7	BD
GHN-KMD-0056	BD	83	5	50	253	27.8	79	45
GHN-KMD-0065	BD	87	46	190	552	40.7	79	37
GHN-KMD-0071	BD	73	0	35	256	26.8	64	40
GHN-KMD-0072	8.3	67	49.6	69.3	486.9	20.7	60.6	BD
GHN-KMD-0073	9.7	106	44	61	426	33.5	100	40
GHN-KMD-0074	BD	92	22	135	378	32.2	92	50
GHN-KMD-0079	BD	75	2	67	256	28.2	61	45
GHN-KMD-0081	5.8	61	25	43	238	25	48	30
GHN-KMD-0082	10	84	82	96	1117.5	20	74	BD
GHN-KMD-0088	6	60	31	40	221	20	47	BD
GHN-LFG-0037	8	68	30	41	231	19	49	BD
GHN-LFG-0085	BD	BD	BD	BD	BD	BD	BD	BD
GHN-LFG-0088	BD	BD	BD	BD	BD	BD	BD	BD
GHN-STM-0001	BD	82	0	27	104	20.2	86	76
GHN-STM-0002	BD	7	0	32	47	20.7	23	102
GHN-STM-0003	BD	14	0	27	36	20.6	30	105
GHN-STM-0004	BD	38	0	18	92	20.3	40	99
GHN-STM-0005	BD	5	0	12	75	21.8	43	62
GHN-VTM-0194	9	77	25	56	108	20	52	BD
GHN-VTM-0195	7.5	70	42	102	392	20	62	BD
GHN-VTM-0196	10.5	94	59	158.5	536.3	19	82	BD
GHN-VTM-0197	9	75	50	102	515	20	61	BD
GHN-VTM-0198	5	50	28	102	303	22	39	BD
GHN-VTM-0199	6	55	29	91	350	21	42	BD
GHN-VTM-0200	3	22	14	40	113	25	21	BD
GHN-VTM-0201	6	61	23	95	245	22	44	BD
GHN-VTM-0202	6	66	32	76	288	21	47	BD
GHN-VTM-0203	6	31	31	76	294	21	47	BD
GHN-VTM-0204	9	82	51	139	497	21	71	BD

Table C7 continued.

Sample ID	Sc	V	Ni	Cu	Zn	Ga	Cr	Co
GHN-VTM-0205	7	81	38	173	392	20	62	BD
GHN-VTM-0206	10	82	58	180	571	20	64	BD
GHN-VTM-0207	6	60	40	116	449	22	48	BD
GHN-VTM-0208	BD	BD	BD	BD	BD	BD	BD	BD
GHN-VTM-0209	9	91	59	127	724	21	62	BD
GHN-VTM-0210	9	82	60	99	798	19	60	BD
GHN-VTM-0211	9	84	54	68	462	19	69	BD
GHN-VTM-0212	9	90	63	112	700	20	71	BD
GHN-VTM-0213	9	78	58	78	588	20	65	BD
GHN-VTM-0214	9	91	61	71	468	21	73	BD
GHN-VTM-0215	9	79	57	121	560	20	65	BD
GHN-VTM-0216	10	82	67	183	1033	20	63	BD
GHN-VTM-0217	5	48	25.5	34	184	22	34	BD
GHN-VTM-0417	BD	BD	BD	BD	BD	BD	BD	BD
GHN-VTM-0418	BD	BD	BD	BD	BD	BD	BD	BD
GHN-VTM-0419	BD	BD	BD	BD	BD	BD	BD	BD
GHN-VTM-0420	BD	BD	BD	BD	BD	BD	BD	BD
GHN-VTM-0421	BD	BD	BD	BD	BD	BD	BD	BD
GHN-VTM-0422	BD	BD	BD	BD	BD	BD	BD	BD
GHN-VTM-0423	BD	BD	BD	BD	BD	BD	BD	BD
GHN-VTM-0424	BD	BD	BD	BD	BD	BD	BD	BD
GHN-VTM-0425	BD	BD	BD	BD	BD	BD	BD	BD
GHN-VTM-0426	BD	BD	BD	BD	BD	BD	BD	BD
GHN-VTM-0450	BD	115	35	102	381	32.2	89	42
GHN-VTM-0451	BD	99	16	159	1066	62.2	87	84
GHN-VTM-0452	BD	109	0	80	500	37.6	80	75
GHN-VTM-0453	8	76	72	156	1067	18	63	BD
GHN-VTM-0454	BD	82	0	121	551	40.5	66	105
GHN-VTM-0455	BD	77	2	45	444	35.9	76	55
GHN-VTM-0598	BD	BD	BD	BD	BD	BD	BD	BD
GHN-VTM-0602	BD	BD	BD	BD	BD	BD	BD	BD
GHN-VTM-0603	12	94	32	79	224	20	49	BD
GHN-VTM-0605	BD	BD	BD	BD	BD	BD	BD	BD
GHN-VTM-0606	4	39	15	36	94	22	25	BD
GHN-VTM-0607	7	65	21	30	129	21	40	BD
GHN-VTM-0612	4	36	24	12	634	16	8	BD
GHN-VTM-0614	11	97	12	9	71	18	36	BD
GHN-VTM-0624	9	85	35	34	266	18	42	BD

Table C8: Part 1 of modal mineralogy results. Qtz = quartz, Kfs = K-feldspar, Plg = plagioclase, Epi = epidote, Cal = calcite, Pyr = pyrite, Fe/Mn/Ti_Ox = oxides of Fe, Mn and Ti, Goe = goethite; TR = trace amounts, ND = not determined.

Sample ID	Qtz	Kfs	Plg	Epi	Cal	Pyr	Fe/Mn/Ti_Ox	Goe
GHN-ACT-0001	59	18	11	0	0	0.22	1	0.01
GHN-ACT-0003	51	23	14	0	TR	0.38	1	0
GHN-ACT-0004	55	18	11	0	0	0.92	1	0
GHN-ACT-0011	38	23	18	5	TR	0.42	2	0.1
GHN-ACT-0012	33	20	16	9	2	0.63	3	0
GHN-ACT-0013	34	20	16	9	3	0.94	2	0.02
GHN-ACT-0019	43	18	11	6	0	1.06	2	0.09
GHN-ACT-0020	51	16	11	1	TR	0.74	2	0
GHN-ACT-0029	33	22	16	9	2	0.78	1	0
GHN-ACT-0030	33	20	17	9	TR	0.68	4	0.1
GHN-KMD-0013	40	15	11	4	0	0.67	8	0.17
GHN-KMD-0014	34	13	11	12	0	0.95	3	0
GHN-KMD-0015	33	14	11	11	0	0.65	6	0.16
GHN-KMD-0016	32	12	11	14	1	0.91	4	0.04
GHN-KMD-0017	44	6	5	2	0	2.87	0	0.01
GHN-KMD-0018	41	18	13	7	0	0.25	4	0.12
GHN-KMD-0019	26	15	13	16	2	0	3	ND
GHN-KMD-0026	50	16	11	2	1	0	2	ND
GHN-KMD-0027	43	16	11	5	1	0	4	ND
GHN-KMD-0051	39	14	10	9	2	0	5	ND
GHN-KMD-0053	47	17	12	5	TR	0	3	ND
GHN-KMD-0056	43	16	12	5	TR	0	3	ND
GHN-KMD-0065	41	17	13	3	0	0	10	ND
GHN-KMD-0071	40	17	12	7	TR	TR	3	ND
GHN-KMD-0073	36	14	12	10	2	TR	3	ND
GHN-KMD-0074	40	13	10	8	0	0	5	ND
GHN-KMD-0079	49	10	8	5	0	0	4	ND
GHN-KMD-0081	47	8	6	8	0	TR	3	ND
GHN-KMD-0082	37	13	11	12	0	0	7	ND
GHN-KMD-0096	66	8	5	0	0	0	2	ND
GHN-LFG-0085	49	20	12	1	TR	TR	2	ND
GHN-LFG-0086	36	15	12	8	TR	0	3	ND
GHN-LFG-0088	33	14	11	11	3	TR	4	ND
GHN-VTM-0194	59	6	5	1	0	2.51	1	0
GHN-VTM-0195	42	16	12	7	0	0.51	4	0.11
GHN-VTM-0196	35	17	13	9	0	0.59	5	0.3
GHN-VTM-0197	42	13	10	7	0	0.42	4	0.07
GHN-VTM-0198	44	13	9	6	0	0.33	5	0.09
GHN-VTM-0199	49	13	9	4	0	0.5	4	0.12
GHN-VTM-0200	45	14	9	3	1	0.38	8	0
GHN-VTM-0202	48	14	9	4	TR	TR	4	ND
GHN-VTM-0204	41	16	13	6	TR	0	4	ND
GHN-VTM-0205	44	11	9	5	2	0	6	ND
GHN-VTM-0206	37	16	13	5	TR	0	10	ND
GHN-VTM-0207	42	16	13	5	1	0	7	ND
GHN-VTM-0208	43	14	12	8	TR	0	2	ND

Table C8 continued.

Sample ID	Qtz	Kfs	Plg	Epi	Cal	Pyr	Fe/Mn/Ti_Ox	Goe
GHN-VTM-0209	41	15	12	8	1	0	4	ND
GHN-VTM-0211	41	14	12	7	2	0	4	ND
GHN-VTM-0212	38	16	14	9	TR	TR	4	ND
GHN-VTM-0213	34	16	13	10	3	0	5	ND
GHN-VTM-0214	35	17	14	8	3	0	5	ND
GHN-VTM-0215	35	15	13	9	2	0	8	ND
GHN-VTM-0216	37	14	12	8	3	0	5	ND
GHN-VTM-0217	48	16	11	2	1	0	3	ND
GHN-VTM-0398	54	8	5	6	0	TR	2	ND
GHN-VTM-0417	47	14	9	1	TR	2	10	ND
GHN-VTM-0418	58	8	5	0	TR	2	1	ND
GHN-VTM-0419	54	9	6	2	TR	3	3	ND
GHN-VTM-0420	33	16	13	8	2	1	5	ND
GHN-VTM-0421	33	18	15	9	TR	0	4	ND
GHN-VTM-0422	36	19	15	8	TR	0	4	ND
GHN-VTM-0423	36	18	14	7	TR	0	4	ND
GHN-VTM-0424	52	18	11	1	1	0	2	ND
GHN-VTM-0425	34	18	14	8	TR	1	3	ND
GHN-VTM-0426	32	16	13	10	0	0	7	ND
GHN-VTM-0450	33	18	14	9	2	0	5	ND
GHN-VTM-0451	35	17	14	9	0	0	2	ND
GHN-VTM-0452	35	17	13	9	2	1	2	ND
GHN-VTM-0453	43	6	5	10	4	2	1	ND
GHN-VTM-0454	45	13	10	6	1	TR	3	ND
GHN-VTM-0606	49	12	8	0	TR	TR	1	ND
GHN-VTM-0612	51	2	2	1	3	TR	4	ND
GHN-VTM-0614	45	1	1	0	0	0	0	ND
GHN-VTM-0624	25	14	12	5	TR	0	1	ND

Table C9: Part 2 of modal mineralogy results. Hem = hematite, Chl = chlorite, A_gy = authigenic gypsum, D_gy = detrital gypsum, Phl_bio = phlogopite and biotite, Clay = clay minerals, Kao = kaolinite, Ill_sme = illite and smectite, Cop = copiapite, Jar = jarosite, Sph = sphalerite; TR = trace amounts, ND = not determined.

Sample ID	Hem	Chl	A_gy	D_gy	Phl_bio	Clay	Kao	Ill_sme	Cop	Jar	Sph
GHN-ACT-0001	0.01	0	0	TR	TR	2	ND	9	0.01	0.09	0
GHN-ACT-0003	0	0	TR	1	TR	5	ND	5	0.01	0.08	0.01
GHN-ACT-0004	0	0	0	1	1	3	ND	9	0.02	0.08	0.03
GHN-ACT-0011	0.65	4	1	0	TR	6	ND	2	0.02	0.02	0
GHN-ACT-0012	0.42	8	TR	TR	0	6	ND	2	0.02	0.02	0
GHN-ACT-0013	0.02	8	TR	TR	0	4	ND	3	0.02	0.04	0
GHN-ACT-0019	0	4	TR	2	0	7	ND	6	0.01	0.06	0.04
GHN-ACT-0020	0	0	0	1	0	8	ND	9	0.01	0.33	0.02
GHN-ACT-0029	0.02	7	1	TR	0	7	ND	2	0.02	0.02	0
GHN-ACT-0030	0.06	5	1	TR	TR	8	ND	2	0.02	0.02	0
GHN-KMD-0013	0.3	4	2	3	TR	ND	1	9	0.17	0.01	0
GHN-KMD-0014	0.75	6	2	2	0	ND	1	9	0.19	0.01	0
GHN-KMD-0015	0.06	8	0.9	2.1	0	ND	2	9	0.15	0.01	0
GHN-KMD-0016	0.35	10	1	1	0	ND	1	10	0.11	0	0
GHN-KMD-0017	0.04	1	1	7	0	ND	2	27	0.06	0.08	0.01
GHN-KMD-0018	0.08	3	1	1	0	ND	1	11	0.07	0	0
GHN-KMD-0019	ND	12	2	1	0	7	ND	3	ND	ND	ND
GHN-KMD-0026	ND	0	2	2	0	5	ND	9	ND	ND	ND
GHN-KMD-0027	ND	3	1	1	0	8	ND	7	ND	ND	ND
GHN-KMD-0051	ND	6	TR	3	0	ND	1	9	ND	ND	ND
GHN-KMD-0053	ND	2	0.9	2.1	0	ND	1	10	ND	ND	ND
GHN-KMD-0056	ND	5	TR	2.55	0	ND	1	10	ND	ND	ND
GHN-KMD-0065	ND	5	1.75	3.25	TR	ND	0	4	ND	ND	ND
GHN-KMD-0071	ND	5	2	2	0	6	ND	6	ND	ND	ND
GHN-KMD-0073	ND	8	2.04	0.96	0	ND	1	9	ND	ND	ND
GHN-KMD-0074	ND	8	2	2	0	ND	0	9	ND	ND	ND
GHN-KMD-0079	ND	2	1.4	2.6	TR	ND	1	15	ND	ND	ND
GHN-KMD-0081	ND	5	3.78	2.22	0	ND	1	15	ND	ND	ND
GHN-KMD-0082	ND	8	1.29	1.71	TR	3	ND	6	ND	ND	ND
GHN-KMD-0096	ND	0	0.06	2.94	TR	0	ND	16	ND	ND	ND
GHN-LFG-0085	ND	2	1	1	0	6	ND	6	ND	ND	ND
GHN-LFG-0086	ND	7	4.75	TR	0	8	ND	5	ND	ND	ND
GHN-LFG-0088	ND	8	1.95	1.05	0	8	ND	5	ND	ND	ND
GHN-VTM-0194	0	TR	0.9	2.1	0	ND	0	21	0	0.5	0.09
GHN-VTM-0195	0.19	2	1.4	0.6	0	ND	1	11	0.14	0.02	0
GHN-VTM-0196	0.19	5	2.1	0.9	0	ND	1	7	0.23	0.22	0
GHN-VTM-0197	0.49	4	1.3	0.7	0	ND	2	11	0.15	0.01	0
GHN-VTM-0198	0.23	3	0.9	2.1	0	ND	1	15	0.02	0.01	0
GHN-VTM-0199	0.11	3	1.2	0.8	0	ND	1	15	0	0	0
GHN-VTM-0200	0.42	1	0.6	1.4	0	ND	1	14	0	0.03	0
GHN-VTM-0202	ND	4	0.65	TR	1	ND	1	14	ND	ND	ND
GHN-VTM-0204	ND	4	1.4	0.6	0	ND	1	12	ND	ND	ND
GHN-VTM-0205	ND	4	1	1	TR	ND	1	13	ND	ND	ND
GHN-VTM-0206	ND	3	1.2	0.8	0	ND	2	8	ND	ND	ND

Table C9 continued.

Sample ID	Hem	Chl	A_gy	D_gy	Phl_bio	Clay	Kao	Ill_sme	Cop	Jar	Sph
GHN-VTM-0207	ND	2	0.5	1.5	0	ND	1	11	ND	ND	ND
GHN-VTM-0208	ND	6	0.75	TR	0	ND	1	11	ND	ND	ND
GHN-VTM-0209	ND	4	0.65	TR	TR	ND	1	9	ND	ND	ND
GHN-VTM-0211	ND	4	0.75	TR	0	ND	1	9	ND	ND	ND
GHN-VTM-0212	ND	5	0.8	TR	0	ND	1	7	ND	ND	ND
GHN-VTM-0213	ND	6	0.75	TR	0	ND	2	7	ND	ND	ND
GHN-VTM-0214	ND	5	0.8	TR	0	ND	1	8	ND	ND	ND
GHN-VTM-0215	ND	6	0.5	0.5	0	ND	1	8	ND	ND	ND
GHN-VTM-0216	ND	6	0.75	TR	0	ND	1	9	ND	ND	ND
GHN-VTM-0217	ND	2	0.6	TR	0	ND	0	16	ND	ND	ND
GHN-VTM-0398	ND	6	1.8	3.2	0	1	ND	13	ND	ND	ND
GHN-VTM-0417	ND	TR	3.9	2.1	0	3	ND	8	ND	ND	ND
GHN-VTM-0418	ND	0	2.1	3.9	0	5	ND	15	ND	ND	ND
GHN-VTM-0419	ND	1	0.7	1.3	0	6	ND	14	ND	ND	ND
GHN-VTM-0420	ND	8	1	1	0	9	ND	4	ND	ND	ND
GHN-VTM-0421	ND	4	3.2	0.8	0	10	ND	3	ND	ND	ND
GHN-VTM-0422	ND	5	3.2	0.8	0	7	ND	3	ND	ND	ND
GHN-VTM-0423	ND	5	2.25	0.75	0	8	ND	4	ND	ND	ND
GHN-VTM-0424	ND	0	0.7	1.3	0	5	ND	8	ND	ND	ND
GHN-VTM-0425	ND	6	1.95	1.05	0	10	ND	3	ND	ND	ND
GHN-VTM-0426	ND	8	1.6	TR	0	7	ND	4	ND	ND	ND
GHN-VTM-0450	ND	5	3.2	0.8	TR	ND	2	6	ND	ND	ND
GHN-VTM-0451	ND	4	4	1	0	ND	2	7	ND	ND	ND
GHN-VTM-0452	ND	6	1.8	TR	TR	ND	1	7	ND	ND	ND
GHN-VTM-0453	ND	8	1	1	1	ND	1	14	ND	ND	ND
GHN-VTM-0454	ND	3	3	1	0	ND	1	12	ND	ND	ND
GHN-VTM-0606	ND	0	0.4	0.6	TR	20	ND	10	ND	ND	ND
GHN-VTM-0612	ND	1	14.3	0.8	1	4	ND	16	ND	ND	ND
GHN-VTM-0614	ND	0	10.5	4.5	0	24	ND	14	ND	ND	ND
GHN-VTM-0624	ND	2	0.05	0.95	TR	33	ND	2	ND	ND	ND